

# Cost-Effective Bird Collision Mitigation for North Sea Offshore Wind Farms

Nino Pérez Pérez



# Cost-Effective Bird Collision Mitigation for North Sea Offshore Wind Farms

Master Thesis by

Nino Pérez Pérez

In partial fulfilment of the requirements to obtain the degrees of  
Master of Science in Offshore and Dredging Engineering at Delft University of Technology (TU Delft)

and

Master of Science in Wind Energy Technology at the Norwegian University of Science  
and Technology (NTNU)

under the European Wind Energy Master programme.

To be defended in public on May 22, 2025.

Supervisors: TU Delft - Tim Raaijmakers  
TU Delft - Pim van der Male  
NTNU - Bjørn Egil Asbjørnslett  
Waardenburg Ecology - Abel Gyimesi

Committee Members: TU Delft - Tim Raaijmakers  
TU Delft - Pim van der Male  
NTNU - Bjørn Egil Asbjørnslett  
Waardenburg Ecology - Abel Gyimesi

Student Number: TU Delft - 4644808  
NTNU - 103223

Cover: Northern gannet flying above offshore wind farm (Stories of Purpose The Hague, 2024).

# Preface

This thesis is submitted in partial fulfilment of the requirements for the MSc degree in Offshore and Dredging Engineering at Delft University of Technology (TU Delft), as well as the MSc degree in Wind Energy Technology at the Norwegian University of Science and Technology (NTNU), under the European Wind Energy Master (EWEM) programme. This thesis focuses on reducing seabird collision risks in offshore wind farms by evaluating the economic feasibility of design changes that support more nature-inclusive strategies.

I would like to express my sincere gratitude to my supervisors, Ir. Tim Raaijmakers from TU Delft, Dr.ir. Pim van der Male from TU Delft, Prof. Bjørn Egil Asbjørnslett from NTNU and Ir. Abel Gyimesi from Waardenburg Ecology. Their proactive involvement, critical insights, and constructive feedback have been essential in guiding the direction and quality of this research. Thanks to their combined expertise—spanning engineering, policy, and ecology—the study was able to take an interdisciplinary approach to a complex challenge. I am also grateful for the collaboration with GROW Offshore, whose industry perspectives and data access significantly enriched the practical relevance of this work.

A special word of thanks goes to Ir. Tim Raaijmakers, whose forward-thinking mindset and drive for eco-friendly innovation has been a major influence on this thesis. His guidance helped shape both the direction and practical outcomes of the work, including the development of a prototype version of the EcoWindToolbox. I am particularly grateful for the learning opportunities he created—such as the 2024 WindEurope Hackathon in Bilbao, interviews with industry experts, and the chance to attend the *Kennisdag WOZEP – MONS*. His initiative to organise the *Seawilding Track on Nature-Inclusive Design of Offshore Energy Infrastructure* was especially inspiring, as it brought together engineers and ecologists and sparked my interest in bridging ecology and technology in offshore wind. Tim’s energy and flow of ideas continue to motivate me to carry this message forward—ensuring that future innovation not only serves human ambition, but also safeguards and rewilds the natural life that shares the offshore environment.

Many thanks go to the ecologists from Waardenburg Ecology and Wageningen Marine Research, whose expertise and openness to collaboration provided invaluable practical insights into the ecological aspects of offshore wind development. In particular, I would like to thank Ir. Abel Gyimesi for his close involvement throughout the thesis. His willingness to engage in frequent discussions and share knowledge created many opportunities to break down the barriers between engineering and ecology. These exchanges were instrumental in shaping an integrated perspective that underpins this work. A full list of experts interviewed during the research can be found in the Appendix.

Looking back, the past three years as a European Wind Energy Master student have been an incredible journey. It was a privilege to study at multiple universities within a single programme. Each semester brought its own unique challenges and rewards—whether through intense group projects, exciting travel opportunities, or unforgettable moments shared with classmates. I am especially thankful to my family and friends for their unwavering support and encouragement throughout this period. Their confidence in me has been a steady source of motivation, both in life and in completing this thesis.

This thesis aims to contribute to the evolving field of offshore wind energy by addressing the growing need for nature-inclusive design. By combining ecological modelling with economic evaluation, it highlights the potential for smarter, more sustainable design choices. I hope this work inspires further research and collaboration towards ecological innovation that allows offshore wind to develop in harmony with the marine environment.

*Nino Pérez Pérez  
Delft, May 5 2025*

# Abstract

This research addresses key challenges and knowledge gaps in avian safety management within offshore wind farm (OWF) development in the North Sea. As the region undergoes rapid expansion of offshore wind energy, there is a growing need to mitigate ecological impacts on seabirds, particularly in relation to their use of airspace as critical habitat. Concerns around bird collisions and broader environmental changes persist, while existing studies highlight considerable uncertainty in avian fatality estimates and migratory behaviour. In response, this thesis seeks to clarify these uncertainties by identifying data gaps, evaluating current methods, and proposing potential solutions.

Central to this effort is the development of a prototype Ecology-Technology Assessment Model. This foundational tool is designed with the mindset to bridge the gap between ecological insight and engineering practice, by integrating wind turbine characteristics, ecological parameters, and project constraints into a flexible optimisation framework. Built on principles from Multi-Disciplinary Analysis and Optimisation (MDAO), the model estimates bird collisions and assesses the economic consequences of potential mitigation measures. While the explicit incorporation of uncertainty lies beyond the current scope, the model is designed to accommodate such extensions in the future. It ultimately supports collaboration between engineers and ecologists and offers a structured platform for continued development.

Building on this framework, the thesis project applied the model to a practical case study at the IJmuiden Ver Alpha offshore wind farm site in the Dutch North Sea. The case study defined relevant ecological and technical input parameters, including wind farm layout, turbine characteristics, wind resource data, and the presence of key seabird species. Using the stochLAB collision risk model (CRM), design variations in minimum tip height (MTH), rotor diameter ( $D_{rotor}$ ), and rated power ( $P_{rated}$ ) were evaluated to assess their effectiveness in reducing seabird collisions. In parallel, the WINDOW model was used to calculate the Levelised Cost of Electricity (LCoE) impacts of these design choices, allowing for an integrated assessment of ecological benefit versus economic feasibility.

Simulation results demonstrated that increasing the minimum tip height is generally the most effective and economically feasible strategy for reducing bird collisions, especially for species with higher baseline collision risks. Increasing rated power was found to be more favourable for reducing a small number of collisions, while varying rotor diameter showed minimal impact on collision reduction within the modelled scenario. Ultimately, the findings emphasise that no universal design solution exists, and that the optimal collision mitigation strategy is highly dependent on the project location, site-specific bird characteristics, and wind farm design constraints. The study concludes by highlighting the importance of combining technical modelling with ecological knowledge, and provides recommendations for future research to improve data availability, model accuracy, and integration between ecological and technical disciplines in offshore wind development.

# Contents

<b>Preface</b>	<b>i</b>
<b>Summary</b>	<b>ii</b>
<b>1 Introduction</b>	<b>1</b>
1.1 Background . . . . .	1
1.2 Problem Statement . . . . .	4
1.3 Research Objective . . . . .	5
1.4 Research Questions . . . . .	6
1.5 Report Outline & Research Methodology . . . . .	6
<b>2 OWF Development Impacts on Birds</b>	<b>9</b>
2.1 Offshore Wind Development in the North Sea . . . . .	9
2.2 Avian Diversity in the North Sea . . . . .	10
2.3 Impact of Offshore Wind Farms on Avian Species . . . . .	14
2.4 Mitigation Measures . . . . .	18
2.5 Monitoring and Impact Assessment Methods . . . . .	21
2.6 Regulatory Framework and Policies . . . . .	23
2.7 Research Gaps and Future Directions . . . . .	25
<b>3 State-of-the-Art methods for Collision Risk Modelling</b>	<b>28</b>
3.1 Collision Risk Modelling . . . . .	28
3.2 Band Model . . . . .	30
3.3 Improved Band Model with Monte Carlo Simulations . . . . .	34
3.4 Literature Review Summary . . . . .	34
<b>4 Problem Background</b>	<b>36</b>
4.1 Summary of the Problem . . . . .	36
4.2 Arguments from Industry & Literature . . . . .	37
4.3 Introducing the Ecology-Technology Model . . . . .	39
<b>5 Case Study for a Typical Collision Assessment Scenario</b>	<b>41</b>
5.1 Scenario Overview . . . . .	41

---

5.1.1	IJmuiden Ver Alpha Background . . . . .	41
5.1.2	Case Study Parameters . . . . .	44
5.2	Driving Technical Criteria for the Ecology-Technology Model . . . . .	48
5.2.1	Support Structure Design Limits . . . . .	49
5.2.2	Vessel Size Limits . . . . .	50
5.2.3	Turbine Optimal Design Limits . . . . .	51
5.3	Modelling with WINDOW and stochLAB . . . . .	52
5.4	Next Steps . . . . .	54
<b>6</b>	<b>stochLAB Collision Risk Modelling</b>	<b>55</b>
6.1	Model Setup . . . . .	55
6.2	Baseline Results . . . . .	59
6.3	Results for Varying Minimum Tip Height . . . . .	61
6.4	Results for Varying Rotor Diameter . . . . .	64
6.5	Results for Varying Turbine Rated Power . . . . .	67
6.6	Collision Risk Modelling Summary . . . . .	70
<b>7</b>	<b>WINDOW LCoE Modelling</b>	<b>71</b>
7.1	Model Overview . . . . .	71
7.2	Governing Criteria . . . . .	74
7.2.1	Overturning Moment . . . . .	75
7.2.2	Natural Frequency . . . . .	77
7.2.3	Embedded Length . . . . .	80
7.3	Model Setup . . . . .	80
7.3.1	Turbine Geometric Inputs . . . . .	80
7.3.2	Support Structure . . . . .	81
7.3.3	Installation . . . . .	82
7.3.4	Operations and Maintenance (O&M) . . . . .	83
7.3.5	Farm AEP . . . . .	83
7.4	Assumptions Overview . . . . .	83
7.5	Baseline Results . . . . .	84
7.6	LCoE Model Results . . . . .	85
7.6.1	Results for Varying Minimum Tip Height . . . . .	86
7.6.2	Results for Varying Rotor Diameter . . . . .	89
7.6.3	Results for Varying Turbine Rated Power . . . . .	92

---

7.7	LCoE Modelling Summary . . . . .	94
<b>8</b>	<b>Simulation Results &amp; Discussion</b>	<b>95</b>
8.1	Results for Varying Rotor Diameter . . . . .	95
8.2	Results for Varying Minimum Tip Height . . . . .	97
8.3	Varying Turbine Rated Power . . . . .	103
8.4	Evaluating MTH versus $P_{rated}$ . . . . .	109
8.5	Practical Implications . . . . .	113
8.6	Assumption Implications . . . . .	114
<b>9</b>	<b>Conclusion</b>	<b>116</b>
<b>10</b>	<b>Recommendations</b>	<b>119</b>
	<b>References</b>	<b>120</b>
<b>A</b>	<b>Expert Interviews</b>	<b>125</b>
A.1	Interview with Ecologists M. Collier, A. Gyimesi & K. Didderen . . . . .	125
A.2	Interview with Marine Ecologists M. Baptist, M. Poot & F. Soudijn . . . . .	126
A.3	Interview with Bird Ecologist A. Gyimesi . . . . .	127
<b>B</b>	<b>Extended Simulation Results</b>	<b>128</b>
<b>C</b>	<b>R Script for Collision Calculations</b>	<b>131</b>
<b>D</b>	<b>Relevant Python Scripts</b>	<b>136</b>

# List of Figures

1.1	Offshore wind farm roadmap in the North Sea. (Heinatz & Scheffold, 2023) . . . . .	1
1.2	Overview of habitats for ten seabird species in the North Sea (Noordzeeloket, 2025). . .	2
1.3	Research plan for investigating the economic feasibility of three collision mitigation measures. . . . .	7
2.1	Offshore wind farm roadmap in the North Sea (Heinatz & Scheffold, 2023). . . . .	10
2.2	Examples of seabirds roaming the North Sea (The Cornell Lab of Ornithology, 2024) (Binda, 2025). . . . .	11
2.3	Density maps of two seabird species in the North- and Norwegian Sea (NINA, 2023). . .	12
2.4	Examples of migratory birds in the North Sea (The Cornell Lab of Ornithology, 2024). .	13
2.5	Offshore wind farm roadmap in the North Sea (Heinatz & Scheffold, 2023). . . . .	14
2.6	Estimated routes of seasonal bird migration (Bradaric, 2022). . . . .	14
2.7	Illustration of macro-, meso- and micro-avoidance (KeyFactsEnergy, 2023). . . . .	15
2.8	Most vulnerable seabird species (The Cornell Lab of Ornithology, 2024). . . . .	16
2.9	Most vulnerable migratory birds (The Cornell Lab of Ornithology, 2024). . . . .	17
2.10	Kernel densities of northern gannets tagged in 2015 (green) and 2016 (blue). OWF status in 2016: dashed black line = under construction, solid black line = operating (Peschko et al., 2021). . . . .	18
2.11	Estimated fatalities of black-legged kittiwake per OWF (Potiek et al., 2022). . . . .	18
2.12	Estimated fatalities of northern gannets per OWF (Potiek et al., 2022). . . . .	18
2.13	Illustration of shutting down procedure during peak bird migration (Rijkswaterstaat, 2022). 20	
2.14	Example of a structured analysis for bird population impact assessment (Brabant et al., 2015). . . . .	22
2.15	Framework for estimating cumulative impacts (Croll et al., 2022). . . . .	24
2.16	Types of uncertainties in OWF impacts on avian species (Searle et al., 2023). . . . .	26
2.17	List of research priorities to be addressed in order to reduce uncertainties in OWF impact assessments (Searle et al., 2023). . . . .	26
3.1	Comparison of collision risk models (A. Cook & Collier, 2015). . . . .	29
3.2	Cruciform bird shape assumption, where $a$ shows the actual bird, and $c$ shows the assumed bird shape by the Band model (E. A. Masden & Cook, 2016). . . . .	32

3.3	<b>Left:</b> How the distribution of birds is assumed by the basic Band model. <b>Right:</b> How the distribution of birds is assumed by an extend version of the Band model (A. Cook & Collier, 2015). . . . .	32
3.4	Example of boxplot output from the improved Band model, showing collision numbers per month (A. Cook & Collier, 2015). . . . .	34
3.5	Example of probability density plot output from the improved Band model (A. Cook & Collier, 2015). . . . .	34
5.1	Site location of IJmuiden Ver Alpha (van der Vliet et al., 2022). . . . .	42
5.2	Illustration of TenneT's 2 GW offshore wind farm to grid connection (TenneT, 2025). . .	43
5.3	Natura 2000 areas surrounding the site of IJmuiden Ver Alpha (van der Vliet et al., 2022). 43	
5.4	Comparison of wind speed distributions for IJmuiden Ver offshore wind conditions. . .	46
5.5	Wind rose for the IJmuiden Ver Alpha site, retrieved from (DOWA, 2017). . . . .	46
5.6	Turbine layout for the base case scenario (Mehta et al., 2024). . . . .	47
5.7	Free body diagram for the offshore wind turbine (McWilliam et al., 2021). . . . .	50
5.8	Examples of WTIV, FIV, and HLV vessels. . . . .	51
5.9	Schematic representation of a soft-stiff turbine design, with respect to the 1P and 3P frequencies (van der Male, 2023). . . . .	52
6.1	Generic flight height distributions used for all species. . . . .	58
6.2	Baseline scenario collisions per month for all species. . . . .	60
6.3	Calculated yearly collisions for various minimum tip heights. . . . .	62
6.4	Illustration of collision risk varying throughout the rotor swept area (van der Vliet et al., 2022). . . . .	63
6.5	Computed yearly collisions for all species vs. minimum tip height. NG = Northern gannet, LBBG = Lesser black-backed gull, HG = Herring gull, GBBG = Great black-backed gull, LG = Little gull, BLK = Black-legged kittiwake. . . . .	64
6.6	Calculated yearly collisions for various rotor diameters. . . . .	65
6.7	Computed yearly collisions for all species vs. rotor diameter. NG = Northern gannet, LBBG = Lesser black-backed gull, HG = Herring gull, GBBG = Great black-backed gull, LG = Little gull, BLK = Black-legged kittiwake. . . . .	66
6.8	Calculated yearly collisions for various rated powers. . . . .	68
6.9	Computed yearly collisions for all species vs. rated power. NG = Northern gannet, LBBG = Lesser black-backed gull, HG = Herring gull, GBBG = Great black-backed gull, LG = Little gull, BLK = Black-legged kittiwake. . . . .	69
7.1	Framework of the Ecology-Technology model, based on the original framework structure from (Mehta et al., 2024). . . . .	72
7.2	Illustration of the simplified foundation stiffness model (Arany et al., 2017). . . . .	77
7.3	Calculated natural frequencies for various minimum tip heights. . . . .	79

7.4	Contribution to LCoE for various CAPEX components, as well as O&M and Decommissioning costs. Note that this is for the base case scenario. . . . .	85
7.5	LCoE values from the WINDOW model for various minimum tip heights. . . . .	86
7.6	<b>(a)</b> Change in CAPEX components with varying minimum tip height. <b>(b)</b> Change in critical farm-level quantities with varying minimum tip height. . . . .	87
7.7	Plot showing the relative variation of CAPEX components for varying MTH. The percentage values on the left and right refer to the component share percentage at 15 and 60 m MTH respectively. . . . .	88
7.8	Simulation results for minimum tip height, illustrating the 'damping' effect of increased AEP. . . . .	88
7.9	LCoE values from the WINDOW model for various rotor diameters. . . . .	89
7.10	<b>(a)</b> Change in components of CAPEX when varying $D_{rotor}$ . <b>(b)</b> Change in crucial farm-level components when varying $D_{rotor}$ . . . . .	90
7.11	Plot showing the relative variation of CAPEX components for varying $D_{rotor}$ . The percentage values on the left and right refer to the component share percentage at 186 and 286 m $D_{rotor}$ respectively. . . . .	91
7.12	Simulation results for rotor diameter, showcasing the effect of AEP 'damping'. . . . .	91
7.13	LCoE values as calculated by WINDOW for various rated power turbines. . . . .	92
7.14	<b>(a)</b> Change in components of CAPEX when varying $P_{rated}$ . <b>(b)</b> Change in crucial farm-level components when varying $P_{rated}$ . . . . .	93
7.15	Plot showing the relative variation of CAPEX components for varying $P_{rated}$ . The percentage values on the left and right refer to the component share percentage at 10 and 23 MW $P_{rated}$ respectively. . . . .	94
8.1	Calculated absolute and relative LCoE values for each reduction or increase in yearly bird collisions, relative to the base case. <b>(a)</b> Northern Gannet. <b>(b)</b> Lesser Black-backed Gull. . . . .	96
8.2	Calculated absolute and relative LCoE values for each reduction or increase in yearly bird collisions, relative to the base case. <b>(a)</b> Herring Gull. <b>(b)</b> Great Black-backed Gull. . . . .	96
8.3	Calculated absolute and relative LCoE values for each reduction or increase in yearly bird collisions, relative to the base case. <b>(a)</b> Little Gull. <b>(b)</b> Black-legged Kittiwake. . . . .	97
8.4	Absolute and relative LCoE values for each reduction or increase in yearly collisions. . . . .	98
8.5	Absolute and relative LCoE values for each reduction or increase in yearly collisions. . . . .	98
8.6	Absolute and relative LCoE values for each reduction or increase in yearly collisions. . . . .	99
8.7	Absolute and relative LCoE values for each reduction or increase in yearly collisions. . . . .	99
8.8	Absolute and relative LCoE values for each reduction or increase in yearly collisions. . . . .	100
8.9	Absolute and relative LCoE values for each reduction or increase in yearly collisions. . . . .	100
8.10	Absolute and relative LCoE values for reducing or increasing yearly collisions due to varying MTH, plotted for all studied species. . . . .	102
8.11	Absolute and relative LCoE values for each reduction or increase in yearly collisions. . . . .	104
8.12	Absolute and relative LCoE values for each reduction or increase in yearly collisions. . . . .	104

---

8.13	Absolute and relative LCoE values for each reduction or increase in yearly collisions. . .	105
8.14	Absolute and relative LCoE values for each reduction or increase in yearly collisions. . .	105
8.15	Absolute and relative LCoE values for each reduction or increase in yearly collisions. . .	106
8.16	Absolute and relative LCoE values for each reduction or increase in yearly collisions. . .	106
8.17	Absolute and relative LCoE values for reducing or increasing yearly collisions due to varying $P_{rated}$ , plotted for all studied species. . . . .	108
8.18	Comparison between the MTH and $P_{rated}$ simulation for the northern gannet. . . . .	109
8.19	Comparison between the MTH and $P_{rated}$ simulation for the lesser black-backed gull. . .	110
8.20	Comparison between the MTH and $P_{rated}$ simulation for the herring gull. . . . .	110
8.21	Comparison between the MTH and $P_{rated}$ simulation for the great black-backed gull. . .	111
8.22	Comparison between the MTH and $P_{rated}$ simulation for the little gull. . . . .	111
8.23	Comparison between the MTH and $P_{rated}$ simulation for the black-legged kittiwake. . .	112
B.1	Full graph for the northern gannet showing the absolute and relative LCoE values for each reduction or increase in yearly collisions, due to varying the minimum tip height. .	128
B.2	Full graph for the black-legged kittiwake showing the absolute and relative LCoE values for each reduction or increase in yearly collisions, due to varying the minimum tip height.129	
B.3	Full graph showing the absolute and relative LCoE values for reducing or increasing yearly collisions due to varying MTH, plotted for all studied species. . . . .	130

# List of Tables

5.1	Reference Farm Specifications. . . . .	45
5.2	Reference Turbine Specifications. . . . .	45
5.3	Lesser black-backed gull inputs. . . . .	47
5.4	Northern gannet inputs. . . . .	47
5.5	Herring gull inputs. . . . .	47
5.6	Great black-backed gull inputs. . . . .	47
5.7	Little gull inputs. . . . .	48
5.8	Black-legged kittiwake inputs. . . . .	48
5.9	Monthly bird density values in birds/km <sup>2</sup> (van der Vliet et al., 2022). Species names abbreviated as: NG = Northern gannet, LBBG = Lesser black-backed gull, HG = Herring gull, GBBG = Great black-backed gull, LG = Little gull, BLK = Black-legged kittiwake. . . . .	48
6.1	Non-trivial input variables used in the <code>stoch_crm()</code> function. . . . .	56
6.2	Blade chord profile for inner to outer radius percentage (IEA, 2025). . . . .	59
6.3	Monthly bird collision estimates per species, including the total collisions for one year. Species names abbreviated as: NG = Northern gannet, LBBG = Lesser black-backed gull, HG = Herring gull, GBBG = Great black-backed gull, LG = Little gull, BLK = Black-legged kittiwake. . . . .	61
6.4	Monthly collision estimates as computed by (van der Vliet et al., 2022). . . . .	61
6.5	Maximum total collisions per year for two wind farm scenarios with 15 and 20 MW turbines, calculated by (van der Vliet et al., 2022). . . . .	70
7.1	Technical parameters for varying minimum tip height. $P_{\text{rated}} = 15$ . . . . .	75
7.2	Estimated monopile diameters for ultimate bending stress analysis. . . . .	76
7.3	Updated monopile diameters values as a result of the natural frequency analysis. . . . .	79
7.4	Updated monopile diameter values, corrected for natural frequency and embedded length requirements. . . . .	80
7.5	Turbine specifications including minimum tip height. . . . .	81
7.6	Vessel types, their purposes, and associated costs, assuming a 15 MW turbine. . . . .	82
7.7	Vessel types and costs, for wind farm O&M assuming a 15 MW turbine. . . . .	83
7.8	Baseline results. . . . .	84
7.9	Farm-level components. . . . .	84

---

7.10 Turbine components. . . . . 84

A.1 Overview of expert interviews. . . . . 125

# Introduction

## 1.1. Background

In line with global climate agreements and the increasing energy demand, offshore wind energy has become a main driver in the energy transition. The North Sea, due to its vast wind resources, has become a prominent and burgeoning hub for offshore wind energy development. The region's strategic location, proximity to densely populated areas, and strong winds make it a prime location for offshore wind farm installations. The growth of offshore wind energy projects in the North Sea has been remarkable, with numerous installations and ambitious expansion plans. The current offshore wind capacity sits at 25 GW, which is owned by the top five European offshore wind energy producers (the UK, Germany, Denmark, the Netherlands and Belgium), and is set to increase tenfold by 2050 (Bradaric, 2022). This rapid development brings forth a unique set of challenges and opportunities regarding avian safety management. To illustrate, Figure 1.1 shows the locations of currently operating wind farms, combined with those planned to be built by 2030 in the Dutch part of the North Sea, with a total capacity of 22 GW (Netherlands Enterprise Agency, 2023).

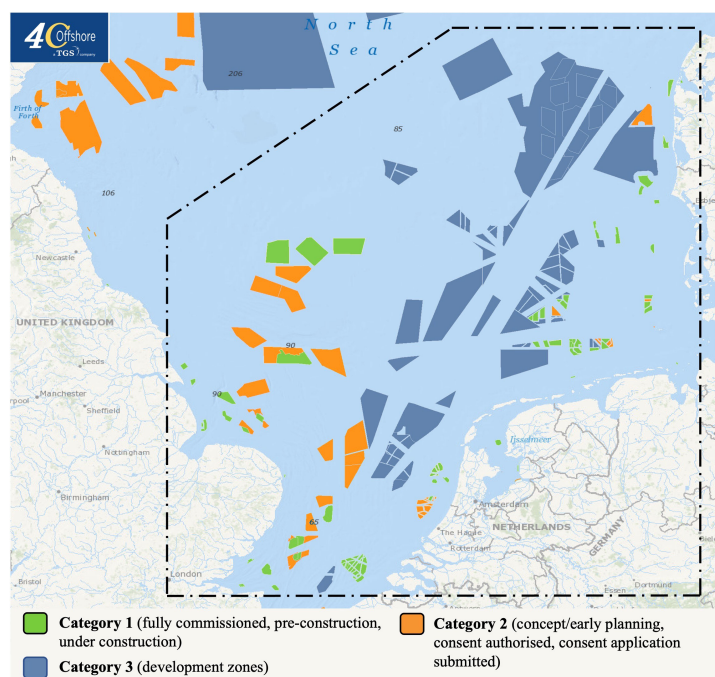


**Figure 1.1:** Offshore wind farm roadmap in the North Sea. (Heinatz & Scheffold, 2023)

The North Sea, with its dynamic avian ecosystem, serves as a compelling case study for understanding the interactions between offshore wind energy and avian species. The airspace above it is an essential and often overlooked habitat for avian species. Birds of various species rely on this three-dimensional domain for breeding, foraging, migration, and general habitat use. This includes airspace above coastline and shallow sea waters, as can be seen in Figure 1.2. In this context, offshore wind farms occupy airspace that is traditionally a critical part of avian ecological networks, making it necessary to address potential conflicts and impacts to ensure the long-term well-being of avian populations. Negative impacts of offshore wind farms (OWFs) on avian species include collisions, habitat loss, and barrier effects. This research focuses on the technical perspective of mitigating seabird collisions with offshore wind farms, while maintaining a competitive Levelised Cost of Electricity (LCoE). However, it is also important to gain knowledge from other perspectives on this topic, since mitigating seabird collisions is a new challenge with many knowledge gaps that span multiple disciplines. An interdisciplinary approach is required to address this issue effectively.

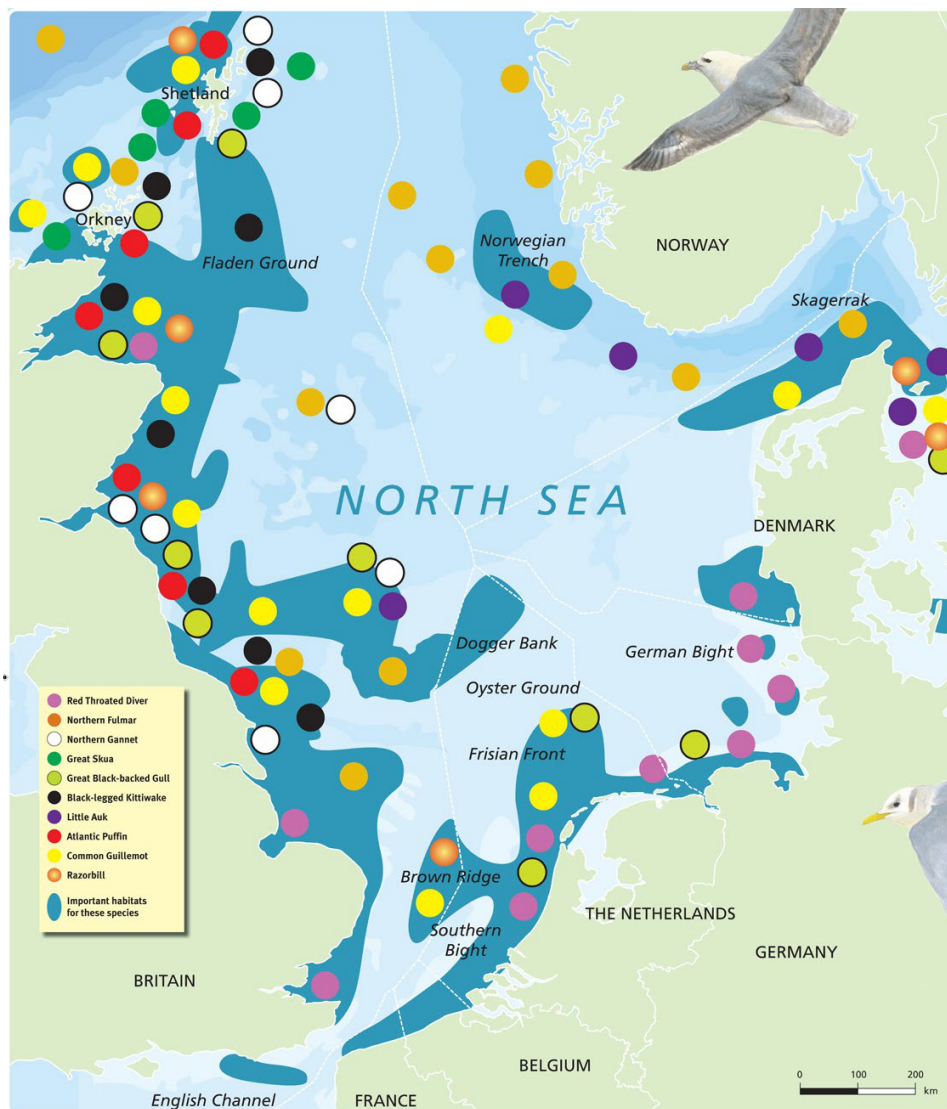


**Figure 1.2:** Overview of habitats for ten seabird species in the North Sea (Noordzeeloket, 2025).

OWFs are rapidly being developed in the North Sea, due to the energy transition. Figure 1.1 showed what the North Sea may look like by the year 2050. With this in mind, and looking at Figure 1.2, it becomes clear that avian life will be affected by the construction of OWFs on such a large scale. Nowadays, there is little known about the magnitude of the impacts of OWF development on birds. Additionally, future

impacts remain difficult to estimate as well. Many players in the energy transition are calling for action on this topic. To obtain a broad understanding of the topic from different perspectives, interviews were conducted with industry experts. A brief overview of the insights from the experts and literature is given below to demonstrate the increasing relevance of research into negative effects of OWFs on seabirds in the North Sea.

### **Legal Perspective**

Despite its importance, the airspace has often been excluded from environmental policies and conservation efforts. There is a growing call among aerocologists to change this and acknowledge the airspace as a critical habitat, due to the increasing challenges it faces from pollution and fragmentation (Lambertucci et al., 2015). Furthermore, the introduction of the Natura 2000 legislation within the European Union has significantly increased the protection of vulnerable species and habitats, including seabirds. Offshore wind farm developments must therefore comply with strict environmental regulations to prevent significant adverse effects on these protected species. Without sufficient monitoring, mitigation, or adaptive management measures in place, there is a risk that future offshore wind expansion could trigger legal challenges similar to the nitrogen crisis in the Netherlands (Adviescollege Stikstofproblematiek, 2019). In that case, large-scale construction projects in the Netherlands were halted due to exceeding environmental limits, demonstrating how environmental protection laws can become a critical bottleneck for infrastructure development if ecological impacts are not properly addressed. The same risk applies to offshore wind farm development projects.

### **Ecological Perspective**

Human activities, including the expansion of offshore wind farms, exert a considerable influence on avian populations in the airspace. The development of renewable energy sources, such as offshore wind, is pivotal in addressing climate change and reducing reliance on fossil fuels. However, the deployment and operation of offshore wind farms have raised concerns about their impact on avian species, with bird collisions with wind turbine blades and alterations to the natural environment being some of the primary concerns. This is mainly due to the fact that there are still a considerable number of knowledge gaps on this topic from an ecological perspective. Some of these gaps have been filled by assumptions based on expert judgement, and others have been filled by pragmatic assumptions. It is essential that the mapping of these knowledge gaps is prioritised and done quickly, as wind energy is being installed at a rapid pace (Platteeuw et al., 2017).

Failing to do so could have drastic consequences. Avian species that are already endangered could go extinct. More importantly, large-scale offshore wind production could lead to population declines of several bird species, which could in turn disturb entire ecosystems (Buij et al., 2018). This last problem is more commonly referred to as 'cumulative effects' in scientific literature. Again, this is particularly important given the rapid growth of the offshore wind sector and the potential for cumulative impacts on entire bird populations due to collisions caused by multiple wind farms (Brabant et al., 2015), (Busch & Garthe, 2018).

### **Economic Perspective**

Negative impacts on birds pose an economic risk to wind farm operators. On May 13 2023, wind turbines in Borssele and Egmond aan Zee were shut down or slowed to mitigate collisions during high-intensity bird migration periods. A scientific model was developed by (Bradaric, 2022), that could predict when peak bird migration was happening. The collaborating wind farm operators agreed to slow or shut down turbines during this predicted peak migration. This is of course an excellent example of reducing harm to nature while still being able to operate a profitable wind farm. However, some may still say that a complete shutdown for wind farm operators is too harsh on profitability, as electricity prices are variable and may be high when shutdowns occur, reducing profitability drastically for operators.

As another example, the impact of wind farms on white-tailed eagles presents a clear economic challenge for operators. At the Smøla Wind Farm in Norway, a total of 133 eagles were killed by turbine collisions

between 2005 and 2023, and the spatial distribution of eagle territories has shifted since the wind farm's construction. While the population of white-tailed eagles has remained stable, there is a slight decline in growth rates, and mortality due to collisions remains a concern, which may lead to the farm being shut down (Stokke & Dahl, 2024). Mitigation strategies, such as painting rotor blades black to increase visibility, have shown promise in reducing bird fatalities. However, should these measures not work, then the wind farm operators run the risk of the wind farm being shut down, which poses an economic risk. This highlights the trade-off that operators must make between the need for wildlife protection and the potential loss of revenue (Raaijmakers, 2025).

### Technical Perspective

Efforts to reduce fatalities of avian species by wind farms have been the topic of many researchers. These can be divided into pre-construction and post-construction measures (Garcia-Rosa, 2022):

#### Pre-construction measures

- **Site Selection:** Careful site selection is crucial to minimise bird collisions. Developers choose sites that avoid critical bird habitats, migration routes, and nesting areas.
- **Turbine Design Modifications:** Some wind turbines are designed with features to reduce bird collisions, such as changing blade colours to improve visibility, using bird-friendly lighting, and implementing avian detection systems.

#### Post-construction measures:

- **Curtailement:** When bird activity is detected in the vicinity of wind turbines, curtailment measures may be applied. Turbine operations may be temporarily halted during migration seasons (Bradaric, 2022), or slowed down to reduce the risk of collisions.
- **Active wind turbine control:** An active control system able to make small adjustments to the rotor speed (in real time), so that the birds can fly through the rotor-swept area without being hit by the blades (Garcia-Rosa, 2022).
- **Deterrents:** Visual and acoustic signals produced by the wind turbines, which are intended to scare birds to prevent them from coming dangerously close to the turbines.
- **Habitat management:** On-site alterations to reduce bird activity by reducing vegetation (on islands) near wind farm sites, and off-site alterations to attract birds elsewhere, like artificial feeding or resting facilities.
- **Painting wind turbines:** Increasing visibility of wind turbine blades and towers by adding high-contrast paint to reduce the risk of collision.

It should be noted that the effectiveness of each method depends on the bird species, since behaviour varies across species. With this in mind, the offshore wind industry, due to its globalised nature, calls for methods that are proven to be most effective for multiple vulnerable species. In addition, better tools for local measures are also required to deal with the species-specific nature of impacts on avian species. To learn more about the technical perspective, an investigation was conducted through a literature review in Chapters 2 and 3.

## 1.2. Problem Statement

At present, there remains considerable ambiguity surrounding avian fatality figures and bird migration patterns in the context of offshore wind energy. Given the rapid expansion of offshore wind farms, it becomes imperative to delve deeper into these aspects. Additionally, the existing bird collision mitigation techniques can appear somewhat excessive. The outright suspension of wind farm operations solely based on predictive models indicating potential bird migration can be financially burdensome for wind farm operators (Bradaric, 2022), due to halting wind farms in moderate wind conditions, when the

energy price is high. In addition, our future energy system will depend heavily on wind energy, which will be a substantial factor in our energy security. Consequently, it is crucial to explore approaches that not only minimise collision risks but also prioritise optimal power generation.

Furthermore, researchers seem to agree that an interdisciplinary approach is needed to overcome the challenges that wind farm development causes on bird populations (E. A. Masden & Cook, 2016). Ecologists, engineers and policy makers will need to actively cooperate to develop solutions. Communication between ecology and engineering fields of expertise will be a crucial part of solving this problem. Up until now, most literature on this topic summarises advancements and challenges regarding avian safety for wind farms, while there are few scientific papers suggesting effective measures to address current challenges. The author's conclusion is that the offshore wind industry could greatly benefit from better means of communication between ecologists and engineers. Connections need to be made between knowledge of bird behaviour and how impact mitigation measures affect wind turbine and farm design. To address this crucial matter, the idea of creating a first-order model that facilitates bird collision estimation and farm-level cost estimation simultaneously is explored in this research.

### 1.3. Research Objective

The aim of this research is to contribute to the field of ecological impact reduction in the wind energy industry. First, a literature study was conducted in the first part of the research, to identify the main knowledge gaps regarding avian safety management for offshore wind farms. In the second part of this research, the thesis project was executed, which focused on understanding the relationship between seabird collision mitigation measures and the Levelised Cost of Electricity of an offshore wind farm. The economic consequences of applying such mitigation measures were identified as a key knowledge gap during the analysis of offshore wind farm impacts on bird species in Chapter 2. Therefore, the research objective was defined as:

*"Quantify the economic impact of implementing design-based mitigation measures to reduce seabird collisions in offshore wind farms in the North Sea."*

This research mainly focused on the influence of offshore wind energy in the North Sea on avian species, specifically seabirds. The influence of renewable energy technology on other lifeforms, while also important, was considered out of the scope of this report. Ecological data about bird species behaviour in an offshore context is increasingly available, and significant progress has been made on the technical understanding of seabird flight behaviour in the context of offshore wind farms (Gyimesi, 2025). Thus, with more ecological data to work with, a technical analysis on seabird collisions in an offshore wind farm context will provide more tangible results. Migratory birds are also a topic of recent research, especially involving prediction models based on weather conditions, which are used to execute coordinated wind farm shut-downs (Bradaric, 2022). However, bird migration happens predominantly on a few nights per season, while seabird interactions with offshore wind farms occur year-round. Therefore, migratory birds were excluded from the scope of this thesis, focusing on seabirds only. In addition, identified impacts on seabirds like habitat loss and barrier effects were left out of the thesis scope as well. Collisions were selected as the primary impact to investigate, mainly because of the available research and existing calculation methods, such as the stochLAB collision risk model (Humphries et al., 2022), in comparison to other impacts (Ijntema, 2024). Collision mitigation is also more relevant to investigate as it directly influences turbine control or design, which operators and engineers have to take into account.

The problem stated in the previous section calls for an interdisciplinary solution across the fields of ecology, engineering and policy, where the latter was excluded from the scope of this research. This research aims to bridge the other two disciplines and investigate wind farm designs and turbine configurations that minimise bird collisions while preserving cost-effectiveness and energy yield. Operational strategies, which are also considered to be effective for collision mitigation, are not included in the thesis scope. Finally, this thesis aims to provide a starting point for developing an integrated ecology-technology assessment model. Such a model could facilitate more effective communication between ecologists and engineers, enabling interdisciplinary discussions with a shared understanding.

The scientific basis for this model was laid out in Chapters 3 and 4, after which its ecology-technology components were developed in Chapters 5, 6, and 7. To evaluate the economic outcome within this model, the Levelised Cost of Electricity (LCoE) was selected as the primary output metric. Other non-economic outcomes, such as life cycle assessments or carbon footprint analyses, were not included within the scope of this thesis, although these are considered valuable additions for future improvements of the ecology-technology model.

## 1.4. Research Questions

The literature study covered the following research questions, aiming to determine the most important knowledge gaps regarding bird impact mitigation within offshore wind farms:

- What are the key challenges and knowledge gaps in avian safety management for offshore wind farms?
- What are the potential solutions to address the identified knowledge gaps in avian safety management?
- What type of choices can be made in the design process of wind turbines, to reduce the risk of collision?
- What are the current state-of-the-art methods for modelling seabird collision risk in offshore wind farms?

For the second phase of this research, the thesis project addressed several research questions to determine the economic impact of applying offshore wind turbine design modifications aimed at mitigating seabird collisions in the North Sea:

- What is a typical scenario for collision risk assessment within an offshore wind farm in the Dutch part of the North Sea?
- How effective are design variations in minimum tip height, rotor diameter, and rated power at reducing seabird collisions within the defined scenario?
- What is the economic feasibility of design variations in minimum tip height, rotor diameter and rated power within the defined scenario?
- Which mitigation measure provides the most cost-effective reduction in seabird collisions within the defined scenario?

## 1.5. Report Outline & Research Methodology

The first four chapters of this research are mostly based on the literature review. The variety of offshore wind farm impacts on bird species are described in Chapter 2. A comprehensive literature search on state-of-the-art methods for collision risk modelling, to help answer the abovementioned research questions, was conducted in Chapter 3. Relevant sources of information related to avian safety management in the context of offshore wind farms were searched for using online databases and search tools, like Google Scholar and ResearchGate. The selected sources included peer-reviewed journal articles, reports, and government documents. The AI tool ChatGPT was also used to uncover the current state of research on the topic. Furthermore, the research is conducted in collaboration with GROW Offshore, a consortium of more than 20 companies/research institutions in The Netherlands. Within GROW, educational institutions like University of Amsterdam (UvA), Leiden University, Wageningen University of Research (WUR), and TU Delft take part in a work package called The EcoWindToolbox. In this work package, the development of a similar model as described in this report is proposed. Furthermore, the ecology consultancy expertise from Waardenburg Ecology was utilised on various occasions through the inclusion of one expert from this company in the exam committee. Information from key players in the field of offshore wind energy will be available through the GROW consortium and Waardenburg Ecology. Interviews with internal experts from GROW and TU Delft also provided

additional knowledge on modelling, which was most useful for the execution of this master's thesis project.

As mentioned in this introductory chapter, the main focus of this thesis was narrowed down to investigating the cost-effectiveness of collision mitigation measures for seabirds. To determine the governing inputs and criteria for such an analysis, a typical scenario for collision risk assessment is described in Chapter 5. The thesis project starts from this chapter and is documented until the end of this report. The Framework for Assessing Ecological and Cumulative Effects report, or KEC 4.0 (Potiek et al., 2022), inspired the selection of critical seabird species. In addition, the recent MER study report for the Ijmuiden Ver wind farm zone (van der Vliet et al., 2022), provided all the necessary ecological details in order to evaluate a relevant and present-day wind farm scenario. Based on the findings of Chapter 3 and an interview with three ecologists from Waardenburg Ecology, the offshore collision risk model developed by Band (Band, 2012), was deemed as the most suitable option for bird collision calculations. In Chapter 6, this model is put into practice via the open source software package called stochLAB, where a stochastic version of the Band model is included. The required function from this package was executed in an R script, where R is a programming language used for statistical research. The resulting collision calculations from stochLAB had to be evaluated next to a Levelised Cost of Electricity calculation of the defined case study. A first-order Levelised Cost of Electricity estimation was done with WINDOW, a publicly available Multi Disciplinary Analysis and Optimisation tool, developed through extensive scientific research at TU Delft (Zaaijer, 2013), (Perez-Moreno et al., 2018). The latest research from (Mehta et al., 2024), used WINDOW to estimate the change in Levelised Cost of Electricity of a wind farm due to scaling of the rotor diameter and rated power of turbines. Based on Chapter 2, three turbine design choices were selected in order to mitigate collisions: increasing minimum tip height, changing rotor diameter and increasing rated power. With some modifications, the latest version of the WINDOW Levelised Cost of Electricity model from (Mehta et al., 2024) was able to calculate the Levelised Cost of Electricity due to these applied changes in turbine design, which is presented in Chapter 7. For a combined analysis, the stochLAB and WINDOW Levelised Cost of Electricity models were constructed into one Python project with multiple scripts, in order to determine the economic feasibility of varying the three abovementioned design parameters.

To provide a clear overview of the thesis project, a simplified illustration of the research plan is shown in Figure 1.3:

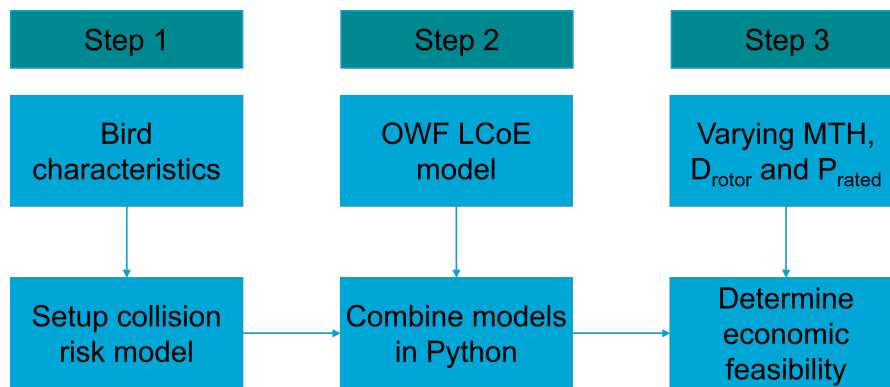


**Figure 1.3:** Research plan for investigating the economic feasibility of three collision mitigation measures.

For step 1 in Figure 1.3, the bird characteristics were determined in Chapter 5 and passed as inputs to the stochastic collision risk model in Chapter 6. In step 2, the offshore wind farm (OWF) Levelised Cost of Electricity was calculated by a modified version of the WINDOW model in Python, as presented in Chapter 7. Combining both models, step three could be executed in order to meet the aforementioned research objective. This last step is presented in Chapter 8, which contains an extensive analysis of the final simulation results. Here, the economic feasibility for varying the minimum tip height, rotor diameter, and rated power to reduce collisions was examined for a total of six critical seabird species.

Lastly, Chapter 9 contains the conclusion, which contains a summary of the key findings, after which suggestions for future research and improvements for the ecology-technology model are specified in Chapter 10.

# 2

## OWF Development Impacts on Birds

This chapter aims to answer the first research question: What are the key challenges and knowledge gaps in avian safety management for offshore wind farms? In addition, it covers the second research question: What are the potential solutions to address the identified knowledge gaps in avian safety management? Finally, it answers the third research question: What type of choices can be made in the design process of wind turbines to reduce the risk of collision? In this chapter, an objective literature review of avian safety management in the North Sea is presented. In the context of burgeoning offshore wind energy developments in regions such as the North Sea, this chapter embarks on a comprehensive literature review that explores the intricate relationship between offshore wind farms and avian species. Beginning with an overview of offshore wind development in the North Sea (Section 2.1), the narrative unfolds through avian diversity in the North Sea (Section 2.2), delving into the rich bird species inhabiting this maritime expanse. Sections 2.3 to 2.7 navigate through the impact of offshore wind farms on avian species, mitigation measures, monitoring and impact assessment methods, the regulatory framework, and policies, culminating in an exploration of research gaps and future directions.

### **2.1. Offshore Wind Development in the North Sea**

The current state of offshore wind energy in the North Sea is characterised by significant growth and development. The offshore wind capacity in the North Sea has increased substantially over the years, with a significant number of offshore wind farms in operation. Europe holds the largest regional market share of offshore wind installations in the Dutch part of the North Sea, accounting for 50.4% of total cumulative global offshore wind installations. The cumulative capacities of grid-connected offshore wind farm projects are projected to surge significantly in the coming years, from 28.4 GW in 2022 to 300 GW by 2050 (Ramírez, 2021). Additionally, the North Sea has been recognised as an attractive location for offshore wind energy infrastructure due to reliable wind resources, shallow waters, and proximity to developed energy and electricity markets (Gusatu et al., 2020). The region has seen rapid growth in installed capacity, with the deployment of large-scale offshore wind farms. Countries such as the UK, Germany, Denmark and The Netherlands have become significant owners of offshore wind farms, further consolidating the North Sea's position as a key area for offshore wind energy development (GWEC, 2022). To illustrate this development, Figure 2.1 shows the distribution of the operating OWFs in the North Sea, as well as OWFs planned for construction.

However, this expansion is not without challenges, particularly concerning potential impacts on avian wildlife. The ecological impacts of offshore wind farms on trophic level species of the marine food chain, especially on avian wildlife, are areas of concern that need to be carefully managed to minimise adverse effects. Thus, the current state of offshore wind energy in the North Sea reflects a promising trajectory towards renewable energy expansion, while also calling for strategic and sustainable management to balance energy generation objectives with environmental conservation priorities.

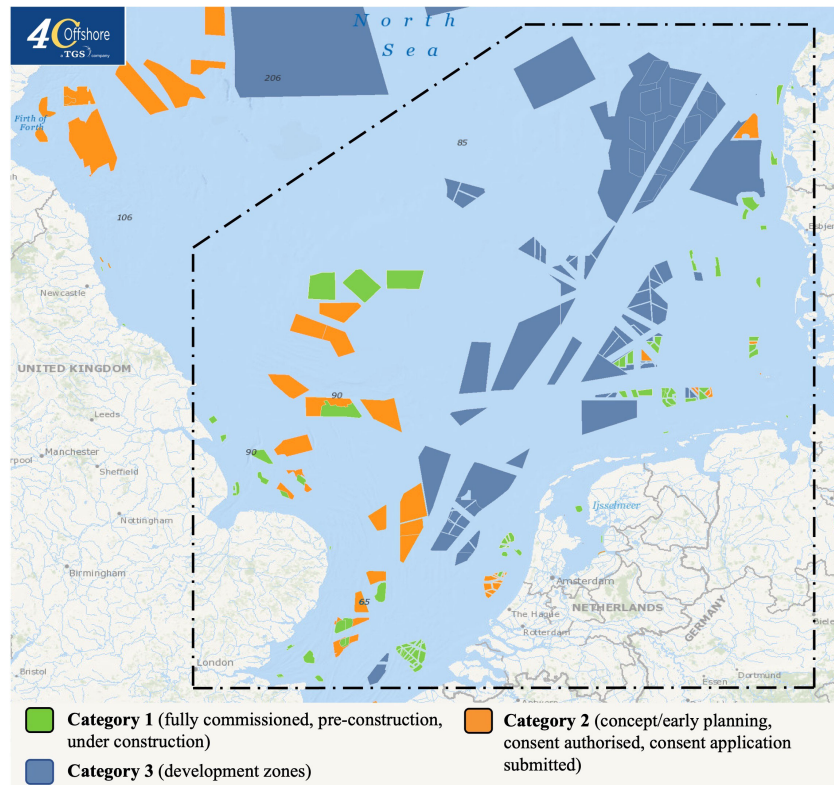


Figure 2.1: Offshore wind farm roadmap in the North Sea (Heinatz & Scheffold, 2023).

## 2.2. Avian Diversity in the North Sea

Birds interact with the North Sea in various ways. These can be categorised into (Platteeuw et al., 2017):

- **Seabirds:** Birds that spend all their time at sea outside the breeding season.
- **Coastal birds:** Living year-round along the coast, for breeding and resting, meaning they fly over the North Sea daily.
- **Migratory birds:** They migrate seasonally along the North Sea shores or cross the North Sea between the European continent and the British Isles.

The North Sea hosts a diverse range of seabird species, including but not limited to the northern gannets (*Morus bassanus*), black-legged kittiwakes (*Rissa tridactyla*), common guillemots (*Uria aalge*), razorbills (*Alca torda*), European shags (*Phalacrocorax aristotelis*), Atlantic puffins (*Fratercula arctica*), and storm-petrels (*Hydrobatidae*) (Camphuysen et al., 2009). Figures of some of these species are shown in Figure 2.2:



(a) Great black-backed gull.



(b) Razorbill.



(c) Atlantic puffin.



(d) Black-legged-kittiwake.



(e) Northern gannet.



(f) Common guillemot.

**Figure 2.2:** Examples of seabirds roaming the North Sea (The Cornell Lab of Ornithology, 2024) (Binda, 2025).

Seabirds, like the northern gannet, spend most of their time at sea, pursuing food sources at distances of up to 200 km offshore, and only return to coastlines (cliffs) for breeding (Kushlan, 2023). According to an ecology expert, most future wind farms are planned at similar distances offshore: 50–100 km, or even further (Gyimesi, pers. comm., 27-06-2024). Therefore, it is most interesting to look into the interaction of seabirds with wind farms in the future, which is in line with the focus of this thesis. Overall, the distribution and density of seabirds in the North Sea depends on the species and location. For example, Figure 2.3 shows the density maps of the great black-backed gull and northern gannet. Looking back

at Figure 2.1, and Figure 1.2 from the previous chapter, raises suspicions that these species could be affected by future OWF development.

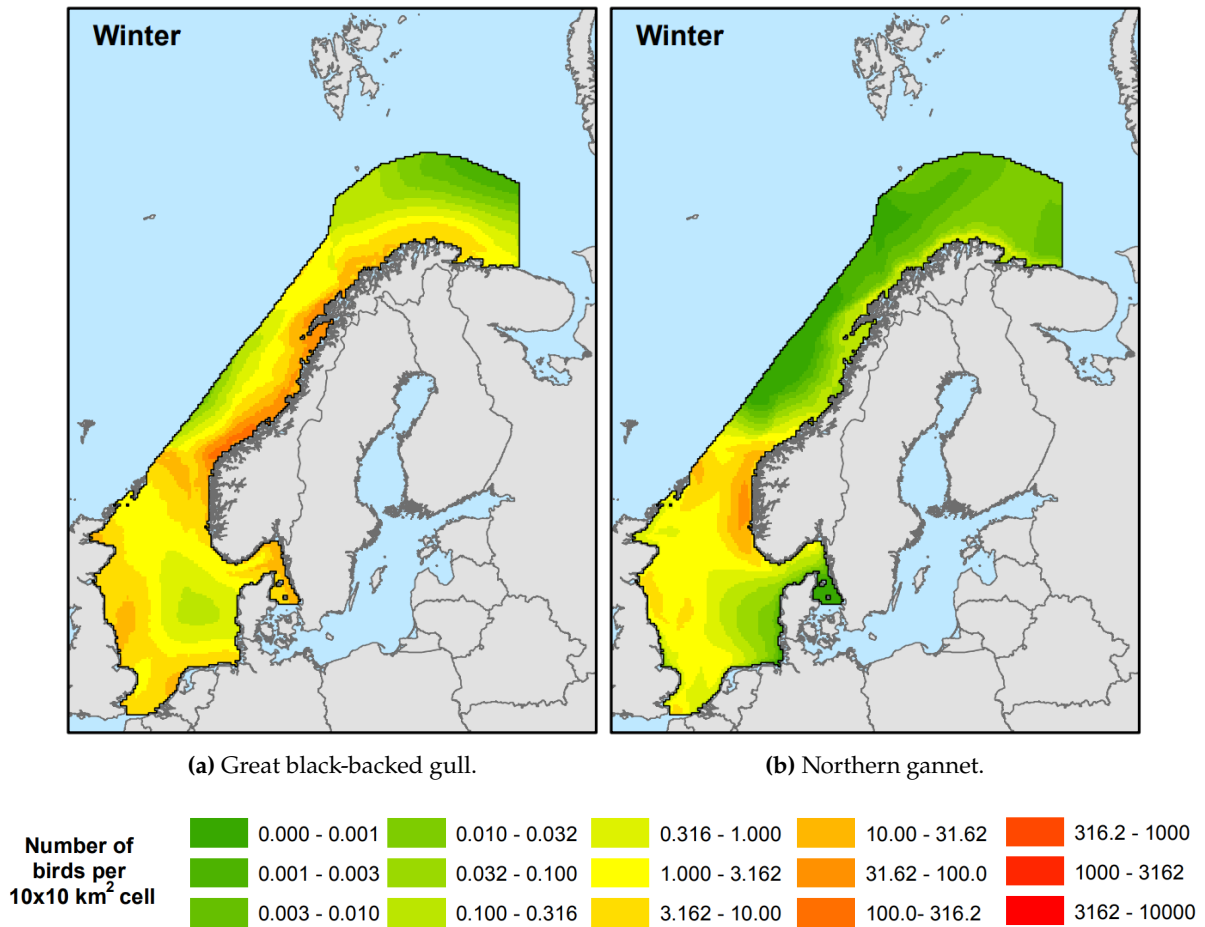


**Figure 2.3:** Density maps of two seabird species in the North- and Norwegian Sea (NINA, 2023).

Birds also interact with the North Sea through migratory routes and seasonal patterns. Typical species that migrate over the North Sea are: blackbirds, starlings, skylarks, various waders, thrushes, and robins, with documented routes including movements between the UK and mainland Europe (Bradarić et al., 2020). The abovementioned migratory birds are shown in Figure 2.4, which were retrieved from The Cornell Lab of Ornithology, 2024:



(a) Skylark



(b) Blackbird



(c) Starling



(d) Robin



(e) Bar-tailed godwit



(f) Red knot

**Figure 2.4:** Examples of migratory birds in the North Sea (The Cornell Lab of Ornithology, 2024).

The North Sea represents a significant crossroads for avian migration within the East-Atlantic flyway. It hosts several hundred million migratory birds of approximately 250 species annually, with a strong presence of nocturnal migrants. These migratory routes extend between Scandinavia and southern Europe, eastern Europe, and the UK (Bradarić et al., 2020). An illustration of estimated migration routes is shown in Figure 2.6. Additionally, the North Sea can act as an ecological barrier for birds during their migratory journeys, and seasonal differences in wind regimes can alter migratory dynamics, including routes, timing, and intensity of migration, especially when considering human structures at sea and the impact of such activities on avian species, which raises conservation concerns (Bradarić et al., 2020). These concerns are better understood when comparing Figures 2.5 and 2.6, which show that bird encounters with wind farms could be more likely to occur in the next 25 years.

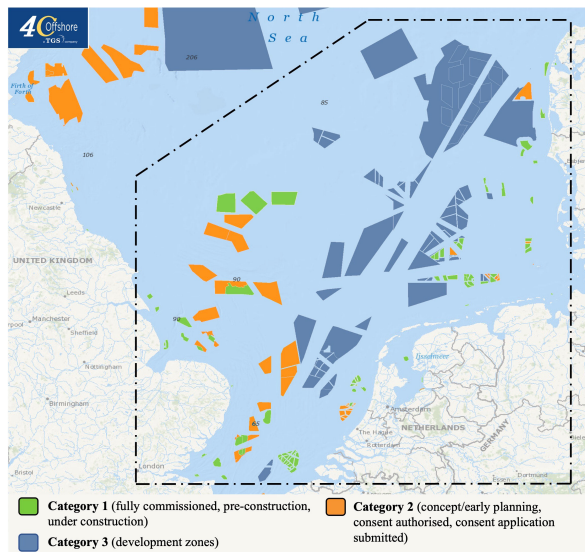


Figure 2.5: Offshore wind farm roadmap in the North Sea (Heinatz & Scheffold, 2023).

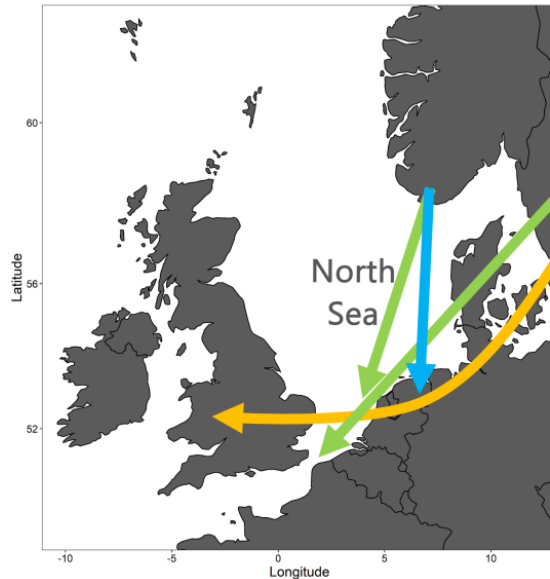


Figure 2.6: Estimated routes of seasonal bird migration (Bradaric, 2022).

## 2.3. Impact of Offshore Wind Farms on Avian Species

### Types of Impacts

In the context of disturbance of avian species by OWFs, literature differentiates between the following impacts (Cook et al., 2018):

1. **Collisions:** These mainly involve birds flying through wind farm areas, either while foraging or during seasonal migration, along the coast or over the North Sea.
2. **Avoidance & Attraction:** Species that tend to avoid wind farms, are displaced. As a result, these species lose a part of their habitat, which is why this effect is often called habitat loss. Other species are attracted to wind farms due to increased foraging and resting opportunities.
3. **Barrier effects:** Wind farms may interfere with essential routes for birds flying to their foraging areas at sea. Birds may be forced to go around the farms, which may lead to greater energy use, loss of foraging time and loss of condition.

Marine birds can be abundant in regions of OWFs and have flight characteristics (flight speed, height, manoeuvrability) that make them vulnerable to collision with turbine blades (Kelsey et al., 2018). Collision risk refers to the likelihood of birds colliding with specific structures or objects, such as offshore wind turbines or power lines. The concept of collision risk is commonly highlighted as a critical factor in understanding the potential effects of offshore wind turbines on marine bird populations (Cook et al., 2018). It involves estimating the probability of birds occupying the same space as the structures, scaling up the risk based on bird density and flight behaviours, and considering avoidance rates to quantify the overall risk of collision with these structures.

Next, observed behaviour of seabirds within offshore wind farms includes both avoidance and attraction effects. Avoidance refers to the behavioural responses of birds, particularly marine birds, to offshore wind farms, as outlined in Cook et al., 2018. It encompasses a spectrum of behaviours at different spatial and temporal scales. According to Cook et al., 2018, avoidance is categorised into:

- Macro-avoidance, which entails birds either taking action to avoid entering a wind farm or being attracted to it.

- Meso-avoidance, which involves the avoidance of individual turbines within a wind farm.
- Micro-avoidance, which represents a last-second action taken by birds to avoid colliding with the rotor blades of turbines.

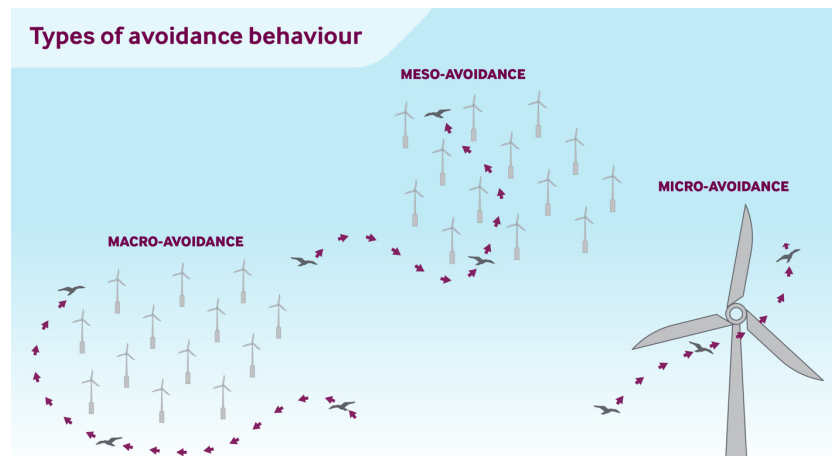


**Figure 2.7:** Illustration of macro-, meso- and micro-avoidance (KeyFactsEnergy, 2023).

These avoidance behaviours are integral to understanding the potential impacts of wind farms on avian populations in the context of displacement effects. Furthermore, avoidance behaviours are also related to collision risk, and thus essential for modelling collision risks (Cook et al., 2018). The impacts of displacement on marine birds vary depending on the location of the OWFs and the timing of the displacement. For example, during the breeding season, OWFs close to breeding colonies may exclude birds from important foraging areas or commuting corridors, potentially increasing the energetic costs of foraging for parents and reducing reproductive output (Vanermen et al., 2014). Additionally, the impacts of displacement can accumulate over time, and may be exacerbated for certain bird species with specific habitat requirements or migratory pathways that overlap with OWFs (Croll et al., 2022).

Attraction of seabirds to wind farms can be influenced by various factors. Specifically, seabirds, being top predators, exhibit a reliance on offshore areas for foraging, resting, and moulting (Peschko et al., 2021). Additionally, the construction and operation of wind farms may lead to the development of more artificial infrastructures within the marine ecosystem, which could have inadvertent attractions for certain species (Wang et al., 2023). However, the precise mechanisms and drivers underlying avian attraction to wind farms are complex and require further research to comprehensively understand these dynamics. Conversely, some seabirds, including lesser black-backed gulls and herring gulls, were observed to be attracted to the wind farm area, with their numbers increasing notably. It is noteworthy that the causes behind the observed attraction effects are not yet fully understood. Additionally, it is mentioned that offshore wind farms offer enhanced feeding opportunities to seabirds due to the turbulence in water caused by offshore structures, which mixes nutrients over the water column, which in turn attracts fish species. Exclusion of fishery activities results in increased food sources for seabirds as well (Dierschke et al., 2016). Understanding the behaviour of seabirds within offshore wind farms involves a complex interplay of habitat changes, hunting opportunities, and potential disturbances caused by the structures.

For certain bird species with specific migratory pathways, overlap with OWF areas exists (Croll et al., 2022). As discussed in Section 2.2, Figures 2.5 and 2.6 show this estimated overlap. Barrier effects, as related to bird interactions with offshore wind farms, refer to instances where the physical presence of wind farms causes birds to take extended flight journeys around the development during migration or when commuting between colonies and foraging areas (Cook et al., 2018). These effects involve avoiding the wind farm by means of flying around it, leading to extended flight paths for birds and potentially impacting their energy costs and foraging or resting habitats (Cook et al., 2018). Additionally, barrier effects are considered a type of evasive behaviour exhibited by birds, particularly during migration, and

can be impulsive or anticipatory, requiring early detection or prior experience (Cook et al., 2018).

### Impacts on Key Species

The presence of offshore wind turbines has led to significant avoidance (displacement) by certain species such as northern gannets, common guillemots, and razorbills, as indicated by (Vanermen et al., 2014). Ecological instances, like Waardenburg Ecology & IMARES, have already indicated that interaction between birds and wind turbines varies per species (Leopold et al., 2015). Leopold et al. have identified the following species as priority species, which are potentially affected by the cumulative impact of OWFs:

#### Seabirds

- Great black-backed gull *Larus marinus*
- Lesser black-backed gull *Larus fuscus*
- Herring gull *Larus argentatus*
- Little gull *Hydrocoloeus minutus*
- Black-legged kittiwake *Rissa tridactyla*
- Northern gannet *Morus bassanus*
- Great skua *Stercorarius skua*
- Arctic skua *Stercorarius parasiticus*
- Common tern *Sterna hirundo*
- Sandwich tern *Thalasseus sandvicensis*

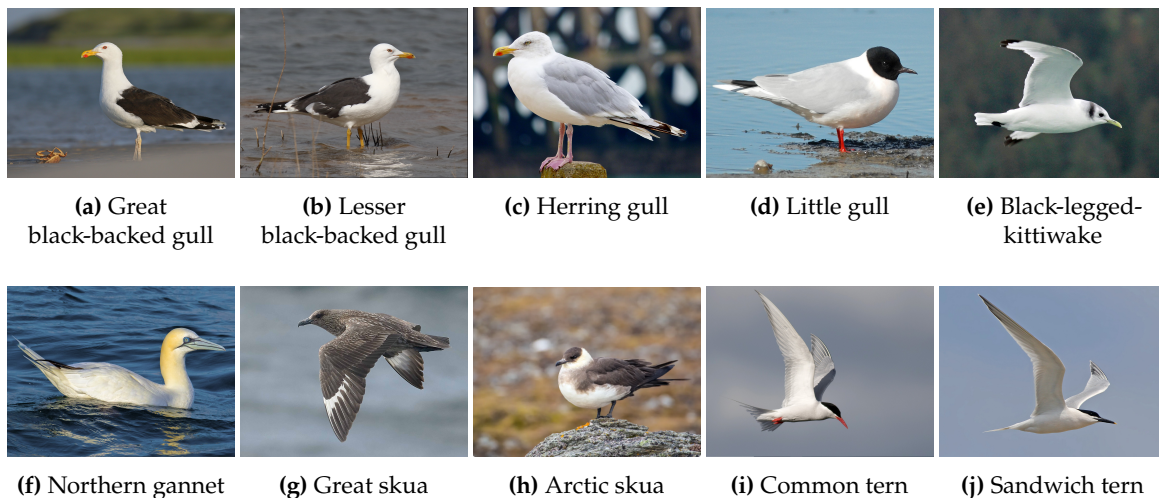


**Figure 2.8:** Most vulnerable seabird species (The Cornell Lab of Ornithology, 2024).

#### Migratory birds

- Brent goose *Branta bernicla*
- Common shelduck *Tadorna tadorna*
- Curlew *Numenius arquata*
- Red knot *Calidris canutus*
- Bar-tailed godwit *Limosa lapponica*
- Black tern *Chlidonias niger*
- Common starling *Sturnus vulgaris*

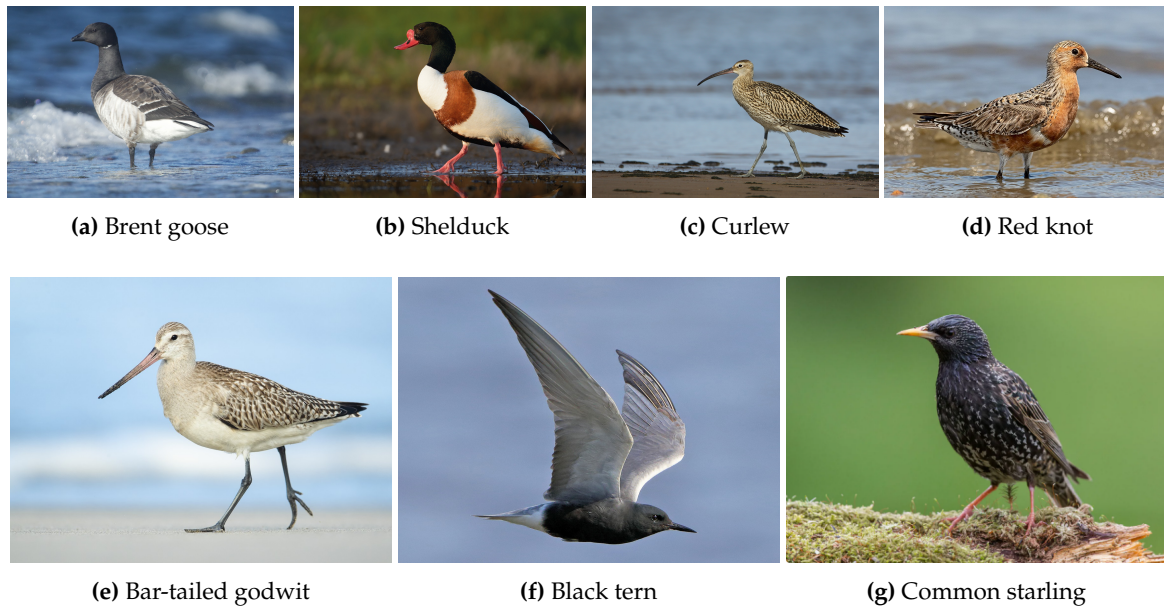


**Figure 2.9:** Most vulnerable migratory birds (The Cornell Lab of Ornithology, 2024).

Taking one of these priority seabird species as an example, the northern gannet, (Peschko et al., 2021) demonstrated that this species is indeed affected by OWFs. According to Peschko et al., gannets have been found to have their habitat overlapping with certain OWF sites, but also that they tend to avoid said wind farms, which is shown in Figure 2.10. For northern gannets, avoidance rates of entire wind farms (macro-avoidance) were estimated at 64%, and avoidance of individual turbines (micro-avoidance) at 99% (Rehfishch et al., 2014). It is interesting to address the sensitivity of avoidance rates in collision risk calculations. According to (SNH, 2010): "This is because although the difference between 99% and 99.98% may appear like a small difference in avoidance rate, it is of course a 50-fold change in the number of predicted collisions." More details on avoidance rates in the context of collision risk models are discussed in Section 2.5. Finally, one can also look at the variations in estimated fatalities between two seabird species. Estimations from Potiek et al. showed that there are significant differences between casualties of black-legged kittiwakes and northern gannets, as can be seen by comparing Figure 2.11 and Figure 2.12. Thus, even within priority species, it is important to look at contributing factors like species-specific density when doing environmental impact assessments (EIAs) of OWFs.

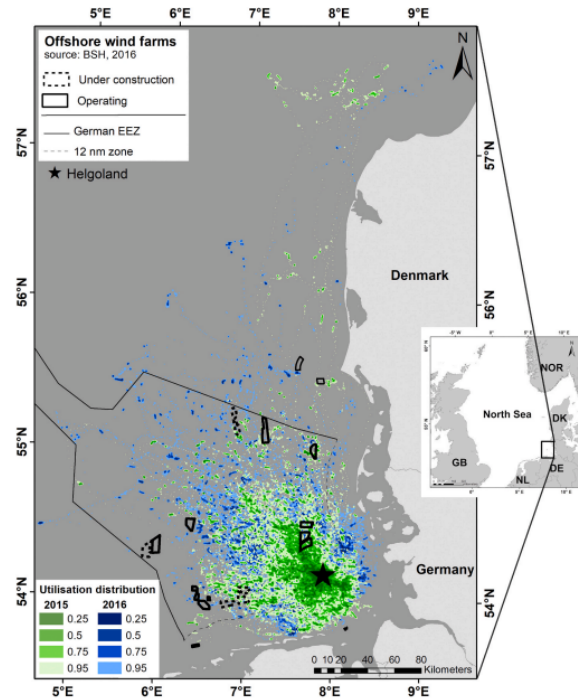


**Figure 2.10:** Kernel densities of northern gannets tagged in 2015 (green) and 2016 (blue). OWF status in 2016: dashed black line = under construction, solid black line = operating (Peschko et al., 2021).

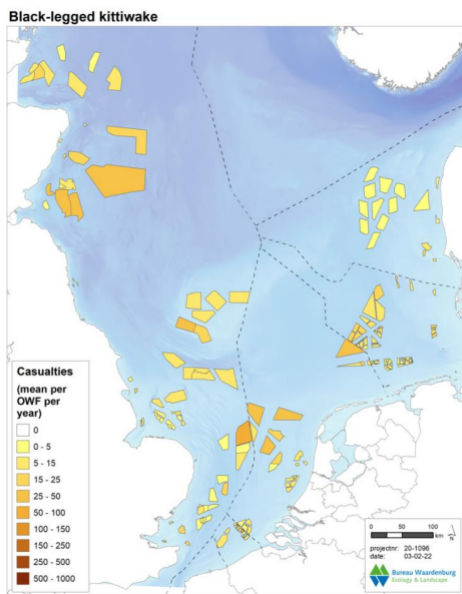


**Figure 2.11:** Estimated fatalities of black-legged kittiwake per OWF (Potiek et al., 2022).

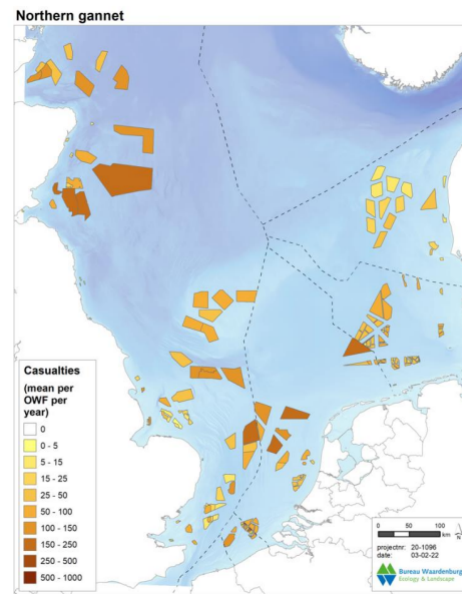


**Figure 2.12:** Estimated fatalities of northern gannets per OWF (Potiek et al., 2022).

## 2.4. Mitigation Measures

In relation to Section 2.3, existing measures to mitigate impacts either try to address collision risk, barrier effects, or habitat loss.

## Mitigating Collision Risk

In general, mitigating collision risk for birds in OWFs may be done either pre-construction or post-construction. A promising pre-construction measure is careful site selection. During the planning phase, an analysis can be made to estimate the collision risk of bird species that inhabit the selected site, and a decision can be made whether to proceed or look for a different site location (Leopold et al., 2015). Other proposed measures to reduce collisions are to adjust the OWF layout by either increasing the space between turbines (Buij et al., 2018), or to introduce so-called "corridors", which would allow safe passage for migratory birds (Leopold et al., 2015). However, according to ecology experts, it is still unknown whether these measures have any significant effect at all (Gyimesi, pers. comm., 27-06-2024) (Poot, pers. comm., 09-02-2024). Other pre-construction methods may be turbine-specific measures. Applying changes in blade colour (to increase visibility) or including acoustic deterrence are potentially effective measures as well (Marques et al., 2014). Furthermore, (Martin & Banks, 2023) propose painting the blades and tower with achromatic patterns. Changing the turbine hub height may also decrease exposure to collision hazards for certain species, depending on the species' flight altitude (May et al., 2015), although this should be considered in the turbine design stage.

Methods to reduce collision risk post-construction have also been the topic of several studies. First and foremost, curtailment is discussed as an effective method for reducing collision risk. Technologies such as radar or cameras can be installed to detect incoming birds in OWFs, which then signal wind turbines to initiate slow-downs or full stops. This can be done in many ways. Technologies like ROBIN Radar, DTBird, and MERLIN SCADA provide real-time measurement and can initiate wind turbine slow- or shutdowns in case risk of collision is high (Salkanović, 2023). Another technology based on active wind turbine control is called SKARV, which aims to avoid collisions by calculating a bird's flight trajectory and slowing down the rotor of a wind turbine (Garcia-Rosa & Tande, 2023). However, these instantaneous curtailment measures result in lower annual energy production (AEP), as well as imbalances in electricity grids. With the latter in mind, (Bradaric, 2022) proposed a better solution for OWF curtailment. The method developed by Bradaric aims to predict seasonal nocturnal bird migration based on weather conditions. It allowed for the prediction of peak migration nights above the North Sea, with an advance notice of two days. Calculations in this research show that collision risk can be minimised for 50% of migratory birds, at the cost of an energy loss of 0.56% in spring and 1.26% in autumn (Bradaric, 2022). However, it should be noted that these values for energy loss do not represent revenue loss, which depends on the actual market price of electricity. Peak migration tends to happen in milder weather conditions (Bradaric, 2022), which means lower wind speeds, which in turn means higher market prices—meaning the impact on revenue can be quite substantial for wind farm operators. As of now, Dutch OWFs at Borssele and Egmond aan Zee are participating in these seasonal curtailment procedures. A schematic for the procedure is shown in the figure below:

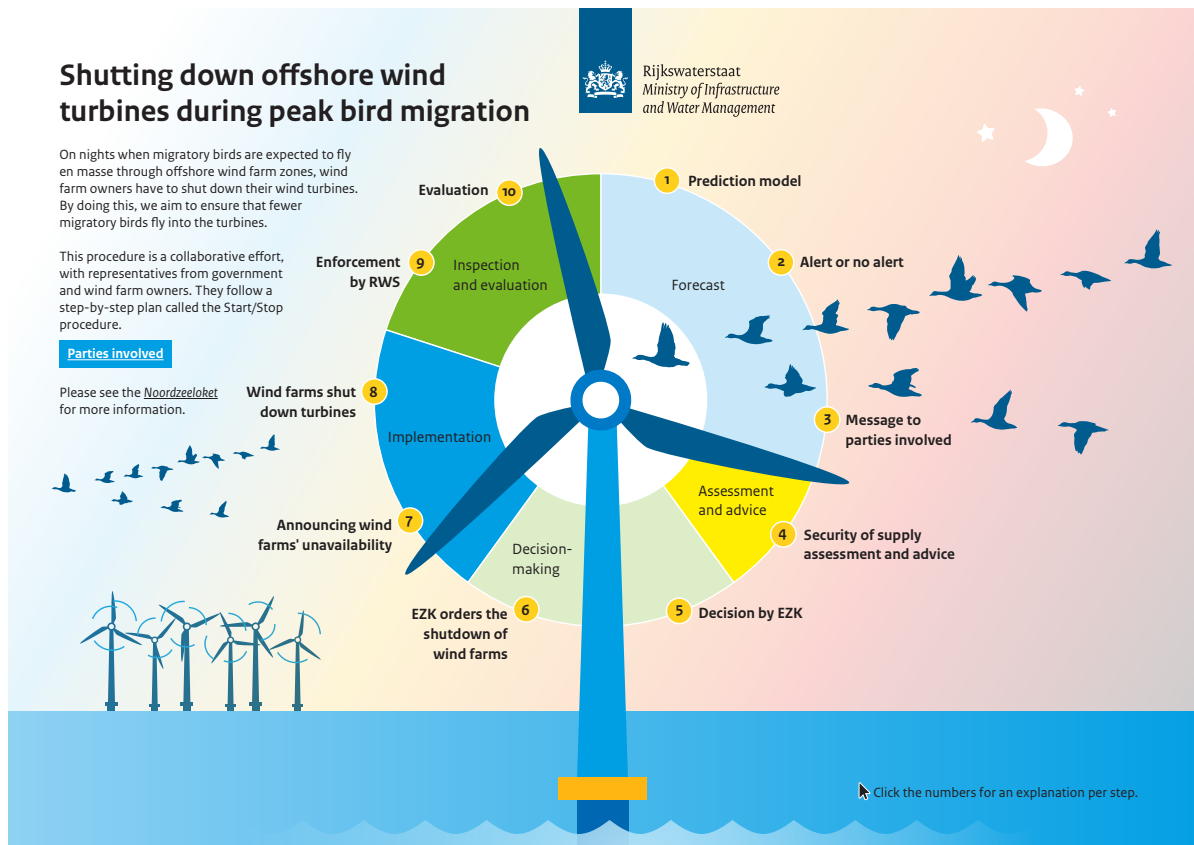


**Figure 2.13:** Illustration of shutting down procedure during peak bird migration (Rijkswaterstaat, 2022).

In summary, there are many more collision reduction measures proposed in the literature. In addition, the geographical distribution of birds varies significantly with the seasons (Peschko et al., 2020). An ecology expert pointed out that scheduling OWF maintenance so that turbines are not operating during the seasons with increased bird activity could reduce collision risk as well (Gyimesi, 27-06-2024). Some state-of-the-art solutions will also be addressed in the GROW pre-proposal, which is further elaborated in Chapter 4. It should be noted that, as of today, most proposed mitigation measures are based on unproven technologies. This can be explained by the fact that validating research through offshore observations is much more difficult than onshore. Additionally, calculations for collisions offshore are also based on models, and there have been very few actual collisions observed in OWFs, according to an ecology expert (Poot, 09-02-2024). This is important context, as mitigating collision risk inevitably impacts OWF development. When talking about reducing collisions in OWFs, this must always be related to electrical output and revenue.

### Mitigating Habitat Loss & Barrier Effects

Most methods to prevent habitat loss onshore, such as modifying vegetation around wind turbines (Parisé & Walker, 2017), cannot be applied offshore. Thus, (Croll et al., 2022) states that there is one main approach to mitigate habitat loss for marine birds due to offshore wind development. This is through careful site selection, which should take into account energy generation potential, human activities, and potential impacts on wildlife and ecosystems. Specifically, after a site has been selected as suitable for OWF development, an ecological analysis should be conducted, including the habitat use of vulnerable marine bird species (Johnston et al., 2014). In addition, (Croll et al., 2022) highlights that careful siting based on models can be improved upon by improving the models themselves. These models rely on empirical datasets of the species' geographical distribution (density) per season or per year. The accuracy of estimating species density can thus be improved with sea survey data or telemetry data (Krüger et al., 2018). Model validation to ensure predictive accuracy remains important, as was the

case for collision mitigation measures as well.

Reducing barrier effects is also possible by applying some of the aforementioned mitigation practices. Careful siting based on models can help predict if a site interferes with bird migration routes or obstructs the flight path towards foraging areas. Similarly, introducing corridors or flyways between wind farms is a promising but as yet unproven solution against barrier effects.

## 2.5. Monitoring and Impact Assessment Methods

### Monitoring Interactions with OWFs

The existing knowledge on avian species in the North Sea region is predominantly derived from sources such as bird ringing, bio-logging, visual observations, and radar studies, showcasing the diverse methodologies used to study avian migration behaviour. Furthermore, the increasing deployment of mobile radars and tracking studies of small migrants is expected to significantly benefit future research on the complex dynamics of migration around the North Sea (Bradarić et al., 2020). An example of such a system is the Motus Wildlife Tracking System (Birds Canada, 2024), which is a network of strategically placed radio antennas worldwide that track the migration movements of smaller migratory species equipped with radio transmitters.

Technologies for measuring avian biodiversity impacts in the wind industry have come a long way, but there is still much to be improved. To this day, human observation of birds appearing near or colliding with wind farms remains a common method for gathering data. Still, this method is logistically challenging to use offshore. Visual censuses from research vessels aimed at estimating local seabird densities and species-specific flight altitudes can be conducted. While this method provides a high taxonomic resolution, it is restricted to daylight and good weather conditions only (Brabant et al., 2015). Next, radar technologies provide information on movements of birds, such as their trajectory and altitude, but these do not allow for species identification. To address this, systems like MUSE (Tjørnløv et al., 2021) combine radars with regular and thermal cameras to enable nocturnal species detection. Still, filtration methods are limited in the dynamic conditions at sea, meaning that not all birds are detected correctly (Tjørnløv et al., 2021). Therefore, data on bird interactions with OWFs is limited, requiring models to assess environmental impacts.

### Environmental Impact Assessment through Models

With limited data on flight behaviour and migration patterns, predictions on the effects of OWFs on seabird population scale are done with models. At their core, these cumulative impact assessments rely heavily on collision risk models (CRMs). Most CRMs calculate the probability of a bird colliding with a wind turbine blade. This collision risk to an individual bird is scaled up based on the number of birds likely to pass through a wind farm (the flux) over a given time period (Cook et al., 2018). A study by Brabant et al., 2015, showed methods to estimate the cumulative impacts on seabirds and migratory birds of Belgian OWFs. In summary, the following 3 step procedure was used, which is also illustrated by Figure 2.14:

#### 1. Data collection:

This step involves two types of data collection techniques: visual counts and radar observations. Visual censuses from research vessels were used to estimate local seabird densities and species-specific flight altitudes. Radar research complemented the visual census data with continuous observations of the flux of birds. The radar system used for this purpose consists of two identical solid state S-band radar antennas, one scanning in the horizontal plane and the other in the vertical plane. These observations provided data on the flux of birds through the area and flight altitudes, assisting in the evaluation of collision risk. These methods allowed the researchers to gather vital information for the subsequent step of collision modelling.

#### 2. Collision risk modelling:

This step involved estimating the bird collision risk based on technical turbine specifications, the number of turbines, and bird-related parameters. A theoretical collision risk model (CRM) was used to estimate bird collision risks, which takes into account various factors such as bird densities, species-specific flight altitudes, and avoidance rates to determine the potential risk of bird collisions with the wind turbines. The output of this CRM is an estimate of the number of collisions for the specified local seabird species and migrating songbird species.

### 3. Extrapolation and impact on population level:

Then, the study extrapolated the CRM results obtained for a specific offshore wind farm (OWF) to estimate the potential number of collisions per turbine per year and scaled it to the expected number of turbines constructed in the study area, considering future wind farm development scenarios. After the extrapolation, the known population size of the bird species at risk and their yearly adult mortality rate were taken into account to estimate the additional mortality resulting from collision fatalities.

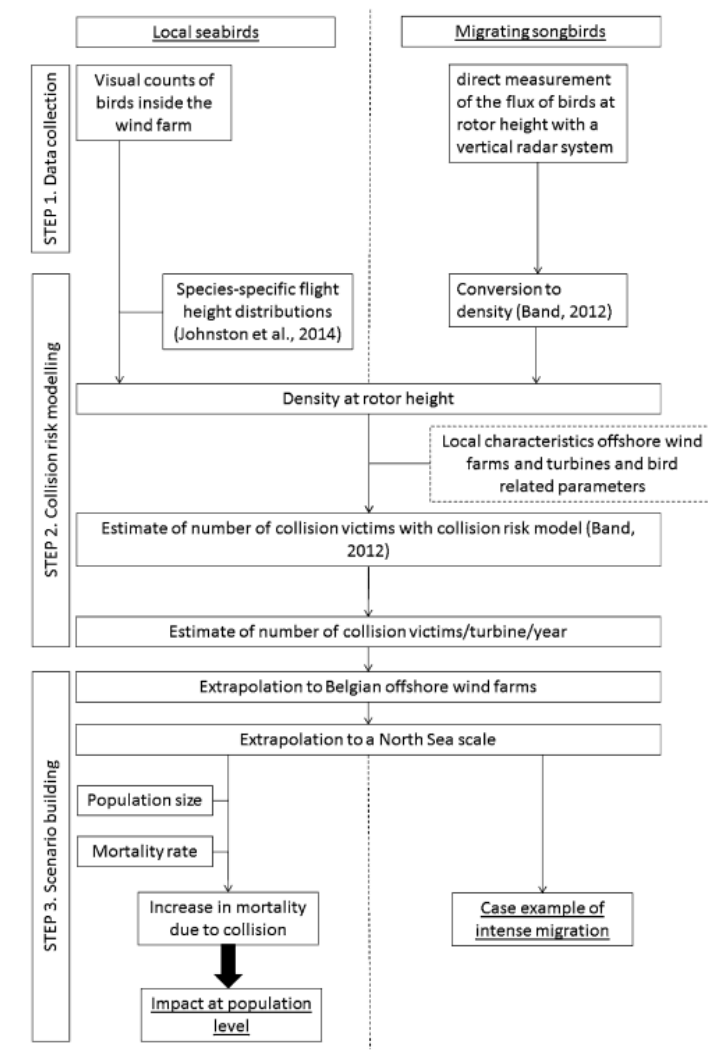


**Figure 2.14:** Example of a structured analysis for bird population impact assessment (Brabant et al., 2015).

It's important to note that the extrapolation and impact assessment are based on theoretical models and carry inherent uncertainties, acknowledging the need for species-specific demographic data and age-specific mortality values to provide more accurate assessments at the population level (Brabant et al., 2015).

As stated by Brabant et al., 2015, the CRM used is the Band model. Up until now, this model is most commonly used for collision impact assessments within offshore wind farms, and is treated in more detail in Chapter 3. In short, the Band model applies the following steps (Band, 2012):

1. **Stage A:** Assemble data on the number of flights that are potentially at risk from wind farm turbines, in the absence of bird displacement or attraction to the wind farm.
2. **Stage B:** Use flight activity data to estimate the potential number of bird transits through the rotors of the wind farm.
3. **Stage C:** Calculate the probability of collision during a single bird rotor transit.
4. **Stage D:** Multiply the results from Stages A, B, and C to yield the potential collision mortality rate for the bird species in question, factoring in the proportion of time that turbines are not operational and assuming current bird use of the site with no avoiding action taken.
5. **Stage E:** Allow for the proportion of birds likely to avoid the wind farm or its turbines, either through displacement or evasive action, and account for any attraction by birds to the wind farm in response to changing habitats.
6. **Stage F:** Express the uncertainty surrounding the collision risk estimate.

It should be noted that limitations of the Band model are:

1. **Uncertainties and Variabilities:** The model involves a large number of sources of variability and uncertainties, including variability in survey data, natural variability in bird populations, uncertain bird avoidance behaviour at sea, and uncertainties in using the collision model itself.
2. **Survey Data Limitations:** Data used in the model is often sampled in time and space and exhibits a high degree of variability, and survey data may be unavailable for certain conditions, such as night-time and storm conditions.
3. **Assumptions and Simplifications:** The model uses simplified geometry for turbine blades and bird shape, assumes a single bird speed, and does not include any risk of collision with turbine towers. Additionally, there may be limited availability of detailed blade dimension and pitch information. Pitch also depends on the control strategy of the turbine, which makes it difficult to include in the model. Finally, yaw angle of the turbine is excluded as well.
4. **Limited Knowledge of Bird Behaviour:** The model's reliance on bird avoidance behaviour as well as bird response to habitat changes caused by wind farms introduces significant uncertainties due to limited experience and knowledge in predicting these behaviours.

Finally, it should be noted that there are more approaches to defining environmental impacts of OWFs on birds. For example, another approach is to model impact assessments through avoidance & attraction. As of now, there have been attempts to model the attraction of birds at wind farm sites. (Salkanović, 2023) discusses the correlations between bird activity at wind farm sites, and features like water bodies and crops, which can cause attraction. (Salkanović, 2023) aimed to address this matter by linking bird activity measurements to location-specific inputs, such as crops.

## 2.6. Regulatory Framework and Policies

It is also important to understand the current legal perspective on this topic from at least one governmental institution, as this translates directly to the planned research and avian safety management measures taken. The effectiveness of current regulatory approaches related to biodiversity conservation, especially for bird species in the context of offshore wind energy development, is a complex and multifaceted issue. In the context provided, (Croll et al., 2022) outlines a framework for assessing and mitigating the impacts of offshore wind energy development on marine birds. The authors present a framework that addresses impacts within the context of multiple stressors across multiple wind energy developments, along with proposing technological and methodological approaches to improve impact estimation and mitigation, which is shown in Figure 2.15. However, the document focuses more on presenting a framework for addressing impacts rather than directly assessing the effectiveness of current regulatory approaches.

On the other hand, (Spijkerboer et al., 2020) details the regulatory mechanisms implemented in the Dutch North Sea for offshore wind energy development. It describes the Round III system, in which the government took control of the development of offshore wind energy in space and time by allowing offshore wind farm (OWF) development only within designated 'wind energy areas' appointed by the national government. The Offshore Wind Energy Act of 2015 introduced the instrument of the plot-decision, where the government determines the coordinates of plots for OWFs within wind energy areas, incorporating provisions to reduce environmental impact, impact on the coast, and coordination with other users.

While the regulatory approaches outlined in (Spijkerboer et al., 2020) represent targeted efforts to govern offshore wind energy development, the effectiveness of these approaches in ensuring biodiversity conservation, specifically for bird species, requires further evaluation. The integration of these regulatory measures with the framework proposed in (Croll et al., 2022) could enhance the assessment and mitigation of impacts on bird species within offshore wind energy development. This framework is further discussed in Section 2.7.

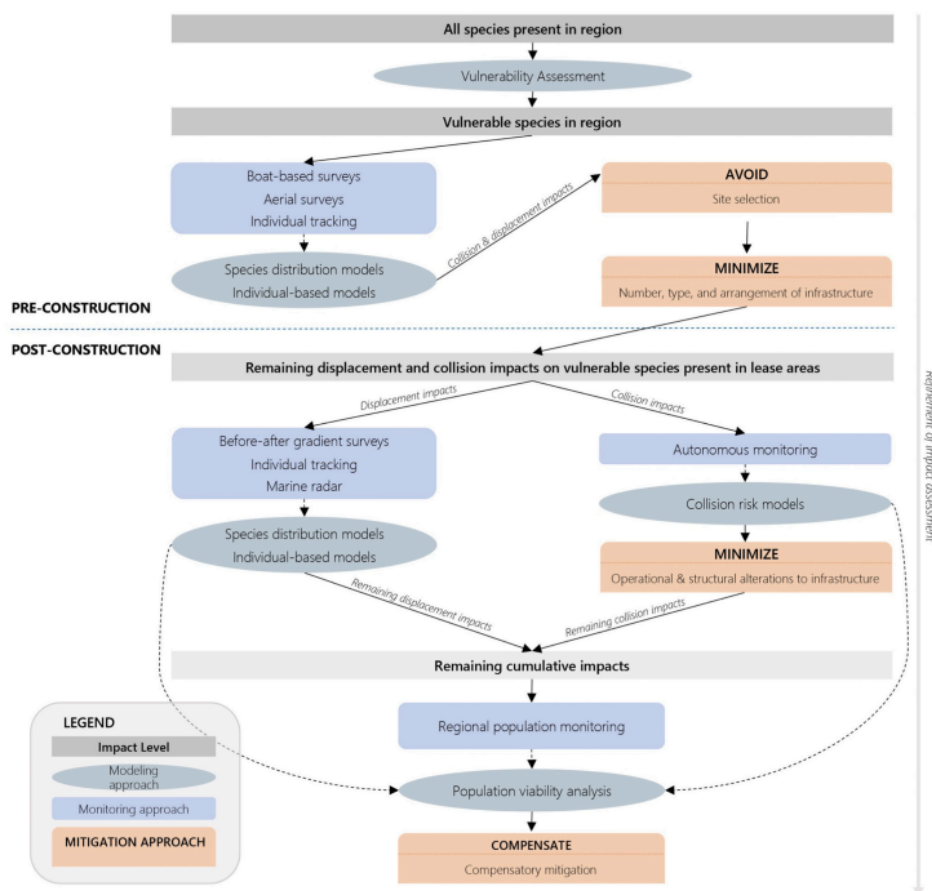


Figure 2.15: Framework for estimating cumulative impacts (Croll et al., 2022).

### Policy in the Netherlands

Finally, the KEC 4.0 report (Potiek et al., 2022) gives some detail on the policy in the Netherlands regarding birds and wind farms.

The assessment of impacts is done by comparing the outcome of the population models with the species-specific Acceptable Levels of Impact, as defined by the Ministry of Agriculture, Nature and Food Quality, which is explained as follows: "For each species, a threshold is defined for the maximally acceptable decline due to wind farms (X) as well as for the maximally acceptable level of causality (PT) (Potiek et al. 2021). Depending on the IUCN status, the threshold value for X is either defined as a

maximally 30% or 15% decline over three generations or 10 years (whichever is longer) as a result of the impact due to wind farms, compared to the population size over the same time span without additional mortality." It is also noteworthy that these threshold values are determined per species. The idea behind the threshold is that each species has a different reproductive rate. In the context of wind turbines, models calculate acceptable levels of surviving number of birds per species. Populations of species with low reproductive rates are therefore more vulnerable to collisions with wind turbines.

Furthermore, there is a measure of accepted level of causality PT, that stands for the maximum acceptable probability of the violation of the above mentioned threshold being due to impacts of wind turbines as opposed to uncertainty in population models. To illustrate (Potiek et al., 2022): "This value for PT can either be 0.5, indicating that maximally 50% of the violations of the X threshold may be due to the impact of wind farms, or 0.1, indicating that maximally 10% of the violations of the X threshold may be caused by wind farms. This means that the threshold of 0.1 is stricter and is violated at a lower impact than the threshold of 0.5."

## 2.7. Research Gaps and Future Directions

In the context of offshore wind farms, there are still many key knowledge gaps in avian conservation. Ecology institutions like Waardenburg Ecology agree with studies stating that the evidence base for assessing collision risk and avoidance behaviour in seabirds is extremely limited (Cook et al., 2018). This limited evidence base directly impacts the precision and reliability of models used to predict collision risk and assess the potential impact of offshore wind farms on avian populations. Further, there are gaps in understanding species-specific responses to wind turbines and how different species adjust their flight paths to avoid collision (Cook et al., 2018). (Bradaric, 2022) found that some migratory birds tend to fly at higher altitudes (+300 m) during some nights of seasonal migration. In addition, this data was collected within offshore wind farms through radars, which is a step up compared to other studies. Still, Bradaric stated that collecting data offshore remains a challenge, due to reflection from waves, harsh rain and strong winds, which can cause radar data to deteriorate. This particularly affected the ability for species-specific identification. Additionally, the influence of offshore wind farms on the behaviour, distribution, and flight heights of seabirds remains an important knowledge gap as well (Cook et al., 2018). These gaps highlight the need for further research to enhance our understanding of the interactions between birds and offshore wind farms as well as the development of robust mitigation measures. Work package 3.1 from GROW's EcoWindToolbox proposal also aims to address this matter.

As for future directions, the focus of future research should be on addressing knowledge gaps in avian avoidance of offshore wind turbines, especially considering differing flight behaviour between onshore and offshore environments (Cook et al., 2018). Furthermore, (Searle et al., 2023) had some concrete suggestions:

- 1. Enhance Quantification of Uncertainty in Ornithological Offshore Wind Energy Assessments:** This should be done through enhancing the precision of estimates and reducing uncertainty through methods such as statistical modelling, improved data collection, or adaptations to the assessment process. By addressing uncertainties in ornithological offshore wind energy assessments, evidence-based decision-making is supported. This could involve funding large-scale studies facilitated through international research collaboration to enhance the quantification of uncertainty in models and data.
- 2. Address End-to-End Uncertainty:** The focus should be on both characterising uncertainty within individual tools and quantifying the propagated uncertainty within the framework, especially when multiple tools are linked together. This is termed end-to-end uncertainty. This can be done by utilising a framework for end-to-end quantification of uncertainty. A comprehensive framework that integrates uncertainty estimates from individual stages of the assessment process should be constructed for general applications in the OWF industry. As a first step, Figure 2.16 shows the different types of uncertainties as identified by Searle et al., 2023. In addition, Figure 2.17 shows a snippet of a research priorities table, which highlights the research gaps that influence uncertainty in OWF impact assessments on avian species.

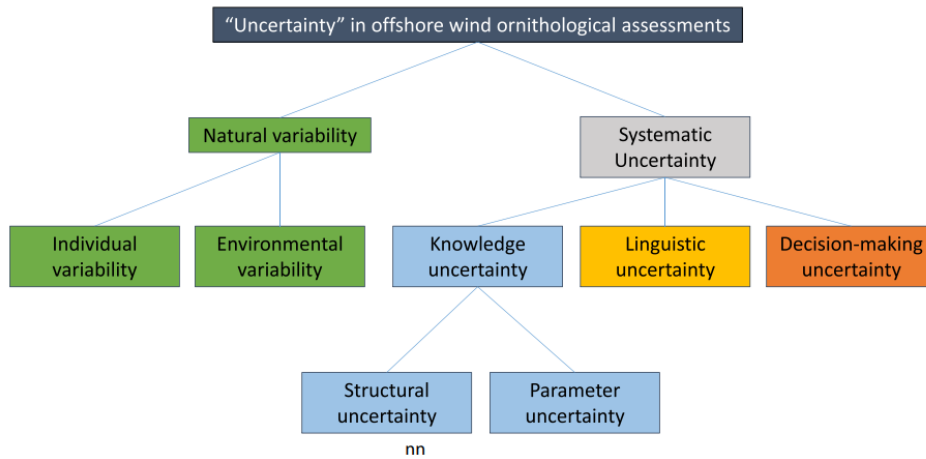


Figure 2.16: Types of uncertainties in OWF impacts on avian species (Searle et al., 2023).

Research priorities and relevant stage of assessment		Contribution to quantifying uncertainty	Contribution to reducing knowledge uncertainty
1	Data integration from different sources and seasons for better knowledge of year-round distributions to quantify and reduce uncertainty <i>Spatial distributions and apportioning</i>	High	High
2	Improving uncertainty quantification in movement models <i>Spatial distributions and apportioning</i>	High	Medium
3	Better understanding and quantification of year-round distributions and impacts of displacement to quantify and reduce uncertainty <i>Spatial distributions, displacement, and apportioning</i>	Medium	High
4	Better understanding and quantification of predator–prey interactions, relationship between prey density and availability, impacts of ORDs on prey distributions and availability to quantify and reduce uncertainty <i>Spatial distributions, displacement, and collision</i>	High	High
5	Estimate link between displacement effects and changes in demographic rates (productivity and survival) to better quantify and reduce uncertainty <i>Spatial distributions, displacement, and apportioning</i>	High	High
6	Effects of displacement on different age classes, e.g. immatures and non-breeders to better quantify and reduce knowledge uncertainty <i>Displacement</i>	Medium	Medium
7	Improve uncertainty quantification within IBMs to better characterize and reduce structural and parameter uncertainty <i>Displacement and collision</i>	High	Medium
8	Assess sensitivity of collision risk model outputs to variation in input and structural parameters; understand and quantify covariance between parameters used in collision risk models to better quantify and reduce structural and parameter uncertainty <i>Collision</i>	Medium	Medium
9	Improve estimates of flight speed and height for species to better characterize and reduce parameter uncertainty, quantify influence of environmental conditions to better characterize natural variability, and understand how variation in flight speed and flight height is related to behaviour (e.g. commuting versus foraging) to reduce knowledge uncertainty <i>Collision</i>	Medium	Medium
10	Improve estimates of avoidance rates and partitioned into micro-, meso-, and macro-avoidance to better quantify and reduce structural and parameter uncertainty; improve understanding of the influence of environmental conditions on avoidance to better characterize natural variability; improve understanding of the contribution of model error to predicted collision rates and the implications of this for estimates of avoidance rates	High	High

Figure 2.17: List of research priorities to be addressed in order to reduce uncertainties in OWF impact assessments (Searle et al., 2023).

Additionally, (Spijkerboer et al., 2020) suggested strategic marine spatial planning. The study called for improving the coordination of sea-uses, particularly in the context of offshore wind energy, through policy development and research. Policymakers should establish a strategic and integrated governance framework, which may involve a more systematic approach to guide new and existing sea-uses. They should pay specific attention to the potential cumulative effects of these uses on the environment.

Finally, the author sees potential in the utilisation of AI applications for bird collision assessments and mitigation strategies. AI can contribute to bird collision risk assessments by analysing radar and acoustic data to enhance the understanding of bird flight patterns and collision risks (May et al., 2015). AI technologies, such as machine learning algorithms, can be employed to process large volumes of flight behaviour data to identify patterns and potential collision hot-spots (Choi et al., 2020). Additionally, AI-enabled predictive modelling can assist in forecasting collision risks based on bird behaviour, turbine

---

characteristics, and environmental factors (May et al., 2015). AI solutions also hold potential for developing real-time collision risk mitigation systems by integrating data from various sensors and environmental parameters to trigger deterrent measures when high collision risks are identified (May et al., 2015).

# 3

## State-of-the-Art methods for Collision Risk Modelling

This chapter aims to address the research question: What are the current state-of-the-art methods for modelling seabird collision risk in offshore wind farms? In this chapter, the collision risk of seabirds interacting with North Sea Offshore Wind Farms (OWFs), employing collision risk modelling as a crucial tool, is investigated. As detailed in Chapter 2, collision risk models (CRMs) play a vital role in estimating the impact of wind turbines on avian species, particularly in cases where monitoring locations are inaccessible. Section 3.1 provides an overview of the general principles underlying CRMs and their reliance on calculating collision risk based on the probability of a turbine blade intersecting with a bird in flight. Section 3.2 focuses on the Band model, a widely used CRM, outlining its methodology, assumptions, limitations, and sensitivities. In Section 3.3, an improved version of the Band model, incorporating Monte Carlo simulations to address uncertainties, is discussed.

### 3.1. Collision Risk Modelling

As mentioned in Chapter 4, the aim of this research is to look into collision risk of seabirds interacting with North Sea OWFs. For many years, this has been done with collision risk models. Collision risk modelling is an important tool used in estimating effects of wind turbines on avian species. This is because collision risk may need to be estimated prior to construction as information for planning. In addition, collision risk modelling is mainly used when wind farm locations are inaccessible for monitoring (A. Cook & Collier, 2015), which is the case for offshore wind farms.

Most collision risk models (CRMs) work in the following manner. All CRMs essentially calculate the collision risk based on the probability of a turbine blade occupying the same space as a bird in flight. The number of collisions is then calculated by (A. Cook & Collier, 2015):

$$\text{number of birds} \times \text{collision risk} = \text{number of collisions} \quad (3.1)$$

where the number of birds is the number of birds flying through the rotor swept area, which is often called the flux. Furthermore, the number of collisions is usually a single output value (A. Cook & Collier, 2015). This calculation reveals the weakness of most CRMs, which lies in the assumption of the amount of birds flying through the rotor swept area of wind turbines. From a total amount of birds flying in an OWF area, a constant flux of birds flying through is assumed. Most CRMs take into account that birds can take evasive action to fly around the rotor swept area. This is also referred to as avoidance, which was discussed in Section 2.3. In addition, evasive behaviour depends on the species and even on the individual, which makes accurately estimating the number of collisions through CRMs an even more difficult task. Thus, by focusing future research on gaining more knowledge about species-specific avoidance behaviour, current CRMs could be improved. Figure 3.1 shows a comparison of some CRMs,

including key characteristics of each model. It should be noted that advancements have been made in the field of CRMs up until now, as there are many more CRMs than shown in Figure 3.1. Specifically, researchers tend to develop their own version based on an older CRM that is applied in a more general sense. This way, situation-specific CRMs are developed when necessary. For now, the next sections will explain two selected CRMs that may be of use during this research.

Model name and reference	Based on...	Number of turbines	Tower included	Wind speed/direction included	Oblique angles of approach	Individual or population	Onshore or offshore example	Stochastic or deterministic	Model output
Band (Band 2000; Band 2012)	-	Multiple	N	N	N	Population	Offshore	D	# birds colliding
Tucker (1996)	-	Single	N	N	N	Individual	-	D	Probability of collision
Biosis (Smales <i>et al.</i> 2013)	-	Multiple	Y	N	Y	Population	Onshore	D	# birds colliding
Podolsky (Podolsky 2008)	-	Multiple	Y	N	Y	Individual	Onshore	D	Probability of collision
McAdam (McAdam 2005)	Band	Single	N	Speed & direction	Y	Individual	Offshore	S	Probability of collision
Desholm (Desholm & Kahlert 2007)	-	Multiple	N	Direction	N	Population	Offshore	S	# birds colliding
Eichhorn (Eichhorn <i>et al.</i> 2012)	Band	Single	N	N	N	Individual	Onshore	S	Mortality rate
Holmstrom (Holmstrom <i>et al.</i> 2011)	Tucker	Single	N	Speed & direction	Y	Individual	-	D	Probability of collision
Bolker (Bolker, Hatch & Zara 2014)	-	Multiple	N	N	Y	Individual	Onshore	D	Probability of collision
USFWS (U.S. Fish and Wildlife Service 2013)	-	Multiple	Not specified	N	N	Population	Onshore	S	Number of fatalities

**Figure 3.1:** Comparison of collision risk models (A. Cook & Collier, 2015).

It is noteworthy that Waardenburg Ecology still used the same method for estimating collision numbers as described in Equation 3.1 in the KEC 4.0 report (Potiek *et al.*, 2022). This report gives the most up-to-date cumulative impact assessment of collisions with existing and planned offshore wind turbines in the southern North Sea, for key seabird and migratory species. More specifically, a stochastic collision risk model (sCRM) was used based on the 2012 Band model. In short, the approach used in KEC 4.0 is as follows (Potiek *et al.*, 2022):

"The sCRM requires several input parameters related to the characteristics of the bird species and the wind turbines to calculate the theoretical collision risk of each species per type of wind turbine. The calculated species-specific collision risk is then multiplied by the species-specific bird flux through the total rotor-swept area of each wind farm and adjusted for the species-specific avoidance behaviour. The estimated number of collision victims per wind farm and per bird species is subsequently calculated for each month."

In addition, the sCRM used also gives standard deviation values for the outputted collision numbers, to illustrate uncertainty in the calculations. The estimations for collision numbers are based on the species-specific flight height distribution, which has been calculated through standard models (Johnston *et al.*, 2014). These standards are updated with GPS-loggers whenever new data is available (Gyimesi, 29-06-2024). This also indicates the effect that current knowledge gaps have on accurately estimating cumulative impacts. Finally, experts from Waardenburg Ecology stated in their interview that this model is the state-of-the-art method for offshore collision calculations (Waardenburg Ecology, pers. comm., 29-01-2024). Therefore, this model will also be used for the collision risk calculations done in Chapter 6. The 2012 Band model is described in more detail in Section 3.2.

## 3.2. Band Model

### Summary of Method

As can be seen in the figure above, a few CRMs are based on the Band collision risk model. The Band model was covered in some detail in Chapter 2. (Band, 2012) improved on the previously developed onshore CRM (Band, 2000), to allow for application in the offshore environment. According to Band, 2012, the model is applicable offshore in the following context:

"The methods used to gather and present information on flight activity, given that direct observations of birds from key vantage points are not usually possible in the marine environment."

Like most CRMs, this model is based on the probability of a bird occupying the same space as a turbine blade, during the time it takes for the bird to pass the rotor swept volume of the turbine. The collision probability relies on bird specifications, like wing span, body length, flight speed flight height and nocturnal flight behaviour.

When talking about the Band model, it should be noted that there are various versions. The basic Band model estimates the number of collisions per year based on:

- i The number of birds flying through the rotor.
- ii The probability of collision with a rotor from a single transit.

This probability of collision is then estimated at fixed intervals along the rotor blade, which is then averaged over the rotor swept area. In addition, the offshore iteration of this model included the use of boat survey data. The first version of this model also included avoidance behaviour, taking into account that a proportion of birds avoid collision (Band, 2012).

### Assumptions & Limitations

The Band model uses several assumptions. What is included in these assumptions directly relates to the limitations of the model. The following **key assumptions** apply when using the Band model (E. A. Masden & Cook, 2016):

- The bird is assumed to have a cruciform shape (see Figure 3.2).
- The turbine blade is assumed to have a width (chord) and a pitch angle but no thickness.
- Only flights parallel to the wind are considered i.e. perpendicular to the rotation plane of the turbine.
- The effects of birds approaching the turbine at oblique angles are assumed to cancel each other out, although this may underestimate collision risk.
- Stationary elements like the turbine tower are excluded.
- Uniform distribution of birds along the rotor swept area (see Figure 3.3).
- Input information about the bird includes wing span, body length, flight speed, flight height, and nocturnal flight activity.
- Input information about the turbine includes blade width, blade length, blade pitch, rotor speed, hub height, and operational time.

The above mentioned assumptions highlight the limitations of the Band model. One notable limitation is the model's simplification of bird representation, assuming a cruciform shape, which may lead to an underestimation of collision risk as real birds are larger and more complex, since the cruciform shape has no thickness (2D representation). Additionally, the model assumes that all flights are perpendicular to the turbine axis, neglecting oblique flight paths, particularly near seabird breeding colonies.

The model's assumption that oblique angles cancel out may also not hold in specific scenarios, potentially impacting the accuracy of risk estimates. To elaborate further on this assumption (Band, 2012):

"A bird approaching a turbine at an oblique angle is exposed both to a reduced probability of flying through the rotor, because the rotor presents an elliptical rather than circular cross-section, and an increased risk of collision if it does so. The model adopted for use here assumes that these two factors exactly offset each other, such that all bird transits can be treated as if making perpendicular approach to the rotor."

(Band, 2012) states that this simplification may lead to as much as 10% less collisions estimated for large birds.

Another limitation lies in the model's exclusion of collisions with stationary components, as it primarily considers the moving rotor. Including stationary elements, like the turbine tower, may be essential for accurate risk assessments.

Furthermore, there are three main turbine related inputs: the rotor blades, rotational speed and blade pitch. Each of these inputs is used in the calculations as described by (Band, 2012) as follows:

- **Rotor blades:** "Rotor blades are assumed to be laminar (i.e. with zero blade thickness) but they have length, a chord width which varies along the length of the blade tapering towards the tip, and a pitch angle (the angle between the blade and the rotor plane) which also varies along the length of the blade."
- **Rotational speed:** "Collision risk should be evaluated using the turbine rotational speed for an operating turbine. Where turbines operate with a range of rotational speeds, the calculation should be done using a mean operational turbine speed. The mean used should be a mean over time, using an analysis of wind data to enable the likely frequency distribution of turbine speeds to be determined."
- **Blade pitch:** "The blade also has a pitch angle – the angle between the blade surface and the axis of the rotor. Pitch angle varies along the length of the blade, from a high angle close to the hub, to a low pitch angle towards the blade tips, ie the blade is twisted. Pitch angle also varies as the pitch is controlled to alter the rotation speed of the turbine. In the model, an average angle is used, representing an average pitch along the blade length. 25-30 degrees is reasonable for a typical large turbine."

Note that in case a frequency distribution cannot be determined, the rated rotor speed is used, which will result in the collision estimate being an upper bound rather than a mean. For the pitch angle, a mean value is assumed, while this tends to vary with control strategy and along the blade. (Band, 2012) stated that the pitch therefore contributes towards uncertainty in the collision estimate, due to the pitch being complex to implement extensively in the calculations, as well as lack of data from manufacturers.

Finally, the deterministic nature of the Band model provides fixed collision risk estimates without comprehensive consideration of data or parameter uncertainty. Estimates should thus be considered indicative rather than absolute due to the inherent limitations and assumptions within this collision risk model.

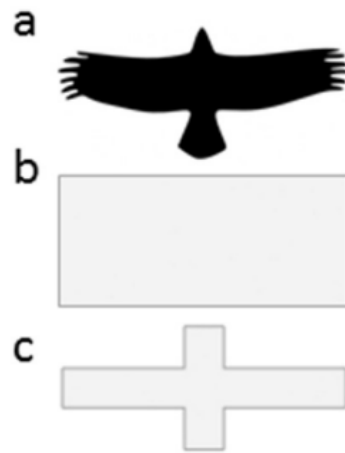


**Figure 3.2:** Cruciform bird shape assumption, where *a* shows the actual bird, and *c* shows the assumed bird shape by the Band model (E. A. Masden & Cook, 2016).

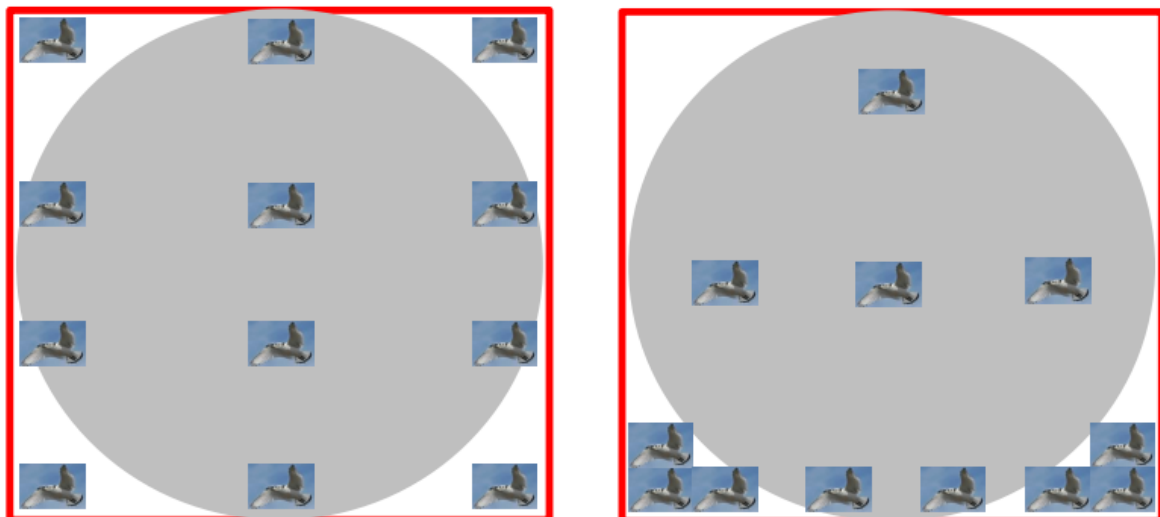


**Figure 3.3:** **Left:** How the distribution of birds is assumed by the basic Band model. **Right:** How the distribution of birds is assumed by an extend version of the Band model (A. Cook & Collier, 2015).

## Sensitivities

The 2012 Band model has some important sensitivities, which are: avoidance rate, flight height and flight speed. Below, each of these sensitivities is elaborated upon.

### Avoidance rate

The avoidance rate is a percentage value that captures a species' tendency to avoid flying through the rotor swept area, as was discussed in Chapter 2. It can be estimated via direct measurement (radar, visual observation), or by comparing data of recorded collisions to the total number of birds in a certain area (A. Cook & Collier, 2015), although this is mainly onshore for practical reasons. Estimating the avoidance rate is challenging due to the different types of avoidance behaviours that bird species have with respect to wind turbines. These are defined as macro-, meso- and micro-avoidance, as was explained in more detail in Chapter 2. Recent studies in wind farm Luchterduinen showed evidence of macro-avoidance of several species, like the northern gannet, razorbill and common guillemot (Leemans

et al., 2022). In addition, studies conducted by (Tjørnløv et al., 2023) and (Leemans et al., 2024) both found significant evidence for meso- and micro-avoidance of several seabird species with in-windfarm measurements. These types of avoidance are about a bird doing an evasive manoeuvre, which can be a few hundred metres in advance or a last-minute manoeuvre. Therefore, meso- and micro-avoidance are particularly interesting inputs for CRMs, while macro-avoidance is directly related to habitat loss. The avoidance rate is related to the number of collisions via (Cook et al., 2018):

$$\text{avoidance rate} = 1 - (\text{observed collisions} / \text{probability of collision} \times \text{flux}) \quad (3.2)$$

It should be noted that a 10% change in avoidance rate results in a 2500% increase in predicted collisions, highlighting the strongest sensitivity of the Band model towards avoidance rate (A. Cook & Collier, 2015). This effect is best demonstrated with the following example (Chamberlain et al., 2006): A total of 109 Bewick's Swans flew at risk height through an area of study. The study used an avoidance rate of 0.9962, giving a final predicted mortality rate of  $0.145$  (collision risk)  $\times$  109 (number of birds at risk)  $\times$  0.0038 (non-avoidance rate) = 0.06 birds over 180 days. A 10% decrease in avoidance rate increases the non-avoidance rate and therefore the mortality rate over 27 times to 1.64 birds (i.e.  $0.145 \times 109 \times (1-0.8962)$ ) over the same period. Note that in this example the non-avoidance rate is  $1 - \text{avoidance rate}$ .

### Flight height

(E. A. Masden et al., 2015) showed that the flight height parameter is also important for the amount of estimated collisions. It is typically estimated with the use of boat surveys, radars, LiDARs, and GPS loggers (Gyimesi, pers. comm., 27-06-2024). More efforts to model flight heights for marine birds were done by (Johnston et al., 2014), with the purpose of increasing the accuracy of CRMs like the Band model. In addition, the flight height is specified as a single value per species. Thus, without any measure for uncertainty, this value has a great influence on the number of estimated collisions, since the flux is calculated with the amount of birds flying at the height of the rotor swept area, which depends on the turbine height. Typically, the distribution of birds is assumed to be equally spaced out by the basic version of the Band model (E. A. Masden & Cook, 2016), as depicted in Figure 3.3. However, studies have shown that this is not the case, and that birds tend to distribute themselves in a more clustered manner at the lower part of the rotor swept area (Figure 3.3) (A. Cook & Collier, 2015). However, (E. A. Masden & Cook, 2016) stated that this also drives up the uncertainty of the model. Still, the flight height ought to be estimated as accurately as possible, because this will allow for a more consistent collision risk estimation. This in turn could allow for a direct evaluation of the influence of turbine height on collision risk, which could be useful for the development of the in Chapter 4 proposed ecology-technology assessment model.

### Flight speed

The Band model is also sensitive to the flight speed to some extent. The flight speed is largely assumed constant by the Band model. Bird parameters like length, wingspan, and flight speed do not have fixed values in reality, but a distribution. The flight speed is used for both estimating flux rate and probability and collision. Larger sample size studies of species-specific flight speed have become increasingly available, mainly for species like: lesser black-backed gull, northern gannet, black-legged kittiwake and herring gull (Gyimesi, pers. comm., 27-06-2024). In addition, (Leemans et al., 2024) also measured horizontal flight speeds of 11 species within Borssele wind farm.

In summary, the Band model has been treated by many researchers as a foundation upon which can be extended. Thus, there are many methods derived in literature to address the original model's limitations. Nevertheless, by adding features to the model, the sensitivity to uncertainty will increase (E. A. Masden & Cook, 2016). A balance must therefore be sought, since factoring in some uncertainty will be useful due to the many knowledge gaps in the seabird collision problem. The next section discusses a method that allows for the implementation of uncertainty in assumptions, when modelling collision risk.

### 3.3. Improved Band Model with Monte Carlo Simulations

#### Summary of Method

(E. A. Masden & Cook, 2016) highlights the importance of addressing uncertainty in collision risk models, because many CRMs are deterministic and do not inherently consider data or parameter uncertainty. The Band model is a deterministic model, and lacks by not providing measures for uncertainty, or context around the produced results. Therefore, (E. A. Masden & Cook, 2016) suggests the use of Monte Carlo methods to introduce stochasticity into a deterministic model like Band's, providing a way to account for uncertainty.

The use of Monte Carlo simulations can improve the Band model for various reasons. First, stochastic modelling allows for the consideration of random variations and uncertainties in input parameters, like avoidance rate, flight height, flight speed, wind conditions, and other factors affecting collision risk. Next, a Monte Carlo-based model can consider joint distributions of wind speed and direction, as well as distributions of flight height, as was shown by (McAdam, 2005). This approach enables a more comprehensive exploration of the combined effects of multiple variables, providing a realistic representation of the complex interactions influencing collision risk. Finally, there is the importance of transparency in collision risk modelling, especially when economically significant decisions, such as wind farm applications, are based on these models. Monte Carlo simulations can provide a transparent way to evaluate the robustness and reliability of the collision risk estimates, contributing to a more informed decision-making process.

Improving the Band model with Monte Carlo simulations means that the following key procedures are included (A. Cook & Collier, 2015):

- Distributional data to estimate uncertainty around input parameters is included in the model.
- Wind speed data is incorporated to model the wind & rotor speed / pitch relationship.
- Results now include boxplots of monthly collision estimates, as is shown in Figure 3.4.
- The end result is a probability plot of collision numbers, as shown in Figure 3.5.

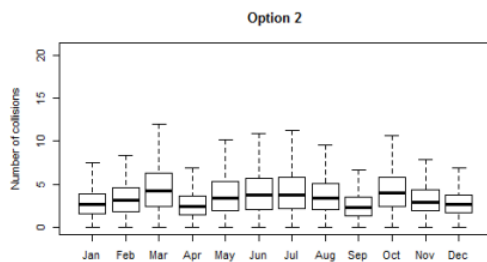


**Figure 3.4:** Example of boxplot output from the improved Band model, showing collision numbers per month (A. Cook & Collier, 2015).

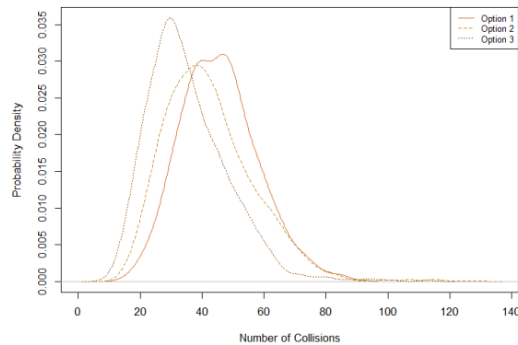


**Figure 3.5:** Example of probability density plot output from the improved Band model (A. Cook & Collier, 2015).

### 3.4. Literature Review Summary

The goal of the broad literature review on offshore wind farms (OWFs) and avian safety was to understand the ecological challenges posed by OWFs in the North Sea and to identify critical knowledge gaps in seabird collision risk management. As offshore monitoring is limited, the review focused on collision risk modelling as a practical assessment tool. Particular attention was given to the widely used Band model, which, despite its application in policy and industry, simplifies key inputs such as bird

geometry and flight behaviour—most notably by neglecting oblique flight paths—and is sensitive to avoidance rates, flight speeds and flight heights. To account for uncertainty, recent advancements have improved the model using Monte Carlo simulations. Still, a lack of offshore data and limited model validation pose challenges for accurate impact assessment. Based on these findings, it was decided to focus from here on modelling the economics of seabird collision risk mitigation for a typical OWF scenario. The next chapter elaborates on the background and relevance of this problem, while Chapter 5 will describe such a scenario in more detail.

# 4

## Problem Background

This chapter delves into a subjective exploration of a problem that was identified through the previous extensive literature review. In addition, this chapter aims to connect the literature study and thesis project by providing present-day background information about the problem stated in Chapter 1. Section 4.1 summarises the overarching problem. Section 4.2 builds on arguments derived from key players, particularly through collaboration with GROW Offshore Wind, outlining the motivations and demands from the offshore wind sector. This section then shifts to arguments derived from the literature, pinpointing specific needs and gaps, such as uncertainties, the lack of tools for collision risk analysis, and uncalibrated mitigation techniques. The chapter concludes by introducing the proposed Ecology-Technology-Integrated-Assessment-Model (ETIAM) in Section 4.3, which will be further developed in subsequent chapters.

### 4.1. Summary of the Problem

Based on the literature review, the author has concluded the existence of the following overarching problem, which is twofold:

First, there remains considerable ambiguity surrounding avian fatality figures and bird migration patterns in the context of offshore wind energy. More research and data are needed on avian interaction with OWFs, particularly offshore. Meanwhile, we are time-constrained due to the rapid scaling-up of offshore wind energy development. Thus, methods to perform environmental impact assessments (EIAs) should be researched and expanded upon. This also applies to technologies and methods for reducing environmental impacts on bird populations due to offshore wind energy development. Furthermore, the technical implications of mitigation methods must always be expressed in terms of Levelised Cost of Electricity (LCoE) and energy security. Therefore, due to the urgency of being ahead of the problem, we are in need of EIA models now, which can be improved and expanded once more ecological data become available.

Second, an interdisciplinary approach is needed to overcome the challenges that wind farm development poses to bird populations. Engineers, ecologists, and policymakers all play a role in present-day offshore wind development. Decisions made by engineers during the design stage translate into the magnitude of impacts that OWFs have on bird populations. This also applies to decisions made by policymakers, since OWF spatial planning relates to the magnitude of bird interactions with OWFs as well. Part of the solution is thus that engineers, ecologists, and policymakers actively cooperate to achieve the most optimal outcomes. It is therefore essential that communication is improved between these disciplines to ensure that methods and measures for reducing environmental impacts are integrated properly into OWF planning, design, construction, and operation, thereby ensuring effective implementation.

## 4.2. Arguments from Industry & Literature

### Arguments from GROW Partners

As stated in Chapter 1, the aim of this thesis is to contribute to finding solutions for the stated problem. The author has partnered up with GROW Offshore Wind, a consortium of 20+ companies & institutions that also invest in finding solutions for the environmental impacts of renewable energy sources. Companies involved include: Boskalis, Shell, Vattenfall, Siemens Gamesa, and TenneT. All partners of GROW are listed on their website (GROW, 2024). Furthermore, educational institutions involved are: TU Delft, University of Amsterdam, Leiden University, and Wageningen University & Research. Through GROW, valuable insight will be gained regarding the needs of key players in the field of offshore wind energy. It should be noted that GROW also collaborates with the ecology consultancy companies, such as Waardenburg Ecology.

Currently, GROW has proposed a project to NWO (NWO, 2024), called the EcoWindToolbox. This project consists of 6 modules or work packages, which all aim to address different types of impacts that offshore wind energy development has on the environment. The work packages have the following topics:

- **WP 1:** Project Management and Knowledge Utilisation.
- **WP 2:** Innovative Foundations to reduce Destratification and Turbidity and Enhance Nature (NID).
- **WP 3:** Managing Bird and Bat Impacts.
- **WP 4:** EMF Impacts and Design of Cable Infrastructure.
- **WP 5:** Holistic Noise and Vibrations Assessment Framework.
- **WP 6:** Ecology-Technology-LCA Integrated-Assessment Framework.

Addressing the impacts of birds and bats of OWFs, and the importance of producing ecology-technology integrated assessment methods, are both included as work packages 3 and 6 in this project proposal. The contents of this report and the author's master's thesis will thus align with work packages 3 and 6 of the GROW EcoWindToolbox proposal. It should also be noted that this entire GROW project is in its proposal phase, meaning the author's master's thesis will be carried out during the proposal phase of NWO's Perspective programme. Thanks to collaboration with GROW, the author has access to some unique insights into the necessities of various players in the North Sea's offshore wind energy development.

Regarding the stated problem, the GROW project proposal gives the following motivations and arguments that are in line with the stated problem from Section 4.1. These arguments are constructed based on discussions with governmental ecological research programmes (WOZEP, MONS) and ecologists within industry, consultancies, and academia:

#### *The need for addressing the uncertainties of OWF impacts:*

Currently, we do not know if wind parks create barriers for birds, and to what extent this is the case. Barriers could be caused by the turbines themselves, but another theory is that the disruption of regional atmospheric conditions at finer spatial scales caused by wind farms contributes to barrier effects. Theories like these need to be verified in order to better understand the extent and magnitude of the problem. Ecological programmes like WOZEP and MONS perform valuable research to understand the impacts of OWFs on ecology. These studies take time, while at the same time offshore wind in the North Sea is growing exponentially. Thus, if it appears that some of these ecological effects are unacceptable, it will most likely be too late to take action. Based on recent calculations, the Acceptable Levels of Impact (ALI) will be violated by 2030 (Potiek et al., 2021). On top of that, it is assumed that policy regulators will make demands to ensure that future offshore wind farms mitigate negative impacts on marine ecology. Without this work, there is a real threat that offshore wind farms will not be built—or at the very least, their development will be delayed—which is an unwanted outcome for all players in the field of offshore wind energy development. Finally, this adds to the risk of countries like The Netherlands failing to meet their EU climate targets. Thus, it makes sense to prioritise mitigating collision risks in offshore wind farms, including for local seabirds.

Examples that the offshore wind sector demands:

- A better understanding of the flight trajectories of birds through wind farms and how to encourage them through corridors in the wind farm whilst avoiding turbines.
- Control strategies for wind turbines to minimise bird collisions whilst reducing the barrier effect of a wind farm.

*The need for integration of multiple disciplines:*

In the context of integration importance, key players have stated that an integrated framework to assess combined ecological-technological solutions on a wide range of performance parameters is completely lacking. For example, calculations from ecological institutes often take existing wind farm technology as a given and assume scaling up and extrapolation in their assessments. However, there are continuous advancements in the offshore wind industry, and these advancements should be included and related to ecological calculations. Furthermore, wind farm operators are willing to make alterations in design and operation strategies, provided that there is sufficient evidence to show that layout design or innovative control can reduce bird impacts and barrier effects without significant increase in offshore wind farm LCoE. What is thus required is a toolbox (or framework) which can balance the demanding requirements of all these stakeholders through a better understanding of the marine ecology and the development of innovative engineering solutions. This will allow informed decisions to be made and these solutions to be implemented, balancing profit, carbon reduction, and environmental impact. Such a toolbox will help remove bottlenecks to offshore wind farm development by reducing uncertainty in terms of environmental impact and by proposing innovative engineering solutions which can be adopted to mitigate impacts (following the precautionary principle) and enhance biodiversity (Nature-Inclusive Design). The modular nature of said framework allows it to include models from other disciplines like ecology, carbon emissions, etc., and to evaluate the impact on marine/bird life or to perform life cycle assessments.

An example that the offshore wind sector demands:

- An analysis of how innovative control strategies balance impacts on marine wildlife with the economic value of wind energy.

## **Extra Benefits**

Finally, there are various extra benefits that result from the development of the above-mentioned demands in the offshore wind sector.

First, constructing a framework for multidisciplinary integration allows it to be expanded to serve many more applications in the offshore wind industry. For example, the framework can include life cycle assessments. Life cycle impacts on the climate—taking into account depletion of scarce resources, global warming effects, ecotoxicity and eutrophication—can be included in OWF design and planning. This could be done by a framework that accounts for a broad range of technological advancements and site-specific parameters, which are then integrated into a spatial analysis that translates the characteristics of certain locations into information usable for optimisations in OWF planning and design. For example, such optimisations could select the optimal locations and technological combinations for offshore wind development with the least material use, embodied greenhouse gas emissions, and life cycle impacts.

Second, when jointly designing solutions from an ecological and technological perspective, not only can reduced ecological impacts be achieved, but even nature enhancement. This is because many species in the North Sea are connected through predator-prey relations. The largest positive effects on ecology are thus achieved if we consider these measures in their coherence. Accelerated roll-out of offshore wind farms may be possible by mitigating their environmental impact and possibly enhancing nature as well.

Third, when this combined ecological-technological design approach is successful, it will provide unique export opportunities for the European offshore wind industry. Countries like The Netherlands—with their tendering procedure for new wind farms—are already including the important roles of ecology

and circularity. Thus, these countries will be ahead of surrounding nations, providing the European offshore wind industry with an edge over competitors in other parts of the world.

### Arguments Derived from Literature

Based on the literature review from Chapter 2, the author derived the following needs for addressing the aforementioned problem. As stated in the last section of Chapter 2, (Searle et al., 2023) suggested that uncertainty in the research landscape should be addressed. Due to the limited evidence base for assessing collision risk, as stated by (Cook et al., 2018), the precision and reliability of models is limited, especially offshore. (Salkanović, 2023) stated that avian collisions can be reduced by careful site selection, but that tools for such analyses are still lacking. As a result, decision makers and wind farm planners are struggling to come up with estimations of collision risk numbers in the wind farm planning phase. Furthermore, (Croll et al., 2022) proposed the development of a framework to enhance OWF impact assessment on bird species. To this day, frameworks and standards for addressing negative impacts are still lacking.

In addition, state-of-the-art collision mitigation techniques are still uncalibrated and can be improved upon. For example, the outright suspension of wind farm operations solely based on predictive models indicating potential bird migration can be financially burdensome for wind farm operators, as is the case for some wind farms participating in shutdowns (Bradaric, 2022). Consequently, it is crucial to explore approaches that not only minimise collision risks but also prioritise optimal power generation. Therefore, a reduction in the number of collisions should always be related to cost, or Levelised Cost of Energy (LCoE). Furthermore, when looking at collision risk models (CRMs), like the Band model, it is important to notice that these models are constructed from an ecological perspective. While CRMs may use technical turbine specifications as input to estimate bird fatalities, no context around the output is produced in relation to possible design changes of turbines or the inclusion of curtailment strategies.

All of the above-mentioned needs can be translated to a demand for an expandable modelling framework that can incorporate improvements in ecological research as time progresses. While uncertainties are addressed in research, the framework should give outputs showcasing probability distributions, to provide context to the results of the modelling framework. Finally, the effectiveness of mitigation measures depends on the type of species (Cook et al., 2018). To find the measures that work best for most species, fast calculations should be produced by simulations of such frameworks, expressing the effectiveness of a proposed mitigation measure.

## 4.3. Introducing the Ecology-Technology Model

In Chapter 1, the research objective for the thesis project was formulated as:

*"Quantify the economic impact of implementing design-based mitigation measures to reduce seabird collisions in offshore wind farms in the North Sea."*

Based on all of the aforementioned gathered information in this report, along with multiple conducted interviews with industry experts, it was decided that the following turbine design alterations will be investigated:

- Varying the minimum tip height (MTH)
- Varying the rotor diameter ( $D_{rotor}$ )
- Varying the turbine rated power ( $P_{rated}$ )

Based on the arguments and needs from key players, and the literature research, the author proposes the develop an **Ecology-Technology-Integrated-Assessment-Model (ETIAM)**. Furthermore, this model may also be referred to as the Ecology-Technology model in this report. Such a model will perform a multi-parameter optimisation, to showcase the relations between engineering and ecological parameters. The offshore wind industry is in need of tools to quantify the impacts of offshore wind farms on birds,

---

prior to site selection. Due to limited knowledge on bird behaviour offshore, the ETIAM shall be designed with the intention of improving the model over time, as more data becomes available on offshore bird behaviour in general, as well as bird behaviour in close proximity to turbines. The model will be developed within the boundaries of the research scope defined in Chapter 1. Furthermore, the methodology and software used for the model will be explored in Chapters 6 and 7. Note that the preliminary framework and design options for such a model were presented in the complete literature research conducted prior to this thesis project (Pérez Pérez, 2023).

# 5

## Case Study for a Typical Collision Assessment Scenario

This chapter covers the research question: What is a typical scenario for collision risk assessment within an offshore wind farm in the Dutch part of the North Sea? To explore the relationship between Levelised Cost of Energy (LCoE) and collision mitigation, simulations are conducted using a collision risk model and LCoE calculation. The input parameters for these simulations, relevant to offshore wind farm operation, are introduced in this chapter. Key factors include site location, proximity to conservation areas, wind farm layout, and the presence of critical seabird species. The first section outlines the selected case study scenario. Thereafter, stochLAB and WINDOW modelling software is introduced, along with details of this research's simulation approach.

### 5.1. Scenario Overview

The current research shall focus on the collision risk estimation of six seabird species at the IJmuiden Ver wind farm site, where multiple substantial offshore wind farms (OWFs) are planned in the future. This section describes the context of a typical collision risk assessment scenario. In addition, the case study parameters are introduced.

#### 5.1.1. IJmuiden Ver Alpha Background

##### Technical perspective

The IJmuiden Ver Wind Farm Zone (IJVWFZ) is a major offshore wind development in the Dutch North Sea, situated approximately 62 km off the west coast of the Netherlands. Spanning around 650 km<sup>2</sup>, the zone consists of three different sites: Alpha, Beta & Gamma. Each of these sites will have a capacity to generate 2 GW of power, contributing to a total capacity of 6 GW. In June 2024, the Dutch government awarded permits for two sites within the IJVWFZ. The IJmuiden Ver Alpha site was granted to the Noordzeker consortium, which includes SSE Renewables, ABP, and APG. Their proposal incorporates ecological innovations, such as bird-friendly turbine designs and artificial reefs, aimed at enhancing marine biodiversity (WindpowerNL, 2024). In contrast, the IJmuiden Ver Beta site was awarded to Zeevonk II, a joint venture between Vattenfall and Copenhagen Infrastructure Partners. Zeevonk II plans to integrate energy system solutions, including a 1 GW electrolyser at the Port of Rotterdam for the production of green hydrogen (WindpowerNL, 2024). The first electricity from these projects is expected by 2029, contributing to the Netherlands' goal of achieving 21 GW of offshore wind capacity by 2032 and 50 GW by 2040 (Netherlands Enterprise Agency, 2023). With grid connections managed by TenneT and innovative energy solutions embedded in the design, the IJVWFZ plays a pivotal role in

advancing a sustainable and resilient energy future. Figure 5.1 shows the location of lots I and II of IJmuiden Ver Alpha.

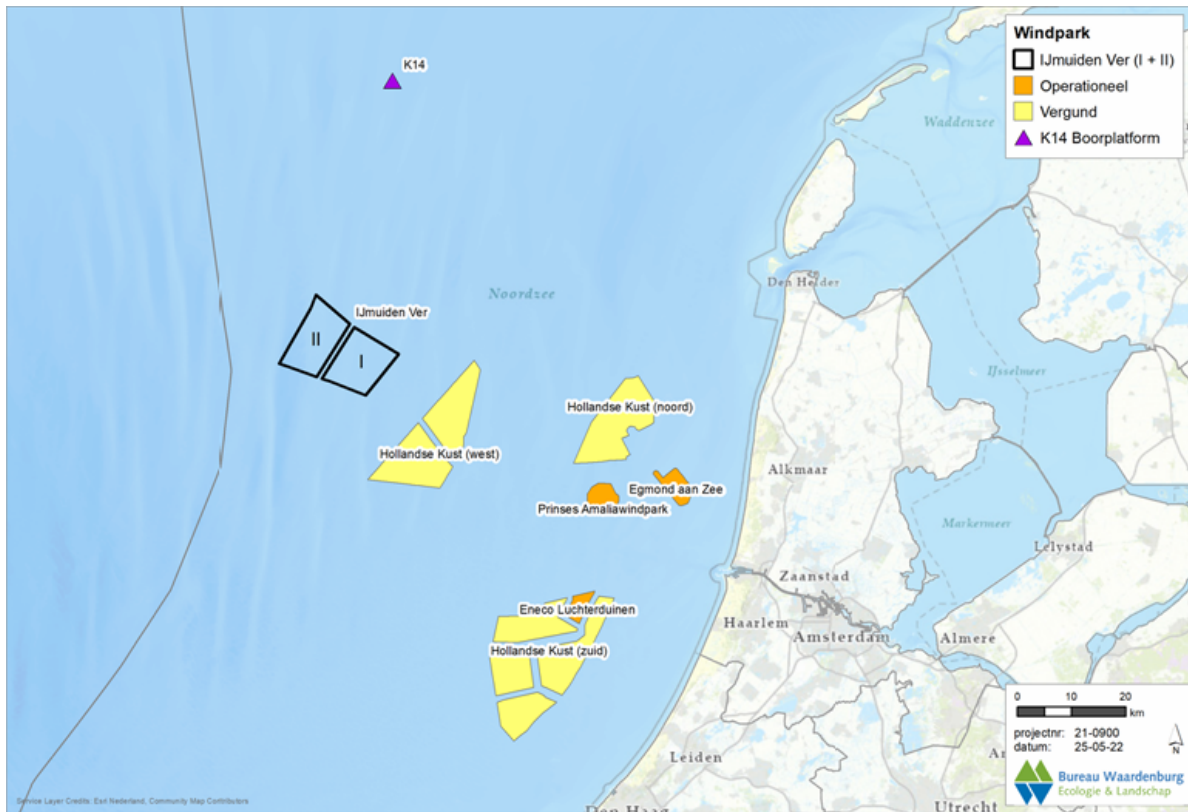


**Figure 5.1:** Site location of IJmuiden Ver Alpha (van der Vliet et al., 2022).

The IJmuiden Ver Wind Farm Zone (IJVWFZ) is also part of TenneT’s 2 GW Program, a large-scale offshore wind transmission initiative designed to connect 14 offshore grid links in the German and Dutch North Sea, each with a 2 GW capacity, totalling 28 GW by 2031. This will account for approximately 30% of the EU’s offshore expansion target. In the Netherlands, the programme includes eight offshore grid connection systems: IJmuiden Ver Alpha, Beta, and Gamma, as well as Nederwiek 1, 2, and 3, and Doordewind 1 and 2. In Germany, six additional systems will be implemented, including BalWin 3 and 4, and LanWin 1, 2, 4, and 5. The first of these connections is expected to be commissioned in 2028, with the remaining systems coming online annually until 2031. A central feature of the programme is its standardised approach, following a “design one, build many” philosophy to improve efficiency and reduce costs by using a uniform high-voltage direct current (HVDC) platform model. Additionally, the programme introduces a 525 kV bipolar cable system, which increases transmission capacity while requiring fewer cables and offshore platforms, thus reducing environmental impact. The large scale of this initiative, combined with the standardisation of many components, makes the 2 GW Program a key framework for future offshore wind farm development. A schematic of such a 2 GW grid connection is shown in Figure 5.2. Additional information on the 2 GW program can be found on the TenneT website (TenneT, 2025).

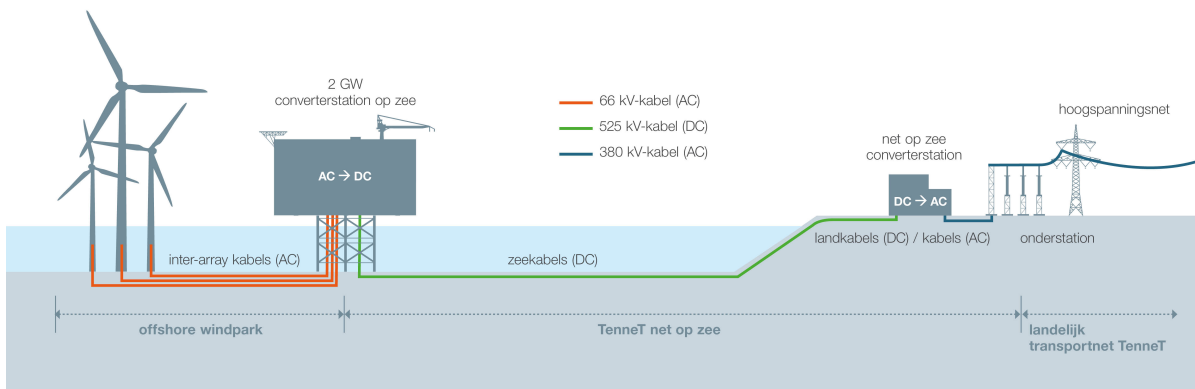


Figure 5.2: Illustration of TenneT’s 2 GW offshore wind farm to grid connection (TenneT, 2025).

**Ecological perspective**

Ecological legislation surrounding the site is governed by EU regulations for habitat and species protection. Species protection laws in Europe are defined under the ‘Birds Directive’ (1009/147/EC), which categorises protection based on the status and sensitivity of individual species. In the Netherlands, the government implemented a policy to safeguard specific habitats, based on the EU Natura 2000 network. Since 1 January 2017, species protection in the Netherlands has been enforced through the Nature Protection Act (Wet natuurbescherming) (van der Vliet et al., 2022). In practice, ecological studies conducted by Waardenburg assess whether the construction, operation, or decommissioning of a wind farm violates species protection laws. For this research, only the operational phase of the wind farm will be evaluated in terms of its potential negative impacts on relevant seabird species due to collisions. Figure 5.3 displays the Natura 2000 areas surrounding the IJmuiden Ver site.



Figure 5.3: Natura 2000 areas surrounding the site of IJmuiden Ver Alpha (van der Vliet et al., 2022).

Only species residing within these areas, and whose foraging range overlaps with the site, are considered for evaluation, provided that specific conservation targets are defined for these species through legislation. Based on these criteria, and considering the vulnerable seabird species identified earlier in the literature review of this research (Chapter 2), the following species are considered critical for collision risk assessment:

- Northern gannet
- Lesser black-backed gull
- Herring gull
- Great black-backed gull
- Little gull
- Black-legged kittiwake

Images of the species mentioned above can be found in Chapter 2. Of the bird species listed above, only the lesser black-backed gull is considered a breeding bird in the Dutch Natura 2000 regions (Figure 5.3). It primarily breeds in the regions Duinen en Lage Land Texel (14,000 pairs), Waddenzee (19,000 pairs), and to some extent in Duinen Vlieland (2,500 pairs) (van der Vliet et al., 2022). Additionally, the northern gannet and black-legged kittiwake are recognised as breeding birds along the Flamborough and Filey Coast region. The closest region of Bruine Bank serves as a foraging location for the northern gannet, little gull, and great black-backed gull. It is important to note that all the aforementioned species also forage in other UK, German, and Danish Natura 2000 regions, which are not specifically highlighted in Figure 5.3. These regions are typically also considered in collision risk assessments by ecological consultants, as birds from these areas may have an action radius that extends to the IJmuiden Ver site (van der Vliet et al., 2022).

## 5.1.2. Case Study Parameters

### Technical input parameters

This section defines the base case by specifying the case study input parameters. First, from various sources, the overall farm specifications are retrieved. A 1 GW capacity is assumed, which is equivalent to one lot of the IJmuiden Ver Alpha site. All parameters specified in Table 5.1 are taken from literature, or assumed when no reference could be found. For example, the distances to grid and harbour are based on grid map drawings from the TenneT 2 GW program (TenneT, 2025). Note that the maximum wave height is the extreme 50 year significant wave height, as defined by RVO studies of site Alpha (Merlaud et al., 2023). All reference farm specifications are shown in Table 5.1.

**Table 5.1:** Reference Farm Specifications.

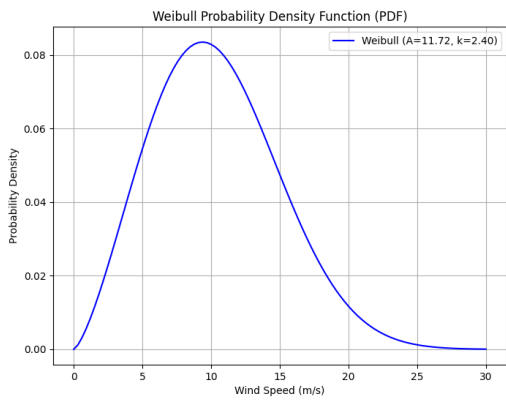
Parameter	Value	Unit
Location	IJmuiden Ver Alpha	-
Installed capacity	1	GW
Farm area	100	km <sup>2</sup>
Number of turbines	67	-
Distance to grid	120	km
Distance to harbour	100	km
Mean water depth	32	m
Mean wind speed at 100 m	10.5	m/s
Maximum wave height (50 year)	7.88	m
Lifetime	35	years

In addition, the base case scenario will assume 15 MW turbines, as this is in line with upcoming OWF development plans for this site. A 236 m diameter, with a hub height of 143 m, is accurate based on literature (van der Vliet et al., 2022). The minimum tip height value is set to 25 m, since this is a relevant value according to industry experts (Gyimesi, pers. comm., 2025). All baseline turbine specifications are shown in Table 5.2.

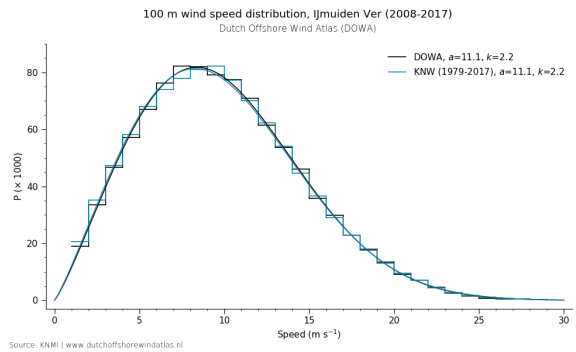
**Table 5.2:** Reference Turbine Specifications.

Parameter	Value	Unit
Rated power	15	MW
Rotor diameter	236	m
Hub height	143	m
Rotational speed	7.6	RPM
Minimum tip height	25	m
Cut-in wind speed	4	m/s
Cut-out wind speed	25	m/s
Rated wind speed	11.4	m/s

For the base case wind data input, a 1 year hourly wind time series is constructed based on 2 year wind measurements at the site location, published by the Dutch Offshore Wind Atlas (DOWA, 2017), for wind speeds and directions at 100 m height. A wind rose is calculated based on this time series, which is shown in Figure 5.5a. For comparison, the wind rose produced by KNMI is shown in Figure 5.5b. The constructed wind time series is therefore representative of the base case scenario. The one-dimensional Weibull plot in Figure 5.4a has similar scale and shape parameters, as well as a similar profile, to the wind speed distribution provided by KNMI (Figure 5.4b). Similar to (Mehta et al., 2024), Figure 5.6 shows the layout for the base wind farm scenario.

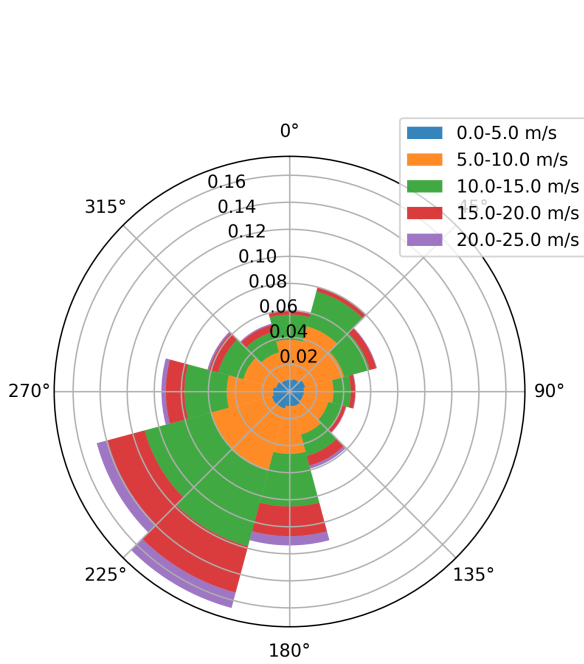


(a) 100 m wind speed distribution, from input wind time series.

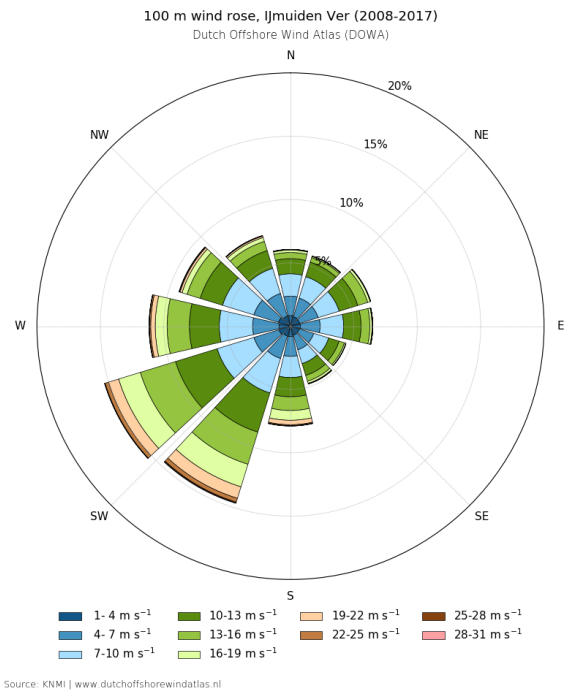


(b) 100 m wind speed distribution for the IJmuiden Ver Alpha site (DOWA, 2017).

**Figure 5.4:** Comparison of wind speed distributions for IJmuiden Ver offshore wind conditions.



(a) Wind rose from input wind time series at 100 m.



(b) Wind rose from (DOWA, 2017).

**Figure 5.5:** Wind rose for the IJmuiden Ver Alpha site, retrieved from (DOWA, 2017).

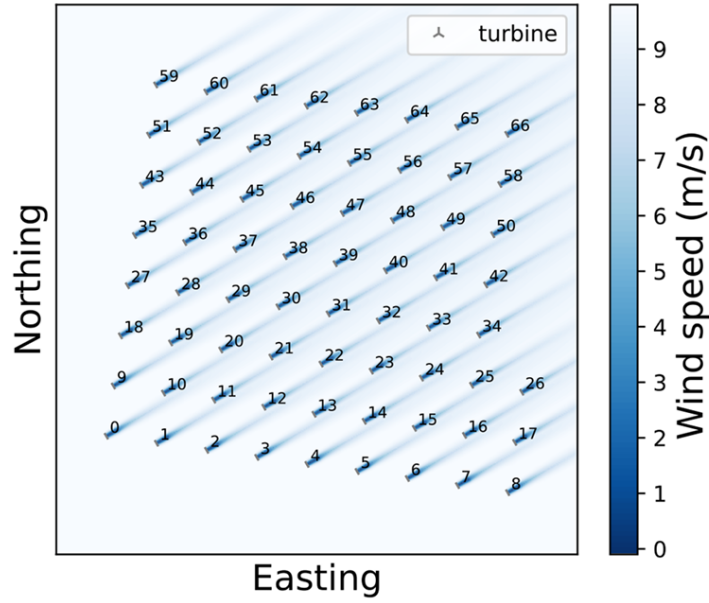


Figure 5.6: Turbine layout for the base case scenario (Mehta et al., 2024).

**Bird input parameters**

The input bird parameters for the base case are species-dependent. The tables below show these parameters, including the mean and standard deviation values, for all relevant species in the base case scenario.

Table 5.3: Lesser black-backed gull inputs.

Parameter	Mean	SD	Unit
Flight speed	9.4	3.92	m/s
Body length	0.58	0.020	m
Wingspan	1.43	0.025	m
Avoidance ratio	0.998	0	-
Nocturnal activity	0.43	0	-

Table 5.4: Northern gannet inputs.

Parameter	Mean	SD	Unit
Flight speed	14.9	2.60	m/s
Body length	0.94	0.022	m
Wingspan	1.73	0.025	m
Avoidance ratio	0.989	0	-
Nocturnal activity	0.08	0	-

Table 5.5: Herring gull inputs.

Parameter	Mean	SD	Unit
Flight speed	11.3	3.91	m/s
Body length	0.60	0.015	m
Wingspan	1.44	0.020	m
Avoidance ratio	0.995	0	-
Nocturnal activity	0.01	0	-

Table 5.6: Great black-backed gull inputs.

Parameter	Mean	SD	Unit
Flight speed	13.7	1.20	m/s
Body length	0.71	0.023	m
Wingspan	1.58	0.025	m
Avoidance ratio	0.995	0	-
Nocturnal activity	0.50	0	-

**Table 5.7:** Little gull inputs.

Parameter	Mean	SD	Unit
Flight speed	11.5	0.10	m/s
Body length	0.26	0.003	m
Wingspan	0.78	0.008	m
Avoidance ratio	0.995	0	-
Nocturnal activity	0.25	0	-

**Table 5.8:** Black-legged kittiwake inputs.

Parameter	Mean	SD	Unit
Flight speed	6.2	3.40	m/s
Body length	0.39	0.003	m
Wingspan	1.08	0.042	m
Avoidance ratio	0.992	0	-
Nocturnal activity	0.50	0	-

These values are obtained from (van der Vliet et al., 2022). In addition, a standard deviation of 0 was assumed in cases where no value was available. Another species-specific input is the bird density at the IJmuiden Ver Alpha site. These values vary throughout the year and are shown in Table 5.9 below. Note that for these species, the bird density values correspond to those determined in the latest KEC 4.0 studies (Potiek et al., 2022).

**Table 5.9:** Monthly bird density values in birds/km<sup>2</sup> (van der Vliet et al., 2022). Species names abbreviated as: NG = Northern gannet, LBBG = Lesser black-backed gull, HG = Herring gull, GBBG = Great black-backed gull, LG = Little gull, BLK = Black-legged kittiwake.

Species	Jan	Feb	Mar	Apr	May	Jun	Jul	Aug	Sep	Oct	Nov	Dec
LBBG	0.0	0.2	0.2	0.4	0.4	0.7	0.7	0.2	0.2	0.2	0.2	0.0
NG	0.4	0.3	0.3	0.4	0.4	0.1	0.1	0.2	0.2	0.6	0.6	0.4
HG	0.5	1.2	1.2	0.1	0.1	0.0	0.0	0.0	0.0	0.2	0.2	0.5
GBBG	0.3	0.3	0.3	0.0	0.0	0.0	0.0	0.1	0.1	0.2	0.2	0.3
LG	0.0	0.1	0.1	1.3	1.3	0.0	0.0	0.0	0.0	0.0	0.0	0.0
BLK	0.9	1.1	1.1	1.0	1.0	0.4	0.4	0.1	0.1	1.3	1.3	0.9

## 5.2. Driving Technical Criteria for the Ecology-Technology Model

The effects of changes in turbine design will be investigated by varying the minimum tip height (MTH), rotor diameter, and turbine rated power. In practice, these measures result in the following design changes:

1. Increasing the minimum tip height results in an increase in hub height at a 1:1 ratio.
2. Increasing the rotor diameter results in an increase in hub height at a 2:1 ratio (see also Section 7.3 in Chapter 7).
3. Increasing the rated power results in a turbine with a larger rotor diameter and increased hub height (see also Chapter 7).

Mitigation measures 1 and 2 place the turbines outside their optimal design envelope, affecting various components at both turbine and farm levels. To identify the most significant effects caused by these proposed design changes, an analysis was conducted based on the three main effects identified. The LCoE model that will be used, called WINDOW, must be modified accordingly. As a first step, the framework of this model, as presented by Mehta et al. (2024), was adapted to incorporate minimum tip height, illustrating the modules impacted by changes in each design parameter. This framework is

discussed in Chapter 7 and illustrated in Figure 7.1, which shows the modified framework including minimum tip height (MTH) as an additional design variable.

In Figure 7.1, all three design variables—MTH,  $D_{rotor}$ , and  $P_{rated}$ —are shown in green boxes. The dark grey boxes labelled as ‘Analysis’ in Figure 7.1 represent the farm-level components that are directly impacted by changes in the respective green-boxed design variables above. Changing the MTH will affect the farm AEP, support structure costs, installation costs, and operations and maintenance (O&M) costs. Varying  $D_{rotor}$  will influence the farm AEP as well as the rotor nacelle assembly (RNA), support structure, installation, and O&M costs. Varying  $P_{rated}$  will impact the number of turbines, as well as the RNA and electrical infrastructure costs. By identifying how each design parameter affects each farm-level component, the most important technical criteria for the Ecology-Technology-Integrated-Assessment-Model (ETIAM) can be established. In the following sections, these technical criteria are explored in a broad sense. This will form the basis for selecting the most critical governing criteria for the ETIAM, which will be listed and discussed in detail in Chapter 7.

### 5.2.1. Support Structure Design Limits

It is expected that an increase in hub height will lead to an increase in support structure cost. The increased hub height requires a longer tower, which increases the amount of steel used. Additionally, the support structure will experience higher loads, which also leads to increased geometry and material requirements, further raising the cost. The loads acting on the turbine structure can be simplified to:

- $T$  — Thrust force at hub height (wind load).
- $q_{aero}$  — Distributed aerodynamic force along the tower, due to wind.
- $q_{hydro}$  — Distributed hydrodynamic force along the monopile, due to waves and currents.
- Gravity force, acting downwards.

By adding the resulting reaction normal force  $N_z$ , shear force  $V_x$ , and moment  $M_y$ , the following free body diagram can be drawn:

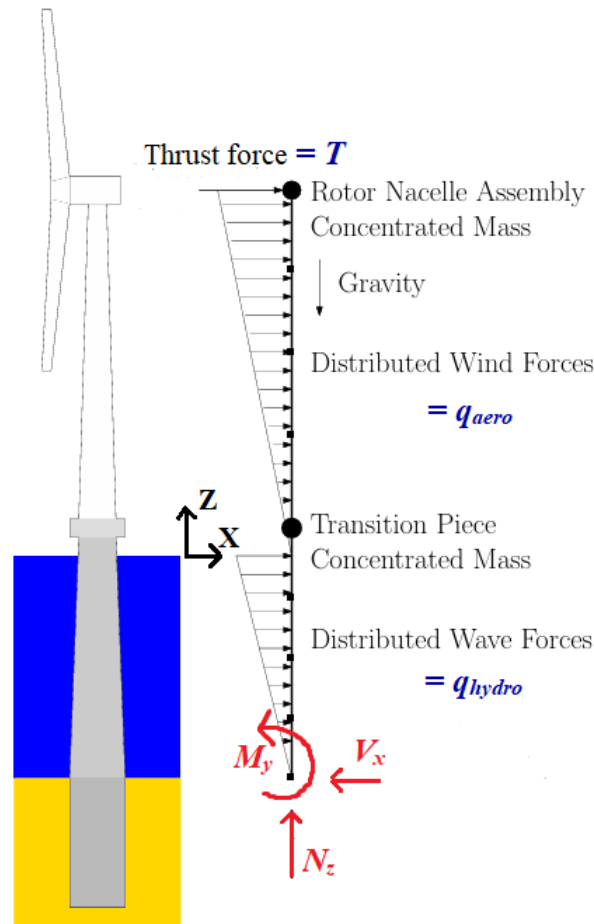


**Figure 5.7:** Free body diagram for the offshore wind turbine (McWilliam et al., 2021).

Firstly, an increase in hub height leads to an increase in  $q_{aero}$  due to a larger area exposed to aerodynamic forces. Additionally, the bending loads in the structure caused by  $T$  and  $q_{aero}$  increase with the greater hub height, resulting in higher bending stresses in the support structure, with the dominant contribution coming from  $T$ . To counteract these increased bending stresses, the monopile diameter  $D_p$  must increase, which also results in an increase in  $q_{hydro}$  due to additional hydrodynamic drag forces. The tower diameter must also increase, leading to additional aerodynamic forces on the tower. Finally, an increase in rotor diameter leads to an increased thrust force  $T$  due to the larger rotor swept area, further increasing the bending stresses in the structure. Overall, the increased support structure cost is caused by the increase in support structure geometry—specifically the length and diameter of the tower and monopile. For this analysis to hold, it is assumed that the structure does not fail, i.e. that the maximum bending stresses in the structure do not exceed the yield stress of steel.

Another condition for the proper functioning of the support structure is having an adequate embedded length  $L_e$  with respect to the monopile diameter. According to an industry expert, a ratio of  $D_p/L_e = 6$  is a good reference value to ensure the monopile is properly embedded and capable of transferring loads to the soil (van der Male, pers. comm., 2025). The expected increase in  $D_p$  would therefore also increase the monopile length, through the additionally required  $L_e$ , contributing further to an increased support structure cost.

### 5.2.2. Vessel Size Limits

For installation and operations and maintenance (O&M) of the wind farm, various large vessels are used. The cost of renting such vessels depends mainly on vessel type, where turbine and support

structure size determine which type of vessel can be used for installation or O&M services. An increase in hub height or rotor diameter is expected to require larger vessels for both installation and O&M. The following vessel types are expected to be dependent on hub height or rotor size:

- Wind turbine installation vessel (WTIV)
- Foundation installation vessel (FIV)
- Heavy lift vessel (HLV)

For increasing turbine size and mass, WTIVs require cranes capable of lifting heavy components to sufficient heights. For example, increasing the hub height limits the pool of WTIVs available due to the required lifting height. In the current market, there are only a limited number of large WTIVs capable of installing the largest turbines, and due to high demand, day rates have increased to the 800–1000 kEUR range (Ummels, pers. comm., 2025). FIVs are more widely available, as some vessels can install monopiles using DP systems; their day rates typically range from 600 to 900 kEUR. For the largest topsides and jackets of offshore substations, only a few suitable HLVs exist, with day rates reaching 1 MEUR (Ummels, pers. comm., 2025). The day rate values mentioned above are assumed to apply to turbines in the 15 to 20 MW range. Therefore, lower day rates may be expected for the installation of smaller turbines. Figure 5.8 shows three examples of present-day vessels in each category.



(a) WTIV: 'Aeolus' (Van Oord, 2025). (b) FIV: 'Orion' (IRO, 2025). (c) HLV: 'Sleipnir' (Heerema, 2025).

Figure 5.8: Examples of WTIV, FIV, and HLV vessels.

### 5.2.3. Turbine Optimal Design Limits

The proposed design changes affect several key properties of the wind turbine. For example, changing the rotor diameter impacts the rotor angular velocity at rated wind speed, or the rated RPM. Wind turbines are designed for an optimal tip speed ratio, and the blade's tangential velocity at the outer radius is limited to 80–100 m/s to minimise noise emissions (Grinderslev & Hansen, 2022). The tip speed ratio ( $\lambda$ ) is given by:

$$\lambda = \frac{\omega R}{V} \quad (5.1)$$

where:

- $\lambda$  is the tip speed ratio (TSR),
- $\omega$  is the rotor angular velocity,
- $R$  is the rotor radius,
- $V$  is the wind speed.

Increasing the rotor radius while maintaining the same rotational speed and tip speed ratio could result in tip speeds that exceed acceptable limits, making the design unfeasible. In general, deviating from the optimal tip speed ratio reduces the aerodynamic efficiency of the rotor, leading to lower power output. Conversely, reducing the turbine rotor radius while maintaining the same rotational speed results in lower power output per turbine. If not compensated by an increase in rotational speed, this would require the installation of more turbines to meet energy targets, increasing overall project cost.

The decrease in produced power due to a smaller rotor swept area can be explained using turbine momentum theory for power production:

$$P = \frac{1}{2} \rho A V_{\infty}^3 C_P \quad (5.2)$$

where:

- $P$  is the power extracted by the wind turbine,
- $\rho$  is the air density,
- $A$  is the rotor swept area,
- $V_{\infty}$  is the free-stream wind speed,
- $C_P$  is the power coefficient, representing the efficiency of power extraction.

The natural frequency of the wind turbine structure can also be affected by an increase in hub height. Wind turbine structures are designed to avoid having their natural frequency coincide with the 1P and 3P frequencies—i.e. the rotor's rotational frequency and the frequency of blade passage in front of the tower. Figure 5.9 shows an example of a soft-stiff design, where the first natural frequency of the structure falls between the maximum 1P and minimum 3P frequencies, mitigating the risk of resonance, which could otherwise lead to large horizontal amplitudes or even catastrophic failure.

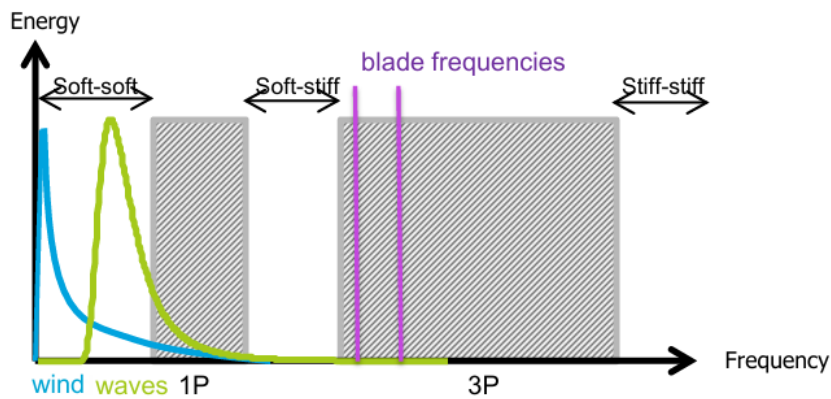


**Figure 5.9:** Schematic representation of a soft-stiff turbine design, with respect to the 1P and 3P frequencies (van der Male, 2023).

An increase in hub height can lead to a reduced natural frequency, as the turbine structure becomes more slender and therefore less stiff. To counteract this effect, an increase in monopile diameter is required to raise the natural frequency again, thus preventing the risk of resonance with the 1P frequency—assuming a soft-stiff design (van der Male, pers. comm., 2025). This increase in monopile diameter also contributes to higher structural costs.

### 5.3. Modelling with WINDOW and stochLAB

To address all research questions (Chapter 1) and in preparation for the EcoWindToolbox work package (Chapter 4), a model will be developed to calculate the Levelised Cost of Energy (LCoE) versus bird collisions for variations on the case study scenario. To investigate the collision risks posed by offshore wind farms to avian species, stochLAB has been selected as the primary tool for this research. For the analysis of LCoE in offshore wind farm projects, the WINDOW openMDAO model has been chosen. These two models will be integrated within Python, with the necessary adjustments made to generate results that contribute to achieving the research objective of this thesis.

## stochLAB Introduction

stochLAB is a stochastic modelling software package designed to simulate and analyse collision risks in scenarios involving uncertainty and variability. It is open source and based on the offshore Band 2012 model (Band, 2012). However, stochLAB's functionalities are more extensive, incorporating improvements such as Monte Carlo simulations, which account for variability in key parameters like bird flight paths, wind speeds, and turbine operability. This is a key advancement for future collision risk assessments, given the persistent research gaps and uncertainties in collision modelling. stochLAB is a user-friendly tool tailored for statistical research, addressing the need for consistent, uniformly applied tools in bird collision simulations, as highlighted in Chapter 4.

stochLAB was mainly developed through the efforts of Dr A. Cook, who based his work on improvements to the Band 2012 model made by (E. A. Masden et al., 2015). One of these improvements is the inclusion of species-specific flight height distributions, rather than assuming a uniform distribution, which makes the model more accurate (van der Vliet et al., 2022). As stated above, stochLAB is a stochastic model, unlike Band's deterministic approach. It incorporates variability in inputs via standard deviation values. Built-in datasets, such as species-specific flight height distributions, include bootstrapping methods, which further help capture uncertainty. This is explained in more detail in Chapter 6. Finally, an ecology expert (Collier, pers. comm., 29-01-2024) stated that stochLAB will increasingly be adopted in practice, particularly to encourage greater uniformity in ecological calculations. For these reasons, stochLAB is chosen as the collision risk model for this research. More information about the tool can be found in the documentation (Humphries et al., 2022).

## WINDOW openMDAO Introduction

WINDOW openMDAO is a publicly available model developed through industry research at TU Delft, based on the Multidisciplinary Design Analysis and Optimization (MDAO) framework. The MDAO framework enables the simultaneous optimisation of multiple disciplines in wind farm design, including layout, electrical collection systems, and support structures. This integrated approach improves overall system performance by identifying trade-offs and balancing the impacts of each discipline on the Levelised Cost of Energy (LCoE). MDAO applications include optimising turbine sizing for offshore wind farms, minimising LCoE, and uncovering crucial interdependencies across wind farm subsystems. Moreover, the framework allows for the assessment of model uncertainties, evolving technologies and costs, varying design conditions, and constraints on optimal turbine design (Mehta et al., 2022; Perez-Moreno et al., 2018).

WINDOW openMDAO employs low-fidelity tools to capture key dependencies between outputs and design variables during the early design stage. While not aimed at providing precise LCoE values or optimum designs, the model serves as an analytical tool that helps identify relationships among components and pinpoint the key drivers influencing turbine sizing—such as technological developments, site conditions, and policy shifts. The WINDOW model has undergone several development phases. It was originally developed in 2012 by M. Zaaijer (Zaaijer, 2013), and later refined through studies such as (Perez-Moreno et al., 2018), who investigated workflow optimisation within MDAO. Most recently, (Mehta et al., 2024) released an updated model in Python 3, which is now publicly available. WINDOW was also proposed for use in Work Package 3 of GROW's pre-proposal, as discussed in Chapter 4. Hence, using this model in this research contributes not only to this thesis, but also to broader research efforts under the GROW programme.

## Simulation Approach

Computing bird collisions with stochLAB for the given scenario is relatively straightforward for the selected critical species. The WINDOW model for LCoE calculations requires some corrections and updates for the assumed input values. Where assumptions are made, they will be clearly stated in Chapter 7. Nevertheless, this model is expected to provide fast, first-order estimations of LCoE for the offshore wind farm scenario. The goal is to run both models in parallel with the same input values, enabling analysis of how variations in technical parameters—such as minimum tip height, rotor

diameter, and rated power—affect both LCoE and bird collision outcomes.

Since *stochLAB* runs in R, a script has been written to call the bird collision model from Python using embedded R code, as *WINDOW* must be run in Python. Initially, the aim was to incorporate the total estimated bird collisions from *stochLAB* into the MDAO optimisation in *WINDOW*. This would allow bird casualties to be integrated into the wind farm optimisation process. However, in the interest of time, a decision was made to run both models separately. In this workflow, collision estimates are first produced using *stochLAB*'s collision risk model (CRM), after which *WINDOW* is run to compute LCoE values for the same set of input parameters.

## 5.4. Next Steps

This chapter has presented a relevant offshore wind farm scenario for estimating bird collisions among critical species. The input parameters defined herein will be used in the collision risk modelling described in Chapter 6, and subsequently in the LCoE calculations presented in Chapter 7. All species introduced in this chapter will be evaluated for collision risk assessment. For the technical calculations, the base case scenario consists of 67 turbines, each with a rated power of 15 MW.

# 6

## stochLAB Collision Risk Modelling

This chapter addresses the research question: How effective are design variations in minimum tip height, rotor diameter, and rated power at reducing seabird collisions within the defined scenario? To evaluate the effectiveness of different mitigation strategies, this chapter presents results from simulations that vary key turbine parameters, such as minimum tip height, rotor diameter, and turbine rated power. The primary focus of these simulations is to assess the impact of these parameters on bird collision risk within the context of an offshore wind farm in the Dutch part of the North Sea. The first section presents the model setup, followed by the baseline results. Subsequent sections contain an analysis of the effect of varying minimum tip height, rotor diameter, and rated power on collision numbers. Key factors influencing the outcomes of these simulations—such as bird flight height distributions and species-specific behaviour—are discussed in relation to the results. The chapter concludes by summarising the effectiveness of each mitigation strategy, setting the stage for the economic analysis in the following chapter.

### 6.1. Model Setup

stochLAB is a collision risk modelling software developed in R. It builds upon the Band offshore collision risk model, originally created in 2012, with enhancements made by Elizabeth Masden in 2015 to incorporate variability and uncertainty (E. Masden, 2015). Details and assumptions of the Band model are explained in Chapter 3. stochLAB, which was recently created by British bird ecologists, is now publicly available and provides a variety of functions for collision risk assessments, particularly for British bird species (Humphries et al., 2022). As stated in the literature study of this research (Chapter 3), the introduction of species-specific flight height probability functions allowed for more accurate estimates of the proportion of the bird population at risk of colliding with turbine blades—an improvement introduced by (Band, 2012). In addition, accounting for uncertainty helps prevent overconfidence in single-value predictions and offers a range of likely collision rates. Placing collision estimates within the context of uncertainty is essential for making informed decisions aimed at reducing turbine or wind farm collisions, and may even influence policy changes in the Netherlands, as discussed in (Pérez Pérez, 2023).

stochLAB offers several useful functions for collision risk modelling. For this research, only one function is used to calculate collisions for the seabird species defined in Chapter 5. This function, called `stoch_crm()`, represents the stochastic collision risk model (SCRM) within the stochLAB package. Using this SCRM, the number of in-flight collisions with offshore wind farm turbines is estimated. The core calculations performed by this function follow the methodology outlined in Masden’s report (E. Masden, 2015). The `stoch_crm()` function offers various options to define the type of input data used in collision risk estimation, starting with four ‘model type’ options:

- Option 1: A basic model that assumes a uniform flight height distribution between rotor limits, using site survey data for birds at risk height.
- Option 2: A basic model that uses a generic flight height distribution instead of site survey data.
- Option 3: An extended model that incorporates a generic flight height distribution.
- Option 4: An extended model that uses a flight height distribution derived from site survey data.

For this research, Option 3 is chosen, as the use of a non-uniform flight height distribution provides more accurate results for the IJmuiden Ver Alpha scenario (as stated by van der Vliet et al., 2022). Additionally, generic flight height distributions are available as built-in functions for nearly all critical species defined in Chapter 5. These distributions are already integrated into the software and ready for use. The extended model also incorporates variability by requiring mean and standard deviation (SD) values for input parameters. Most of these inputs have already been defined in Chapter 5. Any other non-trivial input parameters that were not defined in Chapter 5 are presented in the overview in Table 6.1. Below the table, each of these inputs is discussed, along with how they were obtained or assumed.

**Table 6.1:** Non-trivial input variables used in the `stoch_crm()` function.

Variable Name	Description
<code>n_iter</code>	Number of iterations for the stochastic model
<code>flt_speed_pars</code>	Flight speed parameters
<code>body_ld_pars</code>	Body length parameters
<code>wing_span_pars</code>	Wing span parameters
<code>avoid_ext_pars</code>	Extended avoidance parameters
<code>noct_act_pars</code>	Nocturnal activity parameters
<code>bird_dens_opt</code>	Bird density calculation method
<code>bird_dens_dt</code>	Bird density dataset
<code>flight_type</code>	Flight type category
<code>gen_fhd_boots</code>	General flight height distribution bootstrap
<code>air_gap_pars</code>	Air gap parameters
<code>rtr_radius_pars</code>	Rotor radius parameters
<code>bld_width_pars</code>	Blade width parameters
<code>bld_chord_prf</code>	Blade chord profile
<code>rtn_pitch_opt</code>	Rotor pitch options
<code>bld_pitch_pars</code>	Blade pitch parameters
<code>rtn_speed_pars</code>	Rotor speed parameters
<code>windspd_pars</code>	Wind speed parameters
<code>rtn_pitch_windspd_dt</code>	Rotor pitch and wind speed dataset
<code>trb_wnd_avbl</code>	Turbine wind availability
<code>trb_downtime_pars</code>	Turbine downtime parameters
<code>wf_n_trbs</code>	Number of turbines in the wind farm
<code>wf_width</code>	Wind farm width
<code>wf_latitude</code>	Wind farm latitude

First, the number of iterations is set to 1000, as this is sufficient for the model to converge to a stable solution, according to an industry expert (Gyimesi, 2025). All bird-specific parameters, such as flight speed, body length, wingspan, avoidance, and nocturnal activity parameters, are defined for the base case in Chapter 5. The bird- and month-specific density values are passed to the SCRMs using the mean values defined in Chapter 5, and a standard deviation of 0.001 for each month. The model assumes

that the sampling estimates for these densities follow a truncated normal distribution (since negative bird density values are invalid). Next, the flight type can either be gliding or flapping, and it is set to 'flapping'.

Since Option 3 for the model is used, the generic flight height distributions (FHDs) are called from the built-in functions in the SCRM for each species. These FHDs are derived from research data using GPS loggers and are updated when possible (Gyimesi, 2025). For a given species, the FHD provides the relative frequency distribution of bird flights at various heights starting from the sea surface Humphries et al., 2022. Additionally, each of these FHDs (for up to 25 species) comes with bootstrap estimates. Bootstrapping is commonly used in ecological statistics, as it allows for estimating the variability and uncertainty of flight height distributions by randomly resampling the data. Since the data obtained from these distributions are limited relative to the total seabird population, a method that accounts for low sample sizes is preferred. Still, (van der Vliet et al., 2022) notes that whenever accurate FHD data is unavailable, it is more suitable to use the basic Band model (Band, 2012). Plots of the built-in FHDs used for all species are shown in Figure 6.1. It can clearly be seen that the probability distribution decreases with flight height. It should be noted that the built-in flight height distribution of the little gull was found to be invalid. The flight height distribution of the black-headed gull was used instead, as it represents a bird with similar behaviour and size.

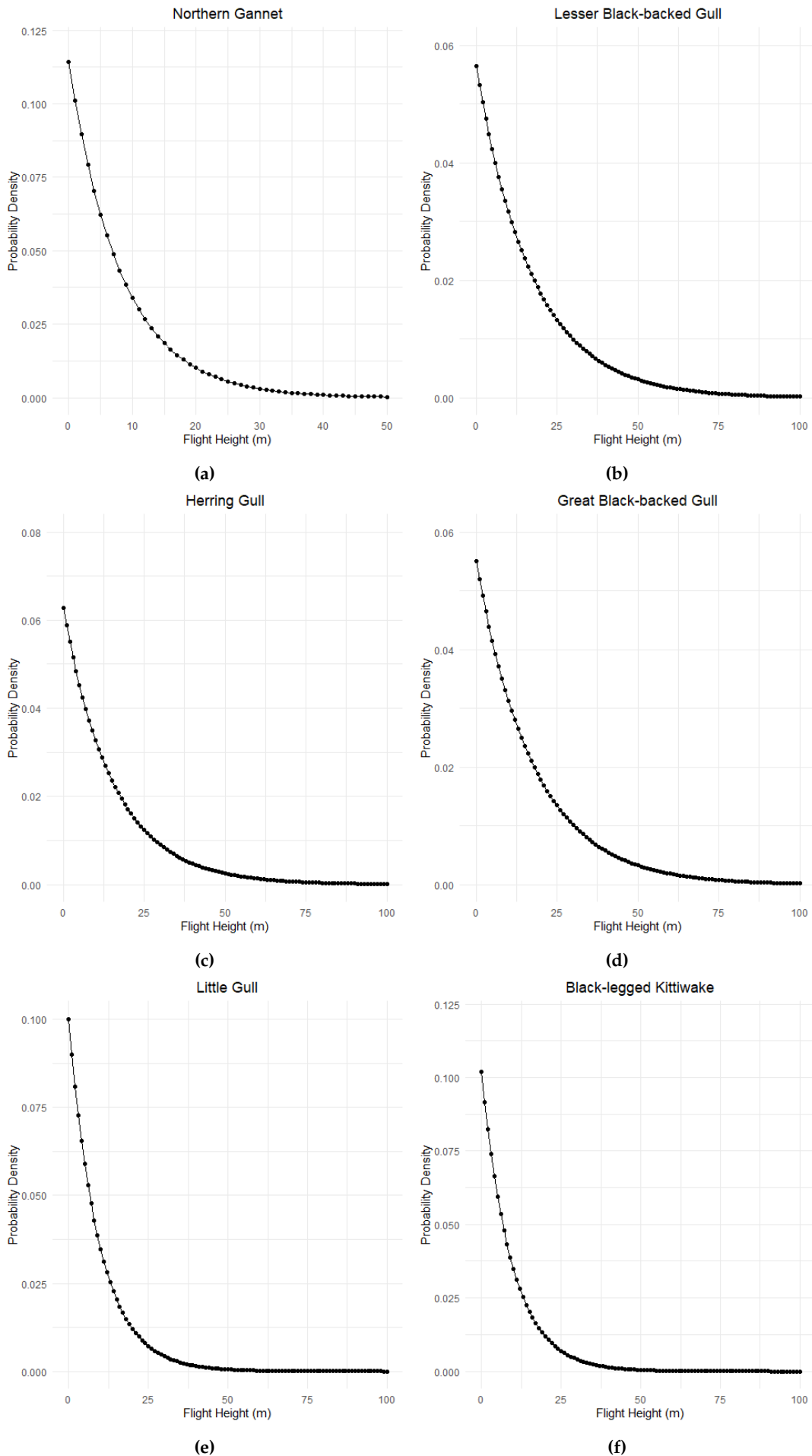


Figure 6.1: Generic flight height distributions used for all species.

For the technical parameters, the air gap is passed as the minimum tip height. The rotor radius is the turbine rotor radius. The blade width is the maximum blade width, which is taken as 5.765 m. The blade chord profile is a data frame that gives the chord width at specific radius intervals, with values proportional to the maximum blade width:

**Table 6.2:** Blade chord profile for inner to outer radius percentage (IEA, 2025).

Radius	0%	10%	20%	30%	40%	50%	60%	70%	80%	90%	100%
Chord	0.982	0.944	1.00	0.931	0.815	0.721	0.637	0.559	0.480	0.393	0.087

The parameter `rtn_pitch_opt` is set to "windSpeedReltn", meaning that both the rotation speed and pitch of the turbine blades are automatically calculated as a function of wind speed. The `stoch_crm()` function applies this using a dataset from the turbine, showing rotational speed and blade pitch for various wind speeds.

The parameter `windspd_pars` takes as input the mean and standard deviation of the wind speed at the wind farm site in m/s. These values are calculated using the scale and shape factor from the generated one-dimensional Weibull distribution plot in Chapter 5, via the following equations (Burton et al., 2011), where  $\lambda$  is the scale parameter,  $k$  is the shape parameter,  $\Gamma(x)$  is the Gamma function,  $\bar{v}$  is the mean wind speed in m/s, and  $\sigma_v$  is the standard deviation in m/s:

$$\bar{v} = \lambda \Gamma\left(1 + \frac{1}{k}\right) \quad (6.1)$$

$$\sigma_v = \sqrt{\lambda^2 \left[ \Gamma\left(1 + \frac{2}{k}\right) - \left(\Gamma\left(1 + \frac{1}{k}\right)\right)^2 \right]} \quad (6.2)$$

Lastly, the dataset that contains the rotational speed and blade pitch as a function of wind speed is retrieved from (IEA, 2025). The turbine wind availability is the percentage of time during which operable wind speeds (between cut-in and cut-out thresholds) occur. Based on the Weibull scale parameter = 11.86 and shape parameter = 2.4, a value of 92.6% is used here. Turbine downtime is set to 2%, representing the time the turbine is non-operational due to maintenance. The number of turbines is equal to the number from Chapter 5. A wind farm width of 11.4 km is used, based on the layout figure in Chapter 5. More detailed descriptions of each input used in the SCRM can be found in (Humphries et al., 2022).

## 6.2. Baseline Results

Before running the simulations for varying minimum tip height, rotor diameter, and turbine rated power, a baseline simulation is performed. The collision results from this simulation serve as a benchmark for evaluating the effectiveness of the proposed mitigation measures, which will be discussed in subsequent sections. The baseline simulation uses all case-specific inputs from Chapter 5, as well as the assumed generic inputs from Section 6.1. In summary, this refers to a wind farm with 67 turbines rated at 15 MW, each with a minimum tip height of 25 m and a rotor diameter of 236 m. Furthermore, the FHDs from Figure 6.1 are applied. The results of this simulation are presented in Figure 6.2 for all six critical bird species.

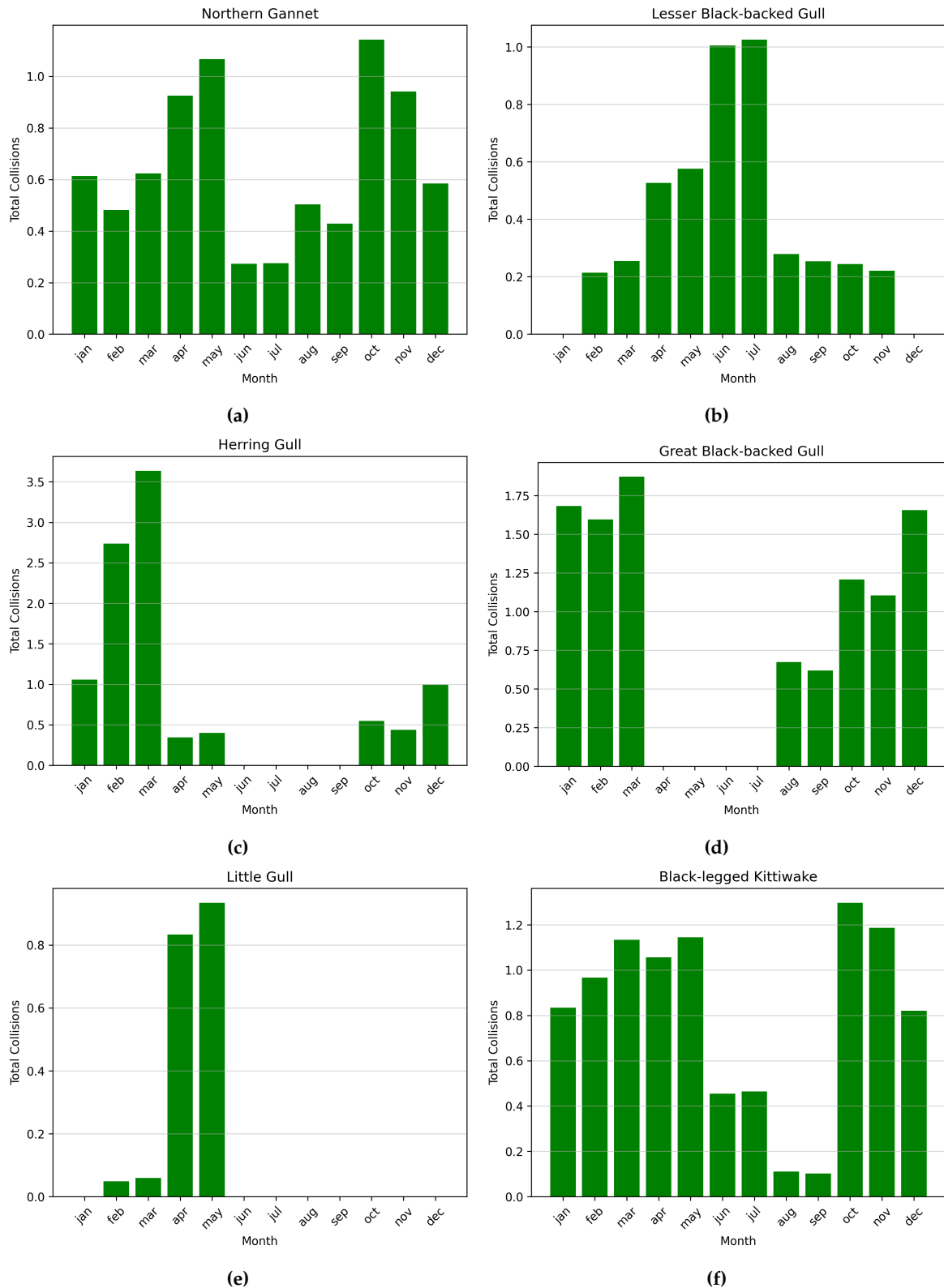


**Figure 6.2:** Baseline scenario collisions per month for all species.

The baseline results clearly show the significant influence of the monthly bird density inputs (Chapter 5). The number of collisions also varies seasonally across all species. Some species, like the little gull, are only active for a short period, while others—such as the northern gannet—are active throughout most

of the year, except for a few months. Offshore wind farms require periodic maintenance, and therefore significant reductions in collision numbers could be achieved by scheduling maintenance during periods when sensitive species are most active. Nevertheless, the proposed mitigation measures in Sections 6.3, 6.4, and 6.5 focus on reducing the total number of collisions over an entire year of wind farm operation.

The corresponding baseline values are also presented in Table 6.3. The last column shows the total yearly estimate as the sum of all monthly values. For comparison, the monthly collision estimates produced by Waardenburg Ecology are shown in Table 6.4. These were generated for the same turbine parameters (minimum tip height, rotor diameter, hub height) to enable verification of the baseline results. At first glance, the outcomes show a similar pattern in monthly collision distributions across all species—especially in the relative proportions. Additionally, for four species, the total yearly collision estimates are close to those shown in Table 6.4. On the other hand, the northern gannet and great black-backed gull show significantly different total collision numbers. It was confirmed that this is due to Waardenburg Ecology using a different FHD for both species (Gyimesi, pers. comm., 2025). In the next section, the SCRM results for varying minimum tip height are discussed.

**Table 6.3:** Monthly bird collision estimates per species, including the total collisions for one year. Species names abbreviated as: NG = Northern gannet, LBBG = Lesser black-backed gull, HG = Herring gull, GBBG = Great black-backed gull, LG = Little gull, BLK = Black-legged kittiwake.

Species	Jan	Feb	Mar	Apr	May	Jun	Jul	Aug	Sep	Oct	Nov	Dec	Sum
NG	0.6	0.5	0.6	0.9	1.1	0.3	0.3	0.5	0.4	1.1	0.9	0.6	<b>8</b>
LBBG	0.0	0.2	0.3	0.5	0.6	1.0	1.0	0.3	0.3	0.2	0.2	0.0	<b>5</b>
HG	1.1	2.7	3.6	0.3	0.4	0.0	0.0	0.0	0.0	0.5	0.4	1.0	<b>10</b>
GBBG	1.7	1.6	1.9	0.0	0.0	0.0	0.0	0.7	0.6	1.2	1.1	1.7	<b>11</b>
LG	0.0	0.0	0.1	0.8	0.9	0.0	0.0	0.0	0.0	0.0	0.0	0.0	<b>2</b>
BLK	0.8	1.0	1.1	1.1	1.1	0.5	0.5	0.1	0.1	1.3	1.2	0.8	<b>10</b>

**Table 6.4:** Monthly collision estimates as computed by (van der Vliet et al., 2022).

Species	Jan	Feb	Mar	Apr	May	Jun	Jul	Aug	Sep	Oct	Nov	Dec	Sum
NG	4.3	3.1	3.8	5.8	6.7	1.1	1.1	3.4	3.0	8.8	7.3	4.1	<b>53</b>
LBBG	0.0	0.3	0.3	0.5	0.6	1.1	1.1	0.3	0.3	0.3	0.2	0.0	<b>5</b>
HG	0.8	2.4	3.0	0.2	0.3	0.1	0.1	0.1	0.1	0.4	0.4	0.8	<b>9</b>
GBBG	2.9	2.1	2.4	0.4	0.4	0.5	0.5	0.6	0.6	1.7	1.6	2.9	<b>17</b>
LG	0.0	0.1	0.1	1.1	1.3	0.0	0.0	0.0	0.0	0.0	0.0	0.0	<b>3</b>
BLK	0.8	0.9	1.0	1.0	1.1	0.5	0.5	0.1	0.1	1.3	1.2	0.8	<b>9</b>

### 6.3. Results for Varying Minimum Tip Height

To investigate the influence of minimum tip height on collision numbers, a simulation is performed for different values of the minimum tip height. All other turbine parameters are kept constant. This way, the relationship between total collisions and minimum tip height can be determined. Figure 6.3 presents the results from varying the minimum tip height from 15 to 60 m. Realistically, the upper limit for the minimum tip height is 40 m, as, according to an expert (Gyimesi, pers. comm., 2025), any turbine design becomes unfeasible at values above 40 m. A minimum of 15 m is chosen in order to demonstrate the effect of decreasing from the base case value of 25 m, while still maintaining an air gap for extreme wave conditions.

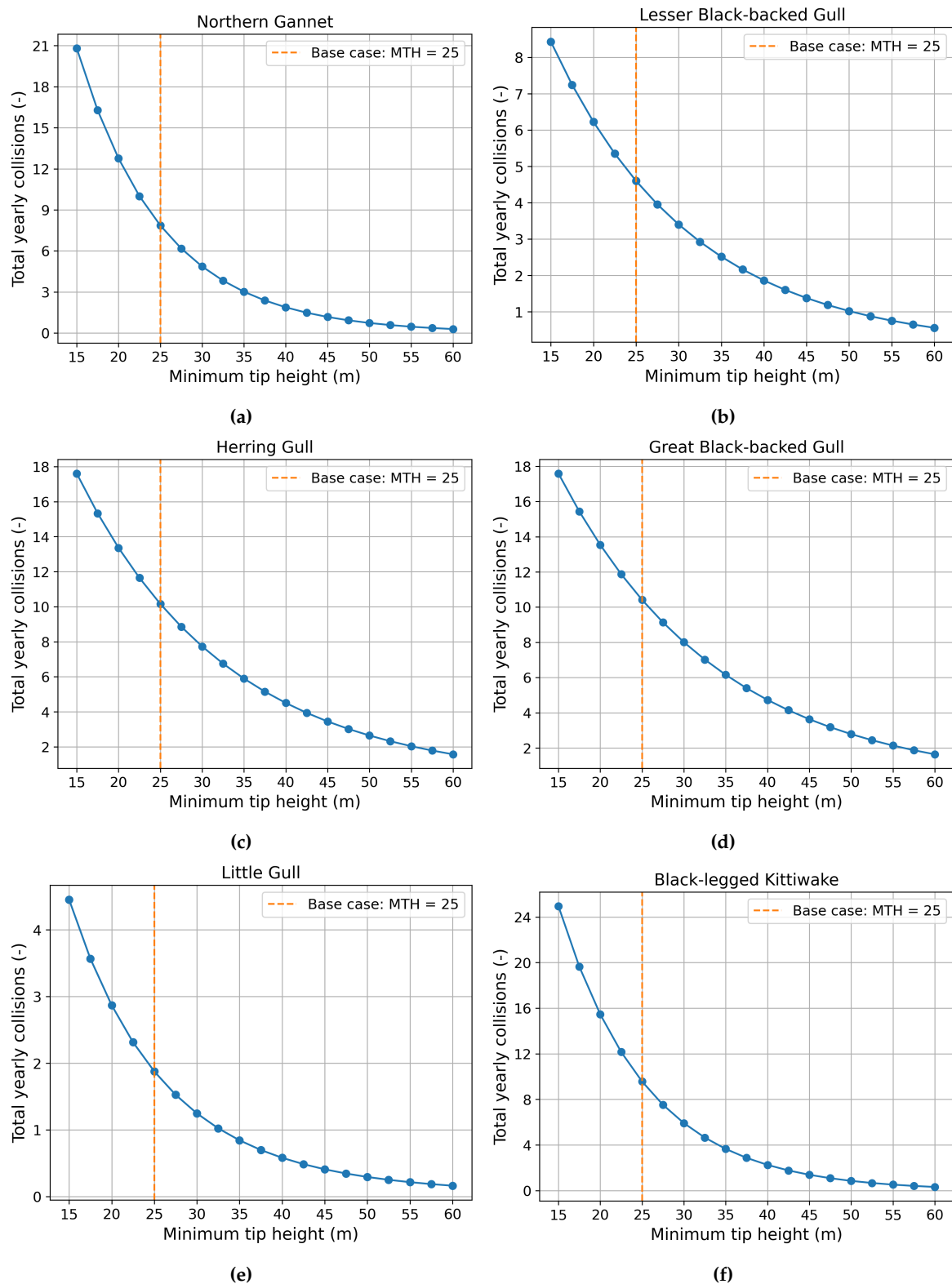


**Figure 6.3:** Calculated yearly collisions for various minimum tip heights.

In Figure 6.3, all plots feature a vertical dashed line indicating the base case value of 25 m for the minimum tip height (MTH). At first glance, it is clear that for all species, collision numbers decrease as minimum tip height increases. The plot for the black-legged kittiwake shows a reduction of almost 5

collisions for a 5 m increase in tip height. The northern gannet, herring gull, great black-backed gull, and lesser black-backed gull show a reduction of at least 2 collisions within the same range. The little gull shows the least reduction, with less than 1 collision avoided for the first 5 m increase in MTH. Furthermore, diminishing returns are evident: the initial metres of tip height increase result in greater reductions than later increments—although this effect varies per species. The total number of avoided collisions also appears proportional to the base case collision estimates. Finally, all species show sharply increasing collision estimates when the tip height is reduced to 15 m.

It is expected that the total number of seabird collisions decreases as the minimum tip height increases, a relationship supported by many studies (Chapter 2). Any seabird flying below the rotor swept area will avoid collision, and increasing MTH raises the probability that birds follow such flight paths. The flight height distributions (FHDs) of seabirds (Figure 6.1) significantly influence how effective increasing MTH is at reducing collisions. This effect is demonstrated by comparing FHDs (Figure 6.1) with the calculated collisions in Figure 6.3. The lesser black-backed gull, great black-backed gull, and herring gull—whose FHDs extend to approximately 75 m—show a more linear decline in collisions with increasing MTH. In contrast, the northern gannet, little gull, and black-legged kittiwake—whose FHDs extend only to around 50 m—show a more curved decline. The effectiveness of increasing MTH therefore depends on the species-specific FHD.

In addition, another phenomenon contributes to the decrease in collisions as MTH increases. Figure 6.4 shows the distribution of target probability (trefkans) and collision probability (aanvaringskans) within the rotor plane. The target probability reflects the likelihood that a bird flies through the rotor swept area. This probability decreases with vertical distance from the rotor centreline—i.e. when birds fly significantly above or below the rotor hub. The collision probability is highest near the hub and lower near the outer blade tips. Together, these two distributions define the overall collision risk within the rotor plane, as illustrated in Figure 6.4. Increasing the MTH results in a higher hub height, which reduces the likelihood of seabirds flying within the rotor swept area (see also Figure 6.1).

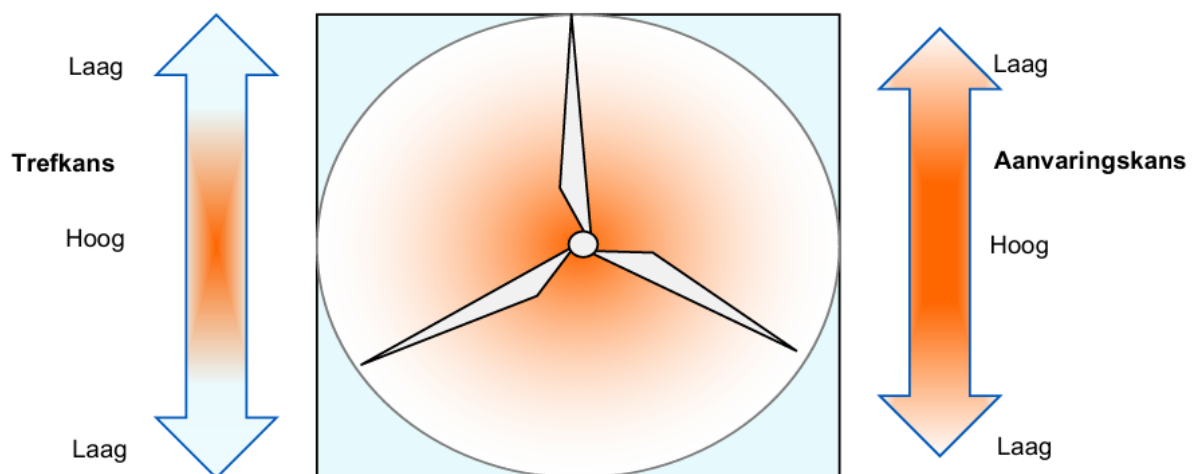


**Figure 6.4:** Illustration of collision risk varying throughout the rotor swept area (van der Vliet et al., 2022).

To provide a clear visualisation of how different species respond to changes in tip height, a combined plot is made for all species. Figure 6.5 shows the total yearly collisions versus minimum tip height for all species. As shown, increasing the MTH significantly reduces bird collisions across all species. The black-legged kittiwake and northern gannet experience the highest collision rates at lower tip heights, with more than 20 collisions per year when the MTH is around 15 m. Meanwhile, the little gull consistently shows the lowest collision numbers across all cases. Overall, increasing the MTH is effective at reducing collisions, but the extent of the reduction varies per species. This is particularly evident for the lesser black-backed gull and herring gull, whose curves are comparatively flatter. Finally, Figure 6.5 shows that even at an MTH of 60 m, the herring gull and great black-backed gull still experience

collisions, likely due to their broader FHDs extending up to 75 m.

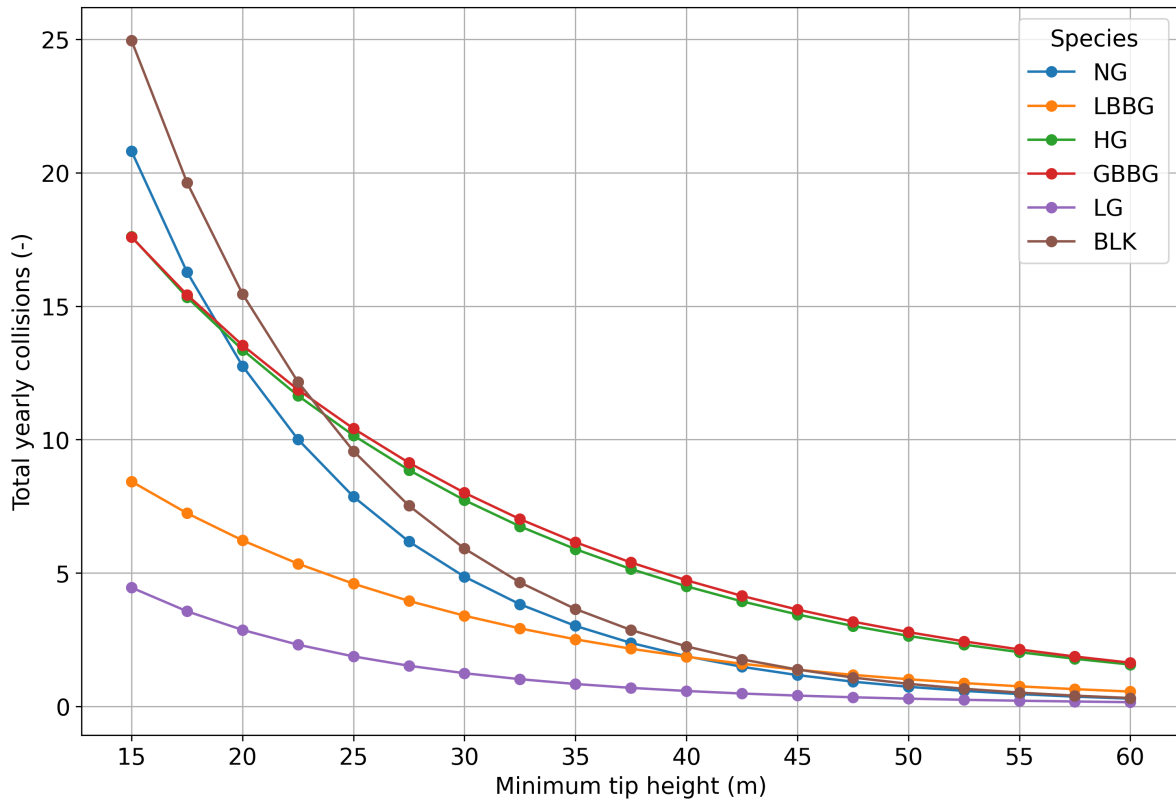


**Figure 6.5:** Computed yearly collisions for all species vs. minimum tip height. NG = Northern gannet, LBBG = Lesser black-backed gull, HG = Herring gull, GBBG = Great black-backed gull, LG = Little gull, BLK = Black-legged kittiwake.

In combination with the results from the LCoE model in Chapter 7, conclusions can be drawn on cost-effectiveness. The next section presents the results for a varying rotor diameter.

## 6.4. Results for Varying Rotor Diameter

To investigate the influence of rotor diameter on bird collisions, a simulation is performed where the rotor diameter is varied, while keeping other turbine parameters as constant as possible. Rotor diameters ranging from 186 m to 286 m are selected, as these values reflect typical lower and upper bounds for present-day wind turbines (10–20 MW). The results are presented in Figure 6.6, showing the relationship between rotor diameter and collision risk for the six critical bird species.

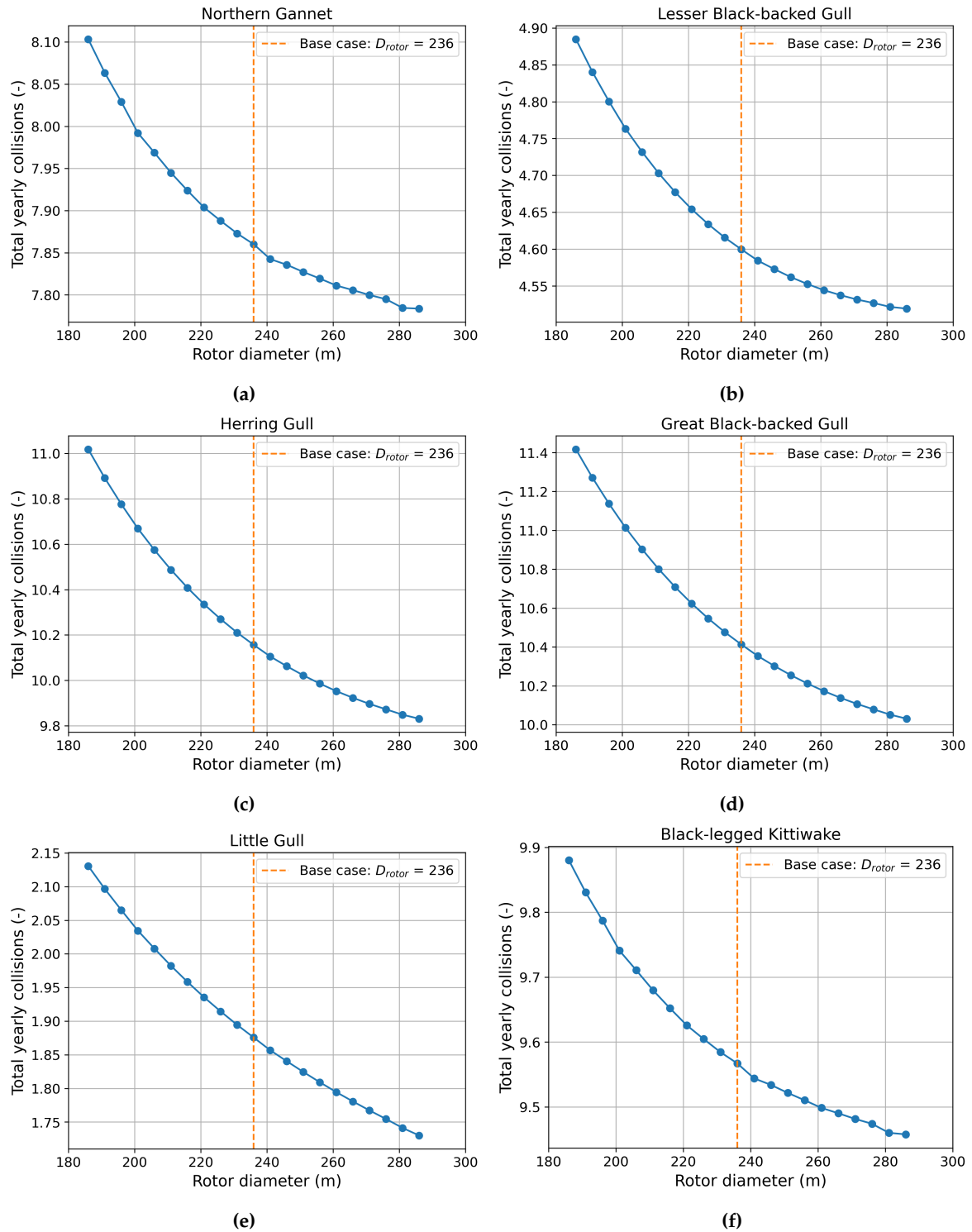


**Figure 6.6:** Calculated yearly collisions for various rotor diameters.

In Figure 6.6, the vertical dashed line marks the base case rotor diameter of 236 m. The results clearly show that changing the rotor diameter is less effective than changing the minimum tip height across all species. The herring gull and great black-backed gull show a reduction of at least one collision when increasing the rotor diameter from 186 m to 286 m. All other species show less than one collision reduction over the entire simulation range. Even relative to the base case, the change in total collisions is minor. Based on these results, it can be concluded that varying rotor diameter has only a small influence

on predicted collision numbers across all species.

The underlying mechanism is similar to that described in the previous section. As shown in Figure 6.4, collision risk is highest near the rotor hub. Increasing the rotor diameter pushes the hub height higher, assuming a fixed minimum tip height of 25 m. While the rotor swept area increases, the elevation of the hub places the high-risk region of the rotor plane at altitudes where fewer birds are flying. This results in a net decrease in predicted collisions, as illustrated in Figure 6.6.

It should be noted that the rotational speed of the rotor was not changed during this simulation. Consequently, the power output is not fully realistic for turbines with significantly different rotor sizes. This limitation is explained in more detail in Chapter 7. The SCRM applies the same rotational speed and blade pitch dataset for all rotor diameters. A more realistic approach would involve adjusting this dataset based on rotor size, such that turbines with smaller rotors have a higher rated RPM and those with larger rotors a lower RPM. With this refinement, the collision values in Figure 6.6 would likely show a greater increase to the left of the dashed line, and a steeper decrease to the right.

To further analyse the impact of rotor diameter across all species, a graph is produced showing total yearly collisions for all species combined (Figure 6.7). This provides insight into the overall effectiveness of rotor diameter adjustments as a mitigation measure. Minimal changes are observed, reinforcing the conclusion that, compared to raising the minimum tip height, increasing the rotor diameter alone is not an effective strategy for reducing seabird collisions.

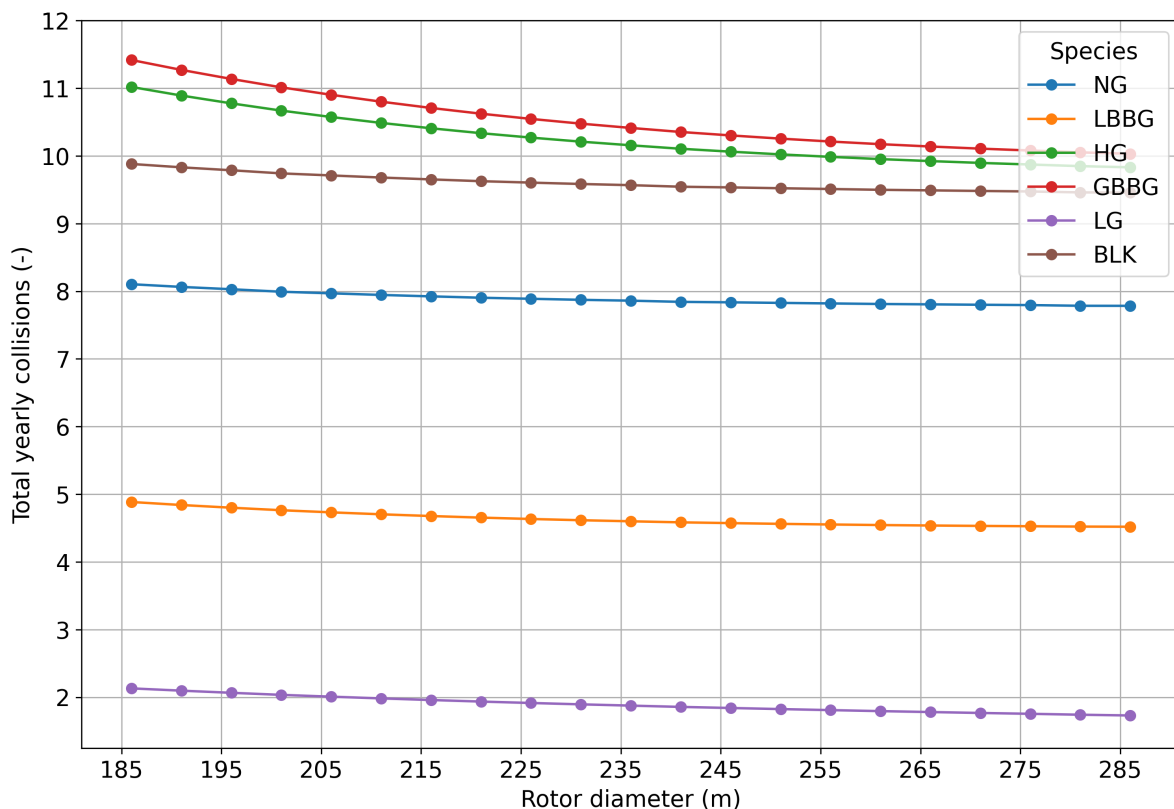


**Figure 6.7:** Computed yearly collisions for all species vs. rotor diameter. NG = Northern gannet, LBBG = Lesser black-backed gull, HG = Herring gull, GBBG = Great black-backed gull, LG = Little gull, BLK = Black-legged kittiwake.

In combination with the results from the LCoE model in Chapter 7, conclusions can be drawn on cost-effectiveness. The next section presents the results for varying the turbine rated power.

## 6.5. Results for Varying Turbine Rated Power

To evaluate how turbine rated power influences bird collision risk, a simulation is conducted in which the rated power is varied. The tested rated power values range from 10 MW to 20 MW, covering both present-day and anticipated future turbine sizes. The minimum tip height remains constant at 25 m, but the rotor diameter and hub height vary accordingly. These values are presented in Chapter 7. In addition, the total yearly collisions for a 20 MW turbine wind farm are compared to collision estimates calculated in (van der Vliet et al., 2022) as a reference. The results of the simulation are presented in Figure 6.8, which illustrates the total yearly collisions for each species under different rated power scenarios.

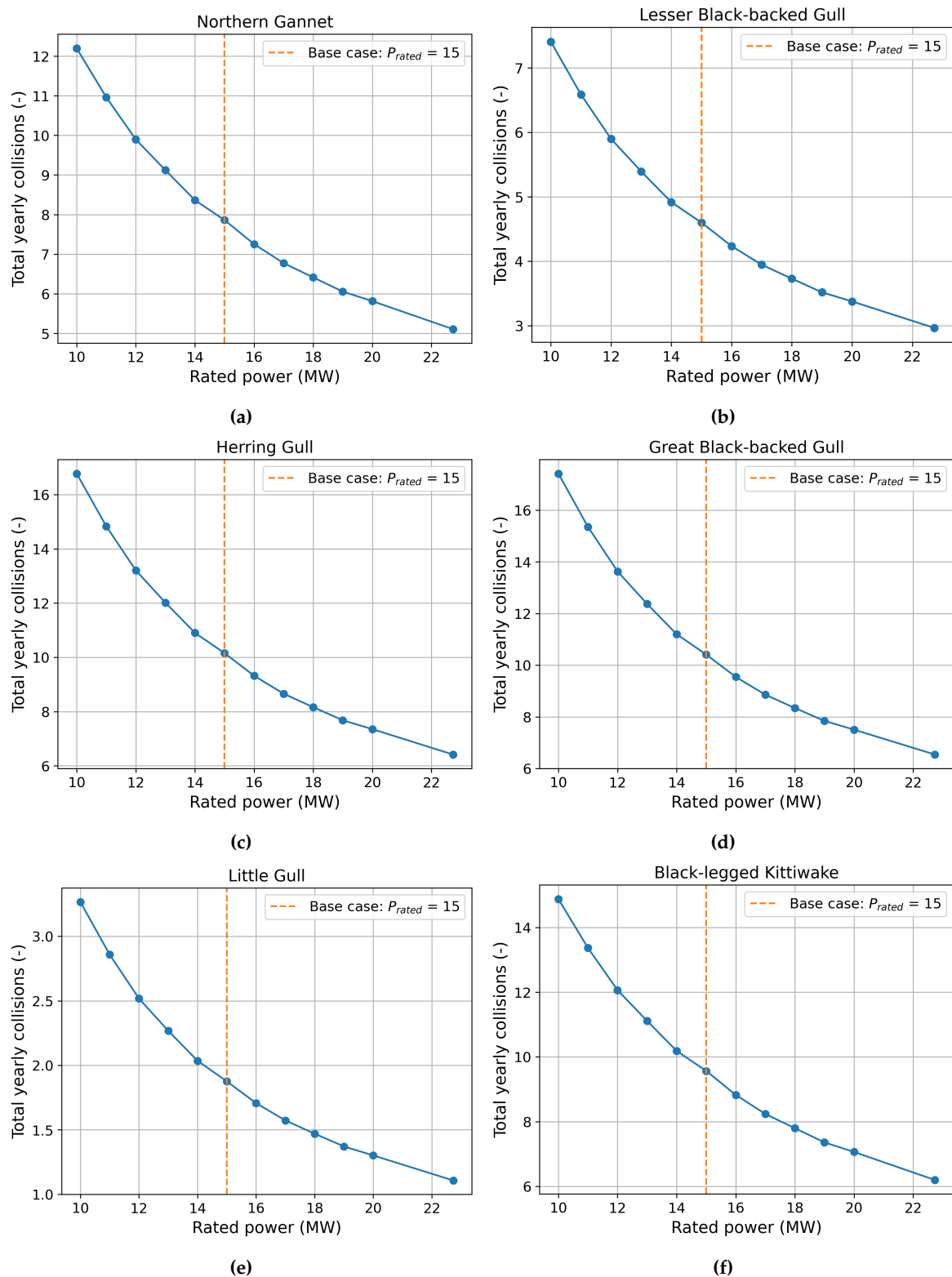


**Figure 6.8:** Calculated yearly collisions for various rated powers.

In Figure 6.8, the vertical dashed line indicates the base case scenario, consisting of 67 turbines rated at 15 MW each. The number of turbines is adjusted to maintain a total installed capacity of 1 GW. The results show that increasing rated power reduces the number of bird collisions for all species. The

smallest reduction is observed for the little gull and the lesser black-backed gull. For the northern gannet, collisions decrease from eight to six compared to the base case. The other three species show a reduction of three collisions for the 20 MW turbine case. A trend of diminishing returns is again visible: increasing from 10 MW to 15 MW results in more pronounced reductions than increasing from 15 MW to 20 MW. The shape of the graphs resembles those seen for minimum tip height variations, suggesting that flight height distributions (FHDs) have less influence here, since the reduction in turbine number becomes the dominant effect. Overall, increasing rated power from 10 MW to 15 MW is more effective than increasing from 15 MW to 20 MW. The results of Figure 6.8 confirm that wind farms with larger turbine capacities can reduce collisions for the six critical bird species.

The decreasing trend in collisions with increasing rated power can be explained by the same principles discussed in Sections 6.3 and 6.4. Larger turbines typically have higher hub heights, which reduces the likelihood of bird collisions. More importantly, the total number of turbines is reduced for the same installed capacity, which significantly lowers total collision estimates. As explained in Chapter 3, the number of turbines is proportional to total collision predictions in the Band model framework.

Again, it must be noted that the RPM vs. wind speed profile is kept constant for all turbine sizes. In practice, 10 MW turbines would rotate faster, while 20 MW turbines would operate at lower rotational speeds. As a result, collision numbers to the left of the orange dashed line would be higher, and those to the right lower, if turbine-specific RPM profiles were used.

A final graph was again created for all species combined, illustrating the overall effectiveness of this mitigation strategy. These results are presented in Figure 6.9.

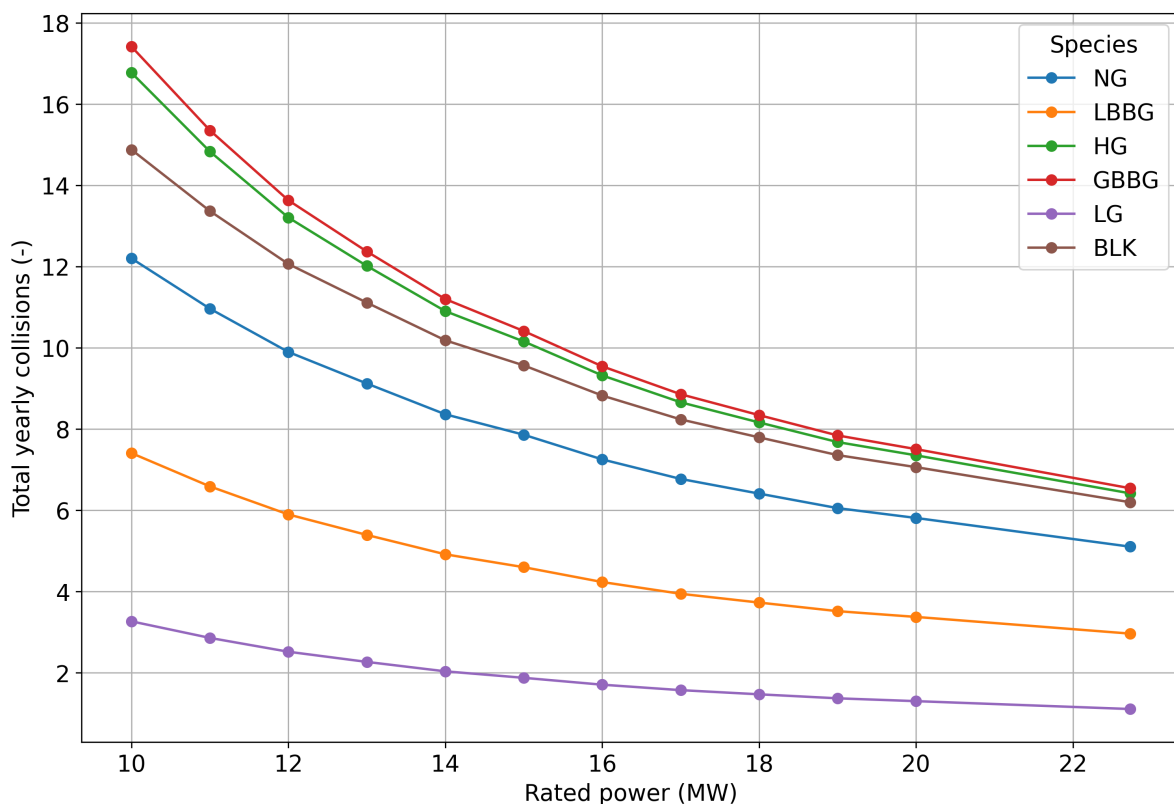


**Figure 6.9:** Computed yearly collisions for all species vs. rated power. NG = Northern gannet, LBBG = Lesser black-backed gull, HG = Herring gull, GBBG = Great black-backed gull, LG = Little gull, BLK = Black-legged kittiwake.

The results show a clear downward trend: increasing the rated power reduces collisions for all species. Species with high collision rates at 10 MW show the most significant decline when increasing to

15 MW. This suggests that the industry-wide trend toward larger turbine capacities may be beneficial for maintaining acceptable collision levels within offshore wind farms. Finally, the total yearly collisions for all species, as calculated by (van der Vliet et al., 2022), are presented in Table 6.5. Comparing these to Figure 6.9 provides an indication of the accuracy of the current results. The calculated collisions for wind farm with 20 MW turbines in this research resemble the value of the herring gull, little gull and black-legged kittiwake from Table 6.5. The calculation for the lesser-black backed gull has a slightly lower estimated value, while the calculations for the great black-backed gull and northern gannet show larger deviations, due to similar reasoning as explained in Section 6.2.

**Table 6.5:** Maximum total collisions per year for two wind farm scenarios with 15 and 20 MW turbines, calculated by (van der Vliet et al., 2022).

Species (group)	Alternative 1	Alternative 2
	67 × 15 MW (236 m diameter)	50 × 20 MW (280 m diameter)
Northern gannet	53	39
Lesser black-backed gull	5	5
Herring gull	9	7
Great black-backed gull	17	14
Little gull	3	2
Black-legged kittiwake	9	7

## 6.6. Collision Risk Modelling Summary

The collision risk modelling results show that increasing the minimum tip height is the most effective measure for reducing bird collisions, particularly during the first few metres of increase. A change in rotor diameter has only a minimal impact on collision numbers. An offshore wind farm with fewer, larger turbines offers the benefit of reduced collision estimates across all six species as well. The next chapter assesses the economic feasibility of these design modifications using Levelised Cost of Energy (LCoE) modelling for offshore wind farm development.

# 7

## WINDOW LCoE Modelling

This chapter addresses the research question: What is the economic feasibility of design variations in minimum tip height, rotor diameter, and rated power within the defined scenario? To evaluate the economic impact of each strategy, this chapter presents the setup and results of a series of simulations using the WINDOW model—a multidisciplinary tool designed to assess key financial drivers in offshore wind farm development. The primary objective of these simulations is to quantify the influence of varying minimum tip height, rotor diameter, and turbine rated power on the Levelised Cost of Electricity (LCoE). The chapter begins by introducing the structure and methodology of the WINDOW model, outlining its core modules and their relevance to this study. Following this, a detailed assessment is provided of how the model was adapted to incorporate new input parameters and meet governing technical criteria. The subsequent sections contain simulation results for each mitigation strategy, including both absolute and normalised LCoE values. Trends and cost sensitivities across key components—such as support structure, installation, and operations and maintenance—are explored in relation to turbine design variations. The chapter concludes by summarising the observed cost trends, providing an economic foundation for the integrated discussion in the following chapter.

### 7.1. Model Overview

WINDOW openMDAO uses multidisciplinary analysis and optimisation (MDAO) to perform calculations across various disciplines in offshore wind farm (OWF) design simultaneously. It offers a range of functionalities to optimise and evaluate key financial drivers in offshore wind development. These include the computation of Levelised Cost of Electricity (LCoE), Levelised Cost of Hydrogen (LCoH), and internal rate of return (IRR). Additionally, the optimisation workflow is customisable based on user needs, as investigated by (Perez-Moreno et al., 2018).

The WINDOW model was most recently updated in the work of (Mehta et al., 2024), which introduced functionality to vary rotor diameter and turbine rated power. As described in Chapter 5, minimum tip height (MTH) is added as an additional design variable in this study. Figure 7.1 presents a schematic overview of all analysis components, including user inputs and design variables, and has been extended to highlight the analysis modules affected by the inclusion of MTH. All source code for WINDOW is publicly available via (Mehta, 2023).

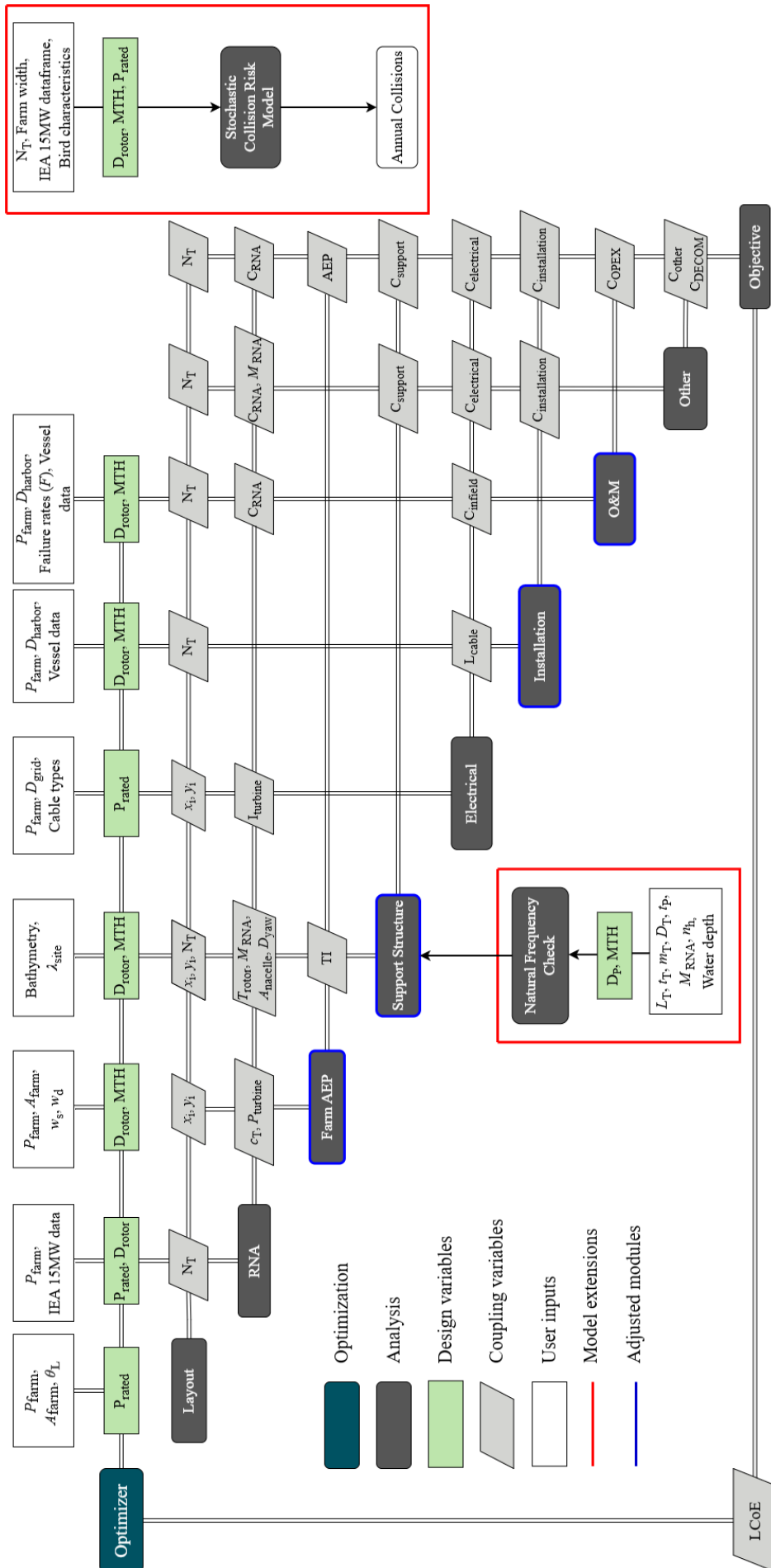


Figure 7.1: Framework of the Ecology-Technology model, based on the original framework structure from (Mehta et al., 2024).

Figure 7.1 presents the framework for the Ecology-Technology model developed in this research. In Figure 7.1, the inputs (white blocks) and design variables (green blocks) are shown above each analysis module (grey blocks). The coupling variables are interchanged between the modules, as indicated by the connecting lines. The model extensions explained later in this chapter are circled in red. The collision risk model is called separately from the WINDOW MDAO analysis and does not communicate with the WINDOW LCoE model during simulation. The natural frequency check is also run before the main LCoE simulation, with its outputs passed to WINDOW prior to the simulation start. Aside from these model extensions, the framework in Figure 7.1 is the same as in the research of (Mehta et al., 2024).

As seen in Figure 7.1, the analysis blocks Farm AEP, Support Structure, Installation, and O&M were identified as the modules that needed modification to correctly incorporate the design variable MTH. These modules are circled with blue. The rationale behind these changes was mainly discussed in Chapter 5. Both the rationale behind the module modifications and the modifications themselves are explained in further detail later in this chapter. Not all modules required extensive adjustments. For example, the Farm AEP module only needed an additional argument to pass the MTH input. This is because hub height already influences AEP through wind speed correction via the power law. The calculation of hub height based on MTH is discussed in the next section.

WINDOW is used in this research to investigate changes in LCoE for a hypothetical wind farm when certain bird collision mitigation measures are applied. As shown in Figure 7.1, the core objective of WINDOW is to calculate an optimised value for the Levelised Cost of Electricity (LCoE). The LCoE is computed using the expression in Equation 7.1, where  $L$  is the operational lifetime of the wind farm,  $r$  is the real discount rate, and  $n$  is the year number. The numerator consists of capital expenditures ( $C_{\text{CAPEX}}$ ), the sum of discounted annual operational expenditures ( $C_{\text{OPEX}}$ ), and decommissioning costs at the end of the project lifetime ( $C_{\text{DECEX}}$ ). The denominator includes the discounted sum of the farm's annual energy production (AEP) (Mehta et al., 2024):

$$\text{LCoE} = \frac{C_{\text{CAPEX}} + \sum_{n=1}^L \frac{C_{\text{OPEX}}}{(1+r)^n} + \frac{C_{\text{DECEX}}}{(1+r)^L}}{\sum_{n=1}^L \frac{\text{AEP}}{(1+r)^n}} \quad (7.1)$$

Equation 7.1 shows that the Levelised Cost of Electricity (LCoE) is influenced by three main cost categories—CAPEX, OPEX, and DECEX—alongside the annual energy production (AEP) of the wind farm. Given the scope and time constraints of this research, it is important to identify which modules contribute most significantly to the LCoE calculation. The relative contributions of various wind farm components to the LCoE, as calculated by the WINDOW model, were examined in the study by (Mehta et al., 2022). CAPEX was identified as the dominant contributor to LCoE. For example, installation costs for the foundation and turbine vary with turbine size due to differences in the required installation vessels. Additionally, the procurement costs of the foundation and tower are sensitive to hub height. Most of these components are also dependent on rotor diameter, a variable already incorporated into the model following the updates by (Mehta et al., 2024).

Operations and maintenance (O&M) costs—classified under OPEX—were also found to constitute a major share of the total LCoE (Mehta et al., 2022). As described in Chapter 5, vessel-related maintenance costs must be scaled based on hub height, making this module particularly relevant for modification in the context of minimum tip height (MTH) variation. Together with the CAPEX contributions mentioned above, OPEX and CAPEX account for approximately 98% of the total LCoE result, enabling a reasonably accurate simulation of design trade-offs related to MTH, should these two components be adjusted correctly.

In contrast, decommissioning costs (DECEX) have a relatively small effect on the overall LCoE. As seen in Equation 7.1, these costs are incurred only at the end of the project lifetime and are therefore substantially reduced by the discounting effect (Zaaijer, pers. comm., 2025). For this reason, decommissioning costs will not be adjusted in relation to MTH variation. Note that Figure 7.4 further in this chapter shows

contribution of individual CAPEX components, as well as OPEX and DECEX to LCoE. The next section explores the technical criteria that govern the integration of ecological and technological objectives for the Ecology-Technology model framework.

## 7.2. Governing Criteria

In Chapter 5, various governing effects associated with applying the proposed design changes to individual turbines were explored. The Ecology-Technology model should be able to perform three simulations: varying the minimum tip height (MTH), rotor diameter  $D_{rotor}$ , and rated power  $P_{rated}$ . It is important to analyse the technical consequences of these variations, as each design change affects the structural configuration of the turbine, which must remain functional over its designated lifetime. For each simulation, the results were assessed to determine whether the governing criteria remained within realistic limits. This research focuses primarily on governing criteria for the support structure design. Furthermore, vessel type selection will also be updated in the model, which is discussed in the next section. Operational limitations were also discussed in Chapter 5, but these are considered out of scope for further analysis. This section focuses on the support structure in terms of bending stress, natural frequency, and embedded length.

The WINDOW model developed by (Mehta et al., 2024) was initially designed to support variations in rotor diameter and rated power. It is intended for fast, first-order estimations with reasonable accuracy, relying on several assumptions as described in the foundational work of (Zaaijer, 2013). Introducing variations in MTH—effectively increasing the hub height—must therefore be implemented without violating any of the governing technical constraints of individual turbine components. However, improving upon the structural design basis of (Zaaijer, 2013) is beyond the scope of this study. The assumptions underpinning the WINDOW model are deemed sufficiently robust for meeting the objectives of this research. Moreover, only the effects of MTH variation on governing criteria are analysed here, as rotor diameter and rated power variations have already been addressed in the work of (Mehta et al., 2024). Limitations of the model regarding all three design variables will be discussed later in more detail.

As previously stated, this section prioritises support structure design criteria, with a particular focus on the foundation (monopile). A key function of the monopile is to safely transfer all loads from the wind turbine to the seabed while staying within allowable deformation limits (Arany et al., 2017). According to Limit State Design philosophy, a wind turbine support structure must satisfy the following limit states over its full operational life (Arany et al., 2017):

- **Ultimate Limit State (ULS):** Ensures structural resistance to extreme loads, primarily overturning moment, lateral load, and vertical load.
- **Serviceability Limit State (SLS):** Limits deformations and ensures the natural frequency of the structure avoids resonant excitation.
- **Fatigue Limit State (FLS):** Evaluates the fatigue life of the monopile under long-term cyclic loading conditions.

The design requirements for the monopile vary depending on which limit state is assessed. Ideally, all three are checked to determine which one governs the final design. In WINDOW, the support structure is optimised based on ULS design. This research primarily considers ULS criteria by analysing bending stresses, and SLS criteria by examining natural frequency and embedded length. A full FLS-based monopile design is outside the scope of this study. However, fatigue is indirectly accounted for in WINDOW through the use of a safety factor (Mehta et al., 2024). The impact of increased MTH on turbine fatigue life will be discussed briefly in Chapter 8.

A focused analysis of key technical parameters for the support structure was carried out by generating simulation results for MTH values ranging from 15 to 60 m. By examining the structural dimensions of the turbine for each case, it was possible to identify which design criteria may become critical. Table 7.1 presents the changes observed in selected technical parameters as the minimum tip height increases. The abbreviations are explained in the next subsection for the overturning moment analysis.

**Table 7.1:** Technical parameters for varying minimum tip height.  $P_{\text{rated}} = 15$ .

$D_{\text{rotor}}$ (m)	$z_{\text{hub}}$ (m)	MTH (m)	$L_T$ (m)	$L_P$ (m)	$L_e$ (m)	$D_P$ (m)	$L_e/D_P$
236.0	133.0	15.0	117.2	73.3	37.0	7.86	4.71
236.0	138.0	20.0	118.8	73.4	37.0	7.88	4.70
236.0	143.0	25.0	123.8	73.7	37.3	7.95	4.69
236.0	147.0	30.0	128.8	74.0	37.5	8.02	4.67
236.0	152.0	35.0	133.8	74.3	37.7	8.10	4.65
236.0	158.0	40.0	138.8	74.7	37.9	8.17	4.64
236.0	163.0	45.0	143.8	75.0	38.1	8.23	4.63
236.0	168.0	50.0	148.8	75.2	38.3	8.30	4.61
236.0	173.0	55.0	153.8	75.5	38.5	8.37	4.60
236.0	178.0	60.0	158.8	75.8	38.7	8.43	4.59

### 7.2.1. Overturning Moment

Using Table 7.1, the first relevant criterion is the monopile's capability to withstand maximum loads, specifically the overturning moment primarily caused by the wind thrust force (see Chapter 5). This overturning moment increases with increasing hub height. The ULS analysis for monopile design in WINDOW considers three ultimate loading conditions (Mehta et al., 2024):

1. **Operational Condition:** The turbine operates at rated wind speed with the maximum wave load occurring in a 1-year extreme sea state.
2. **Parked with Reduced Gust:** The turbine is parked, experiencing a reduced gust in a 50-year average wind speed, along with the maximum wave in a 50-year extreme sea state.
3. **Parked with Maximum Gust:** The turbine is parked under maximum gust conditions in a 50-year average wind speed, accompanied by reduced wave conditions in a 50-year extreme sea state.

For the analysis results from Table 7.5, WINDOW selects load case 1 as governing for this case study, due to the rated wind speed being the main contributor to the total transversal loads, overturning moment, and resulting stresses in the structure. The thrust force at rated wind speed appears to be the dominant factor in monopile sizing, as supported by literature (McWilliam et al., 2021). According to (Zaaijer, 2013), the monopile diameter  $D_P$  is the critical design parameter, estimated by requiring the total bending stress in the monopile to remain below the yield stress of steel. For instance, monopile wall thickness is typically determined to prevent buckling during pile driving.

To compare WINDOW's computed values, several references were consulted. The NREL 15 MW reference turbine has a monopile diameter of 10 m (Gaertner et al., 2020), which aligns with the 15 MW base case turbine in this study. Similarly, DTU's analysis (McWilliam et al., 2021) reports monopile diameters between 9–10 m under comparable conditions. Additionally, (Arany et al., 2017) presents a step-by-step approach to first-order sizing of monopiles, which is used here to verify WINDOW's output.

Given that load case 1 is governing, the wind thrust force can be estimated using the following simplified expression:

$$T = \frac{1}{2} \rho_a A_R C_T U^2 \quad (7.2)$$

where  $\rho_a$  is the air density,  $A_R$  the rotor swept area,  $C_T$  the thrust coefficient, and  $U$  the wind speed. Assuming  $\rho_a = 1.225 \text{ kg/m}^3$ ,  $C_T = 0.812$ , and using base case values from Chapter 5, the thrust force is

calculated as  $T = 2.42$  MN. This value closely matched the output from the WINDOW model, indicating that a static wind load is assumed.

Then, using water depth  $S = 30$  m and hub height  $z_{hub} = 143$  m, the overturning moment at the mudline from wind thrust is:

$$M_{wind} = T(S + z_{hub}) \approx 418 \text{ MNm} \quad (7.3)$$

WINDOW also includes aerodynamic loading on the tower, hydrodynamic loading on the monopile, and gravitational forces. For brevity, these forces are omitted from manual calculation but are internally accounted for in the model. The total overturning moment reported by WINDOW is  $M_y = 492$  MNm. Applying a load factor  $\gamma_L = 1.35$  gives a total design moment of 665 MNm.

The corresponding bending stress in the monopile is evaluated using:

$$\sigma_m = \frac{M_y}{I_P} \cdot \frac{D_P}{2} < \frac{f_{yk}}{\gamma_M} \quad (7.4)$$

where  $\sigma_m$  is the maximum bending stress,  $I_P$  the moment of inertia of the pile cross-section,  $D_P$  the pile diameter,  $f_{yk}$  the yield stress of steel, and  $\gamma_M$  the material factor. The moment of inertia is estimated as:

$$I_P = \frac{1}{8}(D_P - t_p)^3 t_p \pi \quad (7.5)$$

with  $t_p = 86$  mm from WINDOW. Setting  $f_{yk} = 355$  MPa and  $\gamma_M = 1.1$ , the equation can be rearranged to:

$$\frac{D_P}{I_P} < \frac{2f_{yk}}{\gamma_M M_y}$$

Solving this using a root-finding algorithm in Python gives  $D_P \approx 5.65$  m. This is a first-order estimate under static loading. (Arany et al., 2017) recommends verifying other design aspects, such as the use of a dynamic amplification factor (DAF). However, WINDOW applies both DAF and fatigue safety factors internally (Mehta et al., 2024), which partially explains why its output is larger ( $D_P = 7.95$  m).

A further method of verification is comparing how  $D_P$  changes with increasing MTH. The additional overturning moment due to hub height increase mainly results from a longer moment arm. Comparing the  $D_P$  values from Table 7.2 to those from Table 7.1 offers a means to verify that WINDOW correctly estimates the relationship between  $D_P$  and MTH.

**Table 7.2:** Estimated monopile diameters for ultimate bending stress analysis.

MTH (m)	$z_{hub}$ (m)	$D_P$ (m)
25	143	5.65
30	148	5.72
35	153	5.79
40	158	5.85
45	163	5.92
50	168	5.98
55	173	6.05
60	178	6.11

From Table 7.2, an additional diameter of  $6.11 - 5.65 = 0.46$  m is observed for an MTH of 60 m. Comparing this with Table 7.1, WINDOW computes an increase of  $8.43 - 7.95 = 0.48$  m for the same

MTH change from 25 m to 60 m. Based on this analysis, it is assumed that WINDOW estimates the monopile diameter for the ultimate load case in an acceptably accurate manner when varying the minimum tip height.

### 7.2.2. Natural Frequency

A second governing criterion arises from the natural frequency limits of the support structure. As the tower becomes more slender with increasing minimum tip height (MTH), the natural frequency may decrease, potentially violating design constraints. The importance of maintaining the natural frequency between the 1P and 3P excitation frequencies was discussed in detail in Chapter 5. For a first-order approximation, the natural frequency of the turbine can be estimated by modelling the structure as a cantilevered beam with equivalent stiffness properties. Following the methodology provided in the same step-by-step design guide, a three-spring model is used to account for the combined stiffness of the tower, monopile, and soil. This simplified representation, illustrated in Figure 7.2, includes stiffness coefficients  $K_L$ ,  $K_R$ ,  $K_{LR}$ , and  $K_V$ , which define the foundation stiffness and depend on monopile geometry and the soil profile (Arany et al., 2017).

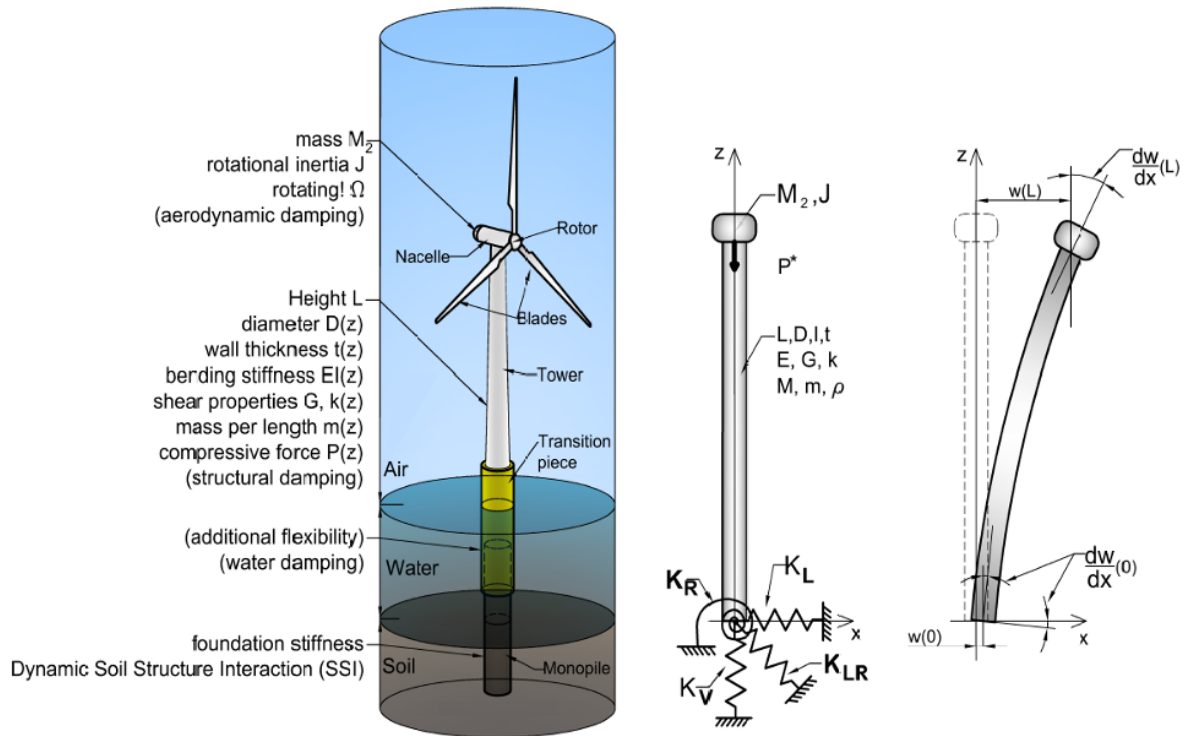


Figure 7.2: Illustration of the simplified foundation stiffness model (Arany et al., 2017).

As discussed in Chapter 5, the turbine is designed with a soft–stiff configuration. This implies that its first natural frequency should lie above the highest 1P excitation frequency and below the lowest 3P excitation frequency. Given a minimum rotor speed of 5 RPM and a maximum of 7.56 RPM, the natural frequency requirement becomes:  $0.126 \text{ Hz} < f_0 < 0.250 \text{ Hz}$ . To assess compliance with this criterion, the natural frequency is calculated using the methodology proposed by Arany et al. (2017), originally developed in Arany et al. (2016). This method estimates the tower's natural frequency based on a cantilever beam formulation, incorporating correction coefficients to account for the flexibility of the monopile foundation. According to this approach, the first natural frequency of the turbine is given by:

$$f_0 = C_L C_R C_S f_{FB} \quad (7.6)$$

where  $C_L$  and  $C_R$  are the lateral and rotational flexibility coefficients for the foundation,  $C_S$  is the substructure flexibility coefficient, and  $f_{FB}$  is the fixed base tower natural frequency. First,  $f_{FB}$  is

calculated with:

$$f_{FB} = \frac{1}{2\pi} \sqrt{\frac{3E_T I_T}{L_T^3 (m_{RNA} + \frac{33}{140} m_T)}} \quad (7.7)$$

where  $E_T$  is the Young's modulus of the tower material,  $I_T$  is the average area moment of inertia of the tower cross-section,  $L_T$  is the tower length,  $m_{RNA}$  is the rotor-nacelle assembly mass, and  $m_T$  is the tower mass. The average area moment of inertia is calculated with:

$$I_T = \frac{1}{16} t_T \pi (D_b^3 + D_t^3) \quad (7.8)$$

where  $t_T$  is the average tower wall thickness,  $D_b$  is the tower bottom diameter, and  $D_t$  is the tower top diameter. Using  $E_T = 210$  GPa for S355 steel, and retrieving values from WINDOW of  $D_b = 8.25$  m,  $D_t = 6.39$  m, average wall thickness  $t_T = (62 + 25)/2 = 43$  mm, tower length  $L_T = 123.8$  m, rotor-nacelle assembly mass  $m_{RNA} = 1059$  t, and tower mass  $m_T = 925.4$  t, the resulting fixed-base natural frequency is calculated as  $f_{FB} = 0.215$  Hz. Next, to compute the spring stiffness coefficients, formulae from (Poulos & Davis, 1980) can be used, assuming a flexible pile in medium sand:

$$K_L = 1.074 n_h^{3/5} (E_P I_P)^{2/5}, \quad K_{LR} = -0.99 n_h^{2/5} (E_P I_P)^{3/5}, \quad K_R = 1.48 n_h^{1/5} (E_P I_P)^{4/5} \quad (7.9)$$

where  $n_h$  is the coefficient of subgrade reaction, taken as  $4.2$  MN/m<sup>3</sup>. This value is used to represent the dominant sand and silt layers, which govern the deflection and stiffness behaviour of the foundation system. The estimation of  $n_h$  is described in more detail by Arany et al. (2017). For this calculation, similar soil conditions are assumed, as an RVO report indicates that sand and silt layers are present in the metocean studies conducted for the IJmuiden Ver Alpha site (RVO, 2023). Using Equation 7.2.2 the following values can be calculated:

$$K_L = 1.05 \text{ GN/m}, \quad K_{LR} = -14.7 \text{ GN}, \quad K_R = 335 \text{ GN/rad} \quad (7.10)$$

The next step is to calculate non-dimensional foundation stiffnesses as:

$$\eta_L = \frac{K_L L_T^3}{EI_\eta} = 1220, \quad \eta_{LR} = \frac{K_{LR} L_T^2}{EI_\eta} = -138.4, \quad \eta_R = \frac{K_R L_T}{EI_\eta} = 25.47 \quad (7.11)$$

where  $EI_\eta$  is the equivalent bending stiffness of the tower, computed as:

$$EI_\eta = E_T I_T \cdot f(q) \quad \text{where} \quad q = \frac{D_b}{D_t}, \quad f(q) = \frac{1}{3} \cdot \frac{2q^2(q-1)^3}{2q^2 \ln q - 3q^2 + 4q - 1} \quad (7.12)$$

The foundation flexibility coefficients can then be calculated as:

$$C_R = 1 - \frac{1}{1 + 0.6 \left( \eta_R \frac{\eta_{LR}^2}{\eta_L} \right)} = 0.854, \quad C_L = 1 - \frac{1}{1 + 0.5 \left( \eta_L \frac{\eta_{LR}^2}{\eta_R} \right)} = 0.996 \quad (7.13)$$

The substructure flexibility coefficient is calculated using the bending stiffness ratio  $\chi = E_T I_T / (E_P I_P) = 0.426$  and the length ratio  $\psi = L_S / L_T = 0.381$ , where  $L_S = 47.2$  m is the distance between the mudline and bottom of the tower. This results in:

$$C_S = \sqrt{\frac{1}{1 + (1 + \psi)^3 \chi - \chi}} = 0.768 \quad (7.14)$$

Finally, the natural frequency can be calculated using Equation 7.2.2:

$$f_0 = 0.996 \cdot 0.854 \cdot 0.768 \cdot 0.215 = 0.140 \text{ Hz} \quad (7.15)$$

Thus, for a minimum tip height of 25 m, the calculated natural frequency is acceptable, as it satisfies the requirement that  $f_0 > 0.126$  Hz. Since the natural frequency is expected to decrease with increasing

minimum tip height, this calculation is repeated for values in the range  $25 < \text{MTH} < 60$  m. The resulting trend is shown in the plot below:

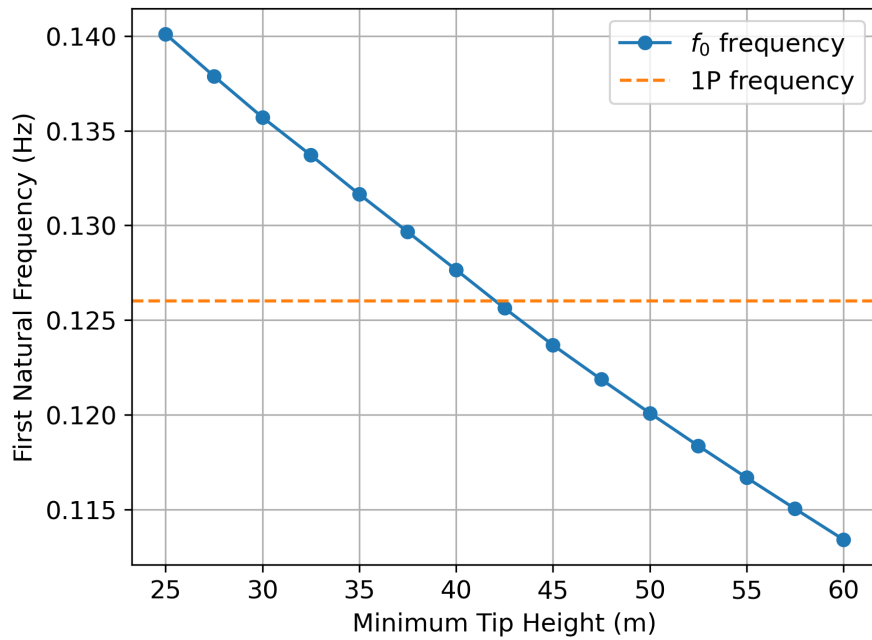


**Figure 7.3:** Calculated natural frequencies for various minimum tip heights.

Figure 7.3 shows that at a minimum tip height of approximately 42.5 m, the natural frequency of the turbine equals the 1P frequency and drops below this limit for MTH values beyond that point. To maintain structural integrity, the monopile diameter must be increased for these higher tip heights (van der Male, pers. comm., 2025). This is addressed by solving a root-finding problem, ensuring that the calculated natural frequency remains above the threshold of 0.126 Hz for all cases. The resulting updated  $D_P$  values for minimum tip heights above 45 m are presented in Table 7.3.

**Table 7.3:** Updated monopile diameters values as a result of the natural frequency analysis.

MTH (m)	$z_{\text{hub}}$ (m)	$D_P$ (m)	$f_0$ (Hz)
25	143	7.95	0.140
30	148	8.02	0.136
35	153	8.10	0.132
40	158	8.17	0.128
45	163	8.41	0.126
50	168	8.81	0.126
55	173	9.27	0.126
60	178	9.81	0.126

Clearly, the monopile diameter must increase significantly to satisfy the natural frequency requirement. For MTH values exceeding 42.5 m, this results in additional monopile costs, which will be reflected in the LCoE calculations presented later. It should be noted that the approach constitutes a simplified representation of a more complex structural dynamic analysis. According to (Arany et al., 2016), the

natural frequencies calculated using this method are therefore likely underestimated. Since this is a first-order calculation, the analysis is deemed sufficient for this research. As a final note, incorporating a safety margin to ensure that  $f_0$  remains sufficiently above the 1P frequency threshold could be a valuable extension of the model; however, this is considered beyond the scope of the present research. With the updated  $D_P$  values now established, the third and final governing criterion—the embedded length—can be analysed.

### 7.2.3. Embedded Length

The third criterion considered in the monopile sizing is the embedded length ( $L_e$ ). This criterion and its importance were introduced in Chapter 5. According to an industry expert, a ratio of  $D_P/L_e = 6$  is desirable for the monopile to effectively transfer loads to the soil (van der Male, pers. comm., 2025), and this value is used as the reference. Table 7.1 showed that for all MTH values, the  $D_P/L_e$  ratio is lower than this requirement. The new values for  $L_e$  are therefore calculated and presented in the table below. Notably, increasing the embedded length does not compromise the natural frequency requirements discussed in the previous section, since it does not affect the monopile length between the tower base and the mudline.

**Table 7.4:** Updated monopile diameter values, corrected for natural frequency and embedded length requirements.

MTH (m)	$z_{\text{hub}}$ (m)	$D_P$ (m)	$f_0$ (Hz)	$L_e$ (m)
25	143	7.95	0.140	47.70
30	148	8.02	0.136	48.12
35	153	8.10	0.132	48.60
40	158	8.17	0.128	49.02
45	163	8.41	0.126	50.46
50	168	8.81	0.126	52.86
55	173	9.27	0.126	55.62
60	178	9.81	0.126	58.86

Increasing  $L_e$  will result in additional monopile costs due to more material being required (additional monopile length). With these values obtained, the next step is to set up the model in order to perform the LCoE calculations. The following section elaborates on the actual changes made to each module in WINDOW.

## 7.3. Model Setup

This section provides an overview of all the relevant modules in the framework. Modules that are expanded for this research are explained in detail. Modules that are not changed are explained in more detail in (Mehta et al., 2024).

### 7.3.1. Turbine Geometric Inputs

For this research, the same workflow as in (Mehta et al., 2024) is used. The only functionality used from WINDOW is the optimisation of the LCoE in the wind farm scenario described in Chapter 5. A simulation will be done for the same range of minimum tip heights, rotor diameters, and rated powers as in Chapter 6. The majority of inputs and data used for the simulations are shown in Chapter 5. For

consistency, predetermined combinations of values for rated power, rotor diameter, hub height, and minimum tip height are chosen.

For 10 MW rated power, a rotor diameter of 178.3 m was chosen, matching the DTU 10 MW reference wind turbine (Gaertner et al., 2020). For the 15 MW and 20 MW turbines, values from (van der Vliet et al., 2022) were adopted, resulting in rotor diameters of 236 m and 280 m, respectively. The rotor diameters for intermediate rated power values are obtained through linear interpolation.

As described in the previous section, WINDOW originally allows users to specify a certain set of rotor diameters and rated power values to perform an LCoE analysis of all possible combinations of these two variables for a specific wind farm case. The model had to be modified to incorporate the minimum tip height as a third variable input. The base minimum tip height is set to 25 m measured from mean sea level (MSL). The hub height is then calculated as:

$$z_{hub} = MTH + \frac{D_{rotor}}{2} \quad (7.16)$$

Along with the assumed values for 10, 15, and 20 MW turbines, the resulting turbine specifications are calculated for rated powers ranging from 10 to 20 MW.

**Table 7.5:** Turbine specifications including minimum tip height.

$P_{rated}$ (MW)	$D_{rotor}$ (m)	$z_{hub}$ (m)	MTH (m)
10	178.3	114.2	25.0
11	189.8	119.9	25.0
12	201.4	125.7	25.0
13	212.9	131.4	25.0
14	224.5	137.2	25.0
15	236.0	143.0	25.0
16	244.8	147.4	25.0
17	253.6	151.8	25.0
18	262.4	156.2	25.0
19	271.2	160.6	25.0
20	280.0	165.0	25.0

Table 7.5 is mainly an indication for the combined values used when varying the rated power. For the MTH and  $D_{rotor}$  simulations, the rated power is equal to the base case value of 15 MW, while the other variables are computed via Equation 7.16.

### 7.3.2. Support Structure

The sizing module for the support structure is based on the work of (Zaaijer, 2013), and (Mehta et al., 2024) explains the most important components of the support structure module in detail. In summary, the module performs an iterative estimation of the tower and monopile geometry, such as length, thickness, and most importantly, diameter. After running calculations for each load case described in Section 7.2, the governing values—mainly the monopile diameter—are selected. The monopile diameter  $D_p$  is initially guessed, after which the value is iteratively updated through analysis of the loads acting on the turbine, including wind thrust force, aerodynamic force on the tower, hydrodynamic forces on the monopile, and gravity forces. Each of these loads is corrected by a partial safety factor, a dynamic

amplification factor, and a fatigue safety factor. The resulting maximum stress (at the mudline) in the monopile then dictates the required diameter  $D_p$ , based on the yield stress requirement.

$D_p$  is the most important parameter for this research, as the monopile mass increases monotonically with it (Zaaijer, 2013), and the monopile mass has a proportional relation with monopile cost. Thus,  $D_p$  gives the strongest sensitivity in monopile cost calculations, which is why a modification was developed in Section 7.2 to produce more accurate results.

The proposed modification to comply with the governing criteria established for the support structure is implemented in WINDOW's Python code. The calculations from Section 7.2 are added to the end results produced by the original support structure module. This means that for all MTH values, the embedded length  $L_e$  is adjusted as done in Table 7.4. For MTH values above 42.5 m, the monopile diameter  $D_p$  is also adjusted, as shown in Table 7.4, to meet the natural frequency requirement.

### 7.3.3. Installation

In Chapter 5, the reasoning for modifying vessel costs was explained. The vessel day rates were updated for the installation cost calculations, which are considered CAPEX costs. Based on expert information, a relationship for scaling vessel costs was derived. For the foundation installation vessel (FIV), a base day rate of 600 kEUR was assumed for a turbine with 15 MW rated power and corresponding hub height (see Table 7.5). A linear scaling function was established to compute the day rate in EUR:

$$dayrate_{FIV} = 600000 \cdot (H_{hub}/143) \quad (7.17)$$

where  $H_{hub}$  is the hub height in metres. This function aims to represent the vessel type required for a given turbine size. For the sake of this research, the possibility of having a hub height that exceeds current vessel capabilities is disregarded.

For the wind turbine installation vessel (WTIV), a similar day rate function is defined:

$$dayrate_{WTIV} = 800000 \cdot (H_{hub}/143) \quad (7.18)$$

where a base day rate of 800 kEUR is assumed for a vessel capable of installing a 15 MW turbine. It should be noted that the day rate for FIV and WTIV vessels in WINDOW originally scaled linearly with the rotor diameter (Mehta et al., 2024). However, a deliberate choice was made to omit a  $D_{rotor}$  term from all vessel day rate equations, as many cost components in WINDOW already scale with rotor radius, and this approach helps preserve overall linear scaling while focussing on the MTH analysis.

Furthermore, for the heavy lift vessel (HLV), which installs the substation, a fixed day rate of 1 MEUR is assumed. Cable lay vessels (CLV) and cable burial vessels (CBV) are assumed to have a day rate of 250 kEUR, based on expert input (Ummels, pers. comm., 2025). Mobilisation costs are also included. According to an expert, mobilisation and demobilisation for an FIV or WTIV can take up to one month. The day rates apply during this period, but fuel costs are reduced, leading to a lower effective rate. A maximum mobilisation cost of 20 MEUR is assumed. To account for different turbine sizes, mobilisation costs are computed as 30 times the day rate, capped at 20 MEUR. For the HLV, a mobilisation cost of 30 MEUR or 30 times the day rate is assumed, reflecting that most large HLVs are rented for a minimum of one month. For the CLV and CBV, a mobilisation time of 5 days in total is assumed, resulting in 1.25 MEUR. An overview of all vessel costs is shown in Table 7.6, based on a 15 MW turbine scenario.

**Table 7.6:** Vessel types, their purposes, and associated costs, assuming a 15 MW turbine.

Vessel type	Purpose	Day rate (EUR)	Mobilisation costs (MEUR)
FIV	Installation: foundation	600 000	18
WTIV	Installation: turbine	800 000	20
HLV	Installation: substation	1000 000	30
CLV	Installation: cable lay	250 000	1.25
CBV	Installation: cable burial	250 000	1.25

It should be noted that the installation model uses additional inputs, such as transit speed, to compute the transit time based on the wind farm’s distance to the nearest port. As these values remain unchanged, they can be found—along with a more detailed explanation of the installation model—in (Mehta et al., 2024).

### 7.3.4. Operations and Maintenance (O&M)

Similar to the installation costs, the O&M cost model in WINDOW was also reviewed. It was found that O&M costs did not scale correctly with increasing hub height, as the model originally applied only a scaling function for rotor diameter. In the O&M context, the WTIV is primarily used for large-scale component replacement (e.g. blades). Following the same approach as in the installation section, the WTIV day rate is scaled with hub height using a base value of 800 kEUR for a 15 MW turbine with a 143 m hub height.

The cable lay vessel (CLV), used for cable maintenance, is assigned the same day rate of 250 kEUR. The mobilisation time for both vessels is assumed to be 1 day in this case. Other vessels used in the model include crew transfer vessels (CTV) and diving support vessels (DSV). Their day rates and mobilisation costs are unchanged from the default settings in WINDOW. An overview of all vessel costs is shown in Table 7.7, based on a 15 MW turbine scenario.

**Table 7.7:** Vessel types and costs, for wind farm O&M assuming a 15 MW turbine.

Vessel type	Purpose	Day rate (EUR)	Mobilisation costs (EUR)
WTIV	O&M	800 000	800 000
CLV	Installation: cable lay	250 000	250 000
CTV	Crew transfer	3 000	–
DSV	O&M: scour repair	75 000	225 000

### 7.3.5. Farm AEP

The module for computing the farm AEP was slightly modified to incorporate the effect of an increased minimum tip height. For the AEP calculation, the hub height is used to project the wind speed at hub level using the power law, with a shear exponent of 0.11 (Mehta et al., 2024). The hub height is calculated based on the provided MTH value and Equation 7.16.

## 7.4. Assumptions Overview

WINDOW has been developed with the aim of analysing trends, rather than providing highly accurate predictions. As such, low-fidelity models are used to enable sensitivity and trade-off exploration. This implies that many assumptions are made, which are mostly documented in (Mehta et al., 2024) and (Zaaijer, 2013). The most important assumptions of this LCoE model are listed below:

- Vessel day rates for installation and maintenance are assumed to scale linearly with the hub height.
- Vessel availability is not constrained by real-world limitations; it is assumed that suitable vessels exist for all hub heights and component sizes.
- No physical supply chain or logistical constraints (e.g., blade transport, vessel access, port size) are modelled.
- O&M cost and downtime modelling relies on generalised assumptions about failure rates, access limits, and maintenance logistics.
- The normalised turbine spacing is fixed, equal to five times  $D_{rotor}$  in both downwind and crosswind directions.
- The wake model used for AEP calculations is the Bastankhah Gaussian wake model.

- A single, fixed 1-year time series is used to calculate the wind distribution, without location-specific or time-varying adjustments.
- The maximum bending stress is assumed to occur at the mudline.
- Decommissioning costs are assumed to remain unchanged across design changes, despite variations in monopile size or installation depth.
- The financial discount rate and project lifetime are fixed.
- The thrust coefficient  $C_T$  and power coefficient  $C_P$  remain constant when varying rotor size.
- To account for low-fidelity, WINDOW applies a general safety factor of 1.5 to various input forces, including the rotor thrust, due to neglecting periodic loads.
- Fatigue is neglected. Hence, a fatigue safety factor of 1.5 is applied when sizing the support structure (Zaaijer, 2013).

Implications of these assumptions are discussed in Chapter 8.

## 7.5. Baseline Results

Before running the simulations for varying minimum tip height, rotor diameter, and turbine rated power, a baseline simulation was performed using the WINDOW model. The results from this simulation provide a benchmark for evaluating the economic cost of the proposed solutions to mitigate bird collisions, which will be discussed in subsequent sections. The base case represents a 1 GW capacity wind farm with 67 turbines of 15 MW rated power, a rotor diameter of 236 m, and a minimum tip height of 25 m. More details on the base case were explained in Chapter 5. The results of the simulation are presented in the tables below. Note that the rated power is set to 14.93 MW, adjusted to match the total farm capacity of 1 GW for 67 turbines. These minor adjustments are applied to all scaled turbines considered in this research, in order to maintain 1 GW capacity.

**Table 7.8:** Baseline results.

**Table 7.9:** Farm-level components.

Parameter	Value	Unit
Rated power	14.93	MW
Rotor diameter	236	m
Hub height	143	m
MTH	25	m
Rated wind speed	10.54	m/s
Farm area	103.7	km <sup>2</sup>
No. of turbines	67	-
Mean wind speed	10.47	m/s
AEP	5277	MWh/year
$C_{CAPEX}$	2740	M€
$C_{DECEX}$	493.0	M€
$C_{OPEX}$	50.55	M€/year
LCoE	45.93	€/MWh

**Table 7.10:** Turbine components.

Parameter	Value	Unit
RNA mass	1059	t
Blade mass	60.55	t
Tower mass	925.4	t
Monopile mass	1402	t
TP mass	326.0	t
Tower length	123.8	m
TP length	19.39	m
Monopile length	84.17	m
Embedded length	47.72	m
Monopile diameter	7.953	m
Monopile thickness	0.0859	m
Tower base diameter	8.25	m
Tower top diameter	6.39	m
Tower min. thickness	0.0250	m
Tower max. thickness	0.0615	m

Furthermore, the overall cost component contribution to the LCoE, after implementing all changes to the WINDOW model as described earlier in this chapter, is shown in Figure 7.4.

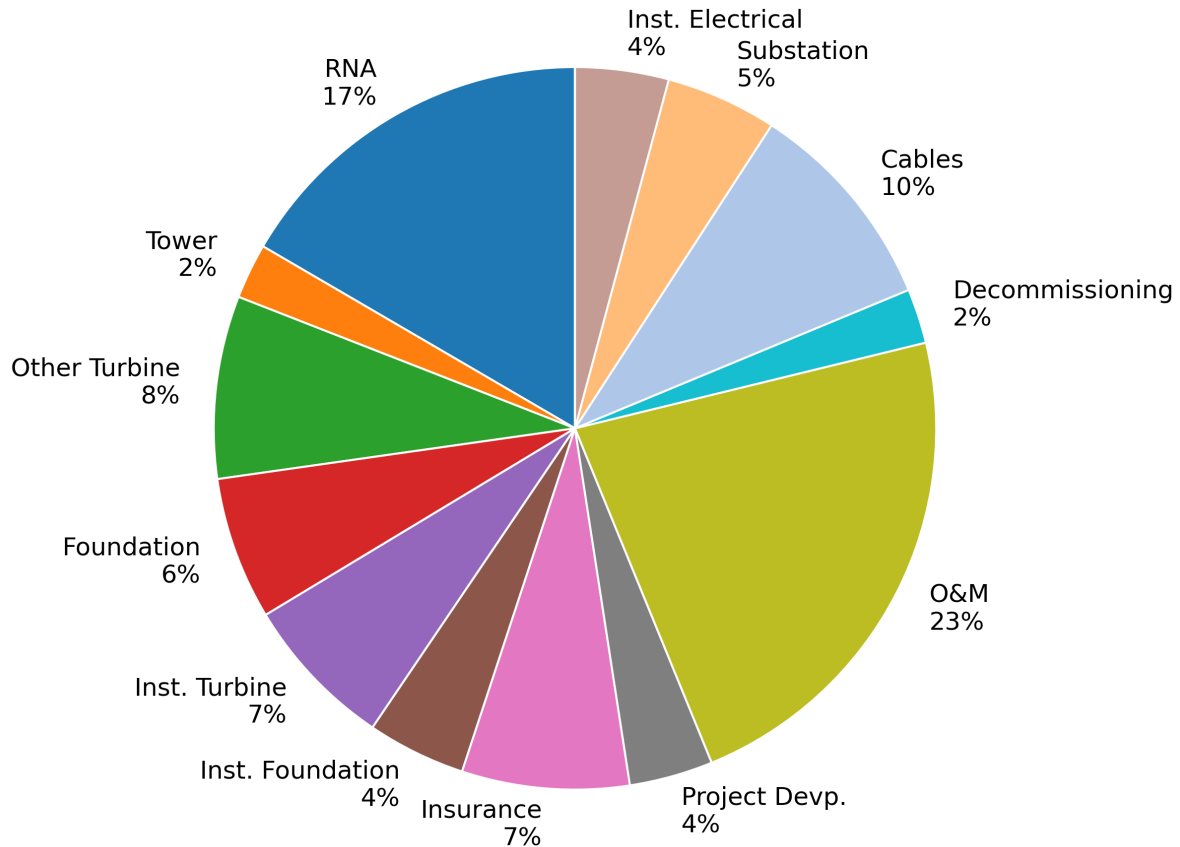


**Figure 7.4:** Contribution to LCoE for various CAPEX components, as well as O&M and Decommissioning costs. Note that this is for the base case scenario.

In Figure 7.4, the percentage contribution to the LCoE calculation, normalised via Equation 7.1, is shown. The various CAPEX components are divided into sub-categories, following the approach used in the study by (Mehta et al., 2024). The O&M and decommissioning costs, which together account for 25% of the total LCoE, are included as well.

Among the CAPEX components, 'RNA' refers to the rotor nacelle assembly. 'Other Turbine' covers costs related to assembly, profit, and warranty. 'Inst. Turbine' represents the cost of installing the turbine, while installation costs are also shown separately for the foundation and for the electrical infrastructure. The latter includes infield cables, export cables, and substation installation. 'Insurance' encompasses insurance and contingency costs, while 'Project Devp.' refers to project development-related expenses, such as management. 'Cables' indicates the procurement of both infield and export cables, and 'Substation' refers to the procurement of the substation itself. It was confirmed that the WINDOW model includes both substation and export cable costs in the LCoE calculation.

The next step is to perform the simulations for varying the minimum tip height, rotor diameter, and rated power, which is done in the next section.

## 7.6. LCoE Model Results

This section presents the results from the LCoE simulations. For each simulation, both absolute and normalised values of the Levelised Cost of Electricity (LCoE) are shown. In addition, insights into model behaviour are presented and discussed, such as the changes of the individual terms in the LCoE equation (Equation 7.1).

### 7.6.1. Results for Varying Minimum Tip Height

In the first simulation, LCoE values were computed for minimum tip heights ranging from 15 m to 60 m. This illustrates the cost increase associated with implementing the proposed solution of increasing the tip height (Chapter 6). According to expert opinion and literature (Gyimesi, pers. comm., 2025), (van der Vliet et al., 2022), 40 m is considered a realistic upper limit for the minimum tip height for offshore wind turbines. Limitations due to vessel availability and turbine design constraints were previously described in Chapter 5. Figure 7.5a shows the results for absolute LCoE values, while Figure 7.5b shows normalised values using the base case as the reference.

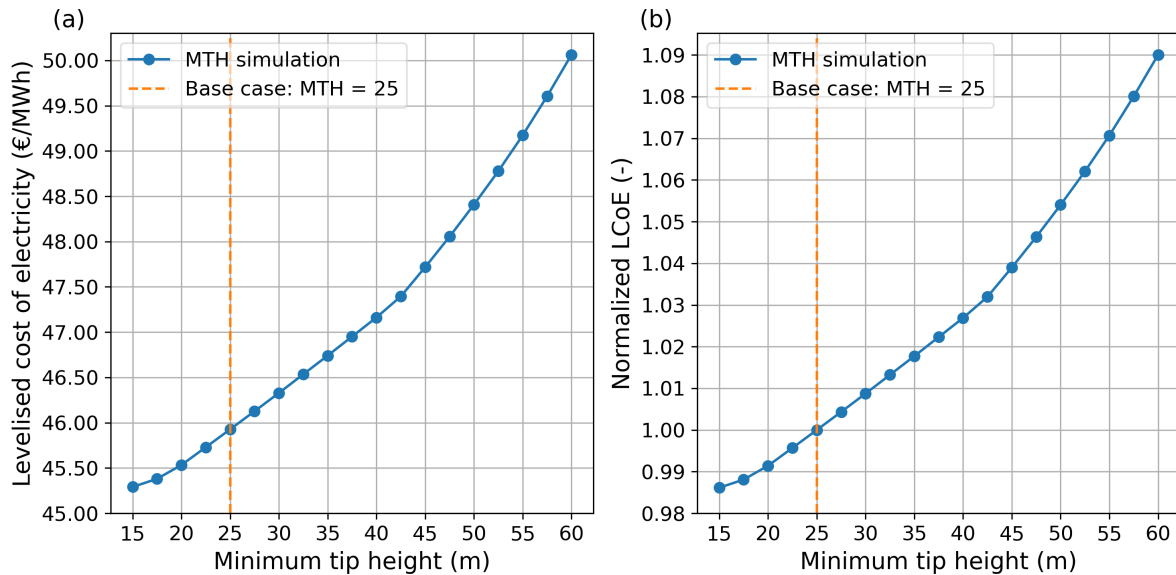


**Figure 7.5:** LCoE values from the WINDOW model for various minimum tip heights.

Figure 7.5 reveals a clear upward trend in LCoE with increasing MTH. For  $15 \text{ m} < \text{MTH} < 42.5 \text{ m}$ , a relatively gentle linear increase is observed. Beyond 42.5 m, a sharper incline appears due to the increased monopile diameter required to satisfy natural frequency constraints (Section 7.2). The base case (MTH = 25 m) is marked with an orange dashed line. Each 10 m increase in MTH leads to an LCoE rise of approximately 0.75 EUR/MWh, up until the 42.5 m threshold. Conversely, reducing MTH to 15 m yields a similar reduction in LCoE. The normalised results show a maximum LCoE increase of around 9% and a reduction of up to 1.5%. While the values reflect model estimations with first-order accuracy, they align in magnitude with results by (Mehta et al., 2024). Future work is advised for improved real-world precision.

Since the proposed mitigation strategies primarily affect capital expenditure (CAPEX), the normalised changes in individual CAPEX components are visualised in Figure 7.6a. Additionally, Figure 7.6b presents key farm-level quantities affected by varying MTH. Note that 'Support structure costs' include the tower, transition piece, monopile, and grout. 'Installation costs' refer to the installation of the turbine, foundation, and electrical components, such as infield cables, export cables, and both onshore and offshore substations. 'Electrical costs' cover the procurement of infield cables, export cables, and substations.

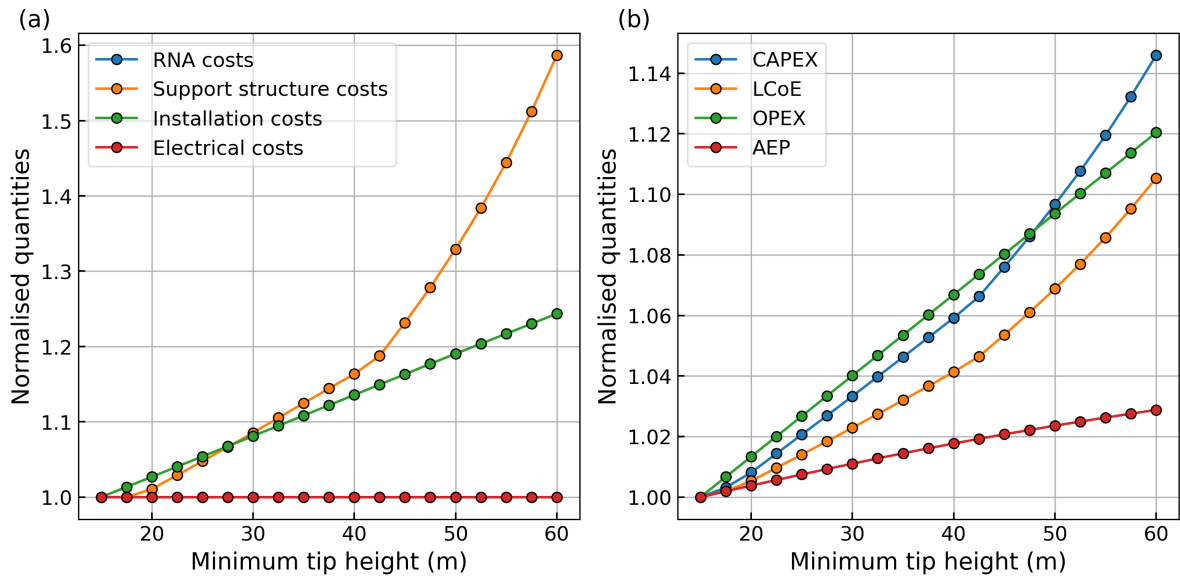


**Figure 7.6:** (a) Change in CAPEX components with varying minimum tip height. (b) Change in critical farm-level quantities with varying minimum tip height.

In Figure 7.6a, the support structure cost exhibits the largest increase. This is first due to the increased overturning moment from higher hub heights and secondly due to the enlarged monopile diameter needed to satisfy the natural frequency requirement—leading to cost increases of up to 60%. Installation costs show a linear rise, driven by hub-height-dependent vessel day rates. Rotor nacelle assembly (RNA) and electrical costs remain unchanged. Note that RNA costs are hidden behind the ‘Electrical costs’ line. Figure 7.6b highlights that CAPEX and OPEX are the main contributors to the observed LCoE increase. The OPEX increase is again attributed to vessel scaling with hub height. A modest AEP increase (up to 3%) helps offset the LCoE rise.

It is also interesting to see how the components from Figure 7.6a vary with respect to each other. Thus, a stacked area plot was made, which is shown in Figure 7.7. Here, the component share of each component is shown by its width at a certain minimum tip height. On the left and right side of the plot, the percentage values of the component shares are shown for MTH values 15 and 60 m respectively. Note that CAPEX costs like project development and insurance, as shown in Figure 7.4, are omitted in this analysis, as these costs do not vary with neither MTH,  $D_{rotor}$  or  $P_{rated}$ . Figure 7.7 shows that the support structure and installation costs increase to 21.4 and 29.1 % respectively for a MTN of 60 m. This is offset by the relative decrease percentage of RNA and electrical costs, as these costs remain constant for this simulation (see Figure 7.6a).

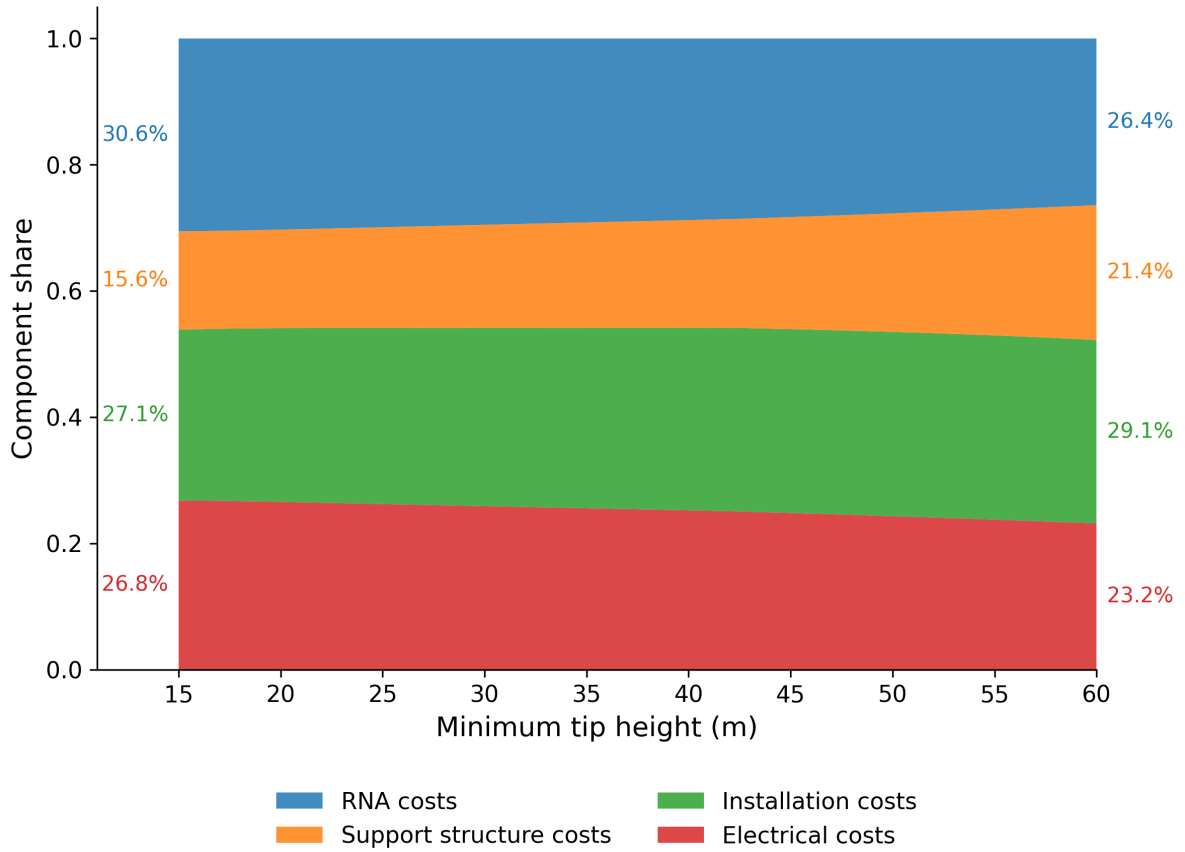


**Figure 7.7:** Plot showing the relative variation of CAPEX components for varying MTH. The percentage values on the left and right refer to the component share percentage at 15 and 60 m MTH respectively.

Finally, to isolate the effect of AEP on LCoE, a comparative simulation was conducted keeping AEP constant. This damping effect is shown in Figure 7.8.

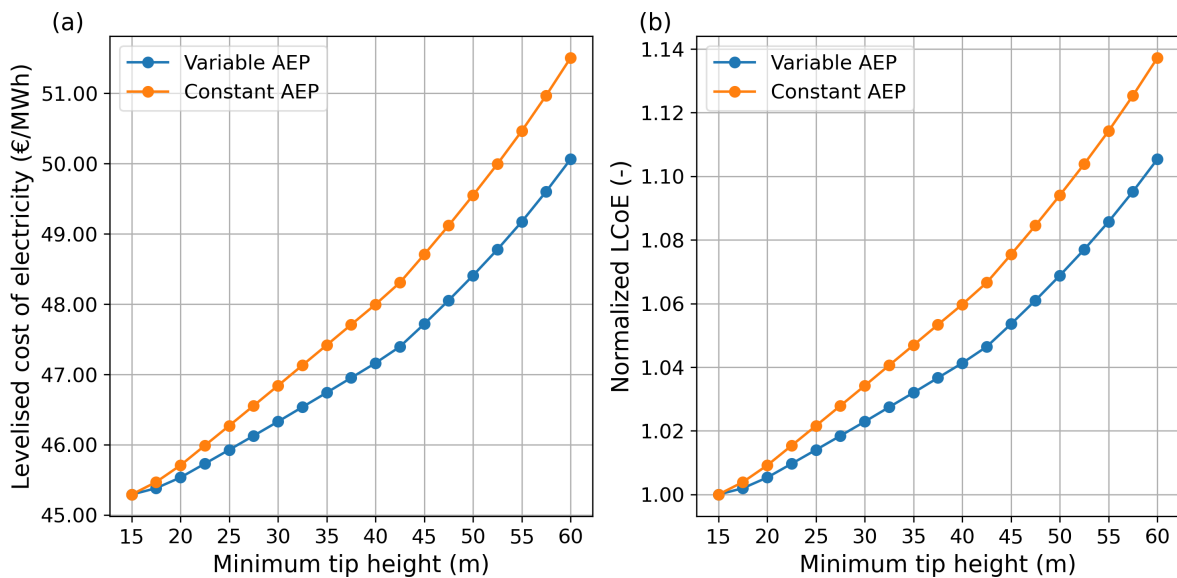


**Figure 7.8:** Simulation results for minimum tip height, illustrating the 'damping' effect of increased AEP.

AEP increases because the hub height increases, leading to higher wind speeds (estimated via the power law using a wind profile at 100 m). This dampens the LCoE increase. Figure 7.8a confirms this, with LCoE values approaching 52 EUR/MWh when AEP is held constant. Figure 7.8b shows that without the AEP increase, LCoE can rise by up to 14%. As discussed by (Zaaijer, 2013), variations in hub height introduce opposing effects: higher costs versus higher energy yield. While this trade-off cannot be precisely captured by low-fidelity models, increasing hub height beyond the necessary minimum is generally not cost-effective.

### 7.6.2. Results for Varying Rotor Diameter

The second simulation examines how varying the rotor diameter from 186 m to 286 m affects LCoE. As in Chapter 6, this is used to assess the proposed mitigation strategy of altering rotor size. The minimum tip height is fixed at 25 m, meaning rotor diameter changes affect hub height. The turbine rated power remains 15 MW. Results for absolute and normalised LCoE values are shown in Figure 7.9, with the orange dashed line indicating the baseline diameter.

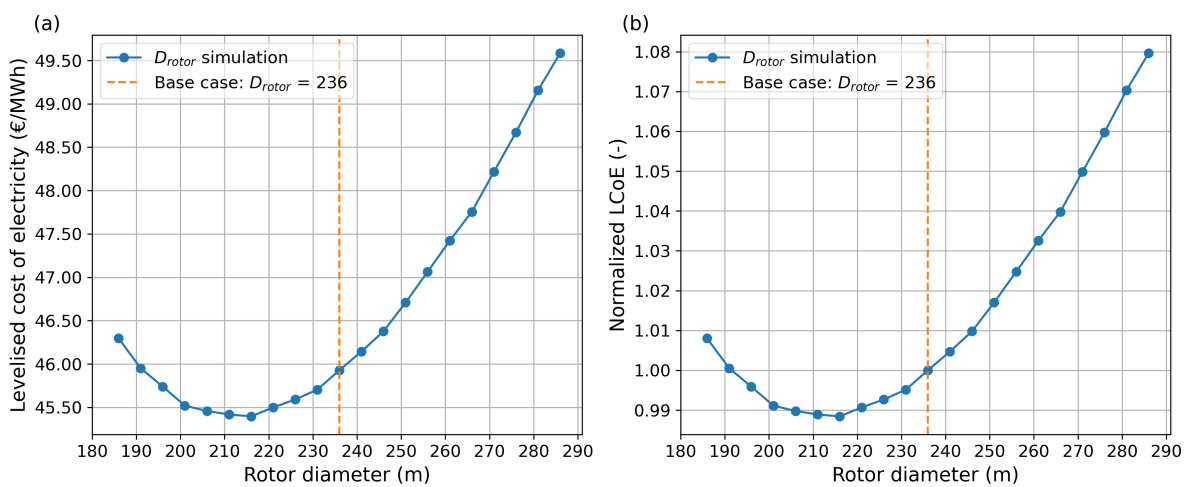


**Figure 7.9:** LCoE values from the WINDOW model for various rotor diameters.

Figure 7.9a shows that the LCoE reaches a minimum at  $D_{rotor} = 216$  m, consistent with WINDOW's known optimal sizing behaviour (Mehta et al., 2024). Beyond this minimum, the LCoE rises, with the increase becoming steeper above the base case diameter. The cost reaches approximately 49.50 EUR/MWh at the largest rotor size. Figure 7.9b shows a maximum reduction of around 1% at 216 m, and an 8% increase at 286 m. These results are in line with previous studies and again represent low-fidelity, first-order calculations. More refined modelling is needed to assess accuracy under real conditions.

To investigate the changes in separate CAPEX components and crucial farm-level parameters due to varying  $D_{rotor}$ , Figures 7.10a and 7.10b are plotted:

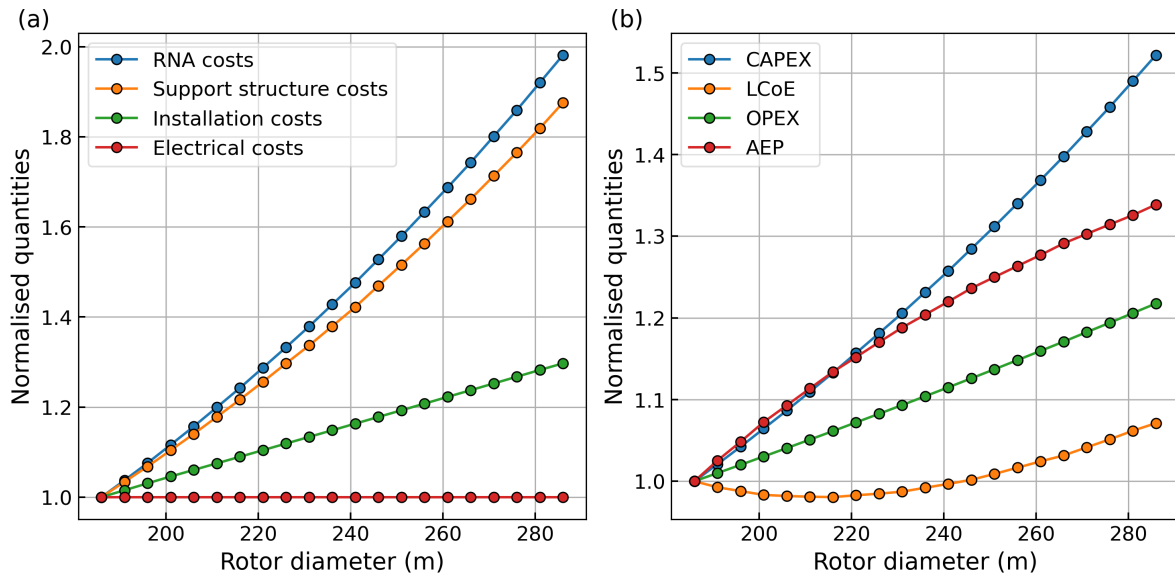


**Figure 7.10:** (a) Change in components of CAPEX when varying  $D_{rotor}$ .  
 (b) Change in crucial farm-level components when varying  $D_{rotor}$ .

In Figure 7.10a, the RNA and support structure costs show the most significant increases—approximately 100% and 90%, respectively. The RNA costs rise due to the larger rotor swept area, which increases both the mass and the aerodynamic loading on the turbine. Simultaneously, the increased hub height leads to higher overturning moments. These factors drive up the dimensions of the tower and monopile, and therefore the support structure costs. Installation costs rise by up to 30%, primarily due to the increased hub height, which necessitates more capable (and costly) installation vessels (Section 7.2). Electrical costs remain unchanged, as was the case for the minimum tip height simulation.

In Figure 7.10b, CAPEX exhibits the largest increase, followed by AEP, OPEX and LCoE. AEP increases significantly due to the unchanged number of turbines and the larger rotor area per turbine. OPEX increases beyond 20%, owing to the higher hub height and associated vessel cost scaling for maintenance. Notably, the WINDOW model originally scaled installation and maintenance costs with  $D_{rotor}$  (Mehta et al., 2024), whereas this research uses hub height as the scaling parameter—leading to different behaviour. The overall LCoE increase remains under 10%, indicating that the AEP increase offsets some of the rising costs.

The relative variation of the mentioned CAPEX components is plotted in Figure 7.11. Here, the strong increase in RNA and support structure costs are seen, despite the increase of the installation costs as shown in Figure 7.10a. The increase in these components are offset by a smaller share of installation cost, although this increases with rotor diameter as well. As the electrical costs do not vary, the share decreases with increasing rotor diameter.

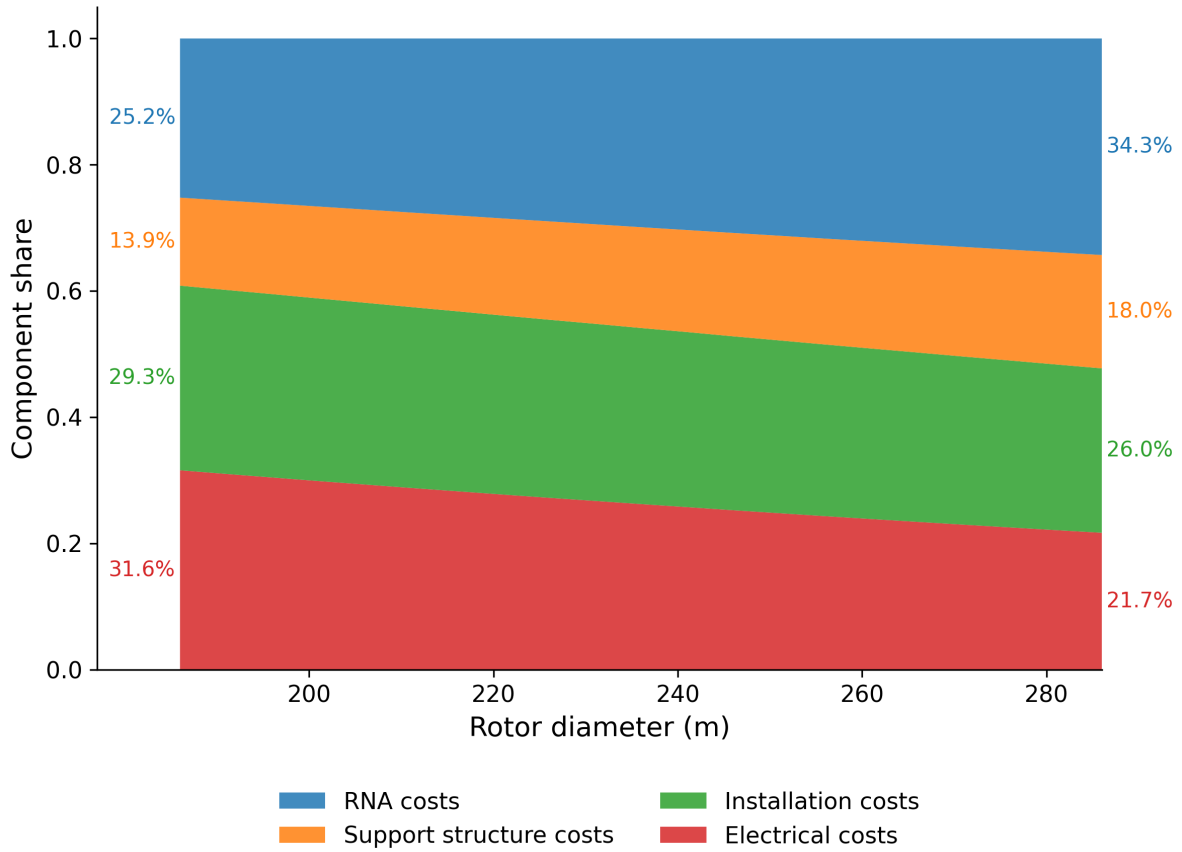


**Figure 7.11:** Plot showing the relative variation of CAPEX components for varying  $D_{rotor}$ . The percentage values on the left and right refer to the component share percentage at 186 and 286 m  $D_{rotor}$  respectively.

Finally, another simulation was conducted with AEP held constant. This is shown in Figure 7.12:

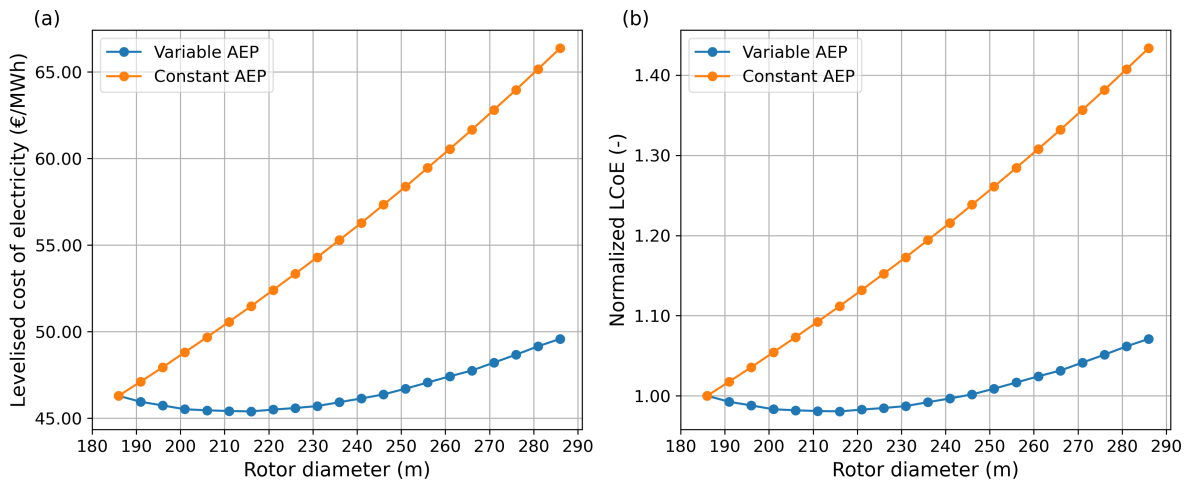


**Figure 7.12:** Simulation results for rotor diameter, showcasing the effect of AEP ‘damping’.

Without AEP increasing, the LCoE rises more steeply, reaching almost 65 EUR/MWh—over 40% higher than the value for  $D_{rotor} = 186$  m. Compared to Figure 7.8, the LCoE model is significantly more

sensitive to changes in  $D_{rotor}$  when AEP is fixed. This is mainly because RNA costs increase substantially with  $D_{rotor}$ , whereas they remain unaffected by MTH. It should be noted that the analysis of varying  $D_{rotor}$  without adjusting the rated RPM accordingly is primarily intended to illustrate model behaviour, rather than to replicate a realistic design scenario. In practice, adjusting the rotor diameter to mitigate collisions would always be done in combination with a corresponding adjustment of the rated RPM, for the reasons explained in Chapter 5.

### 7.6.3. Results for Varying Turbine Rated Power

For the third simulation, LCoE values were computed for offshore wind farms using turbines with rated power ranging from 10 MW to 23 MW. This reflects the proposed solution of using fewer, larger turbines as explored in Chapter 6. Turbine dimensions were defined in Table 7.5. In each case, the total installed capacity was fixed at 1 GW—e.g., 100 turbines for a 10 MW scenario, and 50 turbines for a 20 MW one. Figure 7.13 shows the resulting absolute and normalised LCoE values:

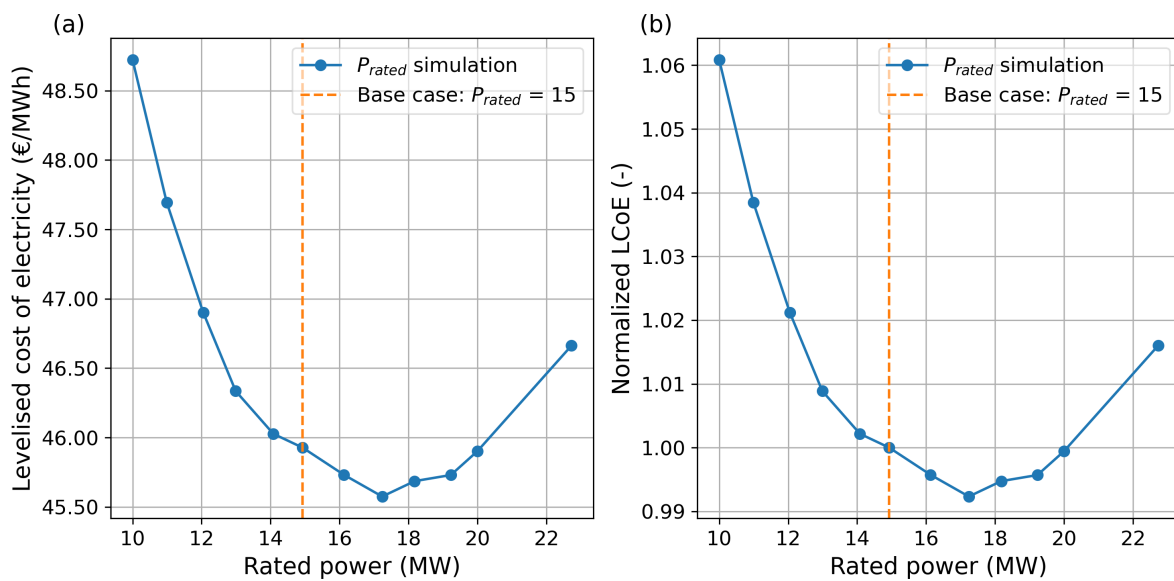
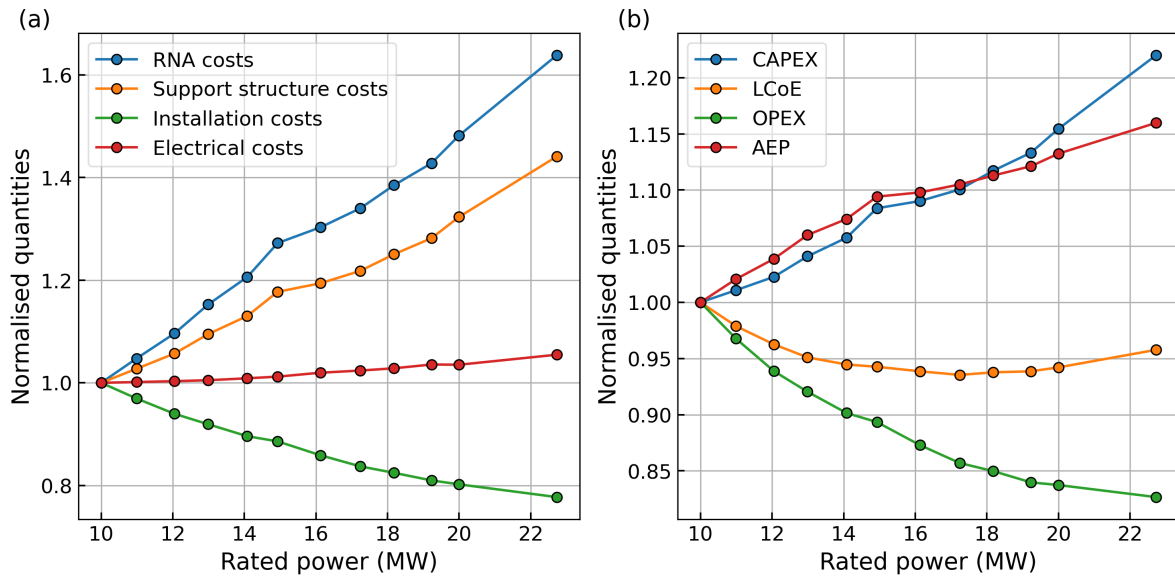


Figure 7.13: LCoE values as calculated by WINDOW for various rated power turbines.

Figure 7.13a shows a minimum LCoE of approximately 45.50 EUR/MWh for a wind farm using 59 turbines rated at 17 MW each. This deviates slightly from (Mehta et al., 2024), which identified 16 MW as the optimum. Up to 17 MW, increasing turbine rated power reduces LCoE. From 17 MW to 20 MW, the LCoE gradually increases again to around 46 EUR/MWh—comparable to the base case of 15 MW. However, the 20 MW scenario remains preferable given its lower bird collision risk (Chapter 6). The normalised results in Figure 7.13b show a maximum LCoE reduction of under 1% and an increase of up to 6% for lower-rated turbines. As with earlier results, these are based on first-order assumptions and warrant further validation.

To better understand the underlying dynamics, CAPEX components and farm-level quantities were visualised in Figure 7.14:



**Figure 7.14:** (a) Change in components of CAPEX when varying  $P_{rated}$ .  
 (b) Change in crucial farm-level components when varying  $P_{rated}$ .

In Figure 7.14a, RNA costs are the primary driver of CAPEX increases, mainly due to larger generators and rotor assemblies. However, the relative increase is smaller than that observed for  $D_{rotor}$  alone, as fewer turbines are required per wind farm. Support structure costs also increase due to higher hub heights, heavier RNAs, and larger wind thrust forces (Mehta et al., 2024). A minor rise in electrical costs is attributed to more expensive infield cables, despite the reduction of infield cable length due to fewer turbines. Installation costs decline due to fewer turbines, despite the greater complexity and vessel size needed for larger turbines.

In Figure 7.14b, OPEX decreases as fewer turbines reduce failure rates and maintenance operations, partially offsetting the increased vessel day rates. AEP increases due to reduced wake losses and higher wind speeds at greater hub heights. These effects collectively result in the observed LCoE optimum at 17 MW.

Finally, the relative variation of CAPEX components for increasing rated power is plotted in Figure 7.15. Again, the RNA and support structure components increase with respect to installation and electrical costs. Looking back at Figure 7.14a, the slight increase in electrical costs is still significantly smaller compared to the increased RNA and support structure cost components, as is seen in Figure 7.15.

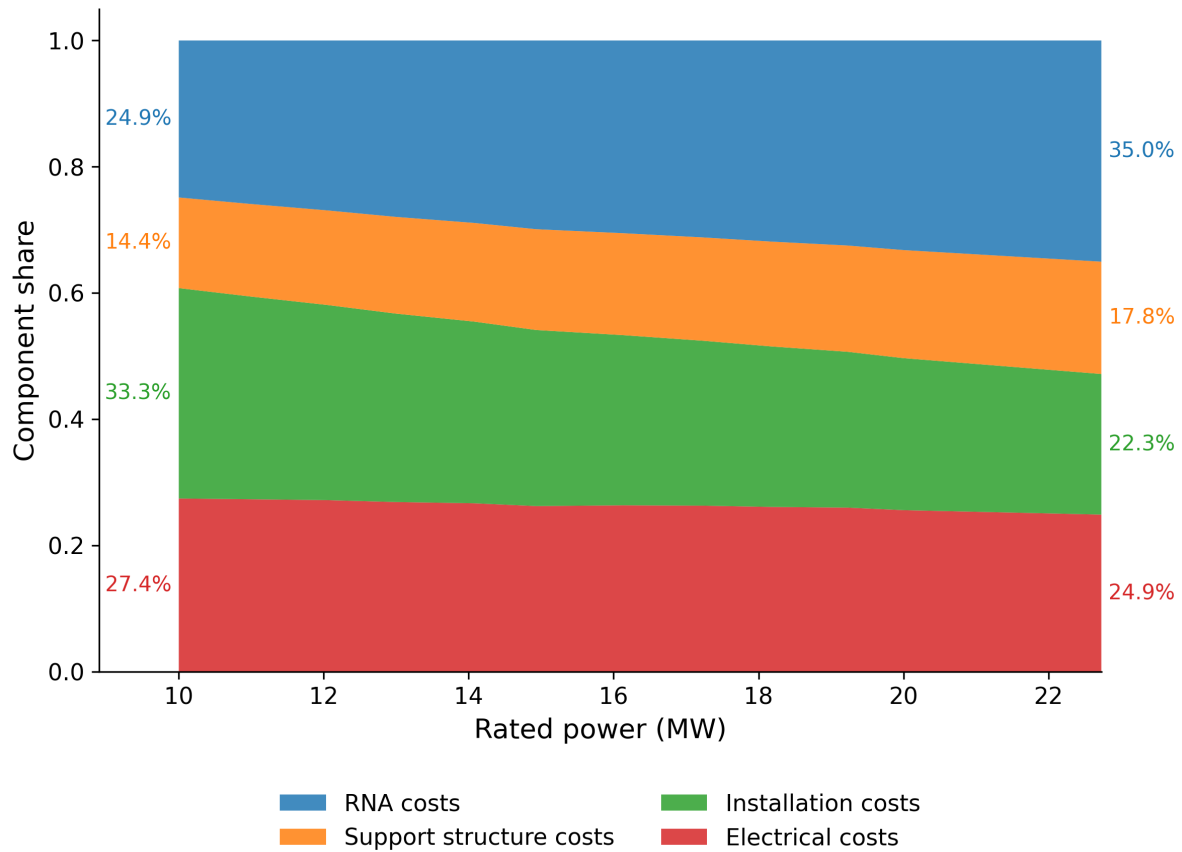


**Figure 7.15:** Plot showing the relative variation of CAPEX components for varying  $P_{rated}$ . The percentage values on the left and right refer to the component share percentage at 10 and 23 MW  $P_{rated}$  respectively.

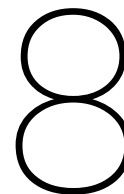
## 7.7. LCoE Modelling Summary

This chapter analysed LCoE variations for the wind farm scenario defined in Chapter 5 by adjusting minimum tip height, rotor diameter, and turbine rated power. The WINDOW model's architecture was outlined in Figure 7.1, and necessary adjustments were made to accommodate governing criteria for realistic turbine design.

The three simulation results showed that:

- Increasing minimum tip height increases LCoE due to rising support structure and vessel costs.
- Increasing rotor diameter beyond the optimal value significantly raises RNA and support structure costs, thereby increasing LCoE.
- Rated power optimisation revealed a minimum LCoE at 17 MW; both smaller and larger turbines led to higher LCoE values.

The following chapter combines these results with the findings from the collision risk model to provide an integrated discussion of trade-offs between ecological impact and cost-effectiveness.



# Simulation Results & Discussion

With the case study scenario defined in Chapter 5, and the CRM and Levelised Cost of Electricity (LCoE) models described in Chapters 6 and 7, the final step is to combine these models to evaluate the trade-off between ecological benefits and economic feasibility of various turbine design changes. This chapter answers the research question: Which mitigation measure provides the most cost-effective reduction in seabird collisions within the defined scenario? Using the CRM and LCoE results as input, this chapter calculates the LCoE cost per collision mitigated for three design variables: rotor diameter, minimum tip height (MTH), and rated power ( $P_{rated}$ ). First, the outcomes for varying rotor diameter are discussed, followed by detailed evaluations of MTH and  $P_{rated}$ . These results are then compared directly to determine the most effective and practical mitigation strategy. Finally, the implications of these findings and the underlying modelling assumptions are examined.

## 8.1. Results for Varying Rotor Diameter

To assess which mitigation measure is the most cost-effective, the simulation results from Chapter 6 and Chapter 7 are combined to calculate the yearly bird collisions per species and the corresponding Levelised Cost of Electricity (LCoE) values. For the purpose of this research, the selected approach is to estimate the LCoE values relative to the base case, for each mitigated collision per year due to the proposed mitigation measure, which can be an increase in one of three design variables: minimum tip height (MTH), rotor diameter  $D_{rotor}$ , or rated power  $P_{rated}$ . Furthermore, the effect on LCoE when allowing for extra collisions by decreasing the design variable in question will also be investigated. In other words, the computed total collisions for the base case, with  $MTH = 25$  m,  $D_{rotor} = 236$  m, and  $P_{rated} = 15$  MW, is the reference point, where no collisions are either increased or reduced. The aim is to compute the LCoE values specifically for each integer value of reduced or increased bird collisions.

First, the produced LCoE and collision risk model (CRM) results are read in Python and combined into one dataframe. The data row that corresponds with the base case is stored. Next, a quadratic 1D interpolation function is constructed for all values in the total yearly collisions and LCoE columns. As stated in the paragraph above, the base case LCoE value of 45.93 EUR/MWh is used as the reference point for the calculation. From this point, each extra reduced or increased collision is passed to the interpolation function, from which the corresponding LCoE value is calculated. The results from Chapter 6 revealed that each species has a specific minimum and maximum number of collisions for the entire simulation. Thus, the interpolation function shall never calculate a reduced number of collisions past the allowable minimum for each species. This applies in both directions, i.e. the interpolation function shall never produce data beyond the maximum collisions per species calculated. The LCoE values are interpolated with a step size of 0.5 collisions. The relative increase ( $\Delta$ ) in LCoE will also be computed, to provide extra insights for informed decision-making. Finally, each value for the relevant design variable will be marked in the plot as well.

For the simulation where  $D_{rotor}$  is varied, the results from Chapter 6 showed that very few collisions can be mitigated for all species across the entire range of simulated values. In addition, in Chapter 7, it was found that varying the rotor diameter from the optimum has a significant increasing effect on the Levelised Cost of Electricity. Based on these results, the conclusion was drawn that the method used in this research for changing  $D_{rotor}$  does not provide useful insight on mitigating collision risk for the case study described in Chapter 5. The results, however, can still give insight into the Ecology-Technology model's behaviour when varying  $D_{rotor}$ . Thus, these results will be presented and discussed first in this chapter, after which the more useful measures of increasing MTH and  $P_{rated}$  will be discussed. Figures 8.1, 8.2, and 8.3 show the calculated absolute and relative LCoE values on the right and left y-axes (vertical axes), respectively. The x-axis (horizontal axis) shows the reduced and increased yearly bird collisions relative to the base case scenario. The round markers on each line show the corresponding  $D_{rotor}$  values for the exact data point they are plotted on.

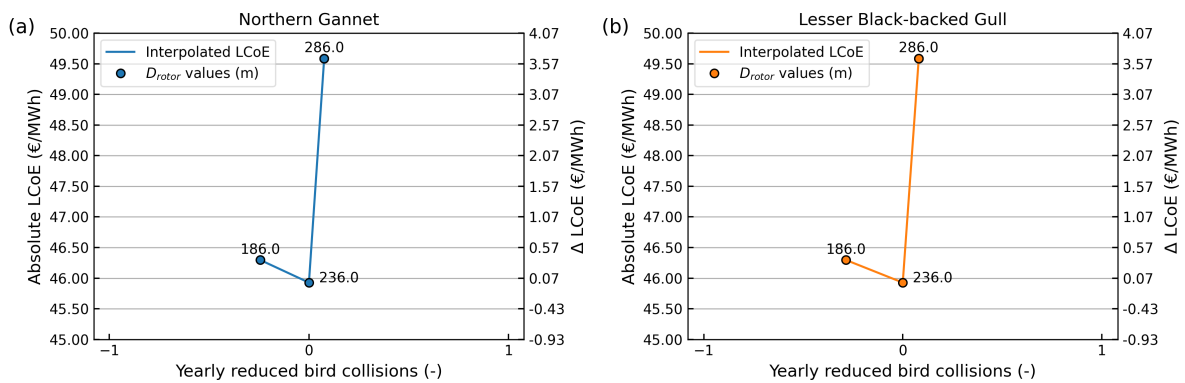


**Figure 8.1:** Calculated absolute and relative LCoE values for each reduction or increase in yearly bird collisions, relative to the base case. **(a)** Northern Gannet. **(b)** Lesser Black-backed Gull.

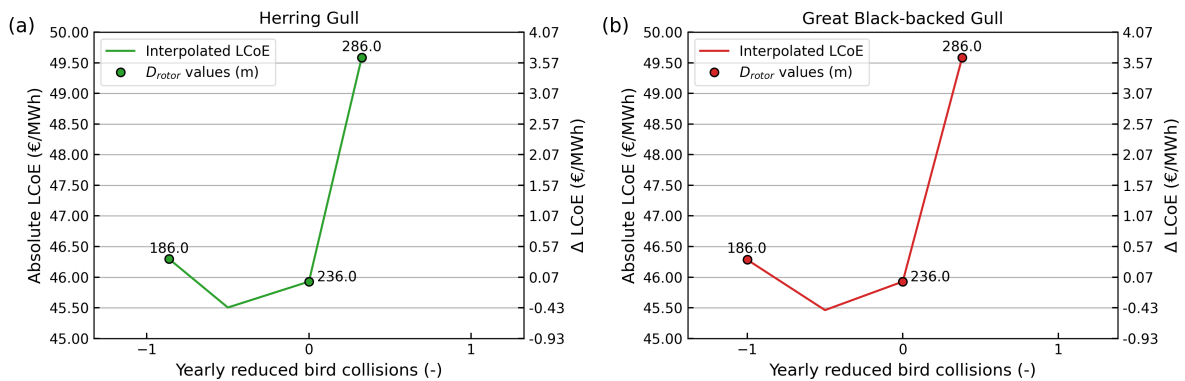


**Figure 8.2:** Calculated absolute and relative LCoE values for each reduction or increase in yearly bird collisions, relative to the base case. **(a)** Herring Gull. **(b)** Great Black-backed Gull.

In Figures 8.1, 8.2 and 8.3, the results show that for all species, no whole collision can be reduced by increasing  $D_{rotor}$  to 286 m. Figures 8.1 and 8.3 show that no whole collision is increased, when reducing to  $D_{rotor} = 186$  m. Figure 8.2 shows a minimum LCoE value at 45.50 EUR/MWh for the herring gull and great black-backed gull, in exchange for a 0.5 increased in yearly collisions. Looking back at Chapter 7, this makes sense, as it was shown that a minimum for the LCoE exists for  $D_{rotor} = 216$  m. Figures 8.1 and 8.3 would also show a minimum LCoE value, in case a smaller step size for the interpolation is used.

The simulation results indicate that, relative to the base case, reducing the rotor diameter to  $D_{rotor} = 216$  m can lower the LCoE by 0.43 EUR/MWh, at the cost of an annual increase of up to 0.5 collisions depending on species. Further reductions beyond 216 m increasing the LCoE can lead to up to one additional

collision per year for herring gulls and great black-backed gulls, while impacts on other species remain below 0.5. The aim was to assess whether a minor rotor diameter adjustment could significantly reduce collisions—a technically simple design change—but the findings show negligible mitigation even at  $D_{rotor} = 286$  m. Thus, all that remains is a slight cost optimisation that is possible at the expense of a small increase in collisions. However, as discussed in Chapter 5, altering the rotor diameter without adjusting the rotational velocity affects aerodynamic performance. This study maintains constant rotational speed, so the computed LCoE minimum at  $D_{rotor} = 216$  m should be validated against aerodynamic design criteria. From a collision mitigation perspective, varying  $D_{rotor}$  as is done in this simulation is therefore not an effective measure.

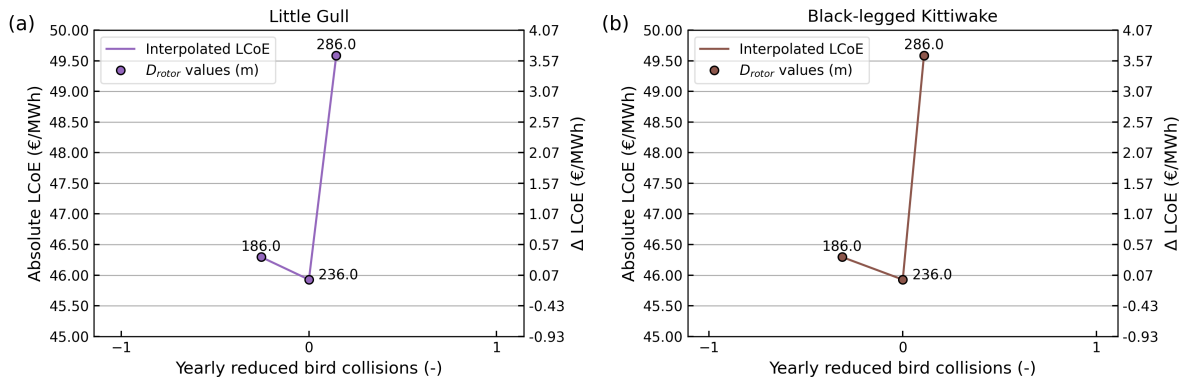


**Figure 8.3:** Calculated absolute and relative LCoE values for each reduction or increase in yearly bird collisions, relative to the base case. (a) Little Gull. (b) Black-legged Kittiwake.

In the next section, the results for varying the minimum tip height are discussed.

## 8.2. Results for Varying Minimum Tip Height

In Chapter 6, the results for varying the minimum tip height (MTH) demonstrated that increasing the minimum tip height has the potential to reduce collisions significantly for most species. Meanwhile, in Chapter 7, the increase in Levelised Cost of Electricity (LCoE) of the hypothetical wind farm as a result of increasing the MTH was calculated. Both of these simulations are combined to plot the total reduced collisions versus the LCoE. As explained in the previous section, the aim of this analysis is to evaluate the cost increase per additional evaded collision. This is done by first checking the SCRM datasets (Chapter 6) for the maximum possible collisions that can be reduced via increasing the MTH. Then, LCoE estimates are calculated for each reduced collision up to the possible maximum relative to the base case. A reduction in LCoE by calculating extra collisions relative to the base case is also computed until the possible minimum. Figures 8.4 to 8.9 present the resulting relation between LCoE and reduced/increased collisions for all six species:

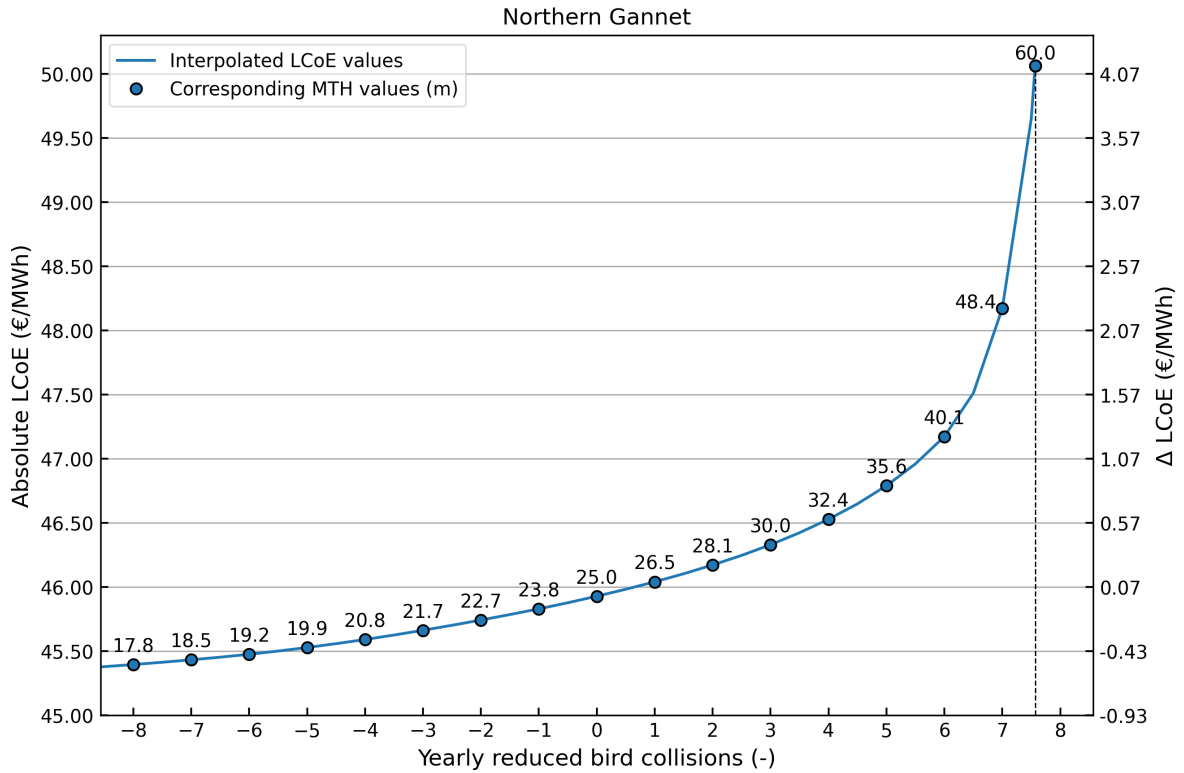


**Figure 8.4:** Absolute and relative LCoE values for each reduction or increase in yearly collisions.

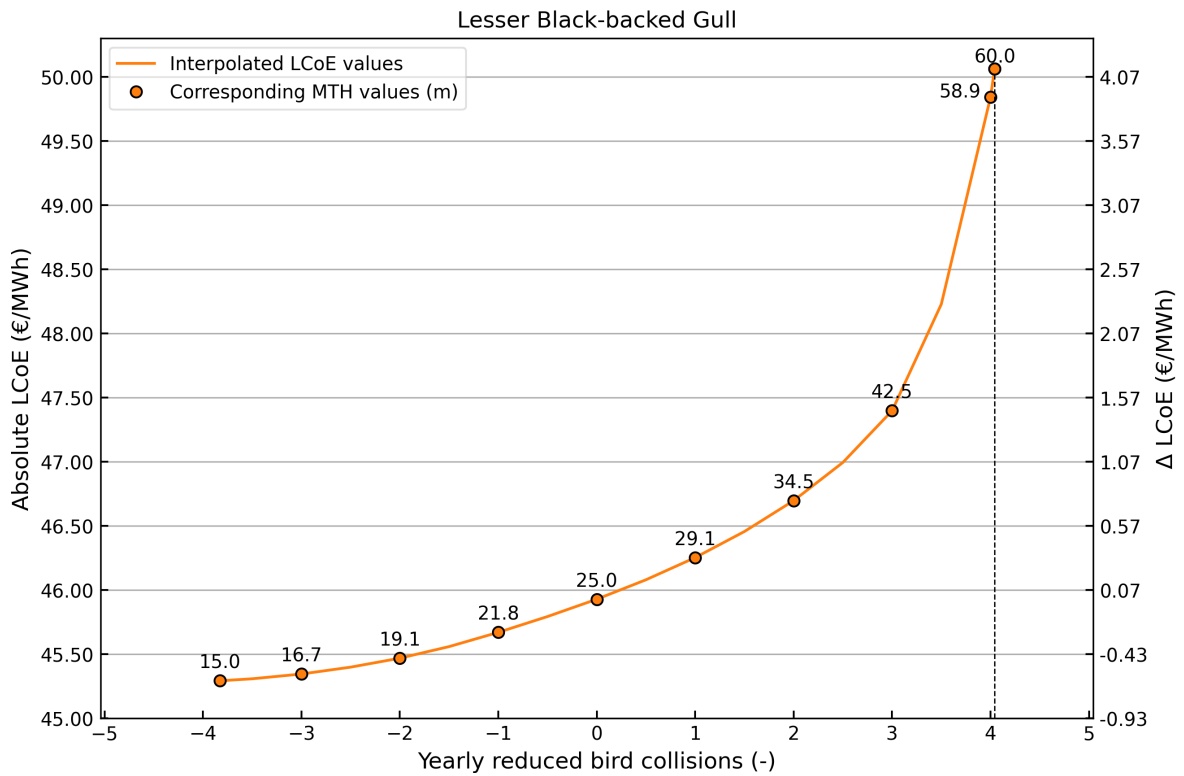


**Figure 8.5:** Absolute and relative LCoE values for each reduction or increase in yearly collisions.

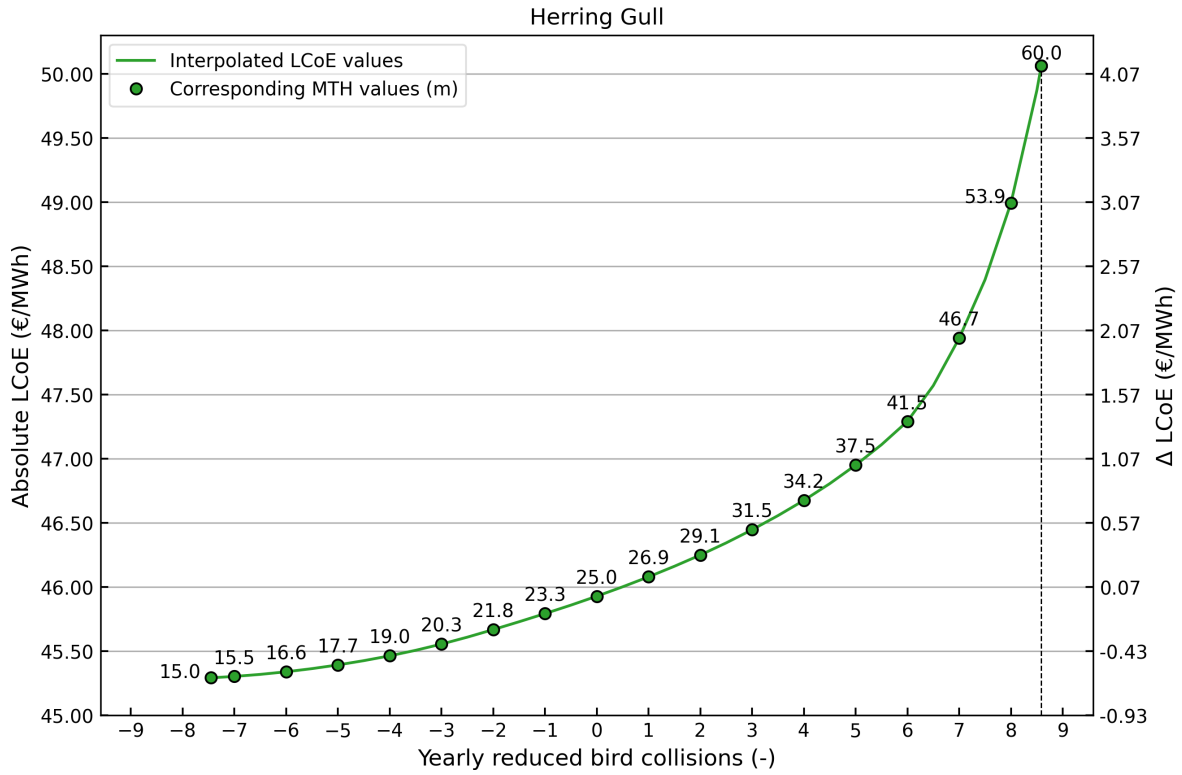


**Figure 8.6:** Absolute and relative LCoE values for each reduction or increase in yearly collisions.

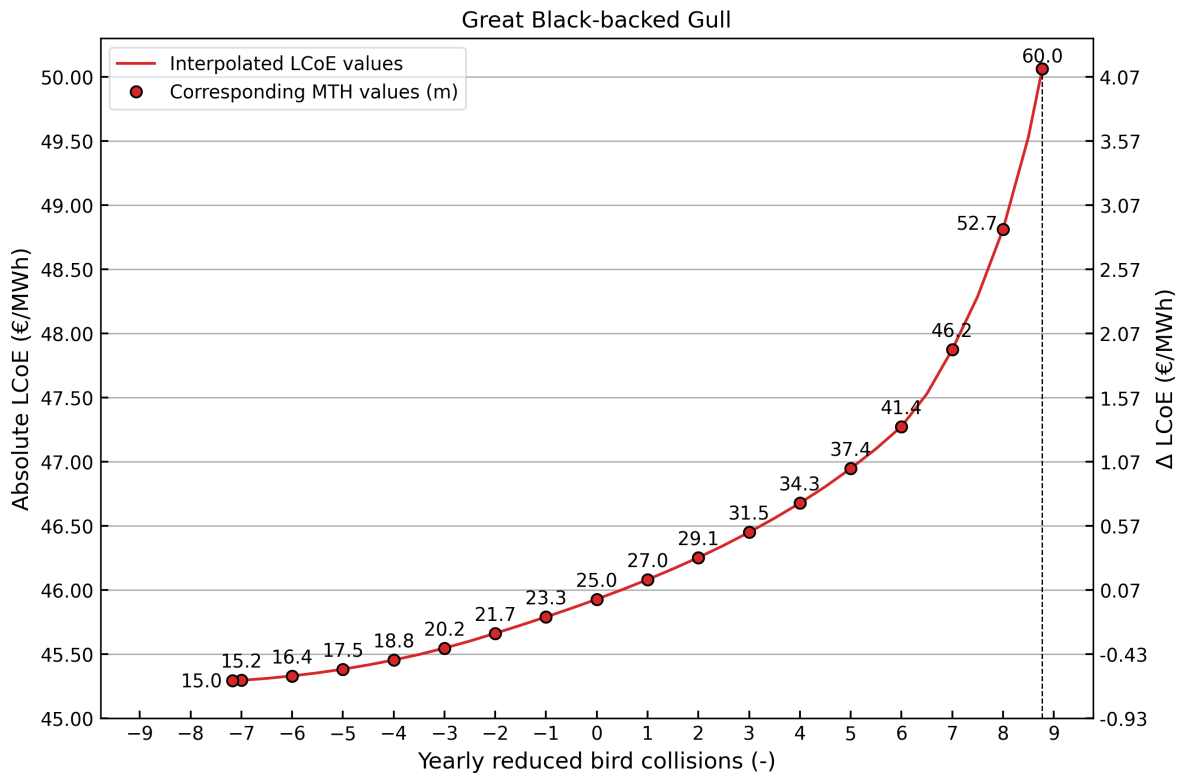


**Figure 8.7:** Absolute and relative LCoE values for each reduction or increase in yearly collisions.

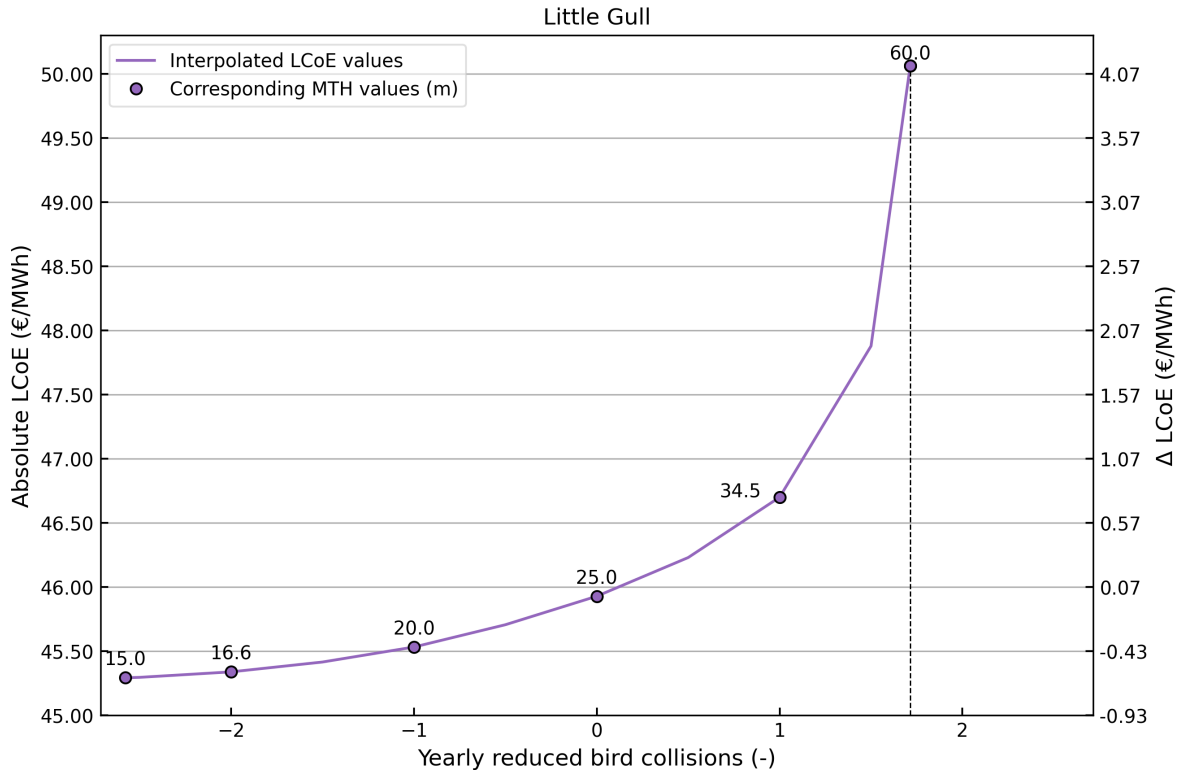


**Figure 8.8:** Absolute and relative LCoE values for each reduction or increase in yearly collisions.

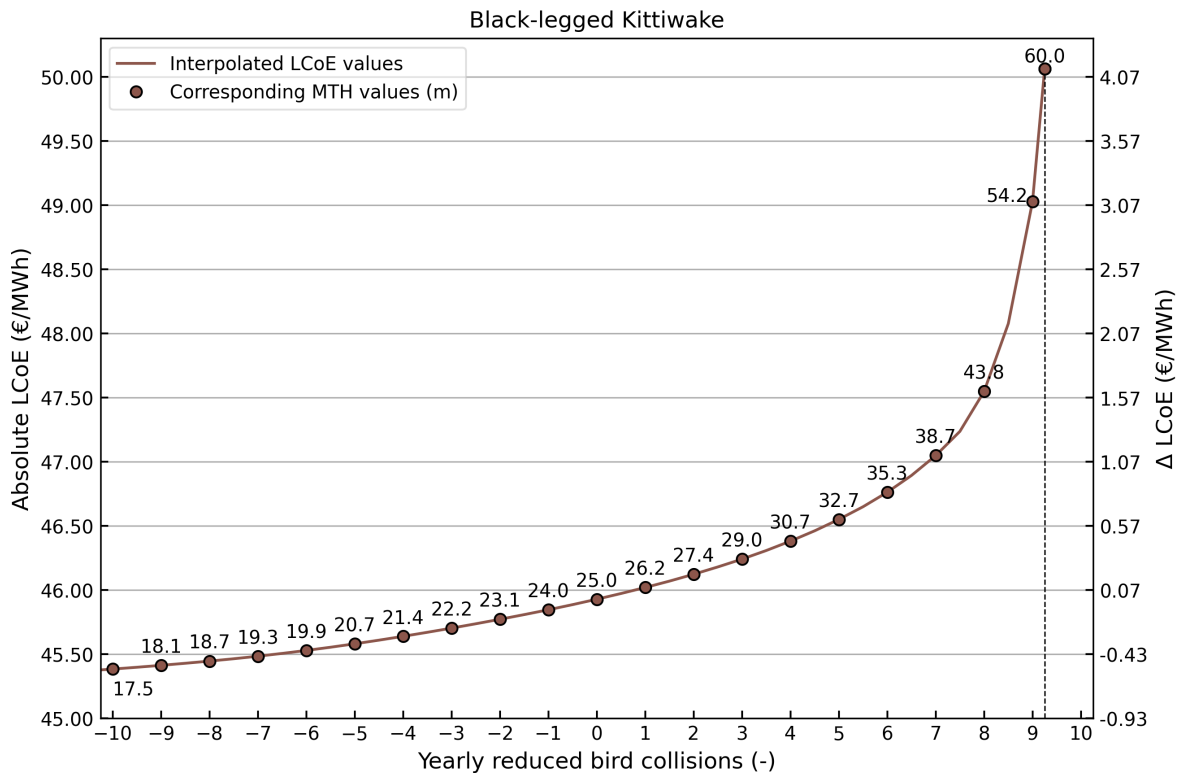


**Figure 8.9:** Absolute and relative LCoE values for each reduction or increase in yearly collisions.

The results for the northern gannet in Figure 8.4 show the increasing trend of LCoE when reducing more collisions. The MTH values are indicated at the blue markers, which correspond to integer reductions in collision numbers, except for the final point at MTH = 60 m. At this point, the maximum achievable reduction of 7.57 collisions is reached, as indicated by the vertical dashed line. Up to around 4 collisions avoided, the LCoE increases moderately to 46.50 EUR/MWh, corresponding to a relative increase of 0.57 EUR/MWh from the base case. Beyond this point, the increments in MTH required to avoid additional collisions increase rapidly, showing the effect of diminishing returns. From 4 to 5 collisions, MTH increases by 3.2 m; from 5 to 6 by 4.5 m; and from 6 to 7 by 8.3 m, before reaching the final MTH of 60 m. This steep exponential increase towards the maximum reduction is a general effect seen across all species. Up to approximately 5 collisions avoided, the LCoE increase remains relatively moderate for the northern gannet, and later in this chapter these values are further put into perspective by comparing them to the  $P_{rated}$  simulation. Reducing MTH below 25 m shows a decrease in LCoE, although this decrease is smaller than the corresponding increase when avoiding collisions. Additionally, the steps of MTH reduction become smaller with each step: from 1.2 m between 0 and -1 collisions to 0.7 m between -7 and -8, indicating that each metre of MTH reduction results in a larger increase in collision risk. Figure 8.4 is a cropped version, while the full extended plot between 15 m and 60 m MTH is provided in Appendix B.

For the lesser black-backed gull, the graph in Figure 8.5 shows the increasing trend of LCoE when reducing more collisions. The MTH values between 15 and 60 m are plotted at each marker, corresponding to integer values of collisions, except where MTH = 15 m and MTH = 60 m. The maximum possible reduction at this latter point is 4.04 collisions, indicated by the vertical dashed line. On the positive x-axis, between 0 and 2 collisions reduced, the LCoE increases moderately towards 46.75 EUR/MWh or 0.82 EUR/MWh from the base case. In this range, the MTH increments to reduce one extra collision increase from 4.1 m (0 to 1) to 8.0 m (2 to 3). Beyond this, the MTH rises steeply, with a 16.4 m increase from 3 to 4 collisions, eventually reaching 60 m. Overall, the LCoE impact remains moderate up to 2 collisions reduced, after which costs escalate rapidly. Reducing the MTH from 25 m results in a decreasing LCoE, with the MTH steps ranging from -3.2 m (0 to -1) to -1.7 m (-3 to -4), indicating that each additional metre reduced leads to a stronger increase in collisions.

The results for the herring gull in Figure 8.6 also show an increasing trend of LCoE when reducing more collisions. The MTH values between 15 and 60 m are plotted at each marker, corresponding to integer values of collisions, except at the simulation limits where MTH = 15 m and MTH = 60 m. The maximum possible reduction at MTH = 60 m is 8.59 collisions, indicated by the vertical dashed line. On the positive horizontal axis, between 0 and 4 collisions reduced, the LCoE increases steadily towards 46.75 EUR/MWh or 0.82 EUR/MWh from the base case. In this range, the MTH increments rise from 1.9 m (0 to 1) to 2.7 m (3 to 4). Beyond this, the increments of MTH become larger, with 3.3 m from 4 to 5 collisions and up to 7.2 m from 7 to 8 collisions. To reach the final reduction of 8.59 collisions, MTH increases to 60 m. On the negative horizontal axis, reducing the MTH from 25 m decreases LCoE, with MTH steps ranging from -1.7 m (0 to -1) to -1.1 m (-6 to -7), indicating that each additional metre reduced leads to a stronger increase in collisions.

For the great black-backed gull, the graph in Figure 8.7 shows the increasing trend of LCoE when reducing more collisions. The MTH values between 15 and 60 m are plotted at the red markers, corresponding to integer values of collisions, except at the simulation limits where MTH = 15 m and MTH = 60 m. The maximum possible reduction at MTH = 60 m is 8.77 collisions, indicated by the vertical dashed line. Between 0 and 4 collisions reduced, the LCoE increases gradually towards 46.75 EUR/MWh or 0.82 EUR/MWh from the base case, while MTH increments increase from 2.0 m (0 to 1) to 2.8 m (3 to 4). Beyond this, MTH steps grow further to 3.1 m (4 to 5) and 6.5 m (7 to 8) before reaching 60 m for the final reduction. Reducing MTH from 25 m decreases LCoE, with step sizes decreasing from -1.7 m (0 to -1) to -1.2 m (-6 to -7), indicating a stronger increase in collisions for each metre reduced here as well.

The results for the little gull in Figure 8.8 also show the increasing trend of LCoE when reducing more collisions. The MTH values between 15 and 60 m are plotted at the purple markers, corresponding to integer values of collisions, except at the simulation limits where MTH = 15 m and MTH = 60 m. The maximum possible reduction at MTH = 60 m is 1.71 collisions, as indicated by the vertical dashed line.

On the positive horizontal axis, the LCoE increases towards 46.75 EUR/MWh or 0.82 EUR/MWh from the base case, with a large MTH increase of 9.5 m from 0 to 1 collision reduced. From 1 to 2 collisions, MTH increases even further by 25.5 m to reach 60 m. Reducing MTH from 25 m results in a decreasing LCoE, with MTH steps ranging from -5.0 m (0 to -1) to -3.4 m (-1 to -2), indicating a stronger increase in collisions for each metre reduced here as well. Due to the limited range of maximum and minimum collisions calculated for the little gull (see also Chapter 6), a sudden change in slope is observed between points 1 and 2.

Lastly, the graph for the black-legged kittiwake in Figure 8.9 shows the increasing trend of LCoE when reducing more collisions. The MTH values are written at the brown markers, corresponding to integer values of reduced collisions, except where MTH = 60 m. At this point, the maximum possible reduction is 9.25 collisions, indicated by the vertical dashed line. On the positive horizontal axis, between 0 and 4 collisions reduced, the LCoE increases steadily towards 46.40 EUR/MWh or with 0.47 EUR/MWh from the base case. The MTH increments increase from 1.2 m (0 to 1) to 1.7 m (3 to 4), after which the increments in MTH increase from 2.0 m (4 to 5) to 5.1 m (7 to 8) and lastly 10.4 m (8 to 9) just before reaching 60 m MTH. Reducing the MTH from 25 m decreases LCoE, with MTH steps ranging from -1.0 m (0 to -1) to -0.6 m (-9 to -10), again showing a growing increase in collisions per metre reduced. The extended version of this plot can be found in Appendix B

For an overall comparison, the same results for all species are plotted together in Figure 8.10.

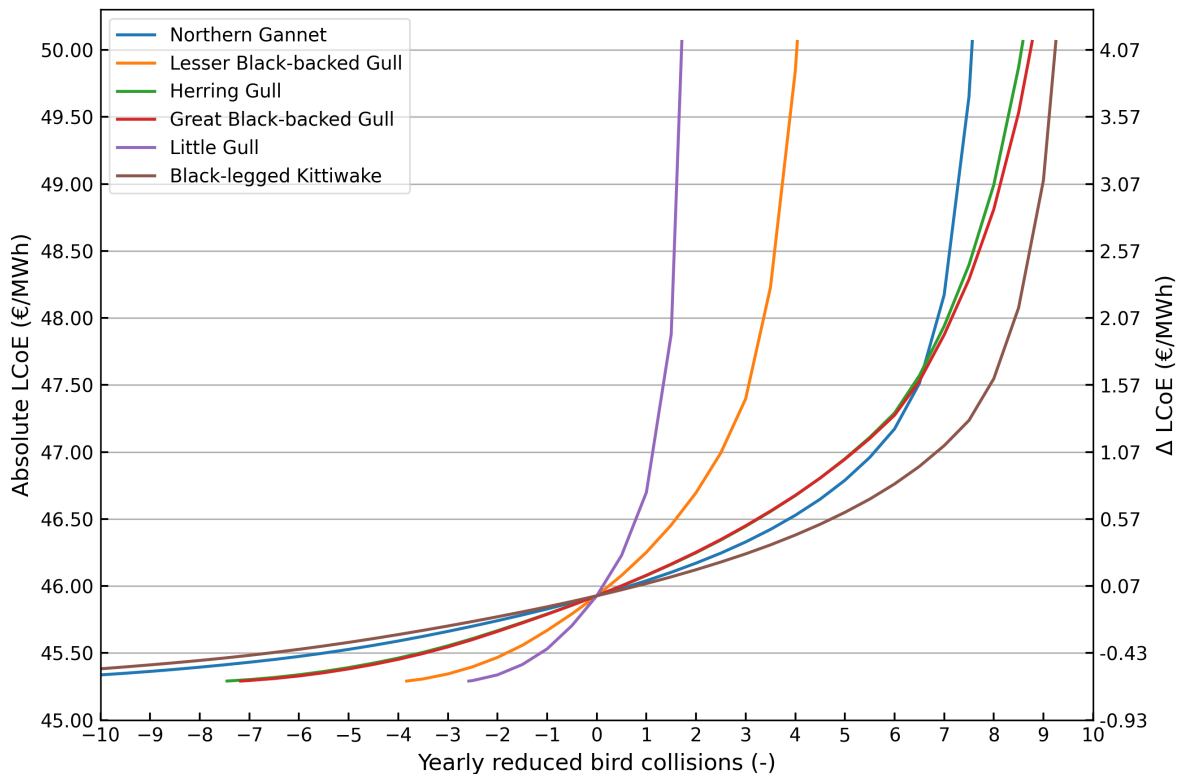


**Figure 8.10:** Absolute and relative LCoE values for reducing or increasing yearly collisions due to varying MTH, plotted for all studied species.

Firstly, all curves in Figure 8.10 show a similar trend and shape across all species, with differences in the total yearly collisions that can be reduced or increased. The black-legged kittiwake, great black-backed gull, herring gull and northern gannet are the species with the highest potential for collision reduction, as their curves become steep at higher numbers of avoided collisions, compared to the lesser black-backed gull and little gull. Out of all species, the black-legged kittiwake has the most reduced collisions at every LCoE value, between 0 and 9 collisions on the positive horizontal axis. In addition, the curves of the

top four species are close together for either +2 or -2 collisions, indicating that within this range, the cost-effectiveness of varying MTH is about the same for these species. Varying the MTH appears to be the least cost-effective for the little gull, with the lesser black-backed gull being slightly better.

Overall, Figure 8.10 illustrates that species with a higher number of collisions calculated in the base case allow for more cost-effective collision mitigation when increasing the minimum tip height. In contrast, species with relatively few collisions, such as the little gull and lesser black-backed gull, face a much more sensitive trade-off between MTH and LCoE. When reducing MTH, the opposite trend is seen: species with lower baseline collisions show a larger decrease in LCoE per collision increased. This highlights the asymmetric behaviour of the trade-off between collision reduction and LCoE across all species.

From  $LCoE = 48.50 \text{ EUR/MWh}$  ( $\approx 50 \text{ m MTH}$ ) and above, the amount of extra reduced collisions that can be realised for each species is less than one, with the exception of the herring gull and great black-backed gull. Furthermore, all curves appear to approach a vertical asymptote, which is in line with the exponential reduction that was seen in collision calculations from Chapter 6. While the curves for some species are limited due to the simulation boundaries, all species show a clear convergence towards a final LCoE value when reducing the MTH (following the negative horizontal axis). Specifically, Figure 8.10 shows that the absolute LCoE values converge to approximately  $45.25 \text{ EUR/MWh}$  when increasing collisions by reducing MTH. This is explained by the findings in Chapters 6 and 7, where it was shown that bird collisions increase exponentially towards lower MTH values, while the LCoE decreases approximately linearly when approaching  $MTH = 15 \text{ m}$ . Conversely, for an LCoE increase of around  $4.07 \text{ EUR/MWh}$  (i.e., a total of approximately  $50 \text{ EUR/MWh}$ ), roughly one collision can be reduced for the little gull, two for the lesser black-backed gull, and more for species with higher baseline collisions.

In the next section, the combined results for varying the rated power are discussed.

### 8.3. Varying Turbine Rated Power

Chapter 6 also presented results for varying rated power, i.e. the size and amount of turbines within the wind farm. It was demonstrated that a wind farm with larger turbines has the potential to reduce collisions to some extent for all seabird species except the little gull. Meanwhile, a varying relationship between LCoE and turbine rated power was calculated in Chapter 7. Both of these simulations are combined to plot the total reduced collisions versus the LCoE, in order to analyse the cost increase associated with avoiding one additional collision. The same method is used as in the previous section for MTH. The SCRM and LCoE simulations that were performed for a range of 10 to 23 MW turbines are combined, and the LCoE values are interpolated for whole numbers of reduced and increased collisions, using the base scenario as the reference point. Figures 8.11 to 8.16 present the resulting relation between LCoE and reduced/increased collisions for all six species:

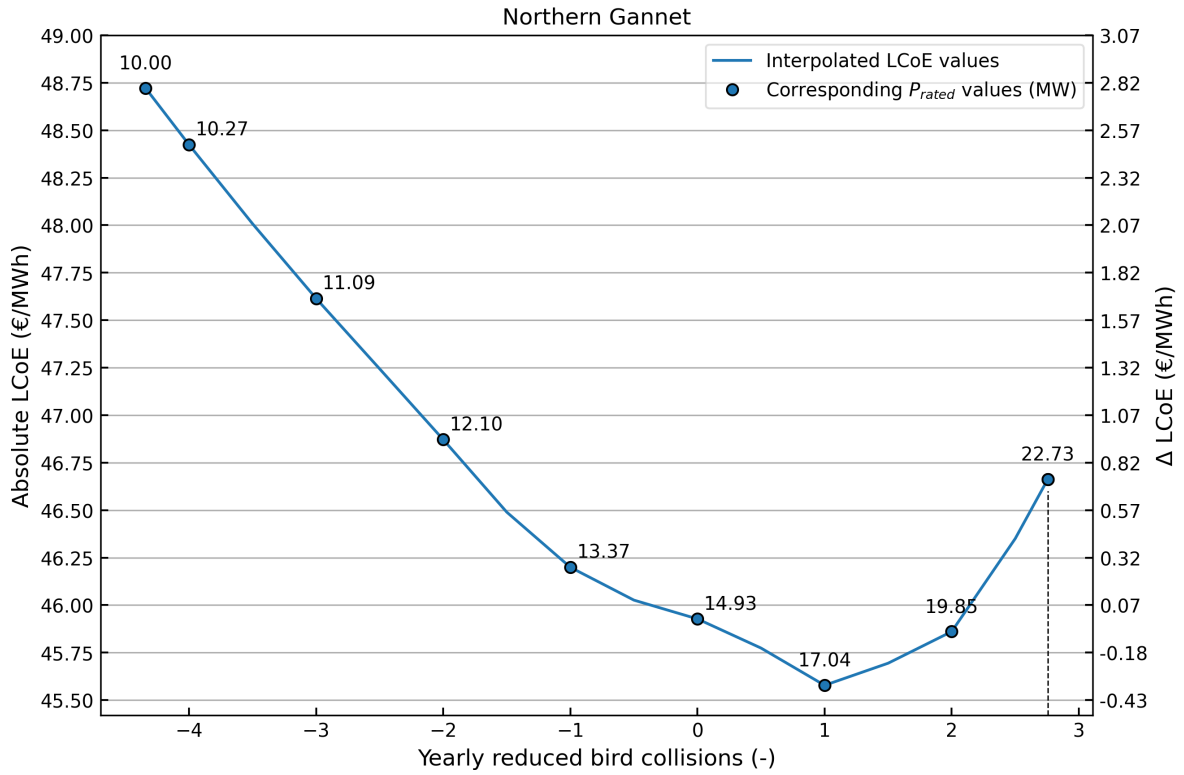


Figure 8.11: Absolute and relative LCoE values for each reduction or increase in yearly collisions.

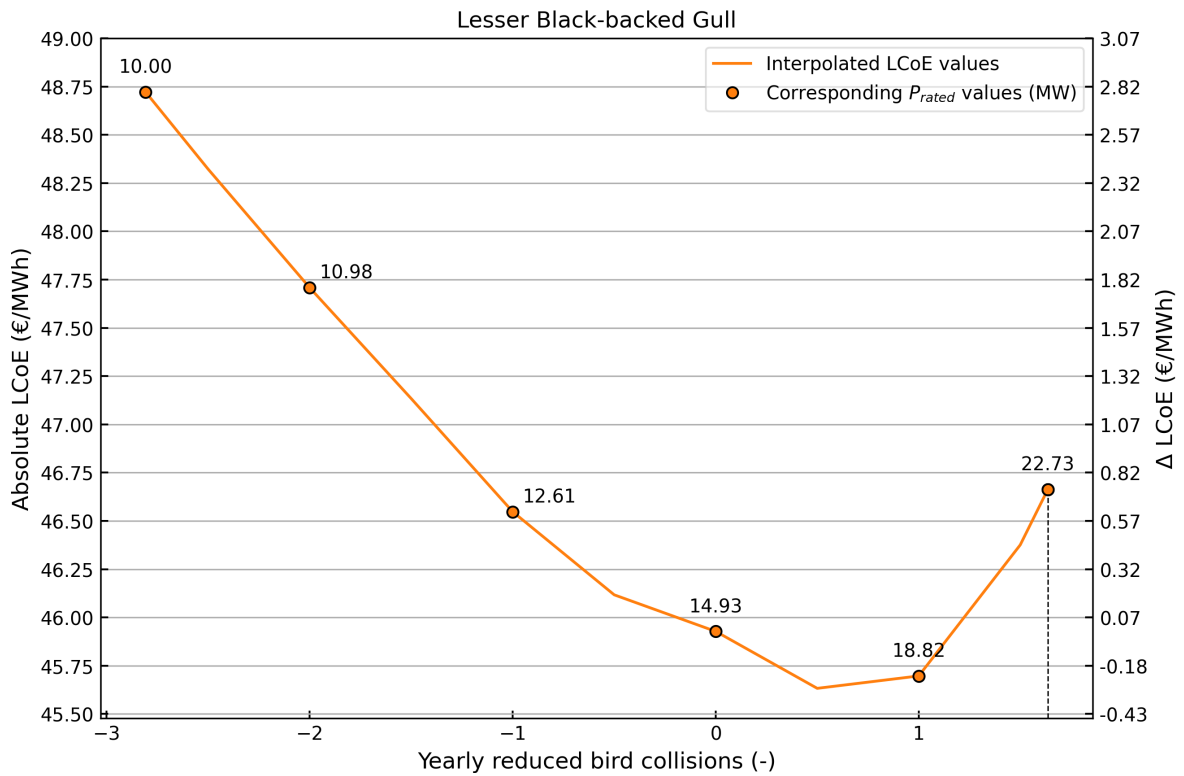


Figure 8.12: Absolute and relative LCoE values for each reduction or increase in yearly collisions.

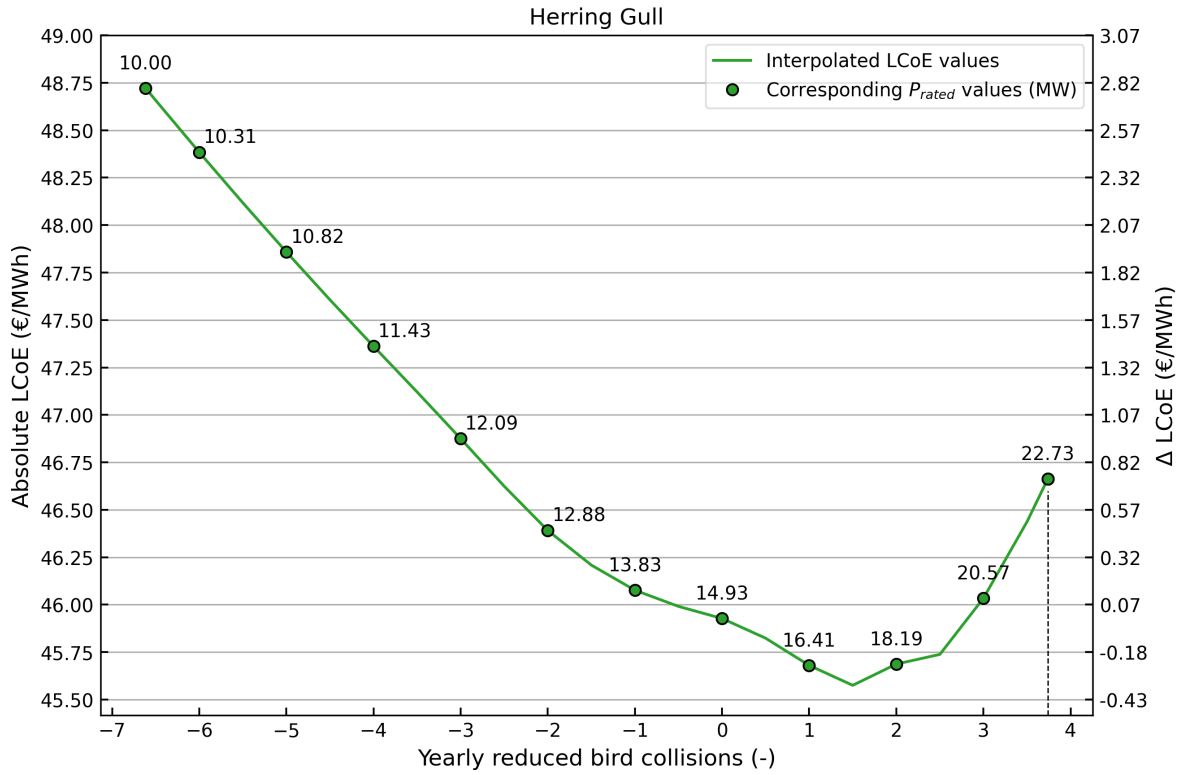


Figure 8.13: Absolute and relative LCoE values for each reduction or increase in yearly collisions.

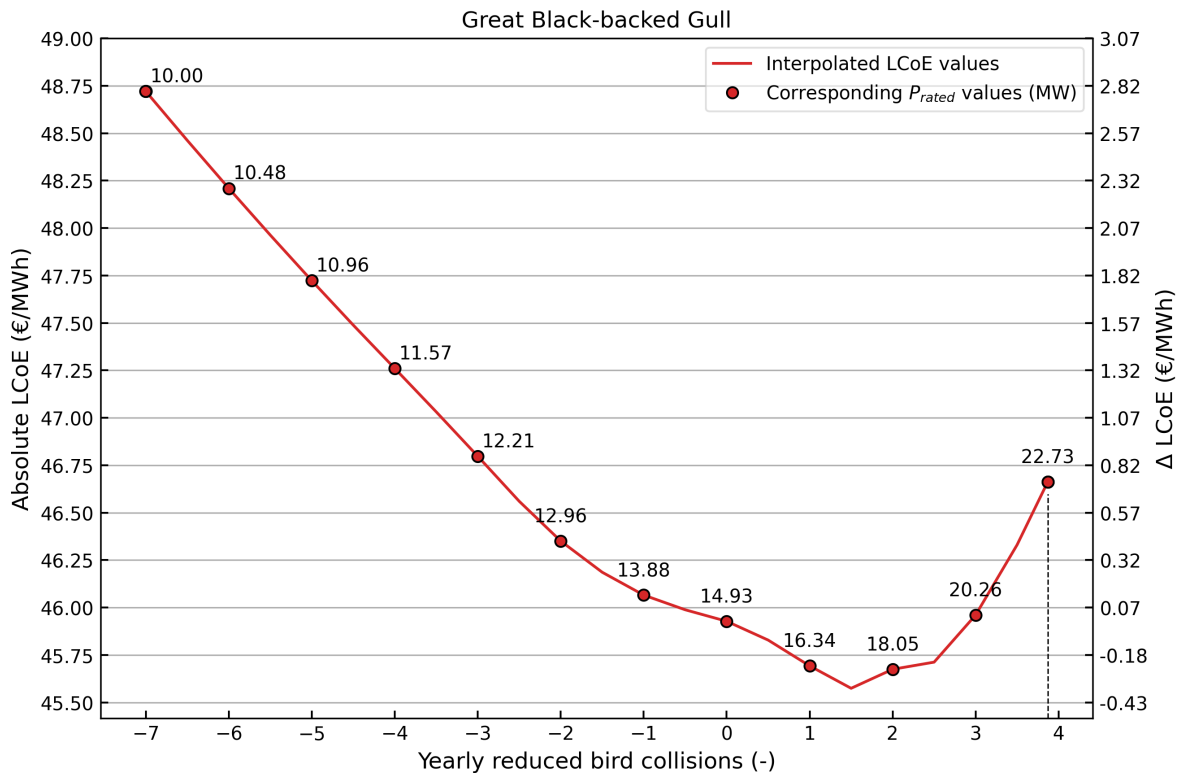


Figure 8.14: Absolute and relative LCoE values for each reduction or increase in yearly collisions.

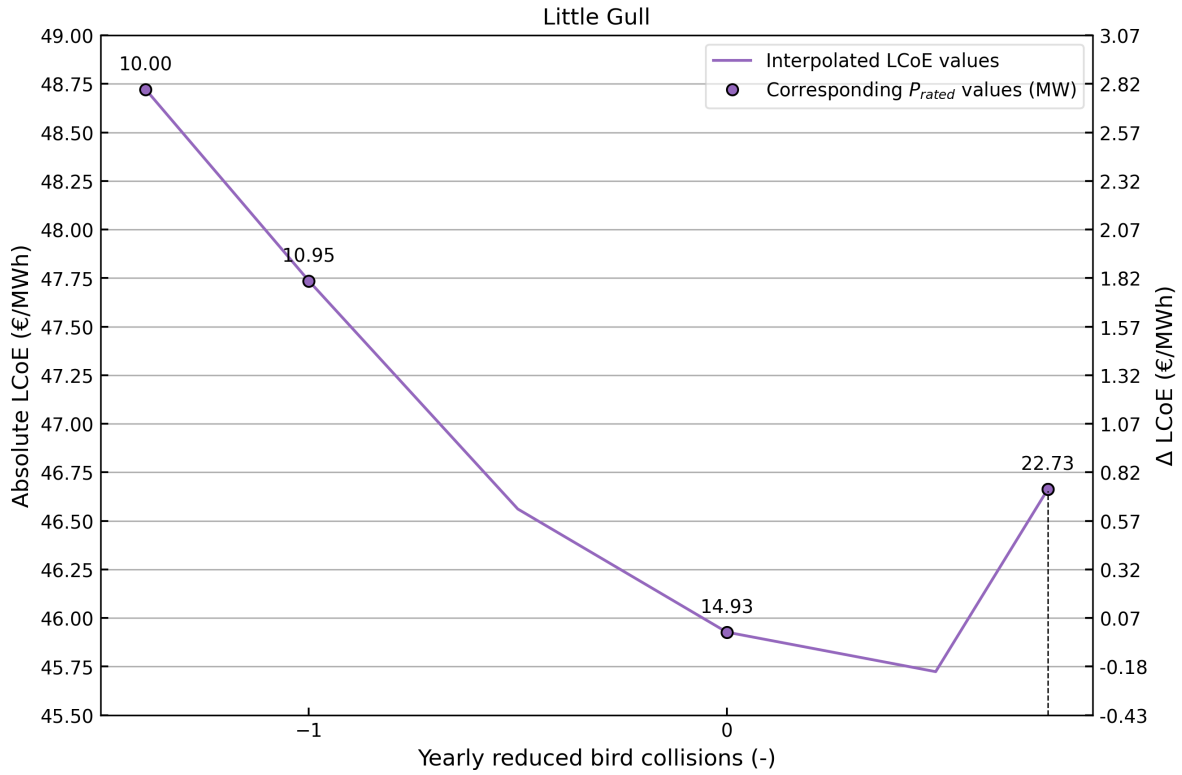


Figure 8.15: Absolute and relative LCoE values for each reduction or increase in yearly collisions.

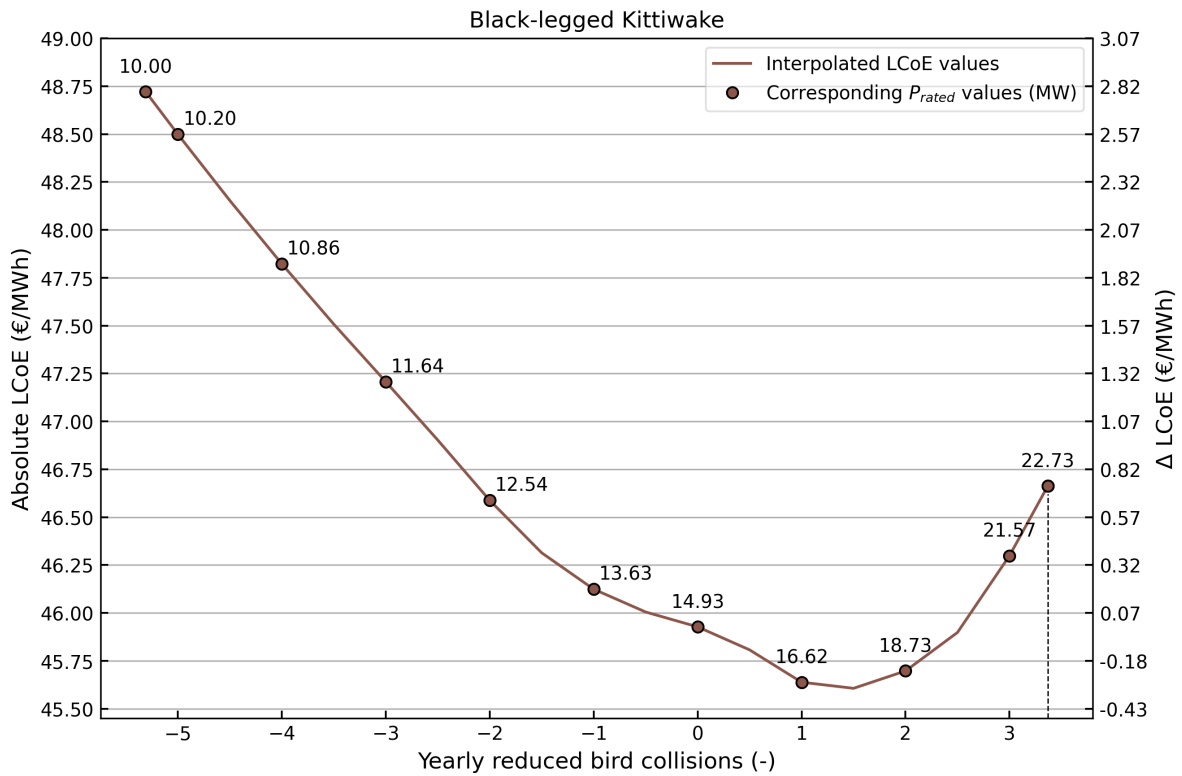


Figure 8.16: Absolute and relative LCoE values for each reduction or increase in yearly collisions.

The graph in Figure 8.11 shows a recognisable curve shape similar to the computed LCoE versus  $P_{rated}$  in Chapter 7 for the northern gannet. In this graph, the  $P_{rated}$  values are plotted at the blue markers, corresponding to integer values of yearly collisions. Along the positive horizontal axis, the maximum possible reduction is 2.76 collisions, as indicated by the vertical dashed line. From 0 to 1 collision reduced, the LCoE decreases, demonstrating the optimum rated power value of 17.04 MW. Thereafter, the LCoE increases between 1 and 2 collisions, and continues to rise towards the final value at  $P_{rated} = 22.73$  MW, where  $LCoE \approx 46.70$  EUR/MWh. Along the negative horizontal axis, decreasing  $P_{rated}$  from the base case of 15 MW shows a smaller increase in LCoE of approximately 0.30 EUR/MWh from 0 to -1 collisions, followed by a more linear increase between -1 and -4 collisions, reaching 48.74 EUR/MWh at  $P_{rated} = 10$  MW.

In Figure 8.12, the  $P_{rated}$  values are shown at the orange markers, corresponding to integer values of reduced yearly collisions for the lesser black-backed gull. The maximum possible reduction is 1.64 collisions, indicated by the vertical dashed line. Between 0 and 1 collision, the LCoE initially decreases to the optimum and then slightly increases, as  $P_{rated} = 18.82$  MW lies beyond the optimal value. The LCoE then increases significantly towards approximately 46.70 EUR/MWh at  $P_{rated} = 22.73$  MW. Along the negative horizontal axis, reducing  $P_{rated}$  from the base case results in a 0.60 EUR/MWh increase from 0 to -1, followed by a steady increase to nearly -3 collisions and an LCoE of 48.74 EUR/MWh.

The plot for the herring gull in Figure 8.13 shows a maximum possible reduction of 3.74 collisions at  $P_{rated} = 22.73$  MW, with an LCoE of approximately 46.70 EUR/MWh. The minimum LCoE lies between 1 and 2 collisions reduced, after which it increases up to the final value. On the negative horizontal axis, reducing  $P_{rated}$  from 15 MW increases the LCoE similarly to the previous species, leading to almost 7 additional collisions and an LCoE of 48.74 EUR/MWh at 10 MW.

Similar collision numbers are seen in the plot for the great black-backed gull in Figure 8.14. Between 0 and 1 collision, the LCoE decreases to its minimum at approximately 1.5 collisions, after which it rises steeply. The maximum possible reduction is 3.87 collisions at  $P_{rated} = 22.73$  MW, with a relative LCoE increase of around 0.77 EUR/MWh from the base case. Along the negative axis, reducing  $P_{rated}$  results in a smaller LCoE increase between 0 and -2 collisions, followed by a sharper rise between -2 and -7 collisions.

For the little gull, the graph in Figure 8.15 shows very limited potential for collision reduction via increased  $P_{rated}$ , with a maximum of 0.77 collision avoided at  $P_{rated} = 22.73$  MW. In the opposite direction, reducing  $P_{rated}$  to 10 MW results in more than one additional collision.

Lastly, the results for the black-legged kittiwake in Figure 8.16 indicate that the minimum LCoE is found between 1 and 2 collisions reduced. Between 2 and the maximum of 3.37 collisions, a steep increase in LCoE is observed, reaching a local maximum of 46.70 EUR/MWh. On the negative side, reducing  $P_{rated}$  to 10 MW results in more than 5 additional collisions, suggesting that this design change is suboptimal for both collision mitigation and economic feasibility.

For an overall comparison, the same results for all species are plotted together in Figure 8.17:

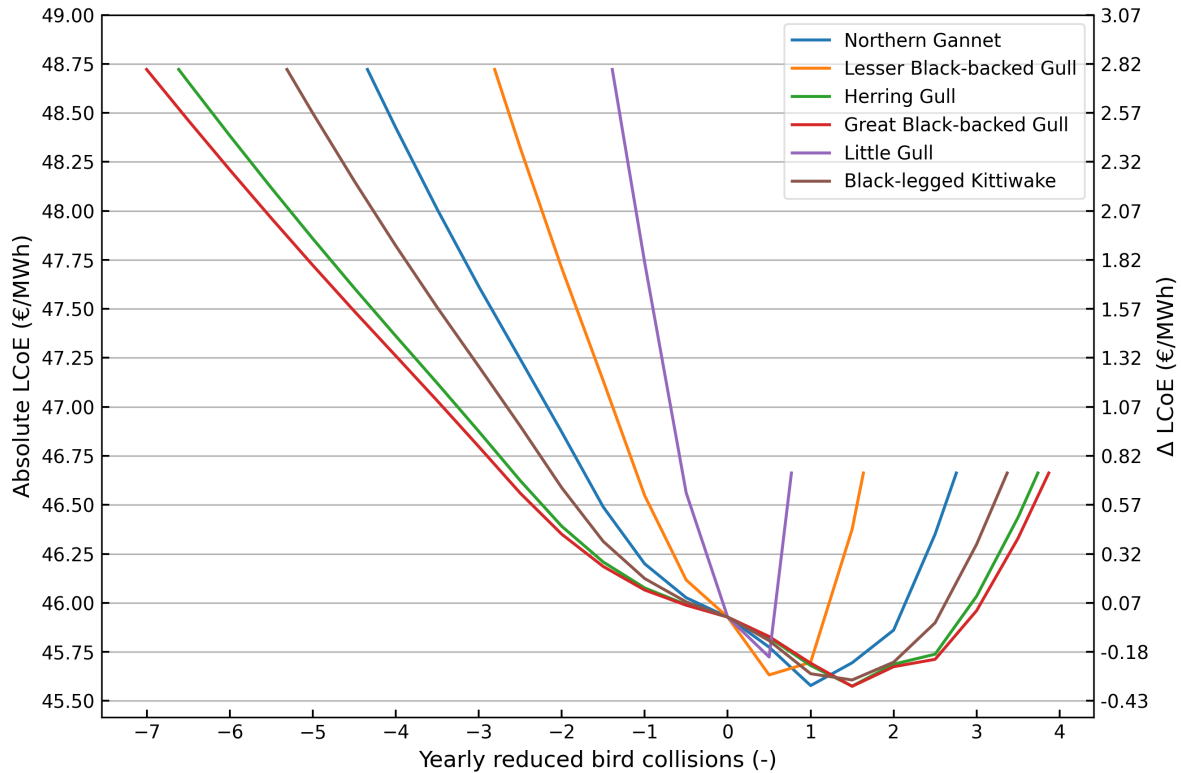


**Figure 8.17:** Absolute and relative LCoE values for reducing or increasing yearly collisions due to varying  $P_{rated}$ , plotted for all studied species.

In comparison to the previous section, Figure 8.17 shows that the great black-backed gull and herring gull achieve the highest maximum reduction in collisions when increasing  $P_{rated}$  up to 22.73 MW. These are followed by the black-legged kittiwake, northern gannet, lesser black-backed gull, and finally the little gull. Along the negative x-axis, where  $P_{rated}$  is reduced towards 10 MW, a similar but reversed order is observed. This indicates that species with the largest potential for collision reduction when increasing  $P_{rated}$  also experience the strongest increase in collisions when decreasing  $P_{rated}$ . The MTH simulation results also showed this relation. In addition, all curves show that reducing the rated power in this scenario is not beneficial for either collisions or costs, regardless of species. Each species has its own optimum reduced collisions value, for a  $P_{rated} \approx 17$  MW at which the Levelised Cost of Electricity (LCoE) is lowest. Except for the little gull, all species appear to reach this optimum at approximately the same LCoE value, indicating that the corresponding optimal  $P_{rated}$  is similar across species. Running another analysis with smaller step size, would therefore produce curves with their minima all at the same minimum LCoE.

Similar to the results for MTH, Figure 8.17 shows that the trade-off between collision reduction and LCoE for a varying  $P_{rated}$  is species dependent. A notable difference, however, is that the curves for all species lie much closer together compared to the MTH results. This indicates that changes in  $P_{rated}$  have a more uniform effect across species within the simulated range. It should be noted, however, that the species curves appear to diverge more strongly towards the edges of the plot, suggesting that this effect would likely increase if  $P_{rated}$  were extended beyond the current simulation limits.

For an increase in LCoE of  $\Delta 0.80$  EUR/MWh, the  $P_{rated}$  simulation in Figure 8.17 shows that approximately 0.8 collisions can be reduced for the little gull, 1.5 for the lesser black-backed gull, 2.8 for the northern gannet, 3.1 for the black-legged kittiwake, 3.8 for the herring gull, and 4 for the great black-backed gull. In contrast, Figure 8.10 shows that under the same LCoE increase, increasing MTH allows for the reduction of approximately 1 LG, 2 LBBG, 4 HG, 4 GBBG, 5 NG, and 6 BLK. These results suggest that, collectively, increasing the minimum tip height (MTH) is the more cost-effective

mitigation strategy. Nonetheless, the  $P_{rated}$  curves reveal a clear optimum point for each species, making it worthwhile to compare the two approaches more closely. This comparison will be made in the next section to further assess the cost-effectiveness of both design measures.

## 8.4. Evaluating MTH versus $P_{rated}$

As a final evaluation, it is useful to compare the results from varying the minimum tip height (MTH) and rated power ( $P_{rated}$ ) more closely. This enables direct conclusions about which of these two mitigation strategies is the most cost-effective for each species. For all species, the absolute and relative Levelised Cost of Electricity (LCoE) values are plotted against the reduction or increase in collisions, measured relative to the base case for both the MTH and  $P_{rated}$  simulations. This comparison is presented in Figures 8.18, 8.19, 8.20, 8.21, 8.22, and 8.23.

Note that the  $P_{rated}$  values correspond with the orange markers and are plotted in a slightly larger font to avoid confusion. At the intersection point at 0 collisions (i.e., the base case), the values for MTH and  $P_{rated}$  are coloured blue and orange, respectively, to emphasise which of the two LCoE curves each value belongs to.

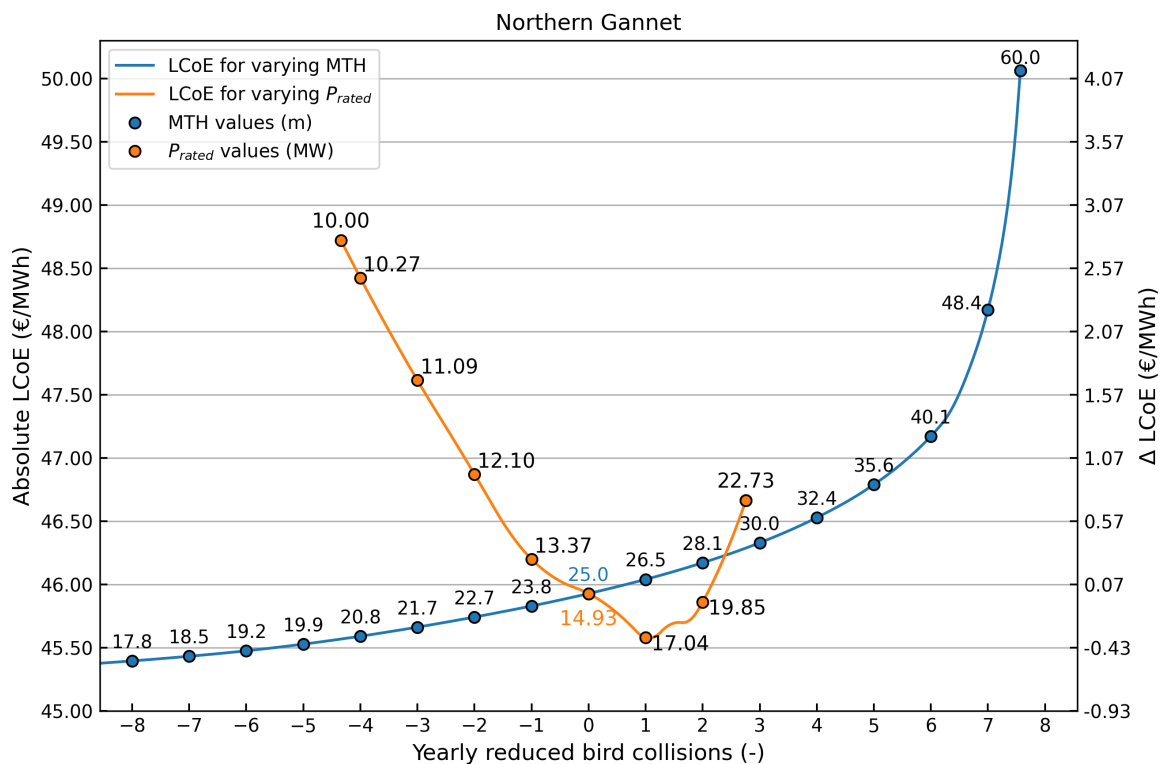


Figure 8.18: Comparison between the MTH and  $P_{rated}$  simulation for the northern gannet.

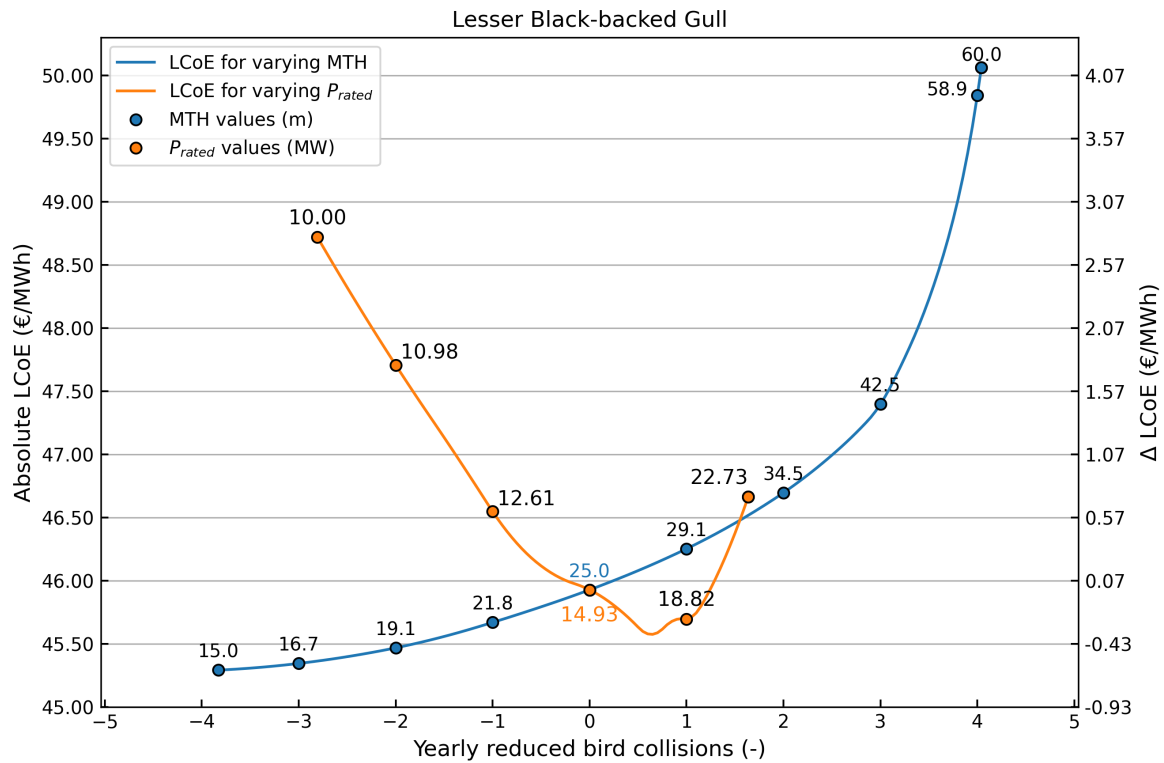


Figure 8.19: Comparison between the MTH and  $P_{rated}$  simulation for the lesser black-backed gull.

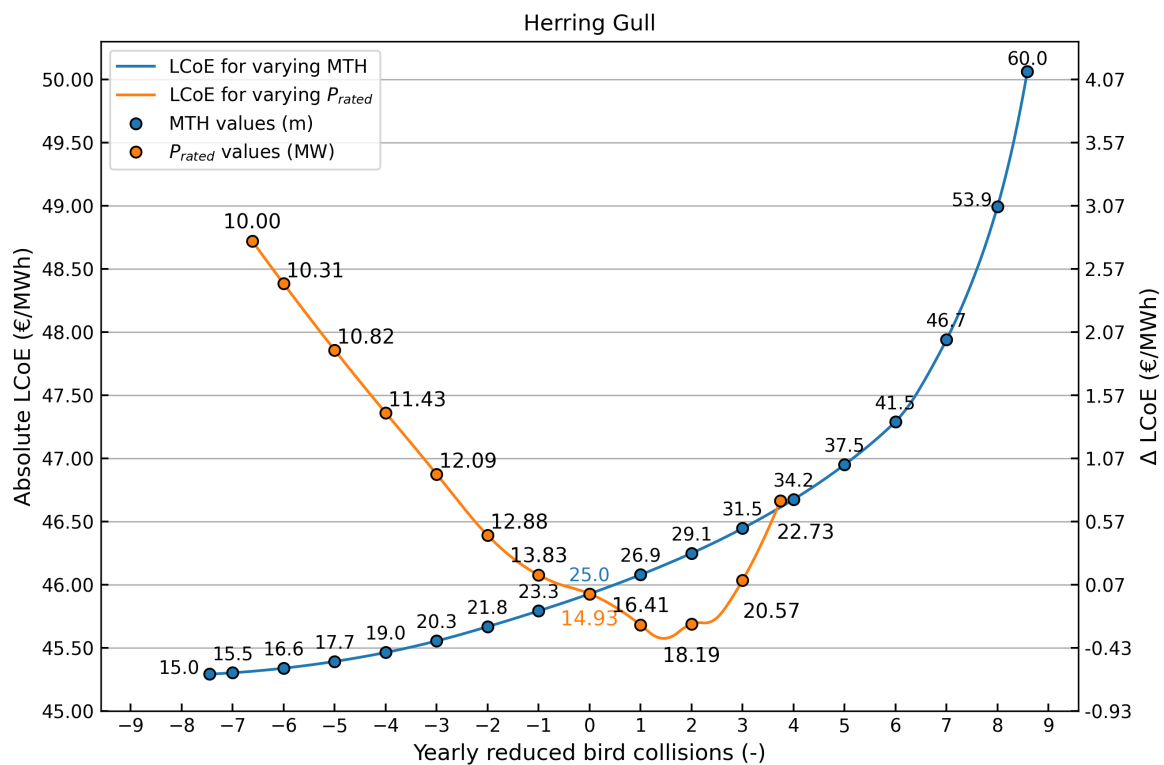


Figure 8.20: Comparison between the MTH and  $P_{rated}$  simulation for the herring gull.

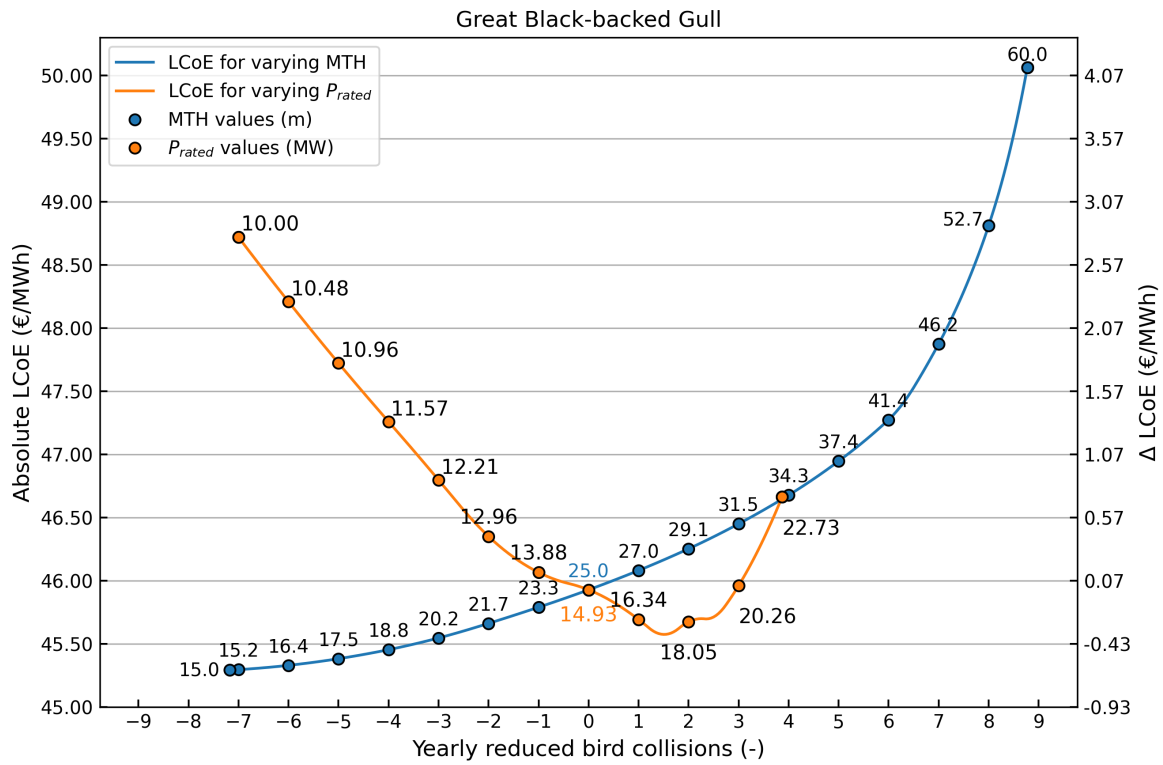


Figure 8.21: Comparison between the MTH and  $P_{rated}$  simulation for the great black-backed gull.

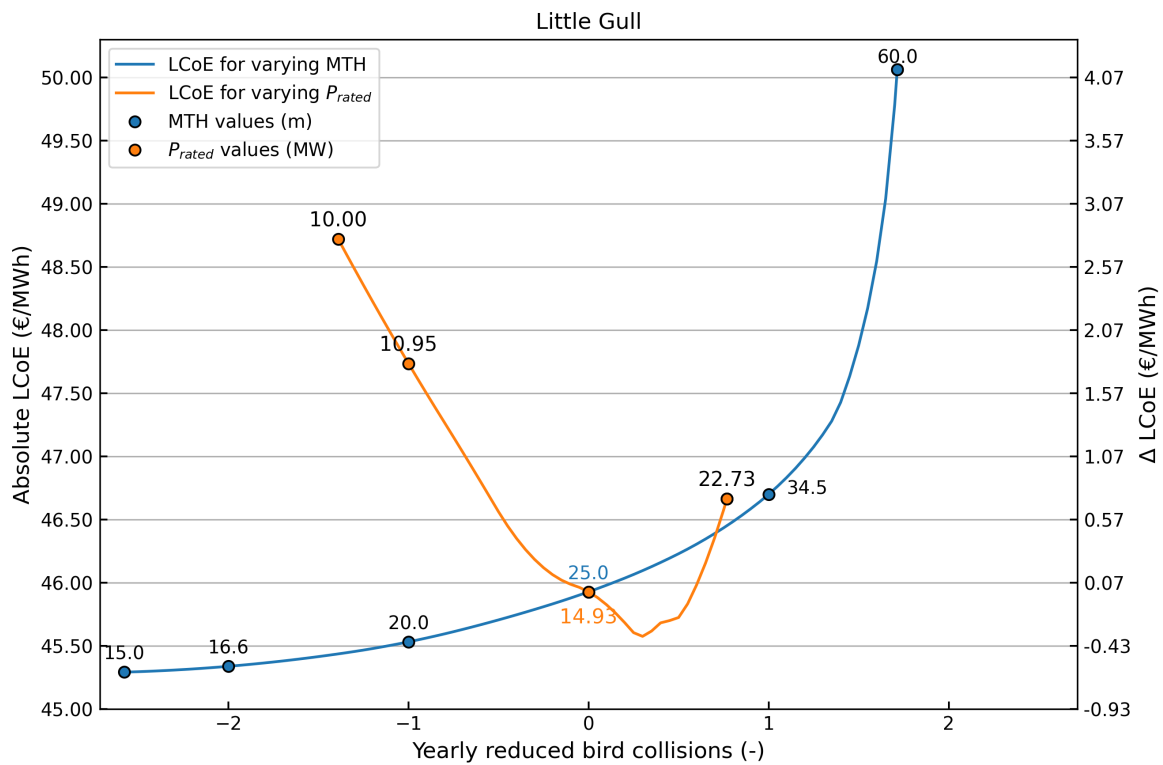
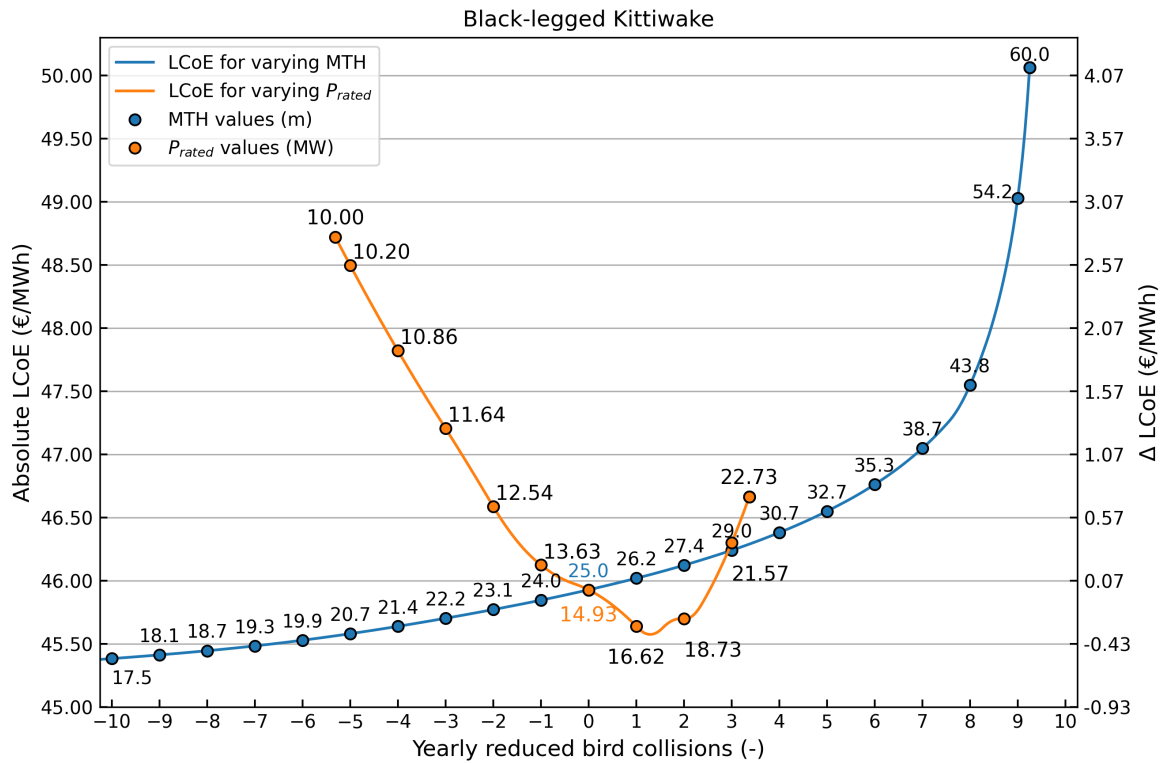


Figure 8.22: Comparison between the MTH and  $P_{rated}$  simulation for the little gull.



**Figure 8.23:** Comparison between the MTH and  $P_{rated}$  simulation for the black-legged kittiwake.

Figure 8.18 shows that, for the northern gannet, increasing the rated power ( $P_{rated}$ ) is initially the more cost-effective measure, up to approximately 2.4 collisions reduced. At this point, the two curves intersect at an LCoE of 46.23 EUR/MWh, corresponding to  $P_{rated}$  = 21.32 MW and MTH = 28.84 m. Beyond this intersection, increasing the minimum tip height (MTH) becomes the more favourable option, with the MTH curve reaching the same LCoE value at around 5 collisions, after which the LCoE increases more steeply.

A similar pattern is observed across all species. The species-specific values for the intersection point between the MTH and  $P_{rated}$  curves are summarised below. For each species, the collision count, corresponding LCoE,  $P_{rated}$  and MTH values are listed, showing up to which point increasing  $P_{rated}$  is more economically favourable than increasing MTH:

- **Lesser black-backed gull:** Up to 1.6 collisions, LCoE = 46.48 EUR/MWh,  $P_{rated}$  = 22.16 MW, MTH = 31.85 m.
- **Herring gull:** Up to 3.7 collisions, LCoE = 46.60 EUR/MWh,  $P_{rated}$  = 22.53 MW, MTH = 33.27 m.
- **Great black-backed gull:** Up to 3.9 collisions, LCoE = 46.64 EUR/MWh,  $P_{rated}$  = 22.66 MW, MTH = 33.81 m.
- **Little gull:** Up to 0.7 collisions, LCoE = 46.40 EUR/MWh,  $P_{rated}$  = 21.91 MW, MTH = 30.90 m.
- **Black-legged kittiwake:** Up to 2.9 collisions, LCoE = 46.23 EUR/MWh,  $P_{rated}$  = 21.32 MW, MTH = 28.87 m.

These findings highlight that increasing  $P_{rated}$  provides a more cost-effective solution for reducing a limited number of collisions across all species. However, once the species-specific intersection point is surpassed, increasing the minimum tip height (MTH) becomes the more economically favourable measure to further mitigate collisions. The exact location of this tipping point depends strongly on the species in question, reflecting the species-dependent outcome of this analysis.

Finally, when considering the negative horizontal axis—where design variables are reduced—lowering the MTH results in a decrease in LCoE, albeit at the expense of increased collisions. In contrast, reducing  $P_{rated}$  not only leads to higher collision numbers but also increases LCoE, making it an unfavourable strategy from both an ecological and economic perspective. Therefore, when aiming to decrease costs while accepting a higher number of bird collisions, adjusting the MTH proves to be the more economically favourable design parameter in this scenario.

## 8.5. Practical Implications

The previous sections emphasised the preferred design parameters for reducing collisions. Among varying MTH,  $D_{rotor}$  and  $P_{rated}$ , significant differences were found. It was shown that varying  $D_{rotor}$  is not a suitable collision mitigation measure within the scope of this research. While varying MTH can potentially reduce more collisions for more species simultaneously, there is a small window where increasing  $P_{rated}$  is the more cost-effective option, as described in the previous section.

From a practical engineering perspective, adjusting either the minimum tip height (MTH) or the rated power ( $P_{rated}$ ) of offshore wind turbines comes with distinct implications for turbine and wind farm design. Increasing the MTH primarily affects the hub height and overall tower length, which can lead to significant structural challenges, as explained in Chapter 7. Even though it appears to be an effective mitigation measure, increasing the MTH ultimately shifts the turbine away from its optimal configuration. As such, applying this measure in practice is complicated, since many more engineering analyses are required to verify feasibility.

In contrast, increasing  $P_{rated}$  is already a trend observed in the development of next-generation offshore wind farms, primarily to minimise operational expenses by reducing the number of turbines needed for a given total power output. This in turn reduces operations and maintenance (O&M) costs. However, scaling up  $P_{rated}$  introduces its own practical limitations. Larger turbines require specialised installation and maintenance vessels, which may not always be available or economically viable. Furthermore, based on current industry projections, it seems unlikely that turbines will exceed  $P_{rated} = 20$  MW in the near future. Thus, while increasing  $P_{rated}$  can offer a cost-effective method to mitigate a limited number of bird collisions, there appears to be a practical upper limit to this strategy. An upper limit also exists for increasing MTH. Manufacturers may find this limit based on their design simulations for the turbine in question.

Both MTH and  $P_{rated}$  scaling were modelled in this research without taking into account manufacturing or logistical constraints. In reality, these constraints may further limit the feasible design space for both parameters, as certain dimensions—such as blade length or tower diameter—are constrained by transport logistics, production facilities, or port infrastructure. It should also be noted that increasing the tip height, and thus the hub height may be an issue with respect to air traffic regulations, which may impose a maximum allowable tip height.

From an ecological and installation perspective, larger turbines with bigger monopiles may require more extensive pile driving during installation. This could increase underwater noise levels, potentially leading to greater disturbance or harm to marine life. Other side effects from an ecological perspective may arise due to the proposed mitigation measures. Therefore, this topic is recommended for further study in future research.

Lastly, it is important to emphasise that the results presented in this research are based on first-order calculations. Therefore, it is difficult to definitively conclude which of the two measures—increasing MTH or increasing  $P_{rated}$ —is the universally preferable option. Instead, the findings should be interpreted as guidelines for exploring the potential of both measures to mitigate bird collisions. Ultimately, the most suitable solution will depend on project-specific characteristics and constraints, which may lead to different outcomes and conclusions for other case studies. The required reduction in bird collisions within the North Sea may depend on the outcomes of cumulative impact assessments or the introduction of stricter environmental regulations as well. While these aspects fall outside the scope of this research, they are highly relevant in practice, as they could strongly influence the decision to which mitigation measure should be implemented, based on the required amount of collisions that

should be mitigated.

## 8.6. Assumption Implications

Overall, both the stochastic collision risk model (SCRM) and WINDOW LCoE model used are first-order models. These come with many simplifications, as can be found in (Humphries et al., 2022), (Zaaijer, 2013), and (Mehta et al., 2024). Assumptions for the stochastic SCRM were explicitly and implicitly discussed in Chapter 3 and Chapter 6 respectively. Implicit and explicit assumptions for the LCoE model were discussed in Chapter 7. The main implications of these assumption are mentioned and discussed briefly in this section.

The findings of this research regarding the effectiveness of increasing minimum tip height (MTH) or increasing the rated power ( $P_{rated}$ ) in reducing collisions align with the findings from ecology studies of the Ijmuiden Ver Alpha site (van der Vliet et al., 2022). Nevertheless, as discussed in Chapters 3 and 7, modelling seabird collision risk and the associated Levelised Cost of Electricity (LCoE) implications in offshore wind farm design involves several assumptions, mainly due to uncertainties in behavioural assessments of seabirds interacting with offshore wind farms. While the use of stochLAB and WINDOW provided a practical framework for first-order assessments, these assumptions inevitably simplify the real-world dynamics of bird behaviour and turbine operation. As such, future validation of the simulation results would strengthen this research, as no real-world case studies are currently available for these simulations.

In Chapter 6, it was mentioned that a fixed mean value for bird densities was used per month, along with a standard deviation for the collision calculations. In reality, bird densities could vary with factors such as wind speed, but this is not reflected in the model. An industry expert stated that data suggesting correlations between seabird activity and wind speed is not currently available (Gyimesi, pers. comm., 2025). The dependency of the Ecology-Technology model on bird densities estimated from studies, naturally introduces uncertainty in the estimated collision number. In addition, no sensitivity analysis was performed in this research. As discussed in Chapter 3, the collision risk model is sensitive to several bird characteristics, with avoidance introducing the largest sensitivity on the results. Thus, it should be noted that the estimated collision numbers may be significantly different, should different bird characteristics be used.

On the technical side, each assumption has its implications for the accuracy of the Ecology-Technology model. Firstly, all simulations were conducted for design variable ranges that may not be feasible for real-world scenarios. While most limitations have been mentioned regarding operation, maintenance, and installation of wind turbines with increased geometry, there may be more constraints on the supply chain or logistical side of offshore wind farm development.

In addition, the support structure sizing module (Chapter 7), neglects fatigue, and therefore applies a fatigue safety factor of 1.5, based on IEC 61400-3 standards (Zaaijer, 2013). It is not explicitly stated by (Zaaijer, 2013) if this causes the support structure to be overdesigned or underdesigned. Thus, the results from this research are to be interpreted with this in mind. A more suitable fatigue analysis calculation may be beneficial for future improvements on this research.

Due to the low-fidelity of calculations, the WINDOW model uses a general safety factor of 1.5 that is applied to various model inputs, including the rotor thrust. This is to account for neglecting the dynamics caused by any periodic loading due to environmental forces such as wind or waves, as well as periodic loads during operation and control, or even a sudden load change due to a turbine failure. For this research, the question remains whether this safety factor is sufficient for ensuring the support structure's integrity over its lifetime, especially in light of the increased minimum tip height. This assumption is particularly relevant considering the natural frequency check discussed in Chapter 7, where the natural frequency was found to be close to the maximum 1P frequency for the base case. Increasing the minimum tip height shifted the natural frequency even closer to the 1P limit, until at 42.5 m MTH, an adjustment in monopile diameter was required to meet the natural frequency requirement. Still, it remains uncertain if this adjustment is sufficient to prevent the excitation frequency of the structure being reached, leading to resonance. Therefore, the results of this research should be

interpreted with this in mind, and it is recommended that a detailed analysis of dynamic loading is conducted to verify whether the general safety factor of 1.5 is acceptable.

Vessel types and costs were estimated in accordance with turbine size, based on linear scaling. In addition, a fixed market price for each vessel category was assumed. In practice, however, vessel availability is variable and day rates are subject to market fluctuations, which can strongly influence installation and maintenance costs. The WINDOW model does not account for this variability. Although vessel day rates were based on expert input, limited availability on real-world vessel day rates introduces significant sensitivity in the cost calculations.

In Chapters 5 and 7, metocean conditions such as waves, currents, soil, and seabed properties were mostly assumed as average or empirical values. For a first-order model, this is sufficient, although it does limit accuracy.

A more detailed implementation of varying MTH would be needed to improve the accuracy of the LCoE calculations. Most turbine-level components are currently scaled using a relationship that takes the rotor diameter. Therefore, these components in the model should be identified, and a decision should be made whether to include  $D_{rotor}$ , MTH, or both in the scaling functions. At present, varying MTH does not scale all turbine-level components in the model as is done when varying  $D_{rotor}$ , which impacts accuracy as well.

Finally, the case study in this research was based on the technical and ecological conditions of the IJmuiden Ver Alpha offshore wind farm zone. All simulations were carried out using site-specific inputs such as wind profiles, water depth, and monthly bird densities. As a result, the findings are closely tied to this location and may not be directly transferable to other offshore sites without appropriate adjustments. Nevertheless, this scenario provides a representative case for the Dutch North Sea context, and applying the results elsewhere would require additional calibration and site-specific data.

# 9

## Conclusion

It is concluded that the rapid growth of offshore wind energy in the North Sea, in combination with the lack of interdisciplinary tools for first-order evaluations, poses challenges for balancing renewable energy targets with avian conservation. In particular, the increased risk of bird collisions with wind turbines has emerged as a key concern in environmental impact assessments, including in the Dutch offshore wind sector. The industry currently faces major knowledge gaps in understanding species-specific bird behaviour offshore, as well as in quantifying the ecological trade-offs of turbine design choices.

While several studies have proposed operational mitigation measures, limited research exists on how wind turbine design itself can be optimised to reduce collision risks without compromising economic feasibility. This research aimed to contribute to this topic by focusing on how technical design choices affect both seabird collision risk and the Levelised Cost of Electricity (LCoE) for offshore wind farms. Therefore, the research objective was defined as:

*"Quantify the economic impact of implementing design-based mitigation measures to reduce seabird collisions in offshore wind farms in the North Sea."*

In short, the conclusion to this research objective is that increasing the minimum tip height is the most economically feasible of the three proposed design choices for reducing bird collisions, offering the highest potential for collision reduction across species. The only exception is a narrow range where increasing the rated power is more cost-effective, typically for the first few collisions avoided.

Several research questions were investigated in this research, in order to come to this conclusion. The first research question was: What are the key challenges and knowledge gaps in avian safety management for offshore wind farms? This question was answered in Chapter 2, where a comprehensive overview on the current state of offshore wind development in the North Sea and its potential impacts on bird species was provided. In this chapter, it was found that the key challenge in avian safety management lies in the limited availability of offshore monitoring data for bird behaviour and interactions with wind farms. This lack of data means that environmental impact assessments rely heavily on collision risk models (CRMs), which themselves are built on uncertain or simplified input parameters such as avoidance rates, flight heights and bird flux. Another critical challenge lies in the determining the species-specific interaction behaviour with offshore wind farms, such as flight characteristics and habitat use. Furthermore, knowledge gaps remain in quantifying habitat displacement effects, species-specific avoidance behaviour, and the cumulative impact of all future offshore wind farms in the North Sea on bird populations. These knowledge gaps ultimately limit the accuracy of current environmental assessments and create uncertainty in designing effective mitigation measures.

In Chapter 2, the second research question was investigated: What are the potential solutions to address the identified knowledge gaps in avian safety management? Proposed solutions include better monitoring of bird behaviour through tracking technologies, such as radars and bio-loggers, improved data collection offshore, and site-specific impact assessments using validated collision risk models

(CRMs). The third research question was: What type of choices can be chosen in the design process of wind turbines, to reduce the risk of collision? The literature review identified that collision risk can potentially be mitigated through measures such as increasing the minimum tip height and applying blade painting for improved visibility. Two more potential design-based mitigation measures were proposed in Chapter 4: varying rotor diameter and increasing turbine rated power.

The fourth research question was formulated as: What are the state-of-the-art methods for modelling seabird collision risk in offshore wind farms? Chapter 3 addressed the fourth research question by providing a detailed overview of current collision risk modelling (CRM) methods used in offshore wind farm (OWF) avian safety management. It was shown that CRMs play a central role in estimating the number of bird collisions at OWFs, particularly in offshore settings where monitoring is challenging. The Band model, specifically its offshore version, was identified as the industry standard for offshore collision calculations, as it was used in recent cumulative impact assessments like the KEC 4.0 report. This model estimates collision numbers based on a combination of bird flux, collision probability, and species-specific avoidance rates. However, the chapter also highlighted several limitations and assumptions within the Band model. Key limitations include the simplified representation of bird shape, the neglect of oblique approaches, and exclusion of stationary components such as the turbine tower. Moreover, the model's strongest sensitivities lie in the avoidance rate, flight height, and flight speed which all carry uncertainty in offshore environments. Recent developments aim to address these shortcomings by integrating Monte Carlo simulations into the Band model, or by allowing uncertainty in model inputs via standard deviation. Nevertheless, even with these improvements, the effectiveness of CRMs still heavily depends on the availability and quality of species-specific input data, particularly for offshore locations where data collection remains challenging.

Next, Chapter 5 addressed the fifth research question: What is a typical scenario for collision risk assessment within an offshore wind farm in the Dutch part of the North Sea? In this chapter, a representative scenario for collision risk assessments at offshore wind farms in the Dutch North Sea was defined, using the IJmuiden Ver Alpha site as a case study location. The scenario included detailed technical and ecological inputs, such as wind farm specifications, turbine design, wind resource data, and bird species distributions. The proximity to Natura-2000 areas made this location a relevant example for collision impact assessments. Six critical seabird species were identified based on their conservation status and overlap in action-radius with the site's area. Species-specific parameters such as flight speed, wingspan, and avoidance rates were presented, along with monthly bird densities. The turbine design for the base case assumed 67 turbines of 15 MW each, with a hub height and rotor diameter of 143 and 236 m respectively. The chapter also identified technical criteria that influence LCoE when design parameters like minimum tip height, rotor diameter, and rated power are varied, such as structural limits, vessel requirements, and aerodynamic efficiency constraints. At the end of this chapter, two key software tools were introduced: *stochLAB*, used for stochastic collision risk modelling, and *WINDOW openMDAO*, used for LCoE analysis through a multidisciplinary design optimisation framework. It was decided to evaluate trade-offs between ecological mitigation and technical feasibility with these models in the subsequent chapters.

In Chapter 6 the sixth research question was investigated: How effective are design variations in minimum tip height, rotor diameter, and rated power at reducing seabird collisions within the defined scenario? First, the *stochLAB* collision risk model was configured using species-specific flight height distributions and key bird and turbine parameters derived from the case study. Varying the minimum tip height proved to be the strategy with the highest potential for collision reductions, with steep reductions in collisions observed in the first few metres of increase, particularly for species with lower flight height distributions. In contrast, changes in rotor diameter showed minimal impact. Increasing the rated power of turbines also reduced total collisions by allowing for fewer turbines in the wind farm.

Chapter 7 addressed the seventh research question: What is the economic feasibility of design variations in minimum tip height, rotor diameter and rated power within the defined scenario? The simulations performed demonstrated that increasing the minimum tip height results in a significant Levelised Cost of Electricity (LCoE) increase, primarily driven by higher support structure costs and, for MTH > 42.5 m, additional costs required to meet the natural frequency limits. For varying rotor diameter, an LCoE optimum was found at  $D_{rotor} = 216$  m, after which further increases lead to significantly higher LCoE

---

values due to increased RNA and support structure costs. Finally, for varying rated power, an LCoE optimum was identified at  $P_{rated} = 17$  MW, while both smaller and larger turbines increased LCoE due to unfavourable scaling of either turbine numbers or component sizes.

The final research question was: Which mitigation measure provides the most cost-effective reduction in seabird collisions within the defined scenario? Simulations combining species-specific collision risk modelling and Levelised Cost of Electricity (LCoE) analysis were presented in Chapter 8. The results showed that increasing the minimum tip height (MTH) is generally the most cost-effective strategy for reducing a higher number of collisions, especially for species with high baseline collisions, such as the black-legged kittiwake and great black-backed gull. In contrast, increasing the rated power ( $P_{rated}$ ) can be more economically favourable for reducing a small number of collisions across species, up to a species-specific tipping point. Beyond this point, MTH becomes the preferred measure. Varying rotor diameter ( $D_{rotor}$ ) did not offer meaningful collision reduction within this model. The findings emphasise that no one-size-fits-all solution exists. Ultimately, the ecological and economic trade-offs are highly species-dependent. Selecting the optimal collision mitigation strategy also depends on the specific location and wind farm project, as these determine the relevant inputs and requirements.

# 10

## Recommendations

The literature review and interviews with industry experts revealed multiple recommendations for research into knowledge gaps related to avian conservation in offshore wind farms:

- Large-scale studies to better understand species-specific density variability under different wind and weather conditions, could be very useful in the context of control-based mitigation measures, by coupling these insights to varying electricity prices with varying wind conditions.
- In addition, improving offshore data on species-specific parameters, such as avoidance, flight speed, and flight height, remains essential to reduce uncertainty and improve the reliability of future collision risk assessments.
- Validating CRM predictions with offshore monitoring data, to strengthen confidence in model outputs used in environmental impact assessments, remains crucial. For example, by conducting extensive experiments with installed radar on offshore wind turbines, particularly to assess the effectiveness of promising collision mitigation measures.

As explained before, the prototype Ecology-Technology model serves as a basis to build upon. Therefore, valuable further research in the following directions is suggested:

- The stochLAB and WINDOW models could be integrated into a single optimisation framework, allowing the Ecology-Technology model to optimise for a certain number of collisions.
- Furthermore, a sensitivity analysis across both the CRM and LCoE models could be done, with a particular focus on key inputs such as avoidance rates, flight height distributions, and technical inputs like vessel data.
- Extensions to the Ecology-Technology model could include: incorporating CO<sub>2</sub> footprint calculations or a full Life Cycle Assessment (LCA); expanding the scenario analysis to multiple case studies with varying ecological and wind resource conditions, to test robustness and generalisability of results; exploring the ecological impacts on other marine life due to the applied mitigation measures; reassessing feasibility limits for increasing MTH and  $P_{rated}$  by integrating real-world constraints such as vessel availability, port capacity, and hub height regulations; including fatigue life calculations and dynamic loading cases to better represent structural demands over time; or even investigating the feasibility of hybrid mitigation strategies that combine design measures (e.g. MTH increase) with control measures such as local curtailment executed by an AI algorithm.
- The overall question remains on how industry standards should evolve to balance ecological constraints with offshore wind energy growth. The prototype Ecology-Technology model could be extended during the EcoWindToolbox project with this in mind, in order to facilitate this interdisciplinary discussion within the industry.

# References

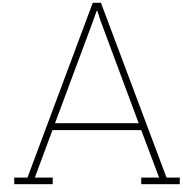
- Adviescollege Stikstofproblematiek. (2019). *Niet alles kan: Eerste advies van het Adviescollege Stikstofproblematiek: aanbevelingen voor korte termijn 25 september 2019*. (tech. rep.). Adviescollege Stikstofproblematiek. <https://edepot.wur.nl/501323>
- Arany, L., Bhattacharya, S., Macdonald, J., & Hogan, S. J. (2017). Design of monopiles for offshore wind turbines in 10 steps. *Soil Dynamics and Earthquake Engineering*, *92*, 126–152. <https://doi.org/10.1016/j.soildyn.2016.09.024>
- Arany, L., Bhattacharya, S., Macdonald, J. H., & Hogan, S. J. (2016). Closed form solution of Eigen frequency of monopile supported offshore wind turbines in deeper waters incorporating stiffness of substructure and SSI. *Soil Dynamics and Earthquake Engineering*, *83*, 18–32. <https://doi.org/10.1016/j.soildyn.2015.12.011>
- Band, B. (2012). *USING A COLLISION RISK MODEL TO ASSESS BIRD COLLISION RISKS FOR OFFSHORE WINDFARMS* (tech. rep.). [www.bto.org/soss](http://www.bto.org/soss).
- Binda, D. (2025). Ireland Auks and Thieves. <https://wildlifepics.nl/index.php/ireland-auks-and-thieves/>
- Birds Canada. (2024). About Motus. <https://motus.org/about/>
- Brabant, R., Vanermen, N., Stienen, E. W., & Degraer, S. (2015). Towards a cumulative collision risk assessment of local and migrating birds in North Sea offshore wind farms. *Hydrobiologia*, *756*(1), 63–74. <https://doi.org/10.1007/s10750-015-2224-2>
- Bradaric, M. (2022). *UvA-DARE (Digital Academic Repository) On the radar* (tech. rep.). <https://www.birdlife.org/worldwide/>
- Bradarić, M., Bouten, W., Fijn, R. C., Krijgsveld, K. L., & Shamoun-Baranes, J. (2020). Winds at departure shape seasonal patterns of nocturnal bird migration over the North Sea. *Journal of Avian Biology*, *51*(10). <https://doi.org/10.1111/jav.02562>
- Buij, R., Jongbloed, R., Geelhoed, S., van der Jeugd, H., Klop, E., Lagerveld, S., Limpens, H., Meeuwssen, H., Ottburg, F., Schippers, P., Tamis, J., Verboom, J., van der Wal, J. T., Wegman, R., Winter, E., & Schotman, A. (2018). *Kwetsbare soorten voor energie-infrastructuur in Nederland : overzicht van effecten van hernieuwbare energie-infrastructuur en hoogspanningslijnen op de kwetsbare soorten vogels, vleermuizen, zeezoogdieren en vissen, en oplossingsrichtingen voor een natuurinclusieve energietransitie* (tech. rep.). <https://doi.org/10.18174/449804>
- Burton, T., Jenkins, N., Sharpe, D., & Bossanyi, E. (2011). *Wind Energy Handbook* (3rd ed.). John Wiley & Sons.
- Busch, M., & Garthe, S. (2018). Looking at the bigger picture: The importance of considering annual cycles in impact assessments illustrated in a migratory seabird species. *ICES Journal of Marine Science*, *75*(2), 690–700. <https://doi.org/10.1093/icesjms/fsx170>
- Camphuysen, C. J., Scott, B. E., & Wanless, S. (2009, December). Distribution and foraging interactions of seabirds and marine mammals in the North Sea: multispecies foraging assemblages and habitat-specific feeding strategies. In *Top predators in marine ecosystems* (pp. 82–97). Cambridge University Press. <https://doi.org/10.1017/cbo9780511541964.007>
- Chamberlain, D. E., Rehfisch, M. R., Fox, A. D., Desholm, M., & Anthony, S. J. (2006). The effect of avoidance rates on bird mortality predictions made by wind turbine collision risk models. *Ibis*, *148*(SUPPL. 1), 198–202. <https://doi.org/10.1111/j.1474-919X.2006.00507.x>
- Choi, D. Y., Wittig, T. W., & Kluever, B. M. (2020). An evaluation of bird and bat mortality at wind turbines in the Northeastern United States. *PLoS ONE*, *15*(8 August). <https://doi.org/10.1371/journal.pone.0238034>
- Cook, A., & Collier, M. (2015). *Understanding avian collision rate modelling and application at the population level Introduction to talk* (tech. rep.). <https://tethys.pnnl.gov/sites/default/files/WREN-Webinar-3-Presentations.pdf>

- Cook, Humphreys, E. M., Bennet, F., Masden, E. A., & Burton, N. H. (2018, September). Quantifying avian avoidance of offshore wind turbines: Current evidence and key knowledge gaps. <https://doi.org/10.1016/j.marenvres.2018.06.017>
- Croll, D. A., Ellis, A. A., Adams, J., Cook, A. S., Garthe, S., Goodale, M. W., Hall, C. S., Hazen, E., Keitt, B. S., Kelsey, E. C., Leirness, J. B., Lyons, D. E., McKown, M. W., Potiek, A., Searle, K. R., Soudijn, F. H., Rockwood, R. C., Tershy, B. R., Tinker, M., . . . Zilliacus, K. (2022, December). Framework for assessing and mitigating the impacts of offshore wind energy development on marine birds. <https://doi.org/10.1016/j.biocon.2022.109795>
- Dierschke, V., Furness, R. W., & Garthe, S. (2016, October). Seabirds and offshore wind farms in European waters: Avoidance and attraction. <https://doi.org/10.1016/j.biocon.2016.08.016>
- DOWA. (2017). Wind farm zone Ijmuiden Ver. <https://www.dutchoffshorewindatlas.nl/atlas/image-library/image-library/wind-farm-zone-ijmuiden-ver>
- Gaertner, E., Rinker, J., Sethuraman, L., Zahle, F., Anderson, B., Barter, G., Abbas, N., Meng, F., Bortolotti, P., Skrzypinski, W., Scott, G., Feil, R., Bredmose, H., Dykes, K., Shields, M., Allen, C., & Viselli, A. (2020). *Definition of the IEA Wind 15-Megawatt Offshore Reference Wind Turbine Technical Report* (tech. rep.). [www.nrel.gov/publications](http://www.nrel.gov/publications).
- Garcia-Rosa, P. B. (2022). *Project memo Review of technology for bird detection and collision prevention* (tech. rep.). [www.sintef.no](http://www.sintef.no)
- Garcia-Rosa, P. B., & Tande, J. O. G. (2023). Mitigation measures for preventing collision of birds with wind turbines. *Journal of Physics: Conference Series*, 2626(1). <https://doi.org/10.1088/1742-6596/2626/1/012072>
- Grinderslev, C., & Hansen, M. (2022, August). *DTU Lecture: Wind Turbine Technology Module 1* (tech. rep.). DTU.
- GROW. (2024). GROW Partners. <https://grow-offshorewind.nl/partners-overview>
- Gusatu, L. F., Yamu, C., Zuidema, C., & Faaij, A. (2020). A spatial analysis of the potentials for offshore wind farm locations in the North Sea region: Challenges and opportunities. *ISPRS International Journal of Geo-Information*, 9(2). <https://doi.org/10.3390/ijgi9020096>
- GWEC. (2022). *GWEC.NET Associate Sponsors Supporting Sponsor Leading Sponsor* (tech. rep.). [www.gwec.net](http://www.gwec.net)
- Heerema. (2025). Sleipnir. <https://www.heerema.com/heerema-marine-contractors/fleet/sleipnir>
- Heinatz, K., & Scheffold, M. I. E. (2023). A first estimate of the effect of offshore wind farms on sedimentary organic carbon stocks in the Southern North Sea. *Frontiers in Marine Science*, 9. <https://doi.org/10.3389/fmars.2022.1068967>
- Humphries, G., Caneco, B., Cook, A., & Masden, E. (2022, December). *Package 'stochLAB'* (tech. rep.). <https://doi.org/10.32614/CRAN.package.stochLAB>
- IEA. (2025). IEA-15-240-RWT. <https://github.com/IEAWindSystems/IEA-15-240-RWT>
- IRO. (2025). DEME's offshore installation vessel 'Orion' successfully completes the near 15 MW turbine foundation installation project in Scotland and heads to US. <https://iro.nl/news-and-press/demes-offshore-installation-vessel-orion-successfully-completes-the-near-15-mw-turbine-foundation-installation-project-in-scotland-and-heads-to-us/>
- Johnston, A., Cook, A. S., Wright, L. J., Humphreys, E. M., & Burton, N. H. (2014). Modelling flight heights of marine birds to more accurately assess collision risk with offshore wind turbines. *Journal of Applied Ecology*, 51(1), 31–41. <https://doi.org/10.1111/1365-2664.12191>
- KeyFactsEnergy. (2023). Bird Behaviour Study is Changing How We Think About Offshore Wind Development. <https://www.keyfactsenergy.com/news/21342/view/>
- Krüger, L., Ramos, J. A., Xavier, J. C., Grémillet, D., González-Solís, J., Petry, M. V., Phillips, R. A., Wanless, R. M., & Paiva, V. H. (2018). Projected distributions of Southern Ocean albatrosses, petrels and fisheries as a consequence of climatic change. *Ecography*, 41(1), 195–208. <https://doi.org/10.1111/ecog.02590>
- Kushlan, J. (2023). Northern Gannet Life History.
- Lambertucci, Shepard, & Wilson. (2015). Extinction risks from climate change: How will climate change affect global biodiversity? *Science*, 348(6234), 501–502. <https://doi.org/10.1126/science.aab2057>
- Leemans, J. J., Brave Rebolledo, E. L., Kuiper, K., Heida, N., van Bemmelen, R. S. A., Ijntema, G. J., Madden, H., & Gyimesi, A. (2024). *Bird research in offshore wind farm Borssele. Fluxes, corridor use, flight-and avoidance behaviour. Report 24-084*. (tech. rep.). Waardenburg Ecology. <https://www.researchgate.net/publication/383841581>

- Leemans, J. J., Van Bemmelen, R. S. A., Middelveld, R. P., Kraal, J., Bravo Rebolledo, E. L., Beuker, D., Kuiper, K., & Gyimesi, A. (2022). *Bird fluxes, flight- and avoidance behaviour of birds in offshore wind farm Luchterduinen*. Bureau Waardenburg Report 22-078 (tech. rep.). Bureau Waardenburg. <https://waardenburg.eco>
- Leopold, Booman, Collier, Davaasuren, Fijn, & Gyimesi. (2015). *A first approach to deal with cumulative effects on birds and bats of offshore wind farms and other human activities in the Southern North Sea* (tech. rep.). <https://library.wur.nl/WebQuery/edepot/329749>
- Marques, A. T., Batalha, H., Rodrigues, S., Costa, H., Pereira, M. J. R., Fonseca, C., Mascarenhas, M., & Bernardino, J. (2014, November). Understanding bird collisions at wind farms: An updated review on the causes and possible mitigation strategies. <https://doi.org/10.1016/j.biocon.2014.08.017>
- Martin, G. R., & Banks, A. N. (2023, April). Marine birds: Vision-based wind turbine collision mitigation. <https://doi.org/10.1016/j.gecco.2023.e02386>
- Masden, E. A., & Cook, A. S. (2016). Avian collision risk models for wind energy impact assessments. *Environmental Impact Assessment Review*, 56, 43–49. <https://doi.org/10.1016/j.eiar.2015.09.001>
- Masden, E. (2015). *Scottish Marine and Freshwater Science Report Vol 6 No 14 Developing an avian collision risk model to incorporate variability and uncertainty* (tech. rep.). <https://doi.org/10.7489/1659-1>
- Masden, E. A., McCluskie, A., Owen, E., & Langston, R. H. (2015). Renewable energy developments in an uncertain world: The case of offshore wind and birds in the UK. *Marine Policy*, 51, 169–172. <https://doi.org/10.1016/j.marpol.2014.08.006>
- May, R., Reitan, O., Bevanger, K., Lorentsen, S. H., & Nygård, T. (2015). Mitigating wind-turbine induced avian mortality: Sensory, aerodynamic and cognitive constraints and options. <https://doi.org/10.1016/j.rser.2014.10.002>
- McWilliam, M. K., Natarajan, A., Pollini, N., Dykes, K., & Barter, G. E. (2021). Conceptual monopile and tower sizing for the IEA Wind Task 37 Borssele reference wind farm. *Journal of Physics: Conference Series*, 2018(1). <https://doi.org/10.1088/1742-6596/2018/1/012025>
- Mehta, M. (2023). mihir0210/WINDOW\_static: Turbine sizing for electricity and hydrogen production (v3.0\_turbine\_sizing). <https://doi.org/https://doi.org/10.5281/zenodo.8380355>
- Mehta, M., Zaaijer, M., & von Terzi, D. (2022). Optimum Turbine Design for Hydrogen Production from Offshore Wind. *Journal of Physics: Conference Series*, 2265(4). <https://doi.org/10.1088/1742-6596/2265/4/042061>
- Mehta, M., Zaaijer, M., & von Terzi, D. (2024). Drivers for optimum sizing of wind turbines for offshore wind farms. *Wind Energy Science*, 9(1), 141–163. <https://doi.org/10.5194/wes-9-141-2024>
- Merlaud, Mendes, & Resende de Paiva. (2023). *Metocean Assessment Analysis Report Ijmuiden Ver Wind Farm Zone* (tech. rep.). [https://offshorewind.rvo.nl/file/download/175dfe66-8458-4182-8e79-80968a469fc5/ijv\\_20231222-dhi-metocean-analysis-report.pdf?utm\\_source=chatgpt.com](https://offshorewind.rvo.nl/file/download/175dfe66-8458-4182-8e79-80968a469fc5/ijv_20231222-dhi-metocean-analysis-report.pdf?utm_source=chatgpt.com)
- Netherlands Enterprise Agency. (2023). Offshore Wind Energy Plans 2030-2050. <https://english.rvo.nl/topics/offshore-wind-energy/plans-2030-2050>
- NINA. (2023). Seabirds at sea. <https://seapop.no/en/distribution-status/distribution/seabirds-at-sea/>
- Noordzeeloket. (2025). Nature and biodiversity. <https://www.noordzeeloket.nl/en/functions-use/natuur/>
- NWO. (2024). What does the Dutch Research Council do? <https://www.nwo.nl/en/what-does-the-dutch-research-council-do>
- Parisé, J., & Walker, T. R. (2017). Industrial wind turbine post-construction bird and bat monitoring: A policy framework for Canada. *Journal of Environmental Management*, 201, 252–259. <https://doi.org/10.1016/j.jenvman.2017.06.052>
- Pérez Pérez, N. (2023, December). *Avian Conservation and Offshore Wind Energy TMR4590: Specialization Project* (tech. rep.).
- Perez-Moreno, S. S., Dykes, K., Merz, K. O., & Zaaijer, M. B. (2018). Multidisciplinary design analysis and optimisation of a reference offshore wind plant. *Journal of Physics: Conference Series*, 1037(4). <https://doi.org/10.1088/1742-6596/1037/4/042004>
- Peschko, V., Mendel, B., Mercker, M., Dierschke, J., & Garthe, S. (2021). Northern gannets (*Morus bassanus*) are strongly affected by operating offshore wind farms during the breeding season. *Journal of Environmental Management*, 279. <https://doi.org/10.1016/j.jenvman.2020.111509>

- Peschko, V., Mendel, B., Müller, S., Markones, N., Mercker, M., & Garthe, S. (2020). Effects of offshore windfarms on seabird abundance: Strong effects in spring and in the breeding season. *Marine Environmental Research*, 162. <https://doi.org/10.1016/j.marenvres.2020.105157>
- Platteeuw, M., Bakker, J., van den Bosch, I., Erkman, A., Graafland, M., Lubbe, S., & Warnas, M. (2017). A Framework for Assessing Ecological and Cumulative Effects (FAECE) of Offshore Wind Farms on Birds, Bats and Marine Mammals in the Southern North Sea. In *Wind energy and wildlife interactions* (pp. 219–237). Springer International Publishing. [https://doi.org/10.1007/978-3-319-51272-3{\\\_}\\\_13](https://doi.org/10.1007/978-3-319-51272-3{\_}\_13)
- Potiek, A., Ijntema, G. J., Van Kooten, T., Leopold, M. F., & Collier, M. P. (2021). *Acceptable Levels of Impact from offshore wind farms on the Dutch Continental Shelf for 21 bird species A novel approach for defining acceptable levels of additional mortality from turbine collisions and avoidance-induced habitat loss Ecology & Landscape* (tech. rep.). [www.buwa.nl](http://www.buwa.nl)
- Potiek, A., Leemans, J. J., Middelveld, R. P., & Gyimesi, A. (2022). *Cumulative impact assessment of collisions with existing and planned offshore wind turbines in the southern North Sea* (tech. rep.). Waardenburg Ecology. [www.buwa.nl](http://www.buwa.nl)
- Ramírez, L. (2021). *Offshore Wind in Europe* (tech. rep.).
- Rehfish, M., Barrett, Z., Brown, L., Buisson, R., Perez-Dominguez, R., & Clough, S. (2014). *ASSESSING NORTHERN GANNET AVOIDANCE OF OFFSHORE WINDFARMS i* (tech. rep.).
- Rijkswaterstaat. (2022). Shutting down offshore wind turbines during peak bird migration. <https://wetswegwijzer.nl/docs/Shuttingdownoffshorewindturbinesduringpeakbirdmigration.pdf>
- RVO. (2023). *Project and Site Description Ijmuiden Ver Wind Farm Zone (Sites Alpha and Beta)* (tech. rep.). <https://english.rvo.nl/subsidies-financing/offshore-wind-energy/ijmuiden-ver>
- Salkanović, E. (2023, June). Protecting avian wildlife for wind farm siting: The Screening Tool Proof of Concept. <https://doi.org/10.1016/j.esd.2023.03.002>
- Searle, K. R., O'Brien, S. H., Jones, E. L., Cook, A. S. C. P., Trinder, M. N., McGregor, R. M., Donovan, C., McCluskie, A., Daunt, F., & Butler, A. (2023). A framework for improving treatment of uncertainty in offshore wind assessments for protected marine birds. *ICES Journal of Marine Science*. <https://doi.org/10.1093/icesjms/fsad025>
- SNH. (2010). *Use of Avoidance Rates in the SNH Wind Farm Collision Risk Model* (tech. rep.). <http://www.snh.gov.uk/docs/A305435.pdf>
- Spijkerboer, R. C., Zuidema, C., Busscher, T., & Arts, J. (2020). The performance of marine spatial planning in coordinating offshore wind energy with other sea-uses: The case of the Dutch North Sea. *Marine Policy*, 115. <https://doi.org/10.1016/j.marpol.2020.103860>
- Stokke, B., & Dahl, E. (2024). *Long-term impacts of the Smøla wind farm on a local population of white-tailed eagles (Haliaeetus albicilla)* (tech. rep.). Norwegian Institute for Nature Research (NINA). <https://tethys.pnnl.gov/publications/long-term-impacts-smola-wind-farm-local-population-white-tailed-eagles-haliaeetus>
- Stories of Purpose The Hague. (2024). How a floating radar from The Hague prevents birds and bats from colliding with offshore wind farms. <https://storiesofpurpose.thehague.com/impact/floating-radar-robin-radar-systems-create-eco-friendlier-wind-farm-birds-and-bats>
- TenneT. (2025). The 2GW Program. <https://www.tennet.eu/about-tennet/innovations/2gw-program>
- The Cornell Lab of Ornithology. (2024). Birds of the World. <https://birdsoftheworld.org/>
- Tjørnløv, R. S., Armitage, M., Skov, H., Schlütter, F., Barker, M., Jørgensen, J. B., Mortensen, L. O., Thomas, K., Uhrenholdt, T., & Hass, M. (2023). *Resolving Key Uncertainties of Seabird Flight and Avoidance Behaviours at Offshore Wind Farms Offshore Wind Farms* (tech. rep.). [www.dhigroup.com](http://www.dhigroup.com)
- Tjørnløv, R. S., Cox, R., Larsen, K., Armitage, M., Skov, H., Barker, M., Cuttat, F., & Thomas, K. (2021). *AOWFL Resolving Key Uncertainties of Seabird Flight and Avoidance Behaviours at Offshore Wind Farms* (tech. rep.).
- van der Male, P. (2023). OSS Lecture 02b: Natural Frequency Analysis.
- van der Vliet, R. E., Bakker, E. G. R., Potiek, A., Kraal, J., Leemans, J. J., Boonman, M., & Gyimesi, A. (2022). *Ecologisch achtergronddocument windenergiegebied Ijmuiden Ver.* (tech. rep.). Bureau Waardenburg, Culemborg.
- Van Oord. (2025). Van Oord Offshore Wind Germany. <https://vanoord.de/en/van-oord-offshore-wind/>
- Vanermen, N., Onkelinx, T., Courtens, W., van de Walle, M., Verstraete, H., & Stienen, E. W. (2014). Seabird avoidance and attraction at an offshore wind farm in the Belgian part of the North Sea. *Hydrobiologia*, 756(1), 51–61. <https://doi.org/10.1007/s10750-014-2088-x>

- Wang, L., Wang, B., Cen, W., Xu, R., Huang, Y., Zhang, X., Han, Y., & Zhang, Y. (2023, May). Ecological impacts of the expansion of offshore wind farms on trophic level species of marine food chain. <https://doi.org/10.1016/j.jes.2023.05.002>
- WindpowerNL. (2024, June). Noordzeker and Zeevonk II winners of IJmuiden Ver Alpha and Beta tenders. <https://windpowernl.com/2024/06/11/noordzeker-and-zeevonk-ii-winners-of-ijmuiden-ver-alpha-and-beta-tenders/>
- Zaaijer, M. (2013). *Great expectations for offshore wind turbines* (tech. rep.).



# Expert Interviews

The interviews with experts both within and outside of the GROW consortium gave valuable practical insights into impacts of offshore wind farms on seabird populations. In addition, these also provided an overview of the current knowledge in this field. I am thankful for all the friendly experts who were willing to share their experiences and ideas to improve the research and to go further than the scarce literature. This appendix sums up the main takeaways from all the interviews. An overview of the interviewees is given in Table A.1 below.

Name	Company	Function	Date
M. Collier, A. Gyimesi, K. Didderen	Waardenburg Ecology	Ecologists	29/01/2024
M. Baptist, M. Poot, F. Soudijn	Wageningen Marine Research	Marine Ecologists	09/02/2024
A. Gyimesi	Waardenburg Ecology	Bird Ecologist	27/06/2024

**Table A.1:** Overview of expert interviews.

## A.1. Interview with Ecologists M. Collier, A. Gyimesi & K. Didderen

Company: Waardenburg Ecology

Date: 29/01/2024

Main takeaways:

- (A.) Ecologists at Waardenburg Ecology also have a need for models that include collision risk in the whole process of OWF planning. They are constantly being asked to redo calculations by tweaking small parameters, which can be done better with a model that is specifically designed for this.
- (A.) The turbine spacing is not yet considered in models to have an effect on bird collisions, since there is no research done on this yet.
- (K.) CRM calculation results are purely quantitative. The context around these results should always be emphasized. For example, one should take into account the footprint of the OWF when doing calculations for a specific site.
- (M.) Interesting to look into: bigger turbines operate in different wind speeds. The cut-in windspeed is typically higher. Any time the turbine is not operative, reduces collision risk. In addition, bigger turbines need less operating time to produce the same amount of electricity, hence collision risk can be reduced as well.
- (M.) The activity and behaviour around OWFs per species is weather and season dependant. This can be used to apply collision mitigation measures smartly, to minimise power production

losses and maximise collision reductions. For example, turbine maintenance is typically done in the summer. This is also the period with the highest seabird density, hence concentrating all maintenance in the summer months may be interesting to investigate.

- (A.) Raising the minimum tip height is already being included in the OWF site requirements (kavelbesluiten) provided by the government for practical reasons. It has also been one of the most discussed mitigation measures for collisions. This is therefore interesting to include in the EcoWindToolbox model.
- (A.) Starting with KEC 5.0, StochLAB will be used as the CRM by Waardenburg Ecology. It can be found on GitHub, and is open source and up-to-date. It is recommended to work with this CRM because in the future Waardenburg Ecology will transition to using this model as well, due to its open source availability and ease for referencing.
- (A.) Calculations for collisions are relatively fast as they were done in KEC 4.0. In case of calculating for many sites and species, calculations may take long, but this is not the case for your thesis.
- (M.) Oblique angles are not included in the StochLAB CRM. This is due to the assumption that oblique angle flight for seabirds does not change the collision risk significantly. As of today, there is no evidence that this assumption is incorrect.
- (A.) The Acceptable Level of Impact (ALI) is purely based on a species population size and trend, and comes forward from legislation. You can therefore assume that all species treated in KEC 4.0 are critical species affected by OWF development.
- (A.) Typically, the government turns to Waardenburg Ecology when it comes to collision risk calculations in the OWF siting phase. In addition, Waardenburg Ecology is involved during the whole siting phase of OWFs. They are also involved in gathering data in operating OWFs on birds interacting with the site.
- (K.) More than 1600 observation hours have been done. This meant that people stood on a platform in OWFs, to look for bird species interacting with wind turbines. Very little activity was observed here, due to the difficulty of spotting birds in those conditions. Observing bird activity in OWFs is still one of the main challenges.
- (M.) In the past years, radars and cameras have been used to monitor 24 hours per day. Still, barely any birds were found to come close to turbines. More technology is coming soon to detect bird species with the help of radars, camera's and AI. However, this technology is tuned to predatory birds on land, and is not yet applicable to seabirds. In general, there is more technology that works on land, but not at sea, hence the uncertainties around cumulative effects of collisions on seabirds.
- (M.) In addition, wind farm operators are not so keen on ecologists installing heavy camera's, radars on their turbines. Holes have to be drilled as well. A solutions is being searched for to accommodate the needs of operators, so that monitoring seabird behaviour in wind farms can be continued.

## **A.2. Interview with Marine Ecologists M. Baptist, M. Poot & F. Soudijn**

Institution: Wageningen Marine Research (WMR)

Date: 09/02/2024

Main takeaways:

- (M. Baptist) Adding a spatial component to the model could be interesting to look into.
- (T.) The model shall aim to combine technical and ecological boundary conditions. The model shall focus on existing wind farms that are located in critical areas, or critical areas where wind farms shall be built in the future.
- (F.) In KEC 4.0 sufficient information can be found about the used parameters and data for cumulative impact assessment.
- (F.) It could be interesting to look into flyways / corridors within wind farms, using your model. This w.r.t. impacts on migratory birds due to wind farms.

- (F.) It could also be worthy to look into the activity of maintenance vessels within wind farms, and their influence on habitat loss of seabirds. And combine this with a cost component in your model for assessment on this matter.
- (M. Poot) The proposed solution of creating corridors / flyways, as far as I know, relate to a different story than what your thesis is about. It mainly applies to nighttime migration, which is only a couple of nights per spring and autumn. In addition, migratory birds mainly fly above rotor heights. However, since the migration is on a massive scale, the Band model does calculate in the order of thousands of bird casualties, which is to be taken seriously.
- (M. Poot) There is very little empirical research done on seabirds and windfarms. In a certain way, the first casualty has yet to be confirmed.
- (M. Poot) The trend of wind turbines becoming bigger is interesting to look into, especially when making a cost-benefits analysis in the ecological sense for seabirds. This is a case that many have been trying to look into in this field. Still, one should keep in mind that this research as of now can only be done theoretically.
- (M. Poot) Keep in mind that your model may lead to a trivial solution.
- (M. Poot) An important part of your story is the flight height distribution. Data for this is available, possibly through Waardenburg Ecology.
- (M. Baptist) Critical species depend on the wind farm location. For example, for Borssele, this is the Northern Gannet (Jan-van-gent).
- (M. Baptist) It could be interesting to look into start-stop mitigations. In case you are focusing on different measures, you could mention these measures in the right context.
- (T.) The perspective programme also wants to look into smart curtailment with AI. But this shall not be the focus for the thesis of Nino.
- (M. Poot) Most of the data you need, can be found in reports, like the parameter of flight height distribution.

### **A.3. Interview with Bird Ecologist A. Gyimesi**

Company: Waardenburg Ecology

Date: 27/06/2024

Main takeaways:

- Use of Ijmuiden Ver as a basecase is relevant. The MER studies done by Waardenburg Ecology provide detailed information about this site, including bathymetry data.
- Relevant critical species in the North Sea indeed include the northern gannet, lesser black-backed gull, greater black-backed gull and the herring gull. Useful to include them in the model.
- Turbine spacing is not considered an important factor on bird collisions, hence it is not included in the state-of-the-art bird collision risk models.
- Ecologists are not necessarily worried about the negative effects of OWFs on seabirds. However, due to laws and legislation, calculations have to be done prior to tendering a site. In the end, the cumulative impact matters, when all planned OWFs are up and running.

# B

## Extended Simulation Results

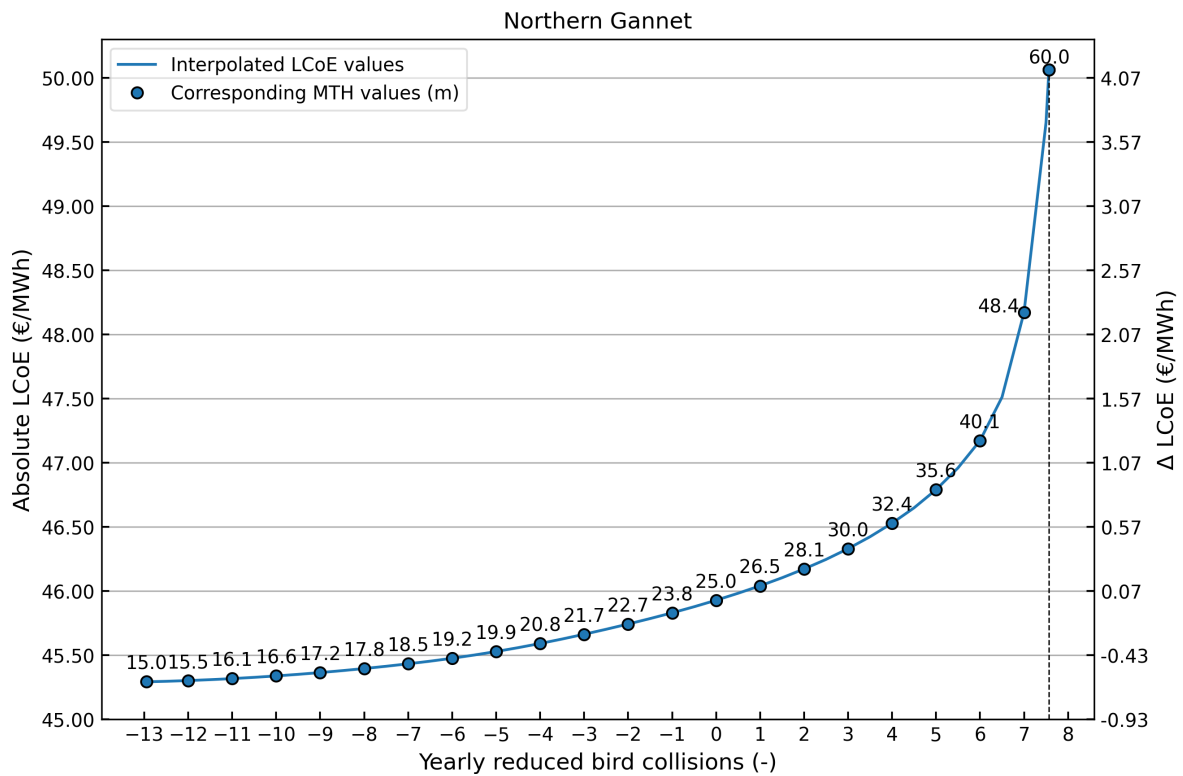


**Figure B.1:** Full graph for the northern gannet showing the absolute and relative LCoE values for each reduction or increase in yearly collisions, due to varying the minimum tip height.

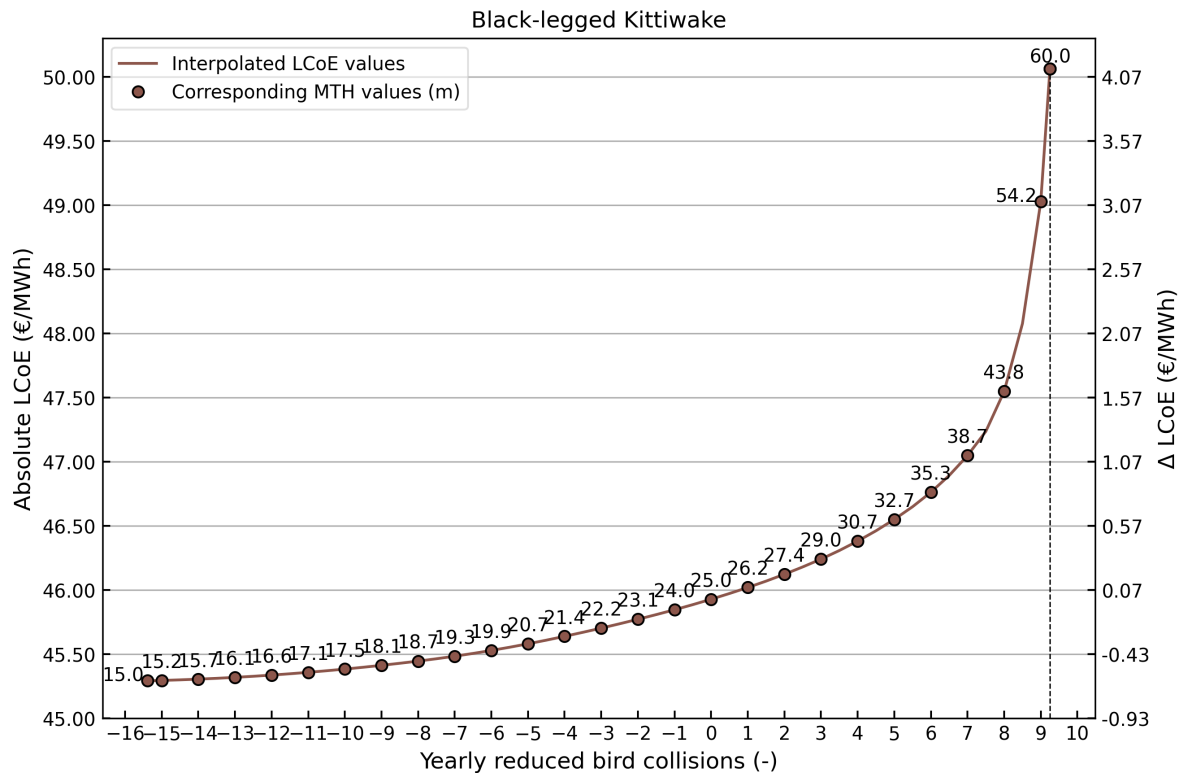


**Figure B.2:** Full graph for the black-legged kittiwake showing the absolute and relative LCoE values for each reduction or increase in yearly collisions, due to varying the minimum tip height.

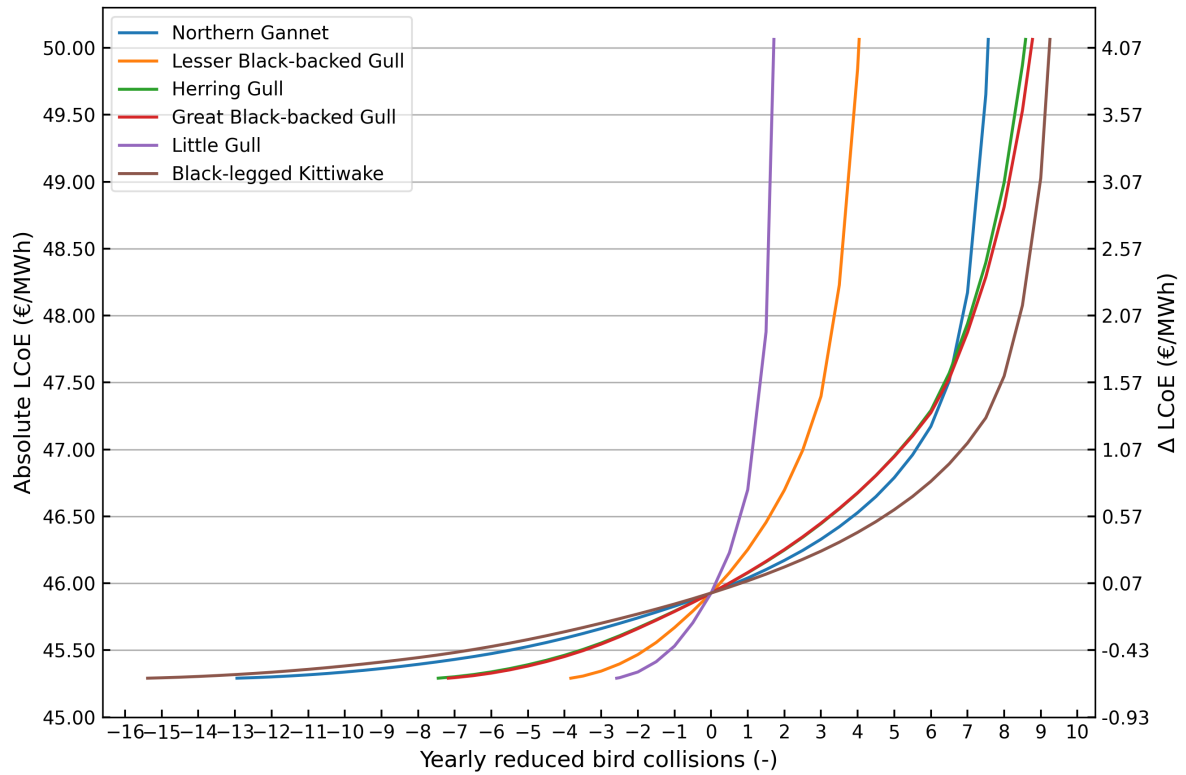
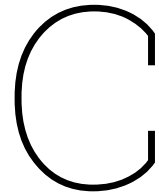


**Figure B.3:** Full graph showing the absolute and relative LCoE values for reducing or increasing yearly collisions due to varying MTH, plotted for all studied species.



## R Script for Collision Calculations

```
1 # ----- stochLAB's Collision Model Learning Script -----
2
3 # Goal Script:
4 # -----
5 # This script is drafted as part of several projects within Waardenburg Ecology
6 # and TU Delft.
7
8 # General Information:
9 # -----
10 # Author(s): Gerben IJntema, MSc; Nino Perez Perez, BSc
11 # Affiliation & Ownership: Waardenburg Ecology, TU Delft
12 # Programmed in: R; version 4.3.2 (2023-10-31)
13 # Last Updated: 2025-04-14
14
15 # Input data files:
16 # -----
17 # Bird Density Files
18 # Bird Characteristics
19 # Windfarm Characteristics
20
21 # Output (data) files:
22 # -----
23 # Reports on bird mortality
24
25
26 # -----
27
28
29 # ----- Setup -----
30
31 # install relevant packages: TODO: more elegant solution available with require
32 # install.packages("stochLAB")
33 # install.packages("dplyr")
34 # install.packages("collections")
35
36 # Load relevant packages:
37 library(stochLAB)
38 library(dplyr)
39 library(collections)
40 library(readxl)
41
```

```

42 args <- commandArgs(trailingOnly = TRUE)
43 if (length(args) == 0) {
44   stop("No input provided. Please provide input arguments.")
45 }
46
47 n_blades <- as.numeric(args[[1]])
48 rtr_radius_pars_mean <- as.numeric(args[[2]])
49 air_gap_pars_mean <- as.numeric(args[[3]])
50 rtn_speed_pars_mean <- as.numeric(args[[4]])
51 bld_width_pars_mean <- as.numeric(args[[5]])
52 trb_wind_avbl <- data.frame(month = month.abb, pctg = rep(as.numeric(args[[6]]),
53   12)
54   ) # DATAFRAME WITH PER EACH MONTH DATA % WIND GOOD
55   ENOUGH FOR RUNstr(trb_downtime_pars),
56 trb_downtime_pars <- data.frame(month = month.abb,
57   mean = rep(as.numeric(args[[7]]), 12),
58   sd = rep(0, 12)) # DATAFRAM WITH PER EACH MONTH
59   DATA % MAINTENANCE DOWNTIME
60
61 wf_n_trbs <- as.numeric(args[[8]])
62 wf_width <- as.numeric(args[[9]])
63 windspd_pars <- data.frame(mean = as.numeric(args[10]), sd = as.numeric(args[11]))
64
65 # Read the Excel file
66 df_rotor <- read_excel("IEA-15-240-RWT_tabular.xlsx", sheet = "Rotor_Performance")
67 # new_df_rotor <- df_rotor[, c(1, 6, 2)]
68
69 # Hardcoded variables for testing -----
70
71 # Variables Needed -Dummies taken from LBBG (bird species)
72 # modeltechnical variables
73 model_options <- 3 # Model type
74 n_iter <- 5 # number of iterations
75 lrg_arr_corr <- TRUE
76 out_format <- "summaries" # Only give summary statistics out not all stochastics
77 draws
78 out_sampled_pars <- FALSE
79 out_period <- "months"
80 verbose <- FALSE
81 log_file <- NULL
82 seed <- 1 # if we want to run reproducibility
83
84 # species specific characteristics, all taken from Ijmuiden ver Alpha WB report
85 flight_type <- "flapping" # conservative type of flying, doesn't matter too much
86 prop_upwind <- 0.5 # default number of flights upwind
87
88 # # jan-van-gent = JVG = NG
89 flt_speed_pars_mean <- 14.9
90 flt_speed_pars_sd <- 2.60
91 body_lt_pars_mean <- 0.94
92 body_lt_pars_sd <- 0.022
93 wing_span_pars_mean <- 1.73
94 wing_span_pars_sd <- 0.025
95 avoid_bsc_pars_mean <- 0.989
96 avoid_bsc_pars_sd <- 0
97 avoid_ext_pars_mean <- 0.989
98 avoid_ext_pars_sd <- 0
99 noct_act_pars_mean <- 0.08
100 noct_act_pars_sd <- 0
101
102 # Species flight height distribution bootstraps
103 gen_fhd_boots <- generic_fhd_bootstraps[["Northern_Gannet"]] # built-in generic

```

```

species specific distributions
99 # gen_fhd_boots <- generic_fhd_bootstraps[["Lesser_Black_Backed_Gull"]] # built-in
generic species specific distributions
100 # gen_fhd_boots <- generic_fhd_bootstraps[["Herring_Gull"]] # built-in generic
species specific distributions
101 # gen_fhd_boots <- generic_fhd_bootstraps[["Great_Black_backed_Gull"]] # built-in
generic species specific distributions
102 # gen_fhd_boots <- generic_fhd_bootstraps[["Little_Gull"]] # built-in generic
species specific distributions
103 # gen_fhd_boots <- generic_fhd_bootstraps[["Black_legged_Kittiwake"]] # built-in
generic species specific distributions
104
105 # Bird Density Data, from WB ijmuiden ver report
106 bird_dens_opt <- "tnorm"
107 # Northern Gannet
108 bird_dens_NG <- data.frame(month = month.abb,
109                             mean = c(0.4, 0.3, 0.3, 0.4, 0.4, 0.1, 0.1, 0.2, 0.2, 0.6,
110                                     0.6, 0.4),
111                             sd = rep(0.001, 12))
112 # LBBG = kleine mantelmeeuw
113 bird_dens_LBBG <- data.frame(month = month.abb,
114                               mean = c(0.0, 0.2, 0.2, 0.4, 0.4, 0.7, 0.7, 0.2, 0.2, 0.2,
115                                       0.2, 0.0),
116                               sd = rep(0.001, 12))
117 # Herring Gull
118 bird_dens_HG <- data.frame(month = month.abb,
119                             mean = c(0.5, 1.2, 1.2, 0.1, 0.1, 0.0, 0.0, 0.0, 0.0, 0.2,
120                                     0.2, 0.5),
121                             sd = rep(0.001, 12))
122 # GBBG
123 bird_dens_GBBG <- data.frame(month = month.abb,
124                               mean = c(0.3, 0.3, 0.3, 0.0, 0.0, 0.0, 0.0, 0.1, 0.1, 0.2,
125                                       0.2, 0.3),
126                               sd = rep(0.001, 12))
127 # Little Gull
128 bird_dens_LG <- data.frame(month = month.abb,
129                             mean = c(0.0, 0.1, 0.1, 1.3, 1.3, 0.0, 0.0, 0.0, 0.0, 0.0,
130                                     0.0, 0.0),
131                             sd = rep(0.001, 12))
132 # BLK
133 bird_dens_BLK <- data.frame(month = month.abb,
134                               mean = c(0.9, 1.1, 1.1, 1.0, 1.0, 0.4, 0.4, 0.1, 0.1, 1.3,
135                                       1.3, 0.9),
136                               sd = rep(0.001, 12))
137
138 # Engineering Technical characteristics of windfarm
139 air_gap_pars_sd <- 0
140 rtr_tradius_pars_sd <- 0
141 bld_width_pars_sd <- 0
142 # bld_chord_prf_pp_radius <- Currently allowed to default to a 5MW default
profile
143 # bld_chord_prf_chord <- see one line above
144 # rtn_pitch_opt <- "probDist"
145 rtn_pitch_opt <- "windSpeedReltn"
146 rtn_pitch_windspd_dt = data.frame(
147   wind_speed = df_rotor$'Wind [m/s]',
148   rtn_speed = df_rotor$'Rotor Speed [rpm]',
149   bld_pitch = df_rotor$'Pitch [deg]')
150 bld_pitch_pars_mean <- 1 # 14 is maximum
151 bld_pitch_pars_sd <- 0
152 rtn_speed_pars_sd <- 0

```

```

147 wf_latitude <- 52.89
148 tidal_offset <- 0.9 # Completely random value, need to tghink further about this
149
150
151 # Variables that cannot be defined as a scalar value and need to be a df/matrix
152 bld_chord_prf <- data.frame(
153   pp_radius = c(0, 0.10, 0.20, 0.30, 0.40, 0.50, 0.60, 0.70, 0.80, 0.90, 1),
154   chord = c(0.90202, 0.94428, 0.99923, 0.93106, 0.81527, 0.72071, 0.63705,
155     0.55872, 0.48011, 0.39288, 0.08673)
156 ) # DATAFRAME WITH % OF MAX WIDTH AT % OF MAX LENGTH
157
158
159 # Put variables that are needed in dfs in dfs
160 flt_speed_pars <- tibble(mean = flt_speed_pars_mean, sd = flt_speed_pars_sd)
161 body_lt_pars <- tibble(mean = body_lt_pars_mean, sd = body_lt_pars_sd)
162 wing_span_pars <- tibble(mean = wing_span_pars_mean, sd = wing_span_pars_sd)
163 avoid_ext_pars <- tibble(mean = avoid_ext_pars_mean, sd = avoid_ext_pars_sd)
164 avoid_bsc_pars <- tibble(mean = avoid_bsc_pars_mean, sd = avoid_bsc_pars_sd)
165 noct_act_pars <- tibble(mean = noct_act_pars_mean, sd = noct_act_pars_sd)
166 air_gap_pars <- tibble(mean = air_gap_pars_mean, sd = air_gap_pars_sd)
167 bld_width_pars <- tibble(mean = bld_width_pars_mean, sd = bld_width_pars_sd)
168 bld_pitch_pars <- tibble(mean = bld_pitch_pars_mean, sd = bld_pitch_pars_sd)
169 rtn_speed_pars <- tibble(mean = rtn_speed_pars_mean, sd = rtn_speed_pars_sd)
170 rtr_radius_pars <- tibble(mean = rtr_radius_pars_mean, sd = rtr_tradius_pars_sd)
171
172 # ----- Start Analysis -----
173 # windSpeedReltn
174 stoch_colls_df <- stoch_crm(
175   model_options = c(3),
176   n_iter = 1000,
177   flt_speed_pars = flt_speed_pars,
178   body_lt_pars = body_lt_pars,
179   wing_span_pars = wing_span_pars,
180   avoid_bsc_pars = avoid_bsc_pars,
181   avoid_ext_pars = avoid_ext_pars,
182   noct_act_pars = noct_act_pars,
183   bird_dens_opt = bird_dens_opt,
184   bird_dens_dt = bird_dens_NG,
185   flight_type = flight_type,
186   prop_upwind = prop_upwind,
187   gen_fhd_boots = gen_fhd_boots,
188   n_blades = n_blades,
189   air_gap_pars = air_gap_pars,
190   rtr_radius_pars = rtr_radius_pars,
191   bld_width_pars = bld_width_pars,
192   bld_chord_prf = bld_chord_prf,
193   rtn_pitch_opt = rtn_pitch_opt,
194   windspd_pars = windspd_pars,
195   rtn_pitch_windspd_dt = rtn_pitch_windspd_dt,
196   trb_wind_avbl = trb_wind_avbl,
197   trb_downtime_pars = trb_downtime_pars,
198   wf_n_trbs = wf_n_trbs,
199   wf_width = wf_width,
200   wf_latitude = wf_latitude,
201   tidal_offset = tidal_offset,
202   lrg_arr_corr = lrg_arr_corr,
203   out_format = out_format,
204   out_sampled_pars = out_sampled_pars,
205   out_period = out_period,
206   verbose = verbose,
207   log_file = log_file,

```

---

```
208   seed = seed
209 )
210
211 result <- stoch_colls_df[[1]]$mean
212 result
```

# D

## Relevant Python Scripts

**Listing D.1:** Python function to call the collision calculation script.

```
1 def batch_birds():
2     ##### Run a batch for birds model #####
3     timestamp = datetime.now().strftime("%m-%d_%H%M")
4     save_directory = 'C:/mihir_phd/window_static/WINDOW_openMDAO-RNA_new/
5         nino_scripts/plotting/csv_outputs'
6     index = 0
7     # species = 'LBBG'
8     species_list = ['NG', 'LBBG', 'HG', 'GBBG', 'LG', 'BLK']
9     species = species_list[4]
10    print(f'Species_{species}')
11
12    # """"Vary min tip height""""
13    # # vals_power = [power_values_1000MW]
14    # simulation_type = 'vary_min_tip'
15    # folder_path = os.path.join(save_directory, species, f"{simulation_type}_{
16        timestamp}")
17    # vals_tip_height = np.arange(15, 62.5, 2.5)
18    # # vals_tip_height = np.arange(25, 27.5, 2.5)
19    # value_rad = 236 / 2
20    # value_power = 15
21    # for val1 in vals_tip_height:
22    #     min_tip_height = val1
23
24    # """"Vary radius""""
25    # simulation_type = 'vary_d_rotor'
26    # folder_path = os.path.join(save_directory, species, f"{simulation_type}_{
27        timestamp}")
28    # vals_rad = np.arange(186, 286+5, 5) / 2
29    # value_power = 15
30    # min_tip_height = 25
31    # for val in vals_rad:
32    #     # print(val)
33    #     value_rad = val
34
35    # """"Vary rated power""""
36    simulation_type = 'vary_p_rated'
37    folder_path = os.path.join(save_directory, species, f"{simulation_type}_{
38        timestamp}")
39    vals_power = [10, 11, 12, 13, 14, 15, 16, 17, 18, 19, 20, 22.73]
40    vals_power = [22.73]
```

```

37 # vals_power_shouldbe = [10.0, 10.99, 12.05, 12.99, 14.08, 14.93, 16.13,
38   17.24, 18.18, 19.23, 20.0]
39 vals_rad = [178.3/2, 189.8/2, 201.4/2, 212.9/2, 224.5/2, 236.0/2, 244.8/2,
40   253.6/2, 262.4/2, 271.2/2, 280.0/2, 306.4/2]
41 vals_rad = [306.4/2]
42 n_t = [100, 91, 83, 77, 71, 67, 62, 58, 55, 52, 50, 44]
43 n_t = [44]
44 min_tip_height = 25
45 for i, val in enumerate(vals_rad):
46     value_rad = val
47
48     """Birds Model"""
49     # Inputs
50     cut_in_speed = 4 # m/s
51     cut_out_speed = 25 # m/s
52     h = min_tip_height + value_rad
53     turbine = '15MW_Mihir'
54     # p_rated = value_power
55     p_rated = vals_power[i]
56     # n_wt = 67
57     n_wt = n_t[i]
58     D_rotor = value_rad * 2
59     rated_RPM = 7.56
60     scale_param = 11.86 # weibull scale parameter A
61     shape_param = 2.4 # weibull shape parameter k
62
63     from bird_functions import calc_operable_pctg, calc_mean_sd_weibull
64
65     n_blades = 3
66     rtr_radius_pars_mean = value_rad
67     air_gap_pars_mean = min_tip_height
68     rtn_speed_pars_mean = rated_RPM # rated RPM = mean RPM for the bird model
69     bld_width_pars_mean = 5.7648
70     trb_wind_avbl = calc_operable_pctg(cut_in_speed, cut_out_speed,
71     scale_param, shape_param)
72     # print(trb_wind_avbl)
73     # exit()
74     trb_downtime_pars = 2
75     wf_n_trbs = n_wt
76     wf_width = 11.4 # km
77     mean_wind_speed, sd_wind_speed = calc_mean_sd_weibull(scale_param,
78     shape_param)
79
80     birds_list = []
81
82     birds = run_r_script_with_packages(f'bird_collisions_{species}.R', [str(
83     n_blades),
84     str(rtr_radius_pars_mean),
85     str(air_gap_pars_mean),
86     str(rtn_speed_pars_mean),
87     str(bld_width_pars_mean),
88     str(trb_wind_avbl),
89     str(trb_downtime_pars),
90     str(wf_n_trbs),
91     str(wf_width),
92     str(mean_wind_speed),
93     str(sd_wind_speed)])
94
95     birds = re.findall(r'\d+\.\d+', birds)
96     # Convert strings to floats
97     birds = [float(x) for x in birds]

```

```

93     birds_list.append([p Rated, D_rotor, rated_RPM, h,
94                       n_blades, rtr_radius_pars_mean, air_gap_pars_mean,
95                       rtn_speed_pars_mean,
96                       bld_width_pars_mean, trb_wind_avbl,
97                       trb_downtime_pars,
98                       wf_n_trbs,
99                       wf_width] + birds)
100
101     birds_df = pd.DataFrame(birds_list,
102                             columns=['p Rated', 'd_rotor', 'rated_RPM',
103                                     'hub_height',
104                                     'n_blades', 'rtr_radius_pars_mean', '
105                                     air_gap_pars_mean',
106                                     'rtn_speed_pars_mean', 'bld_width_pars_mean',
107                                     'trb_wind_avbl',
108                                     'trb_downtime_pars', 'wf_n_trbs', 'wf_width',
109                                     'jan',
110                                     'feb',
111                                     'mar',
112                                     'apr', 'may', 'jun', 'jul', 'aug', 'sep', 'oct
113                                     ', 'nov',
114                                     'dec'])
115
116     header_switch = True if index == 0 else False
117     index += 1
118     birds_df.to_csv('birds_data_nino.csv', mode='a', header=header_switch,
119                    index=False, sep=',')
120     birds_df.to_csv(f'{folder_path}.csv', mode='a', header=header_switch,
121                    index=False, sep=',')
122     print(f'run_{index}_completed')

```

Listing D.2: LCoE model setup script for the defined case.

```

1 def run_main_script(value_rad, value_power, value_elec_ratio, cut_in,
2   min_tip_height):
3     file = open("Input/power_value.txt", "w")
4     file.write(str(value_power))
5     file.close()
6     print(value_power)
7
8     # (Perez Perez, 2025) add
9     # with open("Input/power_value.py", "w") as file:
10    #     file.write(f"p Rated = {value_power}\n")
11
12    with open("Input/min_tip_height_value.py", "w") as file:
13        file.write(f"min_tip_height_support_{min_tip_height}\n")
14
15    # file = open("Input/N_t.txt", "w")
16    # file.write(str(N_t))
17    # file.close()
18    # print(N_t)
19
20    # This file must be run from the 'example' folder that has the 'Input' folder.
21    #from __main__ import value_rad, value_power
22    # Imports OpenMDAO API
23    from openmdao.api import Problem #ScipyOptimizer, view_model, SimpleGADriver
24    import csv
25
26
27
28    # Imports WINDOW workflow

```

```

29
30 # Imports models included in WINDOW
31 # from WINDOW_openMDAO.Turbine.Curves import Curves # Not used in the AEP fast
    calculator.
32 from WINDOW_openMDAO.ElectricalCollection.topology_hybrid_optimiser import
    TopologyHybridHeuristic
33 from WINDOW_openMDAO.SupportStructure.teamplay import TeamPlay
34 from WINDOW_openMDAO.OandM.OandM_models import OM_model3
35 from WINDOW_openMDAO.AEP.aep_fast_component import AEPFast
36 from WINDOW_openMDAO.Costs.teamplay_costmodel import TeamPlayCostModel
37 from WINDOW_openMDAO.AEP.FastAEP.farm_energy.wake_model_mean_new.
    wake_turbulence_models import frandsen
38 from WINDOW_openMDAO.AEP.FastAEP.farm_energy.wake_model_mean_new.
    downstream_effects import JensenEffects as Jensen
39 from WINDOW_openMDAO.AEP.FastAEP.farm_energy.wake_model_mean_new.wake_overlap
    import root_sum_square
40
41 # Imports the Options class to instantiate a workflow.
42 from WINDOW_openMDAO.src.api import WorkflowOptions
43
44 #from WINDOW_openMDAO.multifidelity_fast_workflow_new_UC_static_opt_elec_H2
    import WorkingGroup
45 # Uncomment for H2 or electricity only
46 from WINDOW_openMDAO.multifidelity_fast_workflow_new_UC_static_opt_elec import
    WorkingGroup
47 # from WINDOW_openMDAO.multifidelity_fast_workflow_new_UC_static_opt_elec_H2
    import WorkingGroup
48
49
50 import warnings
51
52 def fxn():
53     warnings.warn("deprecated", DeprecationWarning)
54
55 with warnings.catch_warnings():
56     warnings.simplefilter("ignore")
57     fxn()
58
59
60 def print_nice(string, value):
61     header = '=' * 10 + "□" + string + "□" + '=' * 10 + '\n'
62     header += str(value) + "\n"
63     header += "=" * (22 + len(string))
64     print(header)
65
66
67 options = WorkflowOptions()
68
69 # Define models to be implemented.
70 options.models.aep = AEPFast
71 options.models.wake = Jensen
72 options.models.merge = root_sum_square
73 options.models.turbine = None # Unnecessary for now as long as the power and
    Ct curves are defined below.
74 options.models.turbulence = frandsen
75 options.models.electrical = TopologyHybridHeuristic
76 options.models.support = TeamPlay
77 options.models.opex = OM_model3
78 options.models.apex = TeamPlayCostModel
79
80 # Define number of windrose sampling points

```

```

81 options.samples.wind_speeds = 22 # number of wind samples between cut-in and
    cut-out
82 options.samples.wind_sectors_angle = 30.0 # range of one sector for a windrose
83
84 # Define paths to site and turbine defining input files.
85 # options.input.site.windrose_file = "Input/weibull_windrose_12unique.dat"
86 options.input.site.windrose_file = "Input/weibull_windrose_12unique_IJV_Alpha.
    dat"
87 options.input.site.bathymetry_file = "Input/bathymetry_table.dat"
88
89
90 options.input.turbine.power_file = "Input/power_rna.dat"
91 options.input.turbine.ct_file = "Input/ct_rna.dat"
92 options.input.turbine.num_pegged = 3
93 options.input.turbine.num_airfoils = 50
94
95 options.input.turbine.num_nodes = 50
96 options.input.turbine.num_bins = 62 #31
97 options.input.turbine.safety_factor = 1.5
98 options.input.turbine.gearbox_stages = 3
99 options.input.turbine.gear_configuration = 'eep'
100 options.input.turbine.mb1_type = 'CARB'
101 options.input.turbine.mb2_type = 'SRB'
102 options.input.turbine.drivetrain_design = 'geared'
103 options.input.turbine.uptower_transformer = True
104 options.input.turbine.has_crane = True
105 options.input.turbine.reference_turbine = 'Input/Reference_turbine_15MW.csv'
106 options.input.turbine.reference_turbine_cost = 'Input/
    reference_turbine_15MW_cost_mass.csv'
107 options.input.turbine.rated_power = value_power/15.0
108 options.input.turbine.rotor_radius = value_rad/120.0
109
110 # (Perez Perez, 2025) Add
111 options.input.turbine.cut_in = cut_in
112 options.input.turbine.msl_tip_clearance = min_tip_height
113
114 options.input.site.time_resolution = 8760 #52560 # 98589
115 # options.input.site.wind_file = 'Input/NorthSea_2019_100m_hourly_ERA5_withdir
    .csv'
116 # options.input.site.wind_file = 'Input/
    NL_2019_100m_hourly_ERA5_highwind_withdir.csv'
117 options.input.site.wind_file = 'Input/IJV_Alpha_2023_100m_hourly_withdir.csv'
118
119
120 # options.input.market.spot_price_file = 'Input/NL_2019_spot_price_hourly.csv'
121 options.input.market.spot_price_file = 'Input/NL_2024_spot_price_hourly.csv' #
    Only matters for IRR
122
123 ### H2 addition ###
124 # options.input.hydrogen.electrolyser_ratio = value_elec_ratio #1
125
126 ### FAST addition ###
127
128 options.input.turbine.num_tnodes = 11
129
130 hub_height = min_tip_height + (value_rad)
131 field_names = ['p_rated', 'd_rotor', 'hub_height', 'min_tip_h']
132 description = ['Rated_power_[MW]', 'Rotor_diameter_[m]', 'Hub_height_[m]',
    'Minimum_tip_height_[m]']
133 data = {field_names[0]: [value_power, description[0]], field_names[1]: [
    value_rad*2, description[1]],

```

```

134     field_names[2]: [hub_height, description[2]], field_names[3]: [
135         min_tip_height, description[3]]
136
137 with open('parameters.csv', 'w') as csvfile:
138     writer = csv.writer(csvfile)
139     for key, value in list(data.items()):
140         writer.writerow([key, value[0], value[1]])
141     csvfile.close()
142
143 # (Perez Perez, 2025) add
144 with open('parameters_technical.csv', 'w') as csvfile:
145     writer = csv.writer(csvfile)
146     # **Write the header row first**
147     writer.writerow(['Parameter', 'Value', 'Description'])
148     for key, value in list(data.items()):
149         writer.writerow([key, value[0], value[1]])
150     csvfile.close()
151
152 with open('parameters_CAPEX.csv', 'w') as csvfile:
153     writer = csv.writer(csvfile)
154     for key, value in list(data.items()):
155         writer.writerow([key, value[0], value[1]])
156     csvfile.close()
157
158 with open('parameters_OPEX.csv', 'w') as csvfile:
159     writer = csv.writer(csvfile)
160     for key, value in list(data.items()):
161         writer.writerow([key, value[0], value[1]])
162     csvfile.close()
163
164 with open('parameters_DECEX.csv', 'w') as csvfile:
165     writer = csv.writer(csvfile)
166     for key, value in list(data.items()):
167         writer.writerow([key, value[0], value[1]])
168     csvfile.close()
169
170 # field_names = ['min_tip_height']
171 # description = ['Minimum tip height']
172 # data = {field_names[0]: [min_tip_height, description[0]]}
173 # # data = {field_names[0]: [lcoe[0], description[0]]}
174 #
175 # with open('parameters.csv', 'w') as csvfile:
176 #     writer = csv.writer(csvfile)
177 #     for key, value in list(data.items()):
178 #         writer.writerow([key, value[0], value[1]])
179 #     csvfile.close()
180
181 # import ast
182 # with open('Input/finance.txt', 'r') as file:
183 #     data = file.read()
184 #     d = ast.literal_eval(data)
185 #
186 # target_IRR = d['target_IRR']
187 # options.input.market.target_IRR = target_IRR
188
189 # Instantiate OpenMDAO problem class
190 problem = Problem()
191 problem.model = WorkingGroup(options)
192 problem.setup()
193

```

```

194     ### Uncomment below to plot N2 diagram in a browser.
195     # view_model(problem)
196     from time import time
197
198     start = time()
199     problem.run_model()
200
201
202     #####
203     ##### PARAMS #####
204     #####
205     '''
206     farm_params = ['lcoe.LCOE', 'AeroAEP.AEP', \
207                   'AeroAEP.efficiency', 'AEP.electrical_efficiency',
208                   'Costs.support_structure_investment']
209
210     # Save variables
211     result = {'tsr': problem['design_tsr'],
212              'chord': problem['chord_coefficients'],
213              'twist': problem['twist_coefficients'],
214              'pitch': problem['pitch'],
215              'tf_root': problem['tau_root'],
216              'tf_75' : problem['tau_75']}
217
218
219     # Save Farm parameters
220     for p in farm_params:
221         result[p] = problem[p][0]
222
223     # Save in file
224     result = pd.DataFrame(result)
225     pd.DataFrame(result).to_csv('static_GA.csv')'''
226
227
228
229     lcoe = problem['lcoe.LCOE'][0]
230     aep = problem['FarmAEP.farm_AEP'][0]
231     # subsidy_required = problem['FarmIRR.subsidy_required'][0]
232
233     # lcoh = problem['LCoH.LCoH'][0]
234     # (Perez Perez, 2025) add
235     # print(problem['tower'])
236     # for key in problem.keys():
237     #     print(key)
238     # exit()
239
240
241     print_nice("LCOE", lcoe)
242     # print_nice("LCoH", lcoh)
243     #print_nice("AEP", aep)
244     #print_nice("Subsidy required", subsidy_required)
245
246     '''
247     ### Setup Optimization ###
248     problem.driver = ScipyOptimizer()
249     problem.driver.options['optimizer'] = 'SLSQP'
250     problem.driver.options['tol'] = 1.0e-3
251     problem.driver.options['disp'] = True
252     problem.driver.options['maxiter'] = 1
253
254     problem.model.add_design_var('indep2.tau_root', lower= 0.6, upper=1.1)

```

```

255 problem.model.add_design_var('indep2.tau_75', lower=0.6, upper=1.1)
256 problem.model.add_design_var('indep2.chord_coefficients', lower=[3, 2, 1 ],
    upper=[5, 4, 3])
257 problem.model.add_design_var('indep2.twist_coefficients', lower=[9, 6, 1],
    upper=[16, 12, 6])
258
259
260
261
262 problem.model.add_constraint('Tip_Deflection', upper=7)
263 problem.model.add_constraint('Flapwise_Stress_Skin', upper=700)
264 problem.model.add_constraint('Flapwise_Stress_Spar', upper=1047)
265 problem.model.add_constraint('Stress_Root', upper=700)
266
267
268 # Ask OpenMDAO to finite-difference across the model to compute the gradients
    for the optimizer
269 problem.model.approx_totals()
270
271 problem['indep2.chord_coefficients'] = np.array([3.542, 3.01, 2.313])  #*
    190.8 / 126.0
272 problem['indep2.twist_coefficients'] = [13.308, 9.0, 3.125]
273
274 ### Preprocessor ###
275 problem['indep2.tau_root'] = 1.0
276 problem['indep2.tau_75'] = 1.0
277
278 problem.model.add_objective('LCOE')
279
280
281 problem.run_driver()'''
282
283 print('Executed_in_' + str(round(time() - start, 2)) + '_seconds\n')
284
285 # print outputs
286
287 '''
288 var_list = ['rotor_mass', 'nacelle_mass', 'rna_mass', 'cost_rna', '
    tip_deflection', 'Root_stress', \
289     'Stress_flapwise_skin', 'Stress_flapwise_spar', 'Stress_edgewise_skin
    ', 'Stress_edgewise_te_reinf',
290     'rotor_cp', 'rotor_ct', 'rotor_torque', 'rotor_thrust', \
291     'rated_wind_speed', 'wind_bin', 'elec_power_bin', 'ct_bin', \
292     'scale.hub_height', 'scale.turbine_rated_current', 'scale.
    solidity_rotor']
293
294 saved_output = {}
295 for v in var_list:
296     saved_output[v] = problem['rna.' + v]
297     beautify_dict(saved_output)'''
298 return lcoe

```